FLUID BIOMARKERS IN GENETIC FRONTOTEMPORAL DEMENTIA

EMMA LOUISE VAN DER ENDE

Fluid Biomarkers in Genetic Frontotemporal Dementia

Emma Louise van der Ende

The research described in this thesis was funded by Alzheimer Nederland, the Netherlands Organisation for Scientific Research (NWO), ZonMW Memorabel, the Dioraphte Foundation, and the Bluefield project.

Printing of this thesis was kindly supported by Alzheimer Nederland and the Bluefield project.

Cover design: ProefschriftOntwerp // proefschriftontwerp.nl

Printing: ProefschriftMaken // proefschriftmaken.nl

ISBN: 978-94-6423-320-9

© Emma L. van der Ende, Rotterdam, the Netherlands. All rights reserved. No part of this thesis may be reproduced, stored in a retrieval system or transmitted in any form or by any means without permission of the author. The copyright of previously published articles has been transferred to the respective journals.

Fluid Biomarkers in Genetic Frontotemporal Dementia

Fluïde biomarkers in genetische frontotemporale dementie

Proefschrift

ter verkrijging van de graad van doctor aan de

Erasmus Universiteit Rotterdam

op gezag van de

rector magnificus

Prof.dr. F.A. van der Duijn Schouten

en volgens besluit van het College voor Promoties.

De openbare verdediging zal plaatsvinden op

dinsdag 31 augustus 2021 om 13:00 uur

door

Emma Louise van der Ende

geboren te Vlaardingen

Erasmus University Rotterdam

Promotiecommissie:

Promotor:	Prof.dr. J.C. van Swieten
Overige leden:	Prof.dr. W.M. van der Flier
	Prof.dr. D.W.J. Dippel
	Dr.ing. M.M. Verbeek
Copromotor:	Dr. H. Seelaar

Table of contents

Chapter 1

General introduction

Chapter 1.1

Introduction to the thesis

Frontotemporal dementia (FTD) is a clinically, genetically and pathologically heterogeneous neurodegenerative disorder which accounts for approximately 10% of all dementia diagnoses.[1,2] Typically, patients present with progressive behavioural disturbances (behavioural variant FTD, bvFTD) [3] and / or language impairments (primary progressive aphasia, PPA),[4] which may be accompanied by motor symptoms such as parkinsonism and motor neuron disease.[2] An underlying autosomal dominant genetic mutation is identified in 10-20% of cases, most commonly in *GRN, C9orf72* or *MAPT.*[2,5]

Diagnosing FTD is frequently challenging due to its heterogeneity and overlapping symptomatology with several other neurodegenerative and non-neurodegenerative diseases, and substantial diagnostic delay is not uncommon. With the arrival of therapeutic trials, which may be most effective in early, possibly even preclinical stages of disease, a timely diagnosis of FTD is increasingly important.[5]

Alterations in cerebrospinal fluid (CSF) or blood that reflect FTD-related pathological processes could serve as biomarkers to detect FTD, track disease progression and evaluate the effect of trial medication. Genetic forms of FTD provide an ideal framework to identify such biomarkers, as they offer the opportunity to study mutation carriers as they transition from asymptomatic into clinically overt disese stages.

The aim of this thesis was to identify and validate biomarkers in blood and CSF in genetic forms of FTD.

Chapter 1.2 provides an overview of the current state of fluid biomarker research in sporadic and genetic FTD.

In chapters 2 and 3 we use immunoassays to quantify the levels of potential fluid biomarkers in presymptomatic and symptomatic genetic FTD. Chapter 2.1 describes the longitudinal dynamics of serum neurofilament light chain (NfL), a promising marker of neuroaxonal damage, whereas chapter 2.2 presents neuronal pentraxin 2 (NPTX2) as a novel CSF measure of synapse integrity. Chapter 3 focusses on biomarkers that could reflect immune system dysregulation in FTD. In chapter 3.1, we investigated CSF levels of soluble triggering receptor expressed on myeloid cells-2 (sTREM2), which is thought to reflect microglial activation. Chapter 3.2 describes the measurement of CSF and blood levels of complement proteins.

Chapter 4 explores proteomic and genetic approaches to biomarker identification. Chapter 4.1 descibes the use of unbiased mass spectrometry, followed by a targeted validation step, to identify novel CSF biomarkers. In chapter 4.2, we review the clinical spectrum of the

C9orf72 repeat expansion and discuss genetic factors that might act as biomarkers to predict the phenotype and disease course, with a particular focus on repeat length.

In chapter 5, we use discriminative event-based modelling to shed light on the temporal relationship between various biomarkers. In chapter 5.1, we determine the sequence in which a selection of fluid biomarkers becomes abnormal over the course of FTD, whereas the disease progression model presented in chapter 5.2 includes fluid, neuroimaging and cognitive biomarkers.

Chapter 6 presents the main findings, methodological considerations and possible implications of this thesis as well as recommendations for further research. Finally, chapter 7 summarises the results of this thesis.

References

1. Hogan B, Jetté N, Fiest KM, et al. The prevalence and incidence of frontotemporal dementia: a systematic review. Can J Neurol Sci. 2016;43: Suppl 1:S96-109.
2. Lashley T, Rohrer JD, Mead S, et al. Review: an update on clinical, genetic and pathological aspects of frontotemporal lobar degenerations. Neuropathol Appl Neurobiol. 2015;41(7):858-81.
3. Rascovsky K, Hodges JR, Knopman D, et al. Sensitivity of revised diagnostic criteria for the behavioural variant of frontotemporal dementia. Brain. 2011;134(Pt 9):2456-77.
4. Gorno-Tempini ML, Hillis AE, Weintraub S, et al. Classification of primary progressive aphasia and its variants. Neurology. 2011;76(11):1006-14.
5. Seelaar H, Rohrer JD, Pijnenburg YA, et al. Clinical, genetic and pathological heterogeneity of frontotemporal dementia: a review. J Neurol Neurosurg Psychiatry. 2011;82(5):476-86.
6. Ljubenkov PA, Boxer AL. FTLD Treatment: Current Practice and Future Possibilities. Adv Exp Med Biol. 2021;1281:297-310.

Chapter 1.2

Fluid biomarkers of fronto-temporal lobar degeneration

Emma L. van der Ende and John C. van Swieten

Frontotemporal Dementias. Advances in Experimental Medicine and Biology. Vol. 1281. Cham: Springer; 2021; p.123-139.

Abstract

A timely diagnosis of FTD is frequently challenging due to the heterogeneous symptomatology and poor phenotype-pathological correlation. Fluid biomarkers that reflect FTD pathophysiology could be instrumental in both clinical practice and pharmaceutical trials. In recent years, important progress has been made in developing biomarkers of neurodegenerative diseases: amyloid-β and tau in cerebrospinal fluid (CSF) can be used to exclude Alzheimer's disease, while neurofilament light chain (NfL) is emerging as a promising, albeit non-specific, marker of neurodegeneration in both CSF and blood. Gene-specific biomarkers such as PGRN in *GRN* mutation carriers and dipeptide repeat proteins in *C9orf72* mutation carriers, are potential target engagement markers in genetic FTD trials. Novel techniques capable of measuring very low concentrations of brain-derived proteins in peripheral fluids are facilitating studies of blood biomarkers as a minimally invasive alternative to CSF. A major remaining challenge is the identification of a biomarker that can be used to predict the neuropathological substrate in sporadic FTD patients.

Introduction

The improved understanding of FTD coupled with the emergence of clinical trials has generated much interest in identifying fluid biomarkers that reflect FTD pathophysiology. Generally speaking, a biomarker is a measurable indicator of a normal biological or pathological process. There are currently no FTD-specific fluid biomarkers routinely used in clinical practice.

Diagnosing FTD on clinical grounds alone is frequently challenging, especially in early stages of the disease. A correct and timely diagnosis is needed for appropriate management and support and to exclude treatable causes. At the same time, disease-modifying drugs may be most effective if administered at an early stage, i.e. when neuronal damage is minimal.[1] A biomarker that can identify early disease stages could therefore not only improve clinical management, but also have a key position in participant selection for clinical trials. In light of the relative difficulty of quantifying short-term changes in cognitive functioning or atrophy rates, such biomarkers might also be useful as surrogate markers of treatment effect.

Pathologically, FTD is characterised by frontotemporal lobar degeneration (FTLD) with intracellular inclusions which are most commonly composed of the microtubule-associated protein tau (FTLD-tau) or TAR-DNA binding protein-43 (TDP-43; FTLD-TDP). Less common forms include FTLD-FUS (inclusions composed of FUS protein) and FTLD-UPS (ubiquitin-positive inclusions without immunoreactivity for TDP-43 or FUS).[1,2] While the underlying neuropathology is known in genetic forms of FTD, with *MAPT* mutations leading to FTLD-tau and *GRN*- and *C9orf72*-mutations leading to FTLD-TDP, it is not easily predicted in sporadic FTD based on clinical presentation alone.[1] Fluid biomarkers that can help to identify the pathological substrate will be critical to select patients for etiology-directed therapeutic trials.

This chapter explores the current state of fluid biomarkers in sporadic and genetic FTD and discusses challenges in novel fluid biomarker development.

Fluid biomarker sources

Cerebrospinal fluid

Cerebrospinal fluid (CSF) has gathered the most interest as a source of fluid biomarkers in neurodegenerative diseases. Its proximity to the brain and direct connection with the brain interstitial fluid means that it is most likely to contain brain-derived proteins related to neurological disease. CSF can be obtained through a lumbar puncture, a safe procedure with post-lumbar puncture headache being the most significant complication, occurring in

approximately 10% of patients.[3] However, lumbar puncture is invasive and inconvenient for monitoring disease progression, and variability in the methods used to collect and store CSF can considerably affect the measurement of certain analytes.[4]

Blood

Blood is an attractive alternative to CSF as its collection is minimally invasive and therefore more suitable for repeated collection and disease monitoring. A small fraction of brain proteins that cross the blood-brain barrier can be detected in very low concentrations in the blood.[5] Recent technical developments in the field of ultrasensitive assays and mass spectrometry have greatly improved detection of these brain-derived proteins.[6] Blood biomarker development poses several challenges, including the possibility that the measured analyte is derived from peripheral tissues instead of the brain, interference with immunoassay platforms by resident blood proteins (albumin, immunoglobulins), and potential degradation or masking of pathological markers through protease or protein carrier activity.[5,7]

Other biomarker sources

There is a growing interest in biomarkers in other non-invasively obtained biofluids, including saliva and urine. Several studies have shown that β-amyloid peptides and multiple tau species are detectable in saliva, although results in patients with neurodegenerative diseases are conflicting and require replication.[5,8] While promising, these biomarkers require considerable work to determine their clinical utility and are not discussed further here.

Amyloid-β and tau

Background

The CSF biomarkers amyloid-β_{42} ($A\beta_{42}$), phosphorylated tau_{181} (p-tau_{181}) and total tau (t-tau) are increasingly being used in clinical practice to detect Alzheimer's disease (AD) and are thought to directly reflect hallmark pathological changes of AD, namely cortical amyloid plaques, neurofibrillary tangles and neuronal loss.[9] Amyloid plaques are extracellular aggregates of Aβ peptides which are formed after sequential cleavage of amyloid precursor protein (APP). While most Aβ peptides are 40 amino-acids in length ($A\beta_{40}$), the larger $A\beta_{42}$ is considered more toxic due to its greater tendency to aggregate and misfold.[10, 11] Neurofibrillary tangles are cytoplasmic aggregates of hyperphosphorylated tau protein and are thought to be neurotoxic.[9]

Patients with AD typically have reduced CSF levels of $A\beta_{42}$, due to cortical amyloid deposition, coupled with increased p-tau_{181} due to tangle formation, and increased total tau which is attributed to neuronal loss.[12-16] Together, these findings constitute the so-called AD CSF

profile, which provides good diagnostic accuracy to identify patients with AD,[17] and has recently been incorporated into research diagnostic criteria.[12] Levels of these CSF biomarkers have been shown to correlate with pathological load on post-mortem examination.[13,15,16,18] Of note, these biomarkers can already detect AD pathology in preclinical and prodromal disease stages, and can be used to predict incipient AD in patients with mild cognitive impairment.[17,19]

CSF amyloid-β and tau in FTD diagnosis

In FTD, $A\beta_{42}$ and p-tau_{181} are typically normal and t-tau levels may be normal or elevated, likely due to a release of tau protein following neuronal loss.[20-22] Thus, in the diagnostic work-up of FTD, these biomarkers are useful to exclude underlying AD, but cannot confirm or rule out FTD pathology. An elevated ratio of p-tau_{181}:$A\beta_{42}$ or t-tau:$A\beta_{42}$ provides an especially accurate differentiation of FTD from AD (sensitivity 87-89%, specificity 79-80%).[23] This may be particularly relevant in patients with inconclusive clinical presentations, such as prominent behavioural symptoms, which could be ascribed to behavioural variant FTD or frontal variant AD, or primary progressive aphasia, which can be a feature of either FTD or AD.[24] Correctly identifying patients with underlying AD has become increasingly important with the advent of cholinesterase inhibitors and memantine, which are effective in reducing symptoms in AD but not in FTD and may even worsen FTD symptoms.[25,26]

Remarkably, lower levels of the secreted form of APP (sAPPβ) have been reported in FTD patients compared to both AD patients and cognitively healthy subjects,[27-29] suggesting that APP-derived peptides may be involved in FTD through amyloid-independent mechanisms.

Potential pitfalls of CSF amyloid-β and tau

Importantly, post-mortem studies have revealed that FTD patients frequently have some degree of concomitant AD pathology.[30] Especially in patients over the age of 75 years, some degree of AD pathology is common, and up to 30% of cognitively healthy elderly subjects have an AD CSF profile.[31,32] Therefore, in patients with an AD CSF profile whom are clinically suspected of having FTD, the possibility of AD and FTD co-pathology should be considered.

Furthermore, between-individual variation in overall Aβ production or secretion may cause $A\beta_{42}$ to fall within the normal range despite underlying amyloid pathology; the use of $A\beta_{42/40}$ ratios is thought to provide a more reliable measure of amyloid pathology.[33]

CSF Aβ and tau measurements are sensitive to variations in (pre)analytical conditions. Recommendations for optimal CSF collection include the use of polypropylene collection tubes since $A\beta_{42}$ and other proteins adhere to polystyrene tubes, significantly reducing measured concentrations; similarly, use of lumbar catheters or manometers should be avoided.[4] Variability also exists between and within commercially available ELISA-based assays, calibration peptides and platforms, meaning that interlaboratory and interassay consistency is poor,[34] and direct comparisons between laboratories and across techniques are not reliable.[18] International efforts are underway to harmonise protocols and assays within and between laboratories.[35]

CSF tau to differentiate between pathological subtypes of FTD

Two previous studies did not find a difference in CSF p-tau_{181} between FTD patients with or without underlying tau pathology,[36,37] although one study did reveal an association between the severity of tau pathology and CSF p-tau_{181} levels in FTD patients.[38] The ratio of p-tau_{181} to t-tau is lower in patients with TDP-43 pathology than in those with tau pathology,[1,39-42] although this finding may be driven by the presence of concomitant amyotrophic lateral sclerosis (ALS) (leading to more pronounced neuronal loss and thus higher t-tau levels) in some patients with TDP-43 pathology. Novel tau fragments to distinguish FTD with tau pathology from FTD with TDP-43 pathology have thus far yielded insufficient diagnostic accuracy.[18,43]

Blood amyloid-β and tau

There is a growing interest in the measurement of Aβ and tau species in blood as an alternative to CSF. Although previous results were conflicting, recent studies using ultrasensitive analytical assays have demonstrated decreased levels of blood $A\beta_{42}$ in patients with AD. Blood and CSF $A\beta_{42}$ levels are correlated and blood $A\beta_{42}$ appears to reflect AD-associated pathology with fair diagnostic accuracy.[44,45] Similarly, plasma tau levels are increased in AD patients compared to controls, although not as clearly as in CSF, hampering its diagnostic use.[44,45] These results are promising and warrant further research in larger cohorts.

Neurofilament proteins

Neurofilament proteins (Nfs) are rapidly emerging as the most promising fluid biomarkers for FTD.[46] The discovery that elevation of neurofilament light chain (NfL), which is thought to reflect neuroaxonal damage, can be measured reliably both in CSF and blood has created much interest in NfL as an easily-accessible biomarker across a spectrum of neurological diseases.[47,48]

Background

Nfs are cilindrical heteropolymers located exclusively in the neuronal cytoplasm and are the dominant protein of the axonal cytoskeleton. Nfs consist of three subunits, classified according to molecular weight: neurofilament light chain (NfL), medium chain (NfM) and heavy chain (NfH), of which NfL is the most abundant. Nfs are thought to be critical for stability and radial growth of axons, thereby modulating nerve conduction velocity.[49] Under normal circumstances, Nfs are stable within axons and have a low turnover rate. Upon damage to the axon, Nf molecules are released into the extracellular space, where they traffic to the CSF and, after passing through the blood-brain barrier, enter the bloodstream.[49,50]) The release of Nfs occurs irrespective of the etiology of the neuroaxonal injury; therefore, elevated levels are seen in CSF and blood in patients with various neurological disorders, including dementias, stroke, traumatic brain injury, multiple sclerosis, and Parkinson's disease.[47,48] Due to its relative abundance and solubility, NfL can be more readily quantified in biofluids than NfH and NfM.[49] Blood and CSF NfL levels are highly correlated,[51-53] and advances in ultrasensitive assays (single molecule array, Simoa) have greatly improved the accuracy of blood NfL measurements.[54]

Neurofilament light chain in FTD

A large number of studies have consistently reported strongly elevated NfL levels in CSF and blood of FTD patients, with diagnostic accuracy over 90% to distinguish FTD patients from healthy individuals.[55,56] These NfL increases occur in all FTD phenotypes,[28,57-63] with especially high levels in patients with concomitant ALS.[52,60,64,65] Although higher levels have been reported in patients with confirmed TDP-43 pathology compared to those with tau-pathology, this difference may be driven by patients with concomitant ALS in the TDP-43 group.[41,58,65,66]

NfL levels are significantly higher in FTD than in other frequent causes of dementia, including AD, vascular dementia and dementia with Lewy bodies.[55,62,64,67,68] The pronounced NfL elevations seen in FTD may be related to the anatomical location of neurodegeneration, or due to a higher rate of neuronal death, since especially high NfL levels are also seen in the rapidly progressive Creutzfeldt-Jakob disease.[66,69] However, considerable overlap in NfL levels exists between dementias, and the discriminatory power of NfL on its own to distinguish FTD from disease mimics is only modest.[55] A promising strategy may be to combine NfL with other fluid biomarkers; for instance, the addition of NfL to core AD CSF biomarkers significantly improves the discrimination between AD and FTD compared to AD CSF biomarkers alone.[66,67]

NfL appears be a useful diagnostic biomarker to distinguish FTD from non-neurological disorders, including primary psychiatric disorders, in which NfL levels are typically normal.[70-73] Blood NfL may provide an easily accessible, inexpensive screening tool to identify patients who are likely to have an underlying neurological disease and require further investigation.

Importantly, patients with high NfL levels have more brain atrophy, more functional and cognitive impairment, faster disease progression, and shorter overall survival than patients with low NfL levels,[52,61,62,65,66,68,74,75] demonstrating the value of NfL as a prognostic biomarker. NfL may therefore be a useful tool to inform patients and caregivers about the expected clinical course, and to distinguish patients with clinical hallmarks of FTD who are likely to further decline from those with non-progressing variants (benign or phenocopy FTD syndrome).[76]

Presymptomatic carriers of mutations in *GRN, C9orf72* and *MAPT* typically have low NfL levels,[52,60,65] indicating a low rate of axonal turnover, with sharp increases observed at least 1-2 years prior to symptom onset in one longitudinal study.[65] These increases likely reflect early axonal damage in a prodromal disease stage and suggest that NfL could be a valuable selection tool in clinical trials to identify mutation carriers approaching symptom onset. Another promising application of NfL is as a surrogate marker of treatment effect in clinical trials. In multiple sclerosis, NfL decreases have been observed after treatment with anti-inflammatory drugs,[77] and in AD mouse models, NfL decreased after inhibition of amyloid beta production,[78] suggesting that NfL is a dynamic marker of disease activity. As blood NfL levels are generally stable over the course of FTD,[62,65] a decrease in blood NfL during an FTD trial might reflect a reduced rate of neuroaxonal breakdown in response to the study drug.

CSF and blood NfL levels increase with age among healthy adults, possibly reflecting slow, ongoing axonal turnover as part of physiological ageing.[47,48] This necessitates the development of age-adjusted normal values before NfL can be used in clinical practice. International efforts are underway to harmonise pre-analytical and analytical parameters and to develop universal reference values, which will allow reliable comparison of results from different laboratories.[47]

TDP-43

Background

Aggregation of TDP-43 is a hallmark pathological feature of most tau-negative cases of FTD, as well as almost all cases of ALS.[79-83] Under normal circumstances, TDP-43 is

predominantly localised in the nucleus,[84] where it functions as a transcription factor and regulates important cellular functions such as splicing activity and mRNA stability.[85] In disease, pathological TDP-43 isoforms (phosphorylated and ubiquitinated full-length TDP-43 as well as C-terminal TDP-43 fragments) are redistributed to the cytoplasm, where they form aggregates which are thought to be toxic.[79,82]

Biomarkers of TDP-43 pathology

Underlying TDP-43 pathology can be predicted in patients with a mutation in *GRN* or *C9orf72*, but not in patients with sporadic FTD.[2] Etiology-specific treatment trials will require biomarkers that can detect TDP-43 pathology during the patients' lifetime to select suitable patients. Thus far, efforts to measure disease-specific forms of TDP-43 in biofluids of ALS and FTD patients have yielded inconsistent results.

TDP-43 antibodies used to date have the ability to detect full-length TDP-43 as well as phosphorylated full-length TDP-43 and longer C-terminal fragments, but not the shorter C-terminal fragments which are abundant in brain tissue of ALS and FTD patients.[86] Elevated levels of full-length TDP-43 in CSF of patients with ALS or FTD have been reported,[87-89] albeit with considerable overlap between groups, while another study reported decreased CSF TDP-43 in FTD patients.[42] Phosphorylated TDP-43 in CSF was not different in FTD or ALS compared to controls.[42,90] One small study reported elevated plasma phosphorylated TDP-43 levels in *C9orf72*- or *GRN*-associated FTD;[90] this finding requires replication in a larger cohorts.

Accurate quantification of TDP-43 in CSF or blood is challenging for several reasons. TDP-43 is a ubiquitously expressed protein and is abundant under normal circumstances. The majority of CSF TDP-43 appears to be blood-derived and not brain-derived, although it may be possible to enrich for brain-specific fractions of TDP-43 from exosomes in CSF.[91] Monoclonal antibodies which selectively recognise pathological forms of TDP-43, such as short C-terminal TDP-43 fragments, will therefore be critical.[86] Furthermore, quantification of TDP-43 and especially its phosphorylated form appears limited by very low concentrations or low binding affinity of the antibodies in the presence of abundant immunoglobins or albumin,[92,93] highlighting the need for technical improvements in assays.[83]

Markers of inflammation and astrogliosis

Background

Increasing clinical, genetic and cellular evidence suggests that chronic neuroinflammation plays an important role in FTD. Key observations include microglial and astrocytic activation

in the frontal and temporal cortices both in post-mortem brain tissue and positron-emission tomography (PET), a shared genetic risk between FTD and autoimmune diseases, and a direct link between several FTD-related genes and inflammatory pathways.[94-102] While the exact contribution and timing of neuroinflammation in FTD remains controversial, different disease stages may be characterised by different immune mechanisms, making neuroinflammation an interesting source for potential fluid biomarkers.

Glial markers

Microglia, the resident macrophages of the central nervous system, likely play a central role in neuroinflammation. Resting microglia are involved in homeostasis, and can become activated upon exposure to pathogens or inflammatory stimuli to produce a range of signal molecules, including cytokines, chemokines and complement molecules, which ultimately result in a pro- or an anti-inflammatory CNS microenvironment.[102-105] Similarly, astrocytes are believed to modulate neuroinflammation.[102] The upregulation of microglia and astrocytes in FTD brains has generated interest in biomarkers that can track glial activation in vivo. Candidate glial biomarkers include YKL-40, chitotriosidase-1 (CHIT-1) and glial fibrillar acidic protein (GFAP).

YKL-40, also known as chitinase 3-like 1, is produced primarily by reactive astrocytes but also microglia.[106] CSF YKL-40 is elevated in FTD as well as several other dementias, with especially high levels in aggressive and rapidly progressive dementias.[27,28,107-113] Although YKL-40 is thought to be a non-specific biomarker of glial activation, a positive association has been found with tau deposits, suggesting that YKL-40 upregulation may be particularly sensitive to tau aggregation.[27]

CHIT-1 is an enzyme which is expressed and secreted by activated microglia. A recent study in 72 FTD patients reported elevated CHIT-1 levels compared to controls,[114] although a previous smaller study did not find these elevations.[115] Importantly, CHIT-1 concentration may be reduced in subjects carrying a *CHIT1* polymorphism common in European populations, complicating its use as a biomarker.[115,116]

Glial fibrillar acidic protein (GFAP), a cytoskeletal filament protein in astrocytes, is produced and released by astrocytes during neurodegeneration.[117] High levels of GFAP in blood have been found in several neurodegenerative diseases, with remarkably high levels in FTD,[118,119] suggesting that astrogliosis may be an especially prominent feature of FTD.

The microglial transmembrane receptor TREM2 appears to play a role in microglial homeostatic pathways,[120] and has been investigated as a candidate biomarker for neurodegeneration since genetic variants of *TREM2* are associated with an increased risk of FTD, AD, ALS and PD.[121-126] Its ectodomain can be released into the extracellular space

as a soluble protein (sTREM2), which is measurable in CSF and blood.[127] While small studies reported conflicting results in sTREM2 levels,[128-130] a more recent and larger study observed no differences between FTD patients versus controls except in a small number of *GRN* mutation carriers.[131]

While these glial markers provide further evidence for aberrant microglial and astrocytic activity in FTD, their diagnostic potential is limited as considerable overlap exists with controls. Similarly elevated levels have been reported in several other neurodegenerative diseases, likely reflecting a shared, non-specific glial activation. Furthermore, YKL-40, CHIT-1 and TREM2 are expressed by multiple peripheral cell types, which could affect their measurement.[107,120,132] GFAP, on the other hand, is brain-specific and therefore may be a more interesting candidate.[117]

Cytokine markers

There is extensive, although somewhat conflicting, evidence for altered pro- and anti-inflammatory cytokine profiles in CSF and blood.[102] For instance, increased levels of blood IL-6 were found in *GRN* mutation carriers [133] and sporadic FTD,[134] while another study showed no differences in CSF IL-6 in FTD versus controls.[135] Similarly, TNF-alfa was increased in CSF of patients with sporadic FTD,[136] while another showed a reduction in ten *GRN* mutation carriers.[137] More consistently elevated levels have been found for MCP-1 (monocyte chemoattractant protein 1).[137-139]

These results are mostly derived from small studies and must be interpreted with caution. Peripheral cytokine measurements may be influenced by concurrent infections or other inflammatory conditions outside of the brain. Furthermore, cytokine profiles likely vary depending on the disease stage. Finally, the interpretation of in- or decreased cytokine levels is complex: the original classification of pro-inflammatory and anti-inflammatory cytokines is likely too simplistic, as a given cytokine may behave as either pro- or anti-inflammatory depending on the circumstances [140].

Other candidate biomarkers of neuroinflammation

One study of patients with *GRN*-associated FTD has demonstrated increased CSF levels of the complement proteins C1q and C3b.[141] C1q and C3b are essential components of the classical and alternative complement pathways, which comprise a sequence of protein cleavages and eventually contribute to a pro-inflammatory state. Mouse models showing a potentially important role for complement in synaptic pruning underline the need for replication of complement protein measurements in CSF and blood.[141]

Gene-specific biomarkers

Progranulin in GRN mutation carriers

Background

Progranulin (PGRN) is a ubiquitously expressed growth factor which plays important roles in normal tissue development, cell proliferation and regeneration, and inflammation. In the brain, PGRN is expressed in neurons and microglia and promotes neurite outgrowth, neuronal survival and differentiation, although its exact physiological roles in the nervous system are not fully understood.[142] PGRN also appears to suppress neuroinflammation and modulate neuronal lysosome function, with homozygous mutations in *GRN*, the gene encoding PGRN, leading to the lysosomal storage disease neuronal ceroid lipofuscinosis.[143] PGRN can be cleaved into granulins, which are also biologically active, but often with opposing actions, suggesting that the equilibrium between PGRN and granulins is important for tissue homeostasis.[142]

Progranulin in FTD

Heterozygous mutations in *GRN* are among the most common causes of genetic FTD.[144-146] Most pathogenic *GRN* mutations introduce a premature stop codon that triggers nonsense-mediated decay of *GRN* mRNA, leading to a 50% reduction of PGRN protein levels through haploinsuffiency.[144,145] This reduction in PGRN levels can be detected through immunoassays both in the CSF and blood, enabling accurate recognition of FTD patients due to a *GRN* mutation versus those with sporadic FTD (sensitivity 96%, specificity up to 100%).[147-154] PGRN levels are already decreased in the presymptomatic stage, even in the second or third decade of life, indicating that dysregulated PGRN expression is a very early event during the lifespan of mutation carriers. Blood PGRN levels can therefore also distinguish presymptomatic *GRN* mutation carriers from non-carriers with near perfect sensitivity and specificity.[150,155] Its concentration does not reflect the extent of neurodegeneration and is therefore not useful as a prognostic or disease staging biomarker.[150]

Blood PGRN measurements may be helpful to determine the pathogenicity of novel *GRN* mutations, or to detect mutations not found on standard genetic screening, such as large deletions.[150] Since genetic testing is expensive and time-consuming, blood PGRN determination offers a low-cost, minimally invasive screening tool to identify *GRN* mutation carriers, who should then be subjected to further genetic testing. The ability to screen FTD patients for *GRN* mutations on a large scale is particularly important in light of therapeutic trials aimed at increasing PGRN protein levels.[150]

Since blood PGRN appears to be stable over time,[150,155] PGRN levels can be used to monitor whether a trial drug is effective in increasing PGRN levels. It is important to note that CSF and blood PGRN are only moderately correlated, implying a differential regulation of the two.[155-157] Peripheral PGRN levels may not adequately reflect those in the central nervous system, and the absence of an effect on blood PGRN does not rule out an effect on the brain or PGRN function. Furthermore, the extracellular PGRN levels measured in biofluids might not sufficiently reflect intracellular levels, and it is not clear yet where the loss of PGRN has its main effect.[142]

Much variability in PGRN levels exists within individuals, and various genetic and environmental regulators influence PGRN levels. For example, PGRN levels are elevated in inflammation and other clinical conditions including cancer and pregnancy,[158,159] and certain single nucleotide polymorphisms (SNPs) are associated with increased or decreased PGRN levels, including rs5848 (*GRN*), rs646776 (*SORT1*) and rs1990622 (*TMEM106B*).[155,156,160-162] Further research is needed to elucidate other factors that may confound PGRN measurements.Given the distinct biological properties of granulin peptides, developing antibodies against granulins to study ratios of PGRN to granulins as potential biomarkers could be insightful.[142,149]

Dipeptide repeat proteins in C9orf72 mutation carriers

Background

The *C9orf72* repeat expansion is the most frequent genetic cause of FTD and ALS.[163-168] While the exact mechanism by which *C9orf72* repeat expansions lead to neurodegeneration is unknown, it has been proposed that toxic dipeptide repeat proteins (DPRs) could play a role.[169] The expanded *C9orf72* repeats are bidirectionally transcribed into repetitive RNA, which forms sense and antisense RNA foci. These RNAs can be translated in every reading frame through repeat-associated non-ATG initiated translation (RAN translation), generating five DPRs, in order of abundance: poly(GA), poly(GP), poly(GR), poly(PA) and poly(PR).[170] DPRs are found abundantly in brains of *C9orf72*-FTD/ALS patients,[170-173] mostly in cytoplasmic neuronal inclusions, although remarkably, DPR burden does not coincide neuropathologically with the degree of neurodegeneration.[174-177] Cell and animal models have shown that poly(GR) and poly(PR), and to a lesser extent poly(GA), are toxic when overexpressed, while poly(PA) and poly(GP) are unlikely to be toxic.[169]

Dipeptide repeat proteins in CSF

Poly(GP) can be quantitatively detected by ELISAs in CSF,[178] revealing high levels in patients with ALS or FTD due to *C9orf72* repeat expansions. In sporadic cases, on the other hand, poly(GP) levels were generally very low or undetectable,[178,179] although one study

reported high poly(GP) levels in a small number of patients without the repeat expansion.[180] One possible explanation could be somatic mosaicism, where a pathological repeat is present in the central nervous system but not in peripheral blood, preventing detection of *C9orf72* repeat expansions in peripheral blood. It has been shown in mice that CSF poly(GP) levels correlate with DPR protein pathology, repeat RNA levels and RNA foci burden.[179]

CSF poly(GP) elevations are already observed in presymptomatic *C9orf72* mutation carriers,[180-182] suggesting that DPR protein production emerges prior to neurodegeneration. This is in agreement with the neuropathological detection of DPRs in young presymptomatic *C9orf72* cases.[183-185] CSF poly-GP levels do not correlate with severity of neurodegeneration, disease progression or other clinical characteristics such as age of disease onset,[179-182] limiting the value of poly(GP) as a disease staging or prognostic biomarker.

Since the RNA transcripts of expanded *C9orf72* repeats are believed to play a key role in *C9orf72* pathogenesis, interventions targeting transcription and translation of the repeat expansion are a promising therapeutic strategy. Poly(GP) levels appear to be stable over time,[179] and therefore measurement of poly(GP) before and during treatment presents a feasible approach to measure target engagement. Antisense oligonucleotides (ASOs) targeting repeat RNAs have been shown in mice to reduce CSF poly(GP) levels.[179]

Importantly, poly(GP) can be detected in peripheral blood mononuclear cells (PBMCs); further research is needed to determine its potential as a blood-based biomarker.[179]

Most research to date has focused on measuring poly(GP) in CSF due to its high abundance and solubility, making it the most likely DPR to be accurately measured.[169] Measurements of poly(GA) and poly(GR), which show evidence of toxicity, might uncover associations with clinical features not observed for poly(GP). To date, efforts to measure poly(GA) and poly(GR) in CSF have been unsuccessful, possibly because the currently used assays are not sensitive enough to detect very low concentrations of these DPRs.[186]

Concluding remarks and future directions

Recent years have seen great advances in identifying both general biomarkers of neurodegeneration, such as NfL, as well as gene-specific biomarkers, including PGRN and DPR proteins. There remains an unmet need for biomarkers that specifically reflect FTD pathophysiology and, especially with the advent of clinical trials, biomarkers that can predict the underlying neuropathological substrate in sporadic FTD.

The heterogeneity of FTD complicates biomarker development, and the use of a clinical diagnosis as a reference standard is a potential source of heterogeneity given the high false positive rate of FTD clinical diagnosis.[30] Although novel biomarkers would ideally be validated in post-mortem studies, studying genetic forms of FTD, which enable accurate prediction of the underlying pathological substrate during life, provide a valuable alternative. A combination of analytes that reflect different biological processes is likely to yield more information than single biomarkers alone. Longitudinal studies are needed to determine at what stage during the disease various biomarkers start to become abnormal.

The use of proteomics is a promising strategy to detect differentially regulated proteins in biofluids, although in-depth validation of mass spectrometry results is needed to overcome differences in technical parameters.[187] Candidate proteins that have been identified in multiple independent CSF proteomics studies are likely the most promising and include synaptic proteins, such as neuronal pentraxins and VGF, as well as numerous inflammation-related proteins.[187-193]

A crucial step before a biomarker can be implemented in clinical practice is multicentre standardisation and harmonisation of pre-analytical and assay characteristics, as is currently being done for core AD biomarkers.[35] Developing normal reference values and cut-points is essential and needs to take into account age-related changes in biomarker levels, such as is the case for NfL and several inflammation-related biomarkers.[102] Many of the biomarkers discussed in this chapter are not FTD-specific (e.g. NfL) or brain-specific (e.g. markers of neuroinflammation, TDP-43), and a thorough understanding of potential confounding factors is needed before these biomarkers can be relied upon in a clinical setting.

References

1. Meeter LH, Kaat LD, Rohrer JD, van Swieten JC. Imaging and fluid biomarkers in frontotemporal dementia. Nat Rev Neurol. 2017;13:406-19.
2. Lashley T, Rohrer JD, Mead S, Revesz T. Review: an update on clinical, genetic and pathological aspects of frontotemporal lobar degenerations. Neuropathol Appl Neurobiol. 2015;41:858-81.
3. Duits FH, Martinez-Lage P, Paquet C, Engelborghs S, Lleo A, Hausner L, et al. Performance and complications of lumbar puncture in memory clinics: Results of the multicenter lumbar puncture feasibility study. Alzheimers Dement. 2016;12:154-63.
4. Ahmed RM, Paterson RW, Warren JD, Zetterberg H, O'Brien JT, Fox NC, et al. Biomarkers in dementia: clinical utility and new directions. J Neurol Neurosurg Psychiatry. 2014;85:1426-34.
5. Sancesario G, Bernardini S. AD biomarker discovery in CSF and in alternative matrices. Clin Biochem. 2019;72:52-7.
6. Duffy D. Short Keynote Paper: Single molecule detection of protein biomarkers to define the continuum from health to disease. IEEE J Biomed Health Inform. 2020.
7. Hampel H, O'Bryant SE, Molinuevo JL, Zetterberg H, Masters CL, Lista S, et al. Blood-based biomarkers for Alzheimer disease: mapping the road to the clinic. Nat Rev Neurol. 2018;14:639-52.
8. Ashton NJ, Ide M, Zetterberg H, Blennow K. Salivary Biomarkers for Alzheimer's Disease and Related Disorders. Neurol Ther. 2019;8:83-94.
9. Blennow K, de Leon MJ, Zetterberg H. Alzheimer's disease. Lancet. 2006;368:387-403.
10. McGowan E, Pickford F, Kim J, Onstead L, Eriksen J, Yu C, et al. Abeta42 is essential for parenchymal and vascular amyloid deposition in mice. Neuron. 2005;47:191-9.
11. Portelius E, Westman-Brinkmalm A, Zetterberg H, Blennow K. Determination of beta-amyloid peptide signatures in cerebrospinal fluid using immunoprecipitation-mass spectrometry. J Proteome Res. 2006;5:1010-6.
12. Jack CR, Jr., Bennett DA, Blennow K, Carrillo MC, Dunn B, Haeberlein SB, et al. NIA-AA Research Framework: Toward a biological definition of Alzheimer's disease. Alzheimers Dement. 2018;14:535-62.
13. Buerger K, Ewers M, Pirttila T, Zinkowski R, Alafuzoff I, Teipel SJ, et al. CSF phosphorylated tau protein correlates with neocortical neurofibrillary pathology in Alzheimer's disease. Brain. 2006;129:3035-41.
14. de Souza LC, Chupin M, Lamari F, Jardel C, Leclercq D, Colliot O, et al. CSF tau markers are correlated with hippocampal volume in Alzheimer's disease. Neurobiol Aging. 2012;33:1253-7.
15. Seppala TT, Nerg O, Koivisto AM, Rummukainen J, Puli L, Zetterberg H, et al. CSF biomarkers for Alzheimer disease correlate with cortical brain biopsy findings. Neurology. 2012;78:1568-75.
16. Tapiola T, Alafuzoff I, Herukka SK, Parkkinen L, Hartikainen P, Soininen H, et al. Cerebrospinal fluid {beta}-amyloid 42 and tau proteins as biomarkers of Alzheimer-type pathologic changes in the brain. Arch Neurol. 2009;66:382-9.
17. Olsson B, Lautner R, Andreasson U, Ohrfelt A, Portelius E, Bjerke M, et al. CSF and blood biomarkers for the diagnosis of Alzheimer's disease: a systematic review and meta-analysis. Lancet Neurol. 2016;15:673-84.
18. Bjerke M, Engelborghs S. Cerebrospinal Fluid Biomarkers for Early and Differential Alzheimer's Disease Diagnosis. *J Alzheimers Dis*. 2018;62:1199-209.

19. Mattsson N, Zetterberg H, Hansson O, Andreasen N, Parnetti L, Jonsson M, et al. CSF biomarkers and incipient Alzheimer disease in patients with mild cognitive impairment. Jama. 2009;302:385-93.
20. Riemenschneider M, Wagenpfeil S, Diehl J, Lautenschlager N, Theml T, Heldmann B, et al. Tau and Abeta42 protein in CSF of patients with frontotemporal degeneration. Neurology. 2002;58:1622-8.
21. Schoonenboom NS, Reesink FE, Verwey NA, Kester MI, Teunissen CE, van de Ven PM, et al. Cerebrospinal fluid markers for differential dementia diagnosis in a large memory clinic cohort. Neurology. 2012;78:47-54.
22. van Harten AC, Kester MI, Visser PJ, Blankenstein MA, Pijnenburg YA, van der Flier WM, et al. Tau and p-tau as CSF biomarkers in dementia: a meta-analysis. Clin Chem Lab Med. 2011;49:353-66.
23. Rivero-Santana A, Ferreira D, Perestelo-Perez L, Westman E, Wahlund LO, Sarria A, et al. Cerebrospinal Fluid Biomarkers for the Differential Diagnosis between Alzheimer's Disease and Frontotemporal Lobar Degeneration: Systematic Review, HSROC Analysis, and Confounding Factors. J Alzheimers Dis. 2017;55:625-44.
24. Marshall CR, Hardy CJD, Volkmer A, Russell LL, Bond RL, Fletcher PD, et al. Primary progressive aphasia: a clinical approach. J Neurol. 2018;265:1474-90.
25. McShane R, Westby MJ, Roberts E, Minakaran N, Schneider L, Farrimond LE, et al. Memantine for dementia. Cochrane Database Syst Rev. 2019;3:CD003154.
26. Noufi P, Khoury R, Jeyakumar S, Grossberg GT. Use of Cholinesterase Inhibitors in Non-Alzheimer's Dementias. Drugs Aging. 2019;36:719-31.
27. Alcolea D, Irwin DJ, Illan-Gala I, Munoz L, Clarimon J, McMillan CT, et al. Elevated YKL-40 and low sAPPbeta:YKL-40 ratio in antemortem cerebrospinal fluid of patients with pathologically confirmed FTLD. J Neurol Neurosurg Psychiatry. 2019;90:180-6.
28. Alcolea D, Vilaplana E, Suarez-Calvet M, Illan-Gala I, Blesa R, Clarimon J, et al. CSF sAPPbeta, YKL-40, and neurofilament light in frontotemporal lobar degeneration. Neurology. 2017;89:178-88.
29. Illan-Gala I, Pegueroles J, Montal V, Alcolea D, Vilaplana E, Bejanin A, et al. APP-derived peptides reflect neurodegeneration in frontotemporal dementia. Ann Clin Transl Neurol. 2019;6:2518-30.
30. Irwin DJ, Trojanowski JQ, Grossman M. Cerebrospinal fluid biomarkers for differentiation of frontotemporal lobar degeneration from Alzheimer's disease. Front Aging Neurosci. 2013;5:6.
31. Bouwman FH, Schoonenboom NS, Verwey NA, van Elk EJ, Kok A, Blankenstein MA, et al. CSF biomarker levels in early and late onset Alzheimer's disease. Neurobiol Aging. 2009;30:1895-901.
32. Mattsson N, Rosen E, Hansson O, Andreasen N, Parnetti L, Jonsson M, et al. Age and diagnostic performance of Alzheimer disease CSF biomarkers. Neurology. 2012;78:468-76.
33. Pouclet-Courtemanche H, Nguyen TB, Skrobala E, Boutoleau-Bretonniere C, Pasquier F, Bouaziz-Amar E, et al. Frontotemporal dementia is the leading cause of "true" A-/T+ profiles defined with Abeta42/40 ratio. Alzheimers Dement (Amst). 2019;11:161-9.
34. Verwey NA, van der Flier WM, Blennow K, Clark C, Sokolow S, De Deyn PP, et al. A worldwide multicentre comparison of assays for cerebrospinal fluid biomarkers in Alzheimer's disease. Ann Clin Biochem. 2009;46:235-40.
35. Reijs BL, Teunissen CE, Goncharenko N, Betsou F, Blennow K, Baldeiras I, et al. The Central Biobank and Virtual Biobank of BIOMARKAPD: A Resource for Studies on Neurodegenerative Diseases. Front Neurol. 2015;6:216.

36. Bian H, Van Swieten JC, Leight S, Massimo L, Wood E, Forman M, et al. CSF biomarkers in frontotemporal lobar degeneration with known pathology. Neurology. 2008;70:1827-35.
37. Rosso SM, van Herpen E, Pijnenburg YA, Schoonenboom NS, Scheltens P, Heutink P, et al. Total tau and phosphorylated tau 181 levels in the cerebrospinal fluid of patients with frontotemporal dementia due to P301L and G272V tau mutations. Arch Neurol. 2003;60:1209-13.
38. Irwin DJ, Lleo A, Xie SX, McMillan CT, Wolk DA, Lee EB, et al. Ante mortem cerebrospinal fluid tau levels correlate with postmortem tau pathology in frontotemporal lobar degeneration. Ann Neurol. 2017;82:247-58.
39. Hu WT, Watts K, Grossman M, Glass J, Lah JJ, Hales C, et al. Reduced CSF p-Tau181 to Tau ratio is a biomarker for FTLD-TDP. Neurology. 2013;81:1945-52.
40. Borroni B, Benussi A, Archetti S, Galimberti D, Parnetti L, Nacmias B, et al. Csf p-tau181/tau ratio as biomarker for TDP pathology in frontotemporal dementia. Amyotroph Lateral Scler Frontotemporal Degener. 2015;16:86-91.
41. Pijnenburg YA, Verwey NA, van der Flier WM, Scheltens P, Teunissen CE. Discriminative and prognostic potential of cerebrospinal fluid phosphoTau/tau ratio and neurofilaments for frontotemporal dementia subtypes. Alzheimers Dement (Amst). 2015;1:505-12.
42. Kuiperij HB, Versleijen AA, Beenes M, Verwey NA, Benussi L, Paterlini A, et al. Tau Rather than TDP-43 Proteins are Potential Cerebrospinal Fluid Biomarkers for Frontotemporal Lobar Degeneration Subtypes: A Pilot Study. J Alzheimers Dis. 2017;55:585-95.
43. Foiani MS, Cicognola C, Ermann N, Woollacott IOC, Heller C, Heslegrave AJ, et al. Searching for novel cerebrospinal fluid biomarkers of tau pathology in frontotemporal dementia: an elusive quest. J Neurol Neurosurg Psychiatry. 2019;90:740-6.
44. Molinuevo JL, Ayton S, Batrla R, Bednar MM, Bittner T, Cummings J, et al. Current state of Alzheimer's fluid biomarkers. Acta Neuropathol. 2018;136:821-53.
45. Zetterberg H, Burnham SC. Blood-based molecular biomarkers for Alzheimer's disease. Mol Brain. 2019;12:26.
46. Zetterberg H, van Swieten JC, Boxer AL, Rohrer JD. Review: Fluid biomarkers for frontotemporal dementias. Neuropathol Appl Neurobiol. 2019;45:81-7.
47. Gaetani L, Blennow K, Calabresi P, Di Filippo M, Parnetti L, Zetterberg H. Neurofilament light chain as a biomarker in neurological disorders. J Neurol Neurosurg Psychiatry. 2019;90:870-81.
48. Khalil M, Teunissen CE, Otto M, Piehl F, Sormani MP, Gattringer T, et al. Neurofilaments as biomarkers in neurological disorders. Nat Rev Neurol. 2018;14:577-89.
49. Petzold A. Neurofilament phosphoforms: surrogate markers for axonal injury, degeneration and loss. J Neurol Sci. 2005;233:183-98.
50. Rosengren LE, Karlsson JE, Sjogren M, Blennow K, Wallin A. Neurofilament protein levels in CSF are increased in dementia. Neurology. 1999;52:1090-3.
51. Gisslen M, Price RW, Andreasson U, Norgren N, Nilsson S, Hagberg L, et al. Plasma Concentration of the Neurofilament Light Protein (NFL) is a Biomarker of CNS Injury in HIV Infection: A Cross-Sectional Study. EBioMedicine. 2016;3:135-40.
52. Meeter LH, Dopper EG, Jiskoot LC, Sanchez-Valle R, Graff C, Benussi L, et al. Neurofilament light chain: a biomarker for genetic frontotemporal dementia. Ann Clin Transl Neurol. 2016;3:623-36.
53. Wilke C, Preische O, Deuschle C, Roeben B, Apel A, Barro C, et al. Neurofilament light chain in FTD is elevated not only in cerebrospinal fluid, but also in serum. J Neurol Neurosurg Psychiatry. 2016;87:1270-2.
54. Kuhle J, Barro C, Andreasson U, Derfuss T, Lindberg R, Sandelius A, et al. Comparison of three analytical platforms for quantification of the neurofilament light chain in blood samples:

ELISA, electrochemiluminescence immunoassay and Simoa. Clin Chem Lab Med. 2016;54:1655-61.
55. Forgrave LM, Ma M, Best JR, DeMarco ML. The diagnostic performance of neurofilament light chain in CSF and blood for Alzheimer's disease, frontotemporal dementia, and amyotrophic lateral sclerosis: A systematic review and meta-analysis. Alzheimers Dement (Amst). 2019;11:730-43.
56. Zhao Y, Xin Y, Meng S, He Z, Hu W. Neurofilament light chain protein in neurodegenerative dementia: A systematic review and network meta-analysis. Neurosci Biobehav Rev. 2019;102:123-38.
57. Paterson RW, Slattery CF, Poole T, Nicholas JM, Magdalinou NK, Toombs J, et al. Cerebrospinal fluid in the differential diagnosis of Alzheimer's disease: clinical utility of an extended panel of biomarkers in a specialist cognitive clinic. Alzheimers Res Ther. 2018;10:32.
58. Landqvist Waldo M, Frizell Santillo A, Passant U, Zetterberg H, Rosengren L, Nilsson C, et al. Cerebrospinal fluid neurofilament light chain protein levels in subtypes of frontotemporal dementia. BMC Neurol. 2013;13:54.
59. Ljubenkov PA, Staffaroni AM, Rojas JC, Allen IE, Wang P, Heuer H, et al. Cerebrospinal fluid biomarkers predict frontotemporal dementia trajectory. Ann Clin Transl Neurol. 2018;5:1250-63.
60. Rohrer JD, Woollacott IO, Dick KM, Brotherhood E, Gordon E, Fellows A, et al. Serum neurofilament light chain protein is a measure of disease intensity in frontotemporal dementia. Neurology. 2016;87:1329-36.
61. Scherling CS, Hall T, Berisha F, Klepac K, Karydas A, Coppola G, et al. Cerebrospinal fluid neurofilament concentration reflects disease severity in frontotemporal degeneration. Ann Neurol. 2014;75:116-26.
62. Steinacker P, Anderl-Straub S, Diehl-Schmid J, Semler E, Uttner I, von Arnim CAF, et al. Serum neurofilament light chain in behavioral variant frontotemporal dementia. Neurology. 2018;91:e1390-e401.
63. Steinacker P, Semler E, Anderl-Straub S, Diehl-Schmid J, Schroeter ML, Uttner I, et al. Neurofilament as a blood marker for diagnosis and monitoring of primary progressive aphasias. Neurology. 2017;88:961-9.
64. Bridel C, van Wieringen WN, Zetterberg H, Tijms BM, Teunissen CE, and the NFLG, et al. Diagnostic Value of Cerebrospinal Fluid Neurofilament Light Protein in Neurology: A Systematic Review and Meta-analysis. JAMA Neurol. 2019.
65. van der Ende EL, Meeter LH, Poos JM, Panman JL, Jiskoot LC, Dopper EGP, et al. Serum neurofilament light chain in genetic frontotemporal dementia: a longitudinal, multicentre cohort study. Lancet Neurol. 2019;18:1103-11.
66. Abu-Rumeileh S, Mometto N, Bartoletti-Stella A, Polischi B, Oppi F, Poda R, et al. Cerebrospinal Fluid Biomarkers in Patients with Frontotemporal Dementia Spectrum: A Single-Center Study. J Alzheimers Dis. 2018;66:551-63.
67. de Jong D, Jansen RW, Pijnenburg YA, van Geel WJ, Borm GF, Kremer HP, et al. CSF neurofilament proteins in the differential diagnosis of dementia. J Neurol Neurosurg Psychiatry. 2007;78:936-8.
68. Skillback T, Farahmand B, Bartlett JW, Rosen C, Mattsson N, Nagga K, et al. CSF neurofilament light differs in neurodegenerative diseases and predicts severity and survival. Neurology. 2014;83:1945-53.
69. Zerr I, Schmitz M, Karch A, Villar-Pique A, Kanata E, Golanska E, et al. Cerebrospinal fluid neurofilament light levels in neurodegenerative dementia: Evaluation of diagnostic accuracy in the differential diagnosis of prion diseases. Alzheimers Dement. 2018;14:751-63.

70. Al Shweiki MR, Steinacker P, Oeckl P, Hengerer B, Danek A, Fassbender K, et al. Neurofilament light chain as a blood biomarker to differentiate psychiatric disorders from behavioural variant frontotemporal dementia. J Psychiatr Res. 2019;113:137-40.
71. Eratne D, Loi SM, Walia N, Farrand S, Li QX, Varghese S, et al. A pilot study of the utility of cerebrospinal fluid neurofilament light chain in differentiating neurodegenerative from psychiatric disorders: A 'C-reactive protein' for psychiatrists and neurologists? Aust N Z J Psychiatry. 2020;54:57-67.
72. Katisko K, Cajanus A, Jaaskelainen O, Kontkanen A, Hartikainen P, Korhonen VE, et al. Serum neurofilament light chain is a discriminative biomarker between frontotemporal lobar degeneration and primary psychiatric disorders. J Neurol. 2020;267:162-7.
73. Vijverberg EG, Dols A, Krudop WA, Del Campo Milan M, Kerssens CJ, Gossink F, et al. Cerebrospinal fluid biomarker examination as a tool to discriminate behavioral variant frontotemporal dementia from primary psychiatric disorders. Alzheimers Dement (Amst). 2017;7:99-106.
74. Steinacker P, Huss A, Mayer B, Grehl T, Grosskreutz J, Borck G, et al. Diagnostic and prognostic significance of neurofilament light chain NF-L, but not progranulin and S100B, in the course of amyotrophic lateral sclerosis: Data from the German MND-net. Amyotroph Lateral Scler Frontotemporal Degener. 2017;18:112-9.
75. Skillback T, Mattsson N, Blennow K, Zetterberg H. Cerebrospinal fluid neurofilament light concentration in motor neuron disease and frontotemporal dementia predicts survival. Amyotroph Lateral Scler Frontotemporal Degener. 2017;18:397-403.
76. Valente ES, Caramelli P, Gambogi LB, Mariano LI, Guimaraes HC, Teixeira AL, et al. Phenocopy syndrome of behavioral variant frontotemporal dementia: a systematic review. Alzheimers Res Ther. 2019;11:30.
77. Varhaug KN, Torkildsen O, Myhr KM, Vedeler CA. Neurofilament Light Chain as a Biomarker in Multiple Sclerosis. Front Neurol. 2019;10:338.
78. Bacioglu M, Maia LF, Preische O, Schelle J, Apel A, Kaeser SA, et al. Neurofilament Light Chain in Blood and CSF as Marker of Disease Progression in Mouse Models and in Neurodegenerative Diseases. Neuron. 2016;91:56-66.
79. Arai T, Hasegawa M, Akiyama H, Ikeda K, Nonaka T, Mori H, et al. TDP-43 is a component of ubiquitin-positive tau-negative inclusions in frontotemporal lobar degeneration and amyotrophic lateral sclerosis. Biochem Biophys Res Commun. 2006;351:602-11.
80. Mackenzie IR, Neumann M. Reappraisal of TDP-43 pathology in FTLD-U subtypes. Acta Neuropathol. 2017;134:79-96.
81. Maekawa S, Leigh PN, King A, Jones E, Steele JC, Bodi I, et al. TDP-43 is consistently co-localized with ubiquitinated inclusions in sporadic and Guam amyotrophic lateral sclerosis but not in familial amyotrophic lateral sclerosis with and without SOD1 mutations. Neuropathology. 2009;29:672-83.
82. Neumann M, Sampathu DM, Kwong LK, Truax AC, Micsenyi MC, Chou TT, et al. Ubiquitinated TDP-43 in frontotemporal lobar degeneration and amyotrophic lateral sclerosis. Science. 2006;314:130-3.
83. Steinacker P, Barschke P, Otto M. Biomarkers for diseases with TDP-43 pathology. Mol Cell Neurosci. 2019;97:43-59.
84. Ayala YM, Zago P, D'Ambrogio A, Xu YF, Petrucelli L, Buratti E, et al. Structural determinants of the cellular localization and shuttling of TDP-43. J Cell Sci. 2008;121:3778-85.
85. Buratti E, Baralle FE. Multiple roles of TDP-43 in gene expression, splicing regulation, and human disease. Front Biosci. 2008;13:867-78.
86. Feneberg E, Gray E, Ansorge O, Talbot K, Turner MR. Towards a TDP-43-Based Biomarker for ALS and FTLD. Mol Neurobiol. 2018;55:7789-801.

87. Junttila A, Kuvaja M, Hartikainen P, Siloaho M, Helisalmi S, Moilanen V, et al. Cerebrospinal Fluid TDP-43 in Frontotemporal Lobar Degeneration and Amyotrophic Lateral Sclerosis Patients with and without the C9ORF72 Hexanucleotide Expansion. Dement Geriatr Cogn Dis Extra. 2016;6:142-9.
88. Kasai T, Tokuda T, Ishigami N, Sasayama H, Foulds P, Mitchell DJ, et al. Increased TDP-43 protein in cerebrospinal fluid of patients with amyotrophic lateral sclerosis. Acta Neuropathol. 2009;117:55-62.
89. Steinacker P, Hendrich C, Sperfeld AD, Jesse S, von Arnim CA, Lehnert S, et al. TDP-43 in cerebrospinal fluid of patients with frontotemporal lobar degeneration and amyotrophic lateral sclerosis. Arch Neurol. 2008;65:1481-7.
90. Suarez-Calvet M, Dols-Icardo O, Llado A, Sanchez-Valle R, Hernandez I, Amer G, et al. Plasma phosphorylated TDP-43 levels are elevated in patients with frontotemporal dementia carrying a C9orf72 repeat expansion or a GRN mutation. J Neurol Neurosurg Psychiatry. 2014;85:684-91.
91. Feneberg E, Steinacker P, Lehnert S, Schneider A, Walther P, Thal DR, et al. Limited role of free TDP-43 as a diagnostic tool in neurodegenerative diseases. Amyotroph Lateral Scler Frontotemporal Degener. 2014;15:351-6.
92. Foulds P, McAuley E, Gibbons L, Davidson Y, Pickering-Brown SM, Neary D, et al. TDP-43 protein in plasma may index TDP-43 brain pathology in Alzheimer's disease and frontotemporal lobar degeneration. Acta Neuropathol. 2008;116:141-6.
93. Verstraete E, Kuiperij HB, van Blitterswijk MM, Veldink JH, Schelhaas HJ, van den Berg LH, et al. TDP-43 plasma levels are higher in amyotrophic lateral sclerosis. Amyotroph Lateral Scler. 2012;13:446-51.
94. Broce I, Karch CM, Wen N, Fan CC, Wang Y, Tan CH, et al. Immune-related genetic enrichment in frontotemporal dementia: An analysis of genome-wide association studies. PLoS Med. 2018;15:e1002487.
95. Ferrari R, Hernandez DG, Nalls MA, Rohrer JD, Ramasamy A, Kwok JB, et al. Frontotemporal dementia and its subtypes: a genome-wide association study. Lancet Neurol. 2014;13:686-99.
96. Miller ZA, Rankin KP, Graff-Radford NR, Takada LT, Sturm VE, Cleveland CM, et al. TDP-43 frontotemporal lobar degeneration and autoimmune disease. J Neurol Neurosurg Psychiatry. 2013;84:956-62.
97. Miller ZA, Sturm VE, Camsari GB, Karydas A, Yokoyama JS, Grinberg LT, et al. Increased prevalence of autoimmune disease within C9 and FTD/MND cohorts: Completing the picture. Neurol Neuroimmunol Neuroinflamm. 2016;3:e301.
98. Arnold SE, Han LY, Clark CM, Grossman M, Trojanowski JQ. Quantitative neurohistological features of frontotemporal degeneration. Neurobiol Aging. 2000;21:913-9.
99. Bellucci A, Bugiani O, Ghetti B, Spillantini MG. Presence of reactive microglia and neuroinflammatory mediators in a case of frontotemporal dementia with P301S mutation. Neurodegener Dis. 2011;8:221-9.
100. Cagnin A, Rossor M, Sampson EL, Mackinnon T, Banati RB. In vivo detection of microglial activation in frontotemporal dementia. Ann Neurol. 2004;56:894-7.
101. Lant SB, Robinson AC, Thompson JC, Rollinson S, Pickering-Brown S, Snowden JS, et al. Patterns of microglial cell activation in frontotemporal lobar degeneration. Neuropathol Appl Neurobiol. 2014;40:686-96.
102. Bright F, Werry EL, Dobson-Stone C, Piguet O, Ittner LM, Halliday GM, et al. Neuroinflammation in frontotemporal dementia. Nat Rev Neurol. 2019;15:540-55.

103. Bohlen CJ, Bennett FC, Tucker AF, Collins HY, Mulinyawe SB, Barres BA. Diverse Requirements for Microglial Survival, Specification, and Function Revealed by Defined-Medium Cultures. Neuron. 2017;94:759-73 e8.
104. Grabert K, Michoel T, Karavolos MH, Clohisey S, Baillie JK, Stevens MP, et al. Microglial brain region-dependent diversity and selective regional sensitivities to aging. Nat Neurosci. 2016;19:504-16.
105. Keren-Shaul H, Spinrad A, Weiner A, Matcovitch-Natan O, Dvir-Szternfeld R, Ulland TK, et al. A Unique Microglia Type Associated with Restricting Development of Alzheimer's Disease. Cell. 2017;169:1276-90 e17.
106. Querol-Vilaseca M, Colom-Cadena M, Pegueroles J, San Martin-Paniello C, Clarimon J, Belbin O, et al. YKL-40 (Chitinase 3-like I) is expressed in a subset of astrocytes in Alzheimer's disease and other tauopathies. J Neuroinflammation. 2017;14:118.
107. Baldacci F, Toschi N, Lista S, Zetterberg H, Blennow K, Kilimann I, et al. Two-level diagnostic classification using cerebrospinal fluid YKL-40 in Alzheimer's disease. Alzheimers Dement. 2017;13:993-1003.
108. Illan-Gala I, Alcolea D, Montal V, Dols-Icardo O, Munoz L, de Luna N, et al. CSF sAPPbeta, YKL-40, and NfL along the ALS-FTD spectrum. Neurology. 2018;91:e1619-e28.
109. Janelidze S, Mattsson N, Stomrud E, Lindberg O, Palmqvist S, Zetterberg H, et al. CSF biomarkers of neuroinflammation and cerebrovascular dysfunction in early Alzheimer disease. Neurology. 2018;91:e867-e77.
110. Llorens F, Thune K, Tahir W, Kanata E, Diaz-Lucena D, Xanthopoulos K, et al. YKL-40 in the brain and cerebrospinal fluid of neurodegenerative dementias. Mol Neurodegener. 2017;12:83.
111. Thompson AG, Gray E, Thezenas ML, Charles PD, Evetts S, Hu MT, et al. Cerebrospinal fluid macrophage biomarkers in amyotrophic lateral sclerosis. Ann Neurol. 2018;83:258-68.
112. Zhang H, Ng KP, Therriault J, Kang MS, Pascoal TA, Rosa-Neto P, et al. Cerebrospinal fluid phosphorylated tau, visinin-like protein-1, and chitinase-3-like protein 1 in mild cognitive impairment and Alzheimer's disease. Transl Neurodegener. 2018;7:23.
113. Baldacci F, Lista S, Palermo G, Giorgi FS, Vergallo A, Hampel H. The neuroinflammatory biomarker YKL-40 for neurodegenerative diseases: advances in development. Expert Rev Proteomics. 2019;16:593-600.
114. Abu-Rumeileh S, Steinacker P, Polischi B, Mammana A, Bartoletti-Stella A, Oeckl P, et al. CSF biomarkers of neuroinflammation in distinct forms and subtypes of neurodegenerative dementia. Alzheimers Res Ther. 2019;12:2.
115. Oeckl P, Weydt P, Steinacker P, Anderl-Straub S, Nordin F, Volk AE, et al. Different neuroinflammatory profile in amyotrophic lateral sclerosis and frontotemporal dementia is linked to the clinical phase. J Neurol Neurosurg Psychiatry. 2019;90:4-10.
116. Malaguarnera L, Simpore J, Prodi DA, Angius A, Sassu A, Persico I, et al. A 24-bp duplication in exon 10 of human chitotriosidase gene from the sub-Saharan to the Mediterranean area: role of parasitic diseases and environmental conditions. Genes Immun. 2003;4:570-4.
117. Colangelo AM, Alberghina L, Papa M. Astrogliosis as a therapeutic target for neurodegenerative diseases. Neurosci Lett. 2014;565:59-64.
118. Heller C, Foiani MS, Moore K, Convery R, Bocchetta M, Neason M, et al. Plasma glial fibrillary acidic protein is raised in progranulin-associated frontotemporal dementia. J Neurol Neurosurg Psychiatry. 2020.
119. Ishiki A, Kamada M, Kawamura Y, Terao C, Shimoda F, Tomita N, et al. Glial fibrillar acidic protein in the cerebrospinal fluid of Alzheimer's disease, dementia with Lewy bodies, and frontotemporal lobar degeneration. J Neurochem. 2016;136:258-61.
120. Colonna M. TREMs in the immune system and beyond. Nat Rev Immunol. 2003;3:445-53.

121. Cady J, Koval ED, Benitez BA, Zaidman C, Jockel-Balsarotti J, Allred P, et al. TREM2 variant p.R47H as a risk factor for sporadic amyotrophic lateral sclerosis. JAMA Neurol. 2014;71:449-53.
122. Guerreiro R, Wojtas A, Bras J, Carrasquillo M, Rogaeva E, Majounie E, et al. TREM2 variants in Alzheimer's disease. N Engl J Med. 2013;368:117-27.
123. Guerreiro RJ, Lohmann E, Bras JM, Gibbs JR, Rohrer JD, Gurunlian N, et al. Using exome sequencing to reveal mutations in TREM2 presenting as a frontotemporal dementia-like syndrome without bone involvement. JAMA Neurol. 2013;70:78-84.
124. Jonsson T, Stefansson H, Steinberg S, Jonsdottir I, Jonsson PV, Snaedal J, et al. Variant of TREM2 associated with the risk of Alzheimer's disease. N Engl J Med. 2013;368:107-16.
125. Rayaprolu S, Mullen B, Baker M, Lynch T, Finger E, Seeley WW, et al. TREM2 in neurodegeneration: evidence for association of the p.R47H variant with frontotemporal dementia and Parkinson's disease. Mol Neurodegener. 2013;8:19.
126. Su WH, Shi ZH, Liu SL, Wang XD, Liu S, Ji Y. The rs75932628 and rs2234253 polymorphisms of the TREM2 gene were associated with susceptibility to frontotemporal lobar degeneration in Caucasian populations. Ann Hum Genet. 2018;82:177-85.
127. Wunderlich P, Glebov K, Kemmerling N, Tien NT, Neumann H, Walter J. Sequential proteolytic processing of the triggering receptor expressed on myeloid cells-2 (TREM2) protein by ectodomain shedding and gamma-secretase-dependent intramembranous cleavage. J Biol Chem. 2013;288:33027-36.
128. Heslegrave A, Heywood W, Paterson R, Magdalinou N, Svensson J, Johansson P, et al. Increased cerebrospinal fluid soluble TREM2 concentration in Alzheimer's disease. Mol Neurodegener. 2016;11:3.
129. Kleinberger G, Brendel M, Mracsko E, Wefers B, Groeneweg L, Xiang X, et al. The FTD-like syndrome causing TREM2 T66M mutation impairs microglia function, brain perfusion, and glucose metabolism. Embo J. 2017;36:1837-53.
130. Piccio L, Deming Y, Del-Aguila JL, Ghezzi L, Holtzman DM, Fagan AM, et al. Cerebrospinal fluid soluble TREM2 is higher in Alzheimer disease and associated with mutation status. Acta Neuropathol. 2016;131:925-33.
131. Woollacott IOC, Nicholas JM, Heslegrave A, Heller C, Foiani MS, Dick KM, et al. Cerebrospinal fluid soluble TREM2 levels in frontotemporal dementia differ by genetic and pathological subgroup. Alzheimers Res Ther. 2018;10:79.
132. van Eijk M, van Roomen CP, Renkema GH, Bussink AP, Andrews L, Blommaart EF, et al. Characterization of human phagocyte-derived chitotriosidase, a component of innate immunity. Int Immunol. 2005;17:1505-12.
133. Bossu P, Salani F, Alberici A, Archetti S, Bellelli G, Galimberti D, et al. Loss of function mutations in the progranulin gene are related to pro-inflammatory cytokine dysregulation in frontotemporal lobar degeneration patients. J Neuroinflammation. 2011;8:65.
134. Gibbons L, Rollinson S, Thompson JC, Robinson A, Davidson YS, Richardson A, et al. Plasma levels of progranulin and interleukin-6 in frontotemporal lobar degeneration. Neurobiol Aging. 2015;36:1603 e1-4.
135. Galimberti D, Venturelli E, Fenoglio C, Guidi I, Villa C, Bergamaschini L, et al. Intrathecal levels of IL-6, IL-11 and LIF in Alzheimer's disease and frontotemporal lobar degeneration. J Neurol. 2008;255:539-44.
136. Sjogren M, Folkesson S, Blennow K, Tarkowski E. Increased intrathecal inflammatory activity in frontotemporal dementia: pathophysiological implications. J Neurol Neurosurg Psychiatry. 2004;75:1107-11.

137. Galimberti D, Bonsi R, Fenoglio C, Serpente M, Cioffi SM, Fumagalli G, et al. Inflammatory molecules in Frontotemporal Dementia: cerebrospinal fluid signature of progranulin mutation carriers. Brain Behav Immun. 2015;49:182-7.
138. Galimberti D, Schoonenboom N, Scheltens P, Fenoglio C, Venturelli E, Pijnenburg YA, et al. Intrathecal chemokine levels in Alzheimer disease and frontotemporal lobar degeneration. Neurology. 2006;66:146-7.
139. Galimberti D, Venturelli E, Villa C, Fenoglio C, Clerici F, Marcone A, et al. MCP-1 A-2518G polymorphism: effect on susceptibility for frontotemporal lobar degeneration and on cerebrospinal fluid MCP-1 levels. J Alzheimers Dis. 2009;17:125-33.
140. Cavaillon JM. Pro- versus anti-inflammatory cytokines: myth or reality. Cell Mol Biol (Noisy-le-grand). 2001;47:695-702.
141. Lui H, Zhang J, Makinson SR, Cahill MK, Kelley KW, Huang HY, et al. Progranulin Deficiency Promotes Circuit-Specific Synaptic Pruning by Microglia via Complement Activation. Cell. 2016;165:921-35.
142. Chitramuthu BP, Bennett HPJ, Bateman A. Progranulin: a new avenue towards the understanding and treatment of neurodegenerative disease. Brain. 2017;140:3081-104.
143. Smith KR, Damiano J, Franceschetti S, Carpenter S, Canafoglia L, Morbin M, et al. Strikingly different clinicopathological phenotypes determined by progranulin-mutation dosage. Am J Hum Genet. 2012;90:1102-7.
144. Baker M, Mackenzie IR, Pickering-Brown SM, Gass J, Rademakers R, Lindholm C, et al. Mutations in progranulin cause tau-negative frontotemporal dementia linked to chromosome 17. Nature. 2006;442:916-9.
145. Cruts M, Gijselinck I, van der Zee J, Engelborghs S, Wils H, Pirici D, et al. Null mutations in progranulin cause ubiquitin-positive frontotemporal dementia linked to chromosome 17q21. Nature. 2006;442:920-4.
146. Rademakers R, Neumann M, Mackenzie IR. Advances in understanding the molecular basis of frontotemporal dementia. Nat Rev Neurol. 2012;8:423-34.
147. Almeida MR, Baldeiras I, Ribeiro MH, Santiago B, Machado C, Massano J, et al. Progranulin peripheral levels as a screening tool for the identification of subjects with progranulin mutations in a Portuguese cohort. Neurodegener Dis. 2014;13:214-23.
148. Carecchio M, Fenoglio C, De Riz M, Guidi I, Comi C, Cortini F, et al. Progranulin plasma levels as potential biomarker for the identification of GRN deletion carriers. A case with atypical onset as clinical amnestic Mild Cognitive Impairment converted to Alzheimer's disease. J Neurol Sci. 2009;287:291-3.
149. Finch N, Baker M, Crook R, Swanson K, Kuntz K, Surtees R, et al. Plasma progranulin levels predict progranulin mutation status in frontotemporal dementia patients and asymptomatic family members. Brain. 2009;132:583-91.
150. Galimberti D, Fumagalli GG, Fenoglio C, Cioffi SMG, Arighi A, Serpente M, et al. Progranulin plasma levels predict the presence of GRN mutations in asymptomatic subjects and do not correlate with brain atrophy: results from the GENFI study. Neurobiol Aging. 2018;62:245 e9-e12.
151. Ghidoni R, Benussi L, Glionna M, Franzoni M, Binetti G. Low plasma progranulin levels predict progranulin mutations in frontotemporal lobar degeneration. Neurology. 2008;71:1235-9.
152. Ghidoni R, Stoppani E, Rossi G, Piccoli E, Albertini V, Paterlini A, et al. Optimal plasma progranulin cutoff value for predicting null progranulin mutations in neurodegenerative diseases: a multicenter Italian study. Neurodegener Dis. 2012;9:121-7.
153. Schofield EC, Halliday GM, Kwok J, Loy C, Double KL, Hodges JR. Low serum progranulin predicts the presence of mutations: a prospective study. J Alzheimers Dis. 2010;22:981-4.

154. Sleegers K, Brouwers N, Van Damme P, Engelborghs S, Gijselinck I, van der Zee J, et al. Serum biomarker for progranulin-associated frontotemporal lobar degeneration. Ann Neurol. 2009;65:603-9.
155. Meeter LH, Patzke H, Loewen G, Dopper EG, Pijnenburg YA, van Minkelen R, et al. Progranulin Levels in Plasma and Cerebrospinal Fluid in Granulin Mutation Carriers. Dement Geriatr Cogn Dis Extra. 2016;6:330-40.
156. Nicholson AM, Finch NA, Thomas CS, Wojtas A, Rutherford NJ, Mielke MM, et al. Progranulin protein levels are differently regulated in plasma and CSF. Neurology. 2014;82:1871-8.
157. Wilke C, Gillardon F, Deuschle C, Dubois E, Hobert MA, Muller vom Hagen J, et al. Serum Levels of Progranulin Do Not Reflect Cerebrospinal Fluid Levels in Neurodegenerative Disease. Curr Alzheimer Res. 2016;13:654-62.
158. Han JJ, Yu M, Houston N, Steinberg SM, Kohn EC. Progranulin is a potential prognostic biomarker in advanced epithelial ovarian cancers. Gynecol Oncol. 2011;120:5-10.
159. Todoric J, Handisurya A, Perkmann T, Knapp B, Wagner O, Tura A, et al. Circulating progranulin levels in women with gestational diabetes mellitus and healthy controls during and after pregnancy. Eur J Endocrinol. 2012;167:561-7.
160. Cruchaga C, Graff C, Chiang HH, Wang J, Hinrichs AL, Spiegel N, et al. Association of TMEM106B gene polymorphism with age at onset in granulin mutation carriers and plasma granulin protein levels. Arch Neurol. 2011;68:581-6.
161. Finch N, Carrasquillo MM, Baker M, Rutherford NJ, Coppola G, Dejesus-Hernandez M, et al. TMEM106B regulates progranulin levels and the penetrance of FTLD in GRN mutation carriers. Neurology. 2011;76:467-74.
162. Hsiung GY, Fok A, Feldman HH, Rademakers R, Mackenzie IR. rs5848 polymorphism and serum progranulin level. J Neurol Sci. 2011;300:28-32.
163. Byrne S, Elamin M, Bede P, Shatunov A, Walsh C, Corr B, et al. Cognitive and clinical characteristics of patients with amyotrophic lateral sclerosis carrying a C9orf72 repeat expansion: a population-based cohort study. Lancet Neurol. 2012;11:232-40.
164. DeJesus-Hernandez M, Mackenzie IR, Boeve BF, Boxer AL, Baker M, Rutherford NJ, et al. Expanded GGGGCC hexanucleotide repeat in noncoding region of C9ORF72 causes chromosome 9p-linked FTD and ALS. Neuron. 2011;72:245-56.
165. Majounie E, Renton AE, Mok K, Dopper EG, Waite A, Rollinson S, et al. Frequency of the C9orf72 hexanucleotide repeat expansion in patients with amyotrophic lateral sclerosis and frontotemporal dementia: a cross-sectional study. Lancet Neurol. 2012;11:323-30.
166. Pottier C, Ravenscroft TA, Sanchez-Contreras M, Rademakers R. Genetics of FTLD: overview and what else we can expect from genetic studies. J Neurochem. 2016;138 Suppl 1:32-53.
167. Renton AE, Majounie E, Waite A, Simon-Sanchez J, Rollinson S, Gibbs JR, et al. A hexanucleotide repeat expansion in C9ORF72 is the cause of chromosome 9p21-linked ALS-FTD. Neuron. 2011;72:257-68.
168. van Blitterswijk M, DeJesus-Hernandez M, Rademakers R. How do C9ORF72 repeat expansions cause amyotrophic lateral sclerosis and frontotemporal dementia: can we learn from other noncoding repeat expansion disorders? Curr Opin Neurol. 2012;25:689-700.
169. Jiang J, Ravits J. Pathogenic Mechanisms and Therapy Development for C9orf72 Amyotrophic Lateral Sclerosis/Frontotemporal Dementia. Neurotherapeutics. 2019;16:1115-32.
170. Mori K, Weng SM, Arzberger T, May S, Rentzsch K, Kremmer E, et al. The C9orf72 GGGGCC repeat is translated into aggregating dipeptide-repeat proteins in FTLD/ALS. Science. 2013;339:1335-8.
171. Ash PE, Bieniek KF, Gendron TF, Caulfield T, Lin WL, Dejesus-Hernandez M, et al. Unconventional translation of C9ORF72 GGGGCC expansion generates insoluble polypeptides specific to c9FTD/ALS. Neuron. 2013;77:639-46.

172. Gendron TF, Bieniek KF, Zhang YJ, Jansen-West K, Ash PE, Caulfield T, et al. Antisense transcripts of the expanded C9ORF72 hexanucleotide repeat form nuclear RNA foci and undergo repeat-associated non-ATG translation in c9FTD/ALS. Acta Neuropathol. 2013;126:829-44.
173. Zu T, Liu Y, Banez-Coronel M, Reid T, Pletnikova O, Lewis J, et al. RAN proteins and RNA foci from antisense transcripts in C9ORF72 ALS and frontotemporal dementia. Proc Natl Acad Sci U S A. 2013;110:E4968-77.
174. Davidson YS, Barker H, Robinson AC, Thompson JC, Harris J, Troakes C, et al. Brain distribution of dipeptide repeat proteins in frontotemporal lobar degeneration and motor neurone disease associated with expansions in C9ORF72. Acta Neuropathol Commun. 2014;2:70.
175. Gomez-Deza J, Lee YB, Troakes C, Nolan M, Al-Sarraj S, Gallo JM, et al. Dipeptide repeat protein inclusions are rare in the spinal cord and almost absent from motor neurons in C9ORF72 mutant amyotrophic lateral sclerosis and are unlikely to cause their degeneration. Acta Neuropathol Commun. 2015;3:38.
176. Mackenzie IR, Arzberger T, Kremmer E, Troost D, Lorenzl S, Mori K, et al. Dipeptide repeat protein pathology in C9ORF72 mutation cases: clinico-pathological correlations. Acta Neuropathol. 2013;126:859-79.
177. Schludi MH, May S, Grasser FA, Rentzsch K, Kremmer E, Kupper C, et al. Distribution of dipeptide repeat proteins in cellular models and C9orf72 mutation cases suggests link to transcriptional silencing. Acta Neuropathol. 2015;130:537-55.
178. Su Z, Zhang Y, Gendron TF, Bauer PO, Chew J, Yang WY, et al. Discovery of a biomarker and lead small molecules to target r(GGGGCC)-associated defects in c9FTD/ALS. Neuron. 2014;83:1043-50.
179. Gendron TF, Chew J, Stankowski JN, Hayes LR, Zhang YJ, Prudencio M, et al. Poly(GP) proteins are a useful pharmacodynamic marker for C9ORF72-associated amyotrophic lateral sclerosis. Sci Transl Med. 2017;9.
180. Lehmer C, Oeckl P, Weishaupt JH, Volk AE, Diehl-Schmid J, Schroeter ML, et al. Poly-GP in cerebrospinal fluid links C9orf72-associated dipeptide repeat expression to the asymptomatic phase of ALS/FTD. EMBO Mol Med. 2017;9:859-68.
181. Gendron TF, Group CONS, Daughrity LM, Heckman MG, Diehl NN, Wuu J, et al. Phosphorylated neurofilament heavy chain: A biomarker of survival for C9ORF72-associated amyotrophic lateral sclerosis. Ann Neurol. 2017;82:139-46.
182. Meeter LHH, Gendron TF, Sias AC, Jiskoot LC, Russo SP, Donker Kaat L, et al. Poly(GP), neurofilament and grey matter deficits in C9orf72 expansion carriers. Ann Clin Transl Neurol. 2018;5:583-97.
183. Baborie A, Griffiths TD, Jaros E, Perry R, McKeith IG, Burn DJ, et al. Accumulation of dipeptide repeat proteins predates that of TDP-43 in frontotemporal lobar degeneration associated with hexanucleotide repeat expansions in C9ORF72 gene. Neuropathol Appl Neurobiol. 2015;41:601-12.
184. Proudfoot M, Gutowski NJ, Edbauer D, Hilton DA, Stephens M, Rankin J, et al. Early dipeptide repeat pathology in a frontotemporal dementia kindred with C9ORF72 mutation and intellectual disability. Acta Neuropathol. 2014;127:451-8.
185. Vatsavayai SC, Yoon SJ, Gardner RC, Gendron TF, Vargas JN, Trujillo A, et al. Timing and significance of pathological features in C9orf72 expansion-associated frontotemporal dementia. Brain. 2016;139:3202-16.
186. Riemslagh FW. Molecular Mechanisms of C9orf72-linked Frontotemporal Dementia and Amyotrophic Lateral Sclerosis [Dissertation]: Erasmus Universiteit Rotterdam; 2019.
187. Oeckl P, Steinacker P, Feneberg E, Otto M. Cerebrospinal fluid proteomics and protein biomarkers in frontotemporal lobar degeneration: Current status and future perspectives. Biochim Biophys Acta. 2015;1854:757-68.

188. van der Ende EL, Meeter HH, Stingl C, van Rooij JGJ, Stoop MP, Nijholt DAT, et al. Novel CSF biomarkers in genetic frontotemporal dementia identified by proteomics. Ann Clin Transl Neurol. 2019.
189. Jahn H, Wittke S, Zurbig P, Raedler TJ, Arlt S, Kellmann M, et al. Peptide fingerprinting of Alzheimer's disease in cerebrospinal fluid: identification and prospective evaluation of new synaptic biomarkers. PLoS One. 2011;6:e26540.
190. Ruetschi U, Zetterberg H, Podust VN, Gottfries J, Li S, Hviid Simonsen A, et al. Identification of CSF biomarkers for frontotemporal dementia using SELDI-TOF. Exp Neurol. 2005;196:273-81.
191. Simonsen AH, McGuire J, Podust VN, Hagnelius NO, Nilsson TK, Kapaki E, et al. A novel panel of cerebrospinal fluid biomarkers for the differential diagnosis of Alzheimer's disease versus normal aging and frontotemporal dementia. Dement Geriatr Cogn Disord. 2007;24:434-40.
192. Teunissen CE, Elias N, Koel-Simmelink MJ, Durieux-Lu S, Malekzadeh A, Pham TV, et al. Novel diagnostic cerebrospinal fluid biomarkers for pathologic subtypes of frontotemporal dementia identified by proteomics. Alzheimers Dement (Amst). 2016;2:86-94.
193. Barschke P, Oeckl P, Steinacker P, Al Shweiki MR, Weishaupt JH, Landwehrmeyer B, et al. Different CSF protein profiles in amyotrophic lateral sclerosis and frontotemporal dementia with *C9orf72* hexanucleotide repeat expansion. J Neurol Neurosurg Psychiatry. 2020;In press.

Chapter 2

Biomarkers of neuroaxonal and synaptic integrity

Chapter 2.1

Serum neurofilament light chain in genetic frontotemporal dementia: a longitudinal, multicentre cohort study

Emma L. van der Ende, Lieke H. Meeter, Jackie M. Poos, Jessica L. Panman, Lize C. Jiskoot, Elise G.P. Dopper, Janne M. Papma, Frank Jan de Jong, Inge Verberk, Charlotte Teunissen, Dimitris Rizopoulos, Carolin Heller, Rhian S. Convery, Katrina M. Moore, Martina Bocchetta, Mollie Neason, David M. Cash, Barbara Borroni, Daniela Galimberti, Raquel Sanchez-Valle, Robert Laforce Jr, Fermin Moreno, Matthis Synofzik, Caroline Graff, Mario Masellis, Maria Carmela Tartaglia, James B. Rowe, Rik Vandenberghe, Elizabeth Finger, Fabrizio Tagliavini, Alexandre de Mendonça, Isabel Santana, Chris Butler, Simon Ducharme, Alex Gerhard, Adrian Danek, Johannes Levin, Markus Otto, Giovanni B. Frisoni, Stefano Cappa, Yolande A.L. Pijnenburg, on behalf of the Genetic Frontotemporal dementia Initiative (GENFI), Jonathan D. Rohrer, John C. van Swieten

The Lancet Neurology 2019;18(12):1103-1111.

Abstract

Background: Neurofilament light chain (NfL) is a promising blood biomarker in genetic frontotemporal dementia (FTD), with elevated levels in symptomatic carriers of mutations in *GRN, C9orf72* and *MAPT*. A better understanding of NfL dynamics is essential for upcoming therapeutic trials. We investigated longitudinal NfL trajectories in (pre)symptomatic genetic FTD.

Methods: We included 59 symptomatic and 149 presymptomatic carriers of a mutation in *GRN*, *C9orf72* or *MAPT*, and 127 non-carriers participating in the Genetic FTD Initiative (GENFI), a multicentre cohort study of genetic FTD families across Europe and Canada. We measured NfL by Simoa in 2-6 longitudinal serum samples, collected between June 2012 and September 2017 through annual follow-up visits which also included MR imaging and neuropsychological assessment. Nine presymptomatic carriers became symptomatic during follow-up ('converters'). Using mixed effects models, we analysed NfL changes over time and correlated them with longitudinal imaging and clinical parameters, controlling for age, sex and study site.

Findings: Baseline NfL was elevated in symptomatic carriers (median(interquartile range) 52 pg/ml (24-69)) compared to presymptomatic carriers (9 pg/ml (6-13); p<0.0001) and non-carriers (8 pg/ml (6-11); p<0.0001), and was higher in converters than in non-converting carriers (19 pg/ml(17-28) vs. 8 pg/ml (6-11); p=0.0007) (controlled for age). During follow-up, NfL increased in converters (*b*=0.097; standard error(SE)=0.018; p<0.0001). NfL was stable in symptomatic *C9orf72* and *MAPT* carriers, with an increase in symptomatic *GRN* carriers (*b*=0.040; SE=0.017; p=0.019). Rates of NfL change over time were associated with rate of decline in Mini Mental State Examination and atrophy rate in several grey matter regions.

Interpretation: This study confirms the value of blood NfL as a disease progression biomarker in genetic FTD and suggests that longitudinal NfL measurements could identify mutation carriers approaching symptom onset and capture rates of brain atrophy. The characterisation of NfL over the course of disease provides valuable information for its use as a treatment effect marker.

Introduction

Frontotemporal dementia (FTD) is a common cause of young-onset dementia and is characterised by progressive behavioural and/or language changes.[1,2] Autosomal dominant inheritance is present in 20-30% of cases, most commonly due to mutations in granulin (*GRN*), chromosome 9 open reading frame 72 (*C9orf72*) or microtubule-associated protein tau (*MAPT*).[3] With upcoming therapeutic trials, biomarkers are needed to identify the appropriate moment to start treatment, likely in the preclinical stage, and as surrogate endpoints to measure treatment effect.

Cross-sectional studies have shown that neurofilament light chain (NfL), a constituent of the axonal cytoskeleton, is a promising diagnostic and prognostic blood biomarker in genetic FTD, with low levels in presymptomatic mutation carriers and high levels in symptomatic carriers.[4-6] NfL is elevated in various other neurological diseases, likely reflecting neuroaxonal degeneration.[7] In multiple sclerosis, NfL decreases have been observed after anti-inflammatory treatment,[8] and in Alzheimer's disease (AD) mouse models, decreases were seen following inhibition of amyloid-β deposits,[9] suggesting that NfL is a dynamic marker of disease activity.

Thus far, it is unknown when NfL starts to increase and how NfL changes over the course of FTD. The Genetic FTD Initiative (GENFI), which follows carriers of mutations in *GRN, C9orf72* and *MAPT*, provides an opportunity to prospectively study disease progression from presymptomatic to overt FTD and to identify biomarkers of early pathologic processes.

In this study, we longitudinally measured serum NfL using an ultrasensitive Single Molecule Array (Simoa) in the GENFI cohort to evaluate its temporal profile in genetic FTD. We used corresponding brain imaging and clinical datasets to study whether NfL changes correlate with rates of brain atrophy and clinical decline.

Methods

Subjects

We included 335 subjects from 14 centres collaborating in GENFI, which follows patients with FTD due to a pathogenic mutation in *GRN, C9orf72* or *MAPT* (symptomatic mutation carriers) and healthy at-risk first-degree relatives (either presymptomatic mutation carriers or non-carriers).[10] Participants were included in the current study if at least two serum samples were available with a time interval of six months or more. Exclusion criteria included neurological comorbidities likely to affect NfL, including cerebrovascular events.[7] The final

dataset included 59 symptomatic (25 *GRN*, 24 *C9orf72*, 10 *MAPT*) and 149 presymptomatic (79 *GRN,* 46 *C9orf72,* 24 *MAPT*) mutation carriers and 127 non-carriers. We included 2-6 serum samples for each subject from distinct time points, with a total of 891 samples. A small subset of these samples was collected prior to inclusion in GENFI. The median follow-up duration between the first and last sample was 2.1 years (figure S1, table S1).

As part of GENFI, participants were followed yearly or two-yearly by a semi-structured health interview, neurological and neuropsychological examination, blood sample collection and MR imaging. Knowledgeable informants (e.g. spouse, sibling) were interviewed about potential changes in cognition and/or behaviour. Global cognitive functioning was scored using the Mini Mental State Examination (MMSE) and the Frontotemporal Lobar Degeneration-Clinical Dementia Rating scale (FTLD-CDR); changes in MMSE and FTLD-CDR were used as measures of clinical decline.

Subjects were considered symptomatic (either at baseline or during follow-up) based on international consensus criteria.[1,2] Symptom onset was defined as the moment of first symptoms as noted retrospectively by caregivers. The presence of concomitant amyotrophic lateral sclerosis (ALS) was defined according to revised El Escorial criteria.[11] Presymptomatic mutation carriers had no evidence of motor deficits, behavioural or cognitive changes, as assessed by neurological and neuropsychological examination and structured informant interviews.

Standard protocol approvals and patient consents

Local ethics committees at each site approved the study and all participants provided written informed consent. Clinical researchers were blinded to genetic status of at-risk individuals unless subjects had undergone predictive testing.

Sample collection, processing and storage

Blood was collected by venipuncture in SST-tubes and centrifuged at 2000g for 10 minutes at room temperature within three hours of withdrawal according to a standardised GENFI protocol. After centrifugation, serum was stored at -80°C until use. Participants were not instructed to fast and time of day at blood collection was variable.

Laboratory methods

Serum NfL was measured in duplicate using the Simoa NF-Light Advantage Kit from Quanterix on a Simoa HD-1 Analyzer instrument according to the manufacturer's instructions. The mean coefficient of variation (CV) of duplicate measurements was 4.7% (range 0-15%); samples with a CV>15% were re-measured. Samples were analysed in nine runs; longitudinal samples of each subject were measured in the same run. The mean between-run CV of

quality control samples was 8.3% (range 3.7-12%). Four samples were excluded due to visual hemolysis; one sample was excluded due to a CV>15% and insufficient serum to rerun the measurement. The number of subjects remained unchanged as additional follow-up samples were available for each of these subjects. Laboratory technicians were blinded to clinical information.

Neuroimaging

T1-weighted volumetric imaging was available at baseline in 276 subjects and at follow-up in 258 subjects (2-4 scans per subject, minimum interval between scans: six months). Follow-up imaging was acquired on the same scanner as the baseline visit. All MRI scans were acquired using a standardised GENFI exam card[10] on 3 Tesla MRI scanners and were visually checked for artefacts prior to image processing according to a standardised GENFI protocol. Each MRI scan was coupled to a serum sample with a maximum interval of six months between the serum sample and scan.

T1-weighted MRI scans were parcellated into cortical and subcortical regions as previously described[10] using an atlas propagation and label fusion strategy,[12] combining regions of interest to calculate grey matter cortical volumes (frontal, temporal, parietal, occipital, cingulate and insular cortices), subcortical volumes (hippocampus, amygdala, caudate nucleus, putamen, thalamus) and cerebellar volume of both hemispheres combined (http://www.neuromorphometrics.org:808/seg/). We measured whole-brain grey matter volumes using a semi-automated segmentation method.[13] Total intracranial volume (TIV) was measured with SPM12 (Statistical Parametric Mapping, Wellcome Trust Centre for Neuroimaging, London, UK) as the combination of grey matter, white matter, and CSF segmentations.[14] To ensure accurate delineation of regional volumes, segmentation output files were visually checked by experts.

All grey matter volumes were expressed as a percentage of TIV.

Statistical analyses

Statistical analyses were performed in *R* and IBM SPSS Statistics 24. Statistical significance was set at 0.05 (two-sided).

Cross-sectional analyses of baseline data

For cross-sectional analyses, we identified three groups: symptomatic mutation carriers, presymptomatic mutation carriers (including those who converted to the symptomatic stage during follow-up) and non-carriers. Group comparisons were performed using Kruskal-Wallis tests with post-hoc Dunn's test, as NfL was not normally distributed. NfL was normally

distributed after log-transformation (by Kolmogorov-Smirnov tests and histogram- and Q-Q plots; figure S2), and we additionally compared log(NfL) between clinical groups adjusting for age by ANCOVA; disease duration was included as a covariate in comparisons between symptomatic mutation carriers. NfL was correlated with each of the regional brain volumes (model A1), MMSE (model A2) and FTLD-CDR (model A3) through multiple linear regression, adjusting for age, sex and study site and, in brain volume analyses, for MRI scanner type. MMSE and FTLD-CDR analyses were limited to symptomatic mutation carriers to study whether the severity of cognitive and functional deficits during the course of FTD was correlated with NfL. Diagnostic performance of NfL was assessed by areas under the curve (AUC) obtained by receiver operating characteristic (ROC) analyses, with optimal cut-off levels determined by the highest Youden's index.

We fit a linear regression model to analyse whether baseline NfL in presymptomatic mutation carriers differed compared to non-carriers as they approached their expected disease onset (model B). The large variation in onset age within families would render analyses based on family onset age invalid.[10,15,16] Therefore, we used age as a proxy to approaching symptom onset. We used log-transformed baseline NfL and included age, mutation status (mutation carrier or non-carrier) and an interaction between these terms. Polynomials or natural cubic splines of age did not improve the model fit. In case of a significant interaction term, estimated NfL at ages 40-60 with 2-year intervals was compared between mutation carriers and non-carriers, with Bonferroni correction.

Longitudinal analyses of follow-up data

For longitudinal analyses we identified four groups: symptomatic mutation carriers, presymptomatic mutation carriers (who remained presymptomatic during follow-up), converters (who developed FTD during follow-up) and non-carriers. We analysed NfL changes using linear mixed effects models to account for the correlation between repeated measurements in each subject. We specified the following fixed effects: time (time = 0 at first serum sample), clinical group (non-carrier, presymptomatic carrier, converter, symptomatic carrier, with non-carriers as the reference group), age, sex, study site and an interaction term between time and clinical group (model C). We included random intercepts and slopes of time per subject. NfL was log-transformed to meet the models' assumptions. Appropriate random and fixed effects structures were selected using likelihood ratio tests. Polynomials or natural cubic splines of time did not improve the model fit. Differences in NfL change over time between mutation groups were studied through post-hoc analyses with an interaction term between time and the combination of mutation group and clinical status.

Next, we calculated rates of NfL change using mixed effects models with time as the fixed effect and a random slope and intercept of time per subject (model D). We correlated grey

matter volume with rate of NfL change by mixed effects models with age, sex, study site and MRI scanner type as covariates, and an interaction between time and rate of NfL change to study whether rate of NfL change was associated with grey matter volume change over time (model E1). We correlated NfL change with MMSE- and FTLD-CDR change in symptomatic carriers using the same approach (model E2 and E3).

Formulas for all statistical models are provided in supplementary file 1.

Role of the funding source

The funders of the study had no role in study design, data collection, analysis and interpretation, writing of the report or in the decision to submit for publication. The corresponding author had access to all data and final responsibility in the decision to submit for publication.

Results

Subjects

Baseline subject characteristics are shown in table 1. Nine presymptomatic mutation carriers (6 *GRN,* 1 *C9orf72,* 2 *MAPT*) converted to the symptomatic stage during follow-up. Five symptomatic *C9orf72* mutation carriers had concomitant ALS.

Table 1. Subject characteristics at baseline. Continuous variables are described as medians (interquartile range). Phenotypes of symptomatic mutation carriers: behavioural variant FTD (n=40), primary progressive aphasia (n=11), FTD with amyotrophic lateral sclerosis (n=5), FTD with progressive supranuclear palsy (n=1), memory-predominant FTD (n=1), FTD not otherwise specified (n=1). MMSE, Mini Mental State Examination; FTLD-CDR, Frontotemporal Lobar Degeneration – Clinical Dementia Rating scale.

	Symptomatic carriers			Presymptomatic carriers			Non-carriers	*p*
N	59			149			127	-
Sex, male (%)	36 (61%)			52 (35%)			58 (46%)	0.002[a]
Age, years	63 (58-69)			45 (39-55)			50 (39-59)	<0.0001[b]
MMSE	25 (8-30)			30 (24-30)			30 (25-30)	<0.0001[c]
FTLD-CDR	4.8 (2.5-9.5)			0 (0)			0 (0)	<0.0001[c]
Serum NfL (pg/ml)	52 (24-69)			9 (6-13)			8 (6-11)	<0.0001[d]
Follow-up duration (range)	1.2 (0.5-8.1)			2.1 (0.7-5.6)			2.2 (0.8-4.9)	-
Samples per subject (range)	2 (2-5)			3 (2-6)			2 (2-6)	-
Gene-specific information	*GRN*	*C9orf72*	*MAPT*	*GRN*	*C9orf72*	*MAPT*		
N	25	24	10	79	46	24	-	-
Age, years	61 (56-67)	68 (62-74)	58 (56-63)	48 (39-57)	43 (38-55)	39 (33-45)	-	<0.0001[b]
Age at symptom onset, years	58 (54-63)	63 (55-69)	55 (52-57)	-	-	-	-	0.039[e]
Disease duration at baseline, years	2.6 (1.1-4.6)	4.0 (2.0-6.6)	2.8 (1.3-7.4)	-	-	-	-	0.144[f]

[a]By Pearson Chi-square test; [b]Symptomatic carriers significantly older than presymptomatic carriers and non-carriers, both overall and for each genotype separately (all comparisons p<0.0001 by Kruskal-Wallis test with post-hoc Dunn's test); [c]Symptomatic carriers significantly lower MMSE and higher FTLD-CDR than presymptomatic carriers and non-carriers (both comparisons p<0.0001 by Kruskal-Wallis tests with post-hoc Dunn's test); [d]Symptomatic carriers significantly higher NfL levels than presymptomatic carriers and non-carriers (both comparisons p<0.0001 by ANCOVA on log-transformed NfL levels with correction for age); [e]Symptomatic *C9orf72* mutation carriers significantly older at symptom onset than *MAPT* mutation carriers (p=0.033 by Kruskal-Wallis test with post-hoc Dunn's test); [f]By Kruskal-Wallis test.

Baseline NfL

Baseline NfL in symptomatic mutation carriers (median 52 pg/ml) was significantly higher than in presymptomatic carriers (9 pg/ml) and non-carriers (8 pg/ml; both p<0.0001). These differences were also seen for each mutation group separately. Symptomatic *GRN* mutation carriers had higher baseline NfL (69 pg/ml) than symptomatic *C9orf72 (*39 pg/ml; p=0.005; after exclusion of FTD-ALS cases: 37 pg/ml; p=0.004) and *MAPT* mutation carriers (20 pg/ml; p<0.0001). Correction for age and, in the latter comparison, disease duration on log-transformed NfL yielded similar p-values (figure 1a).

Age correlated significantly with NfL (r_s=0.770; p<0.0001). This correlation was similarly present when limited to non-carriers (r_s=0.754; p<0.0001) with an estimated increase of 1.2% per year. No difference in NfL was found between males and females (9.6 pg/ml versus 9.2 pg/ml; p=0.101).

Overall, baseline NfL did not differ significantly between presymptomatic mutation carriers and non-carriers (p=0.892). However, modelled by age (model B), a significant interaction was found between mutation status and age (p=0.045), with higher NfL in presymptomatic mutation carriers compared to non-carriers from the age of 48 years (contrast estimate at 48 years=0.065; standard error (SE)=0.024; p=0.033) (figure 1b). ROC analyses of baseline NfL showed a high AUC to separate symptomatic from presymptomatic mutation carriers (AUC 0.93 [95% CI 0.90-0.97]); sensitivity 86%, specificity 87% at cut-off level 17 pg/ml) and to separate symptomatic mutation carriers from non-carriers (AUC 0.95 [95% CI 0.92-0.98]; sensitivity 88%, specificity 91% at cut-off level 15 pg/ml) (figure S3).

NfL was correlated with grey matter volume of the whole brain (*b*=-0.021; SE=0.005; p=0.0003), frontal lobe (*b*=-0.115; SE=0.016; p<0.0001), insula (*b*=-0.756; SE=0.183; p=0.0006), cingulate gyrus (*b*=0.331; SE=0.092; p=0.005) and temporal lobe (*b*=-0.084; SE=0.029; p=0.045).

In symptomatic mutation carriers, NfL was correlated with MMSE (n=55; *b*=-0.021; SE=0.007; p=0.003) but not with FTLD-CDR (n=48; *b*=0.009; SE=0.008; p=0.221). No association was found between NfL and disease duration (n=59; *b*=0.003; SE=0.009; p=0.749).

Figure 1. (A) Baseline NfL in presymptomatic and symptomatic mutation carriers and non-carriers. Subjects in orange were presymptomatic at baseline and converted to the symptomatic stage during follow-up. Grey squares indicate symptomatic *C9orf72* mutation carriers with both FTD and amyotrophic lateral sclerosis. Dashed horizontal line indicates the suggested cut-off value of 17 pg/ml to separate symptomatic mutation carriers from presymptomatic mutation carriers. Reported p-values are from ANCOVA on log-transformed NfL levels with correction for age and, in comparisons between symptomatic mutation carriers, disease duration. *p=0.012; **p=0.005; ***p<0.0001. (B) Baseline log(NfL) in pre-symptomatic mutation carriers (blue triangles) and non-carriers (green circles). Curves were drawn by a linear regression model with a significant interaction term for age by carrier status (p=0.045; model B). Shaded areas represent 95% confidence intervals. For blinding purposes, the displayed x-axis range is 25-80 years (9 subjects not shown) and a jitter of ±2 years was added to all subjects (analyses were performed on raw data).

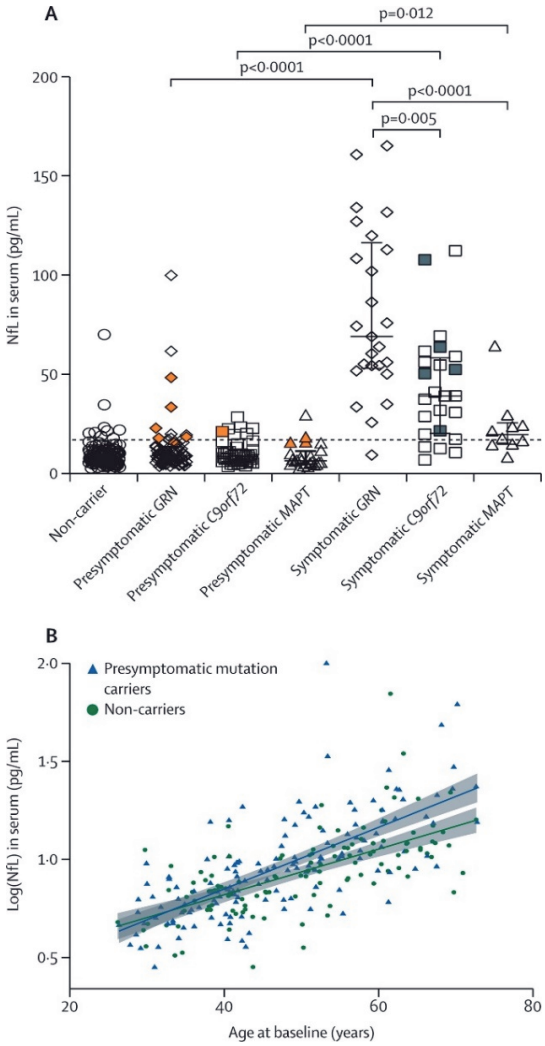

Longitudinal NfL

Non-carriers had relatively stable NfL levels over time during follow-up (figure S4). Two non-carriers had high NfL at baseline with large decreases during follow-up. The mixed effects model (model C) of NfL change over time indicated a significant interaction between time and clinical status on NfL ($F(1,547)=10.6$; $p<0.0001$).

Across all non-converting presymptomatic mutation carriers, a small but significant increase in log(NfL) over time was found ($b=0.015$; SE=0.007; p=0.044). Post-hoc analyses revealed an increase in presymptomatic *C9orf72* ($b=0.030$; SE=0.011; p=0.005), but not in presymptomatic *GRN* (p=0.528) or *MAPT* (p=0.298) mutation carriers. We visually identified seven (non-converting) presymptomatic mutation carriers (4 *C9orf72,* 3 *GRN*, median age at baseline 63 years) with large increases during follow-up (figure S5).

A significant NfL increase over time was found in converters ($b=0.097$;SE=0.018;$p<0.0001$) (figure 2).

Figure 2. Individual NfL trajectories in converters. The dashed horizontal line represents baseline median NfL level in non-converting presymptomatic mutation carriers. *GRN* mutation carriers are shown in green, *C9orf72* mutation carriers in red and *MAPT* mutation carriers in blue.

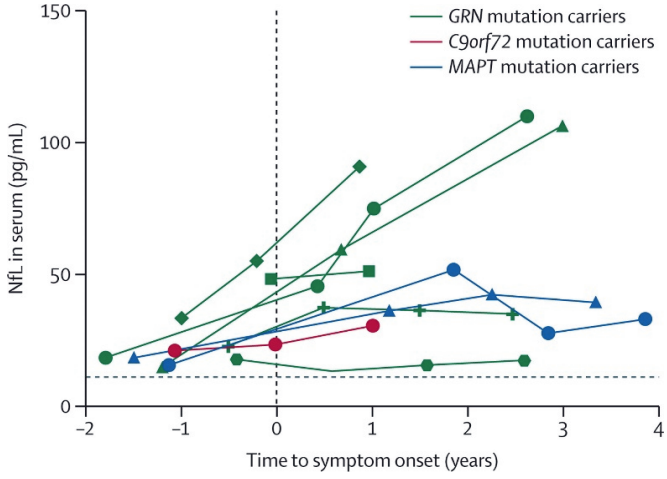

The group of nine converters had higher NfL at baseline (before symptom onset) than non-converting presymptomatic mutation carriers (median 19 versus 8 pg/ml, corrected for age by ANCOVA, p=0.0007). ROC analyses revealed an AUC of 0.93 (95%CI 0.89-0.98) to distinguish converters from presymptomatic mutation carriers using baseline NfL (sensitivity 100%, specificity 84%, cut-off 15.0 pg/ml) (figure S3c). Details for each converter are shown in table S2 and figure S6. In symptomatic mutation carriers, overall, NfL did not change during

follow-up (*b*=0.017; SE=0.010; p=0.101) and remained elevated. Post hoc analyses revealed an increase over time in *GRN* mutation carriers (*b*=0.040; SE=0.017; p=0.019), with much variation in individual NfL trajectories (figure S5), while in symptomatic *C9orf72* and *MAPT* mutation carriers, NfL remained stable over time (p=0.650 and p=0.464 respectively). The estimated NfL trajectories for each clinical group are shown in figure 3a.

Rates of NfL change

The rate of NfL change was significantly higher in converters than in non-carriers and non-converting presymptomatic mutation carriers (both p<0.0001; model D) (figure 3b).

Correlations with longitudinal neuroimaging and clinical parameters

Across all groups, the rate of NfL change was significantly associated with the change over time in volume of the frontal lobe, insula, cingulate gyrus, hippocampus, putamen (all p<0.0001), whole brain volume (p=0.001), temporal lobe (p=0.001), amygdala (p=0.012) and cerebellum (p=0.026) (figure 4; coefficients in table S7). The rate of NfL change was significantly associated with MMSE change over time (n=49; *b*=-94.7; SE=33.9; p=0.003) (figure S7) but not with FTLD-CDR change (n=47; *b*=-3.46; SE=46.3; p=0.941) (models E1-E3). Extended results for all statistical models are provided in tables S3-7.

Figure 3. NfL change over time. (A) Estimated NfL trajectories for each clinical group, with curves drawn using mixed effects modelling (model C), for males of median age. Dashed lines represent 95% confidence intervals. Time indicates number of years since baseline sample. (B) Rates of NfL change per year across clinical groups. The boxes map to the median, 25th and 75th quartiles and whiskers extend to 1.5 x interquartile range. Converters had significantly higher rates of change than presymptomatic mutation carriers and non-carriers (p<0.0001) (by Kruskal Wallis test with Monte Carlo method).

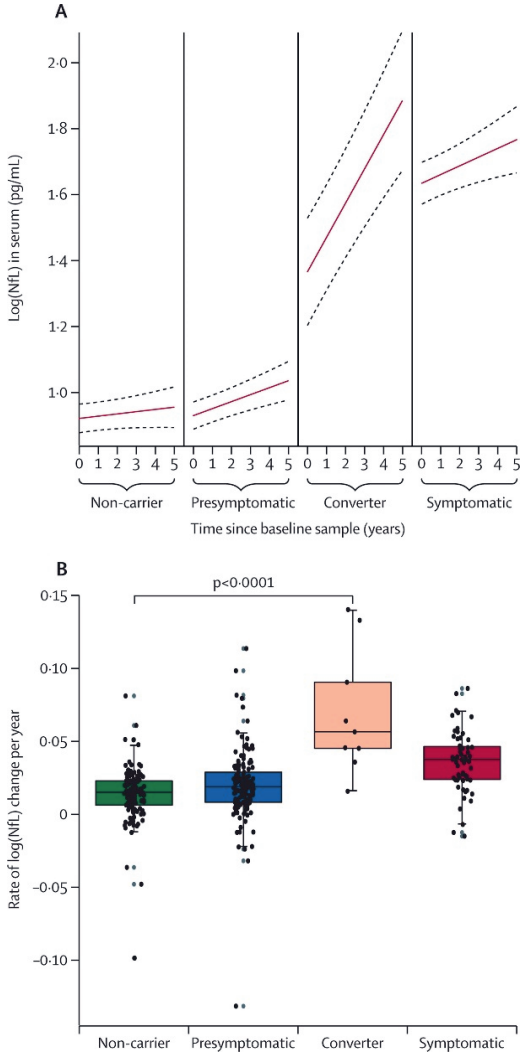

Figure 4. Relationship between the annual rate of log(NfL) change and the rate of (A) frontal volume change and (B) insular volume change, as extracted from linear mixed effects models (model D) in non-carriers (green), presymptomatic carriers (blue), symptomatic carriers (red) and converters (orange). Shaded areas represent 95% confidence intervals. All brain volumes are expressed as a percentage of total intracranial volume.

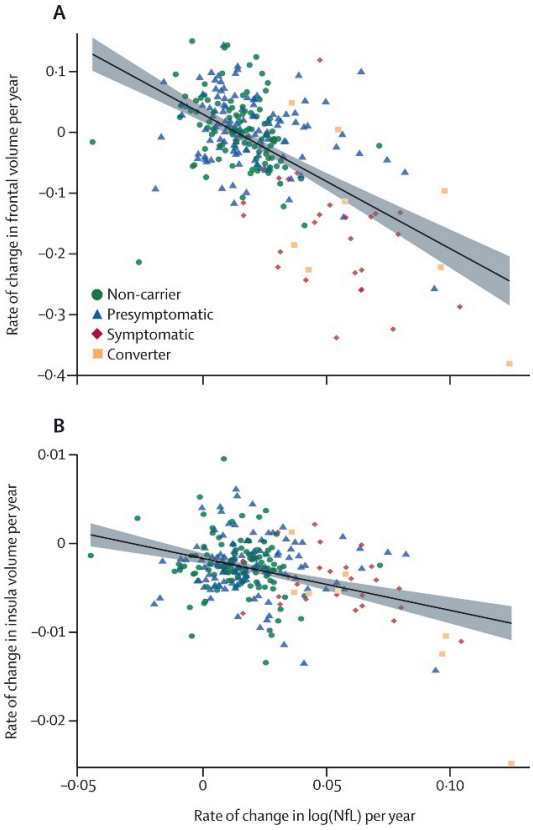

Discussion

The present longitudinal study of the largest cohort of (pre)-symptomatic genetic FTD showed stable NfL levels in most presymptomatic mutation carriers, a significant NfL increase over conversion to the symptomatic stage, and stable, elevated NfL over the course of FTD. Increases in NfL were associated with more pronounced atrophy rates in several brain regions.

We found markedly elevated blood NfL in patients with genetic FTD, with good diagnostic accuracy to distinguish symptomatic from presymptomatic mutation carriers, in accordance with previous cross-sectional studies.[4-6] The correlation between cross-sectional NfL and

MMSE supports the clinical relevance of this biomarker. We confirmed the previous finding of especially high NfL in *GRN*-associated FTD,[4,5,17,18] which may be due to extensive white matter pathology.[19]

We describe three major findings regarding presymptomatic NfL increases. First, in converters, baseline NfL (1-2 years before symptom onset) was higher than in non-converting presymptomatic mutation carriers. Similar findings have been reported in familial ALS.[20] Second, we found higher baseline NfL in presymptomatic mutation carriers compared to non-carriers from the age of 48 years. These presymptomatic NfL increases likely reflect early axonal damage in a prodromal disease stage,[21] which may be a promising intervention-time for disease-modifying therapies. The good diagnostic accuracy of baseline NfL to distinguish converters from non-converting carriers (albeit in small numbers) underlines the potential value of serum NfL as a candidate selection tool. More pre-conversion data is needed to determine whether the rate of NfL change might be even more sensitive to imminent conversion. Most converters in the present study were *GRN* mutation carriers, which may to some extent have driven the overall NfL increase in converters. In future studies it will be interesting to study possible gene-specific differences in the timing of NfL increases. Finally, the large NfL increases observed in a small number of non-converting presymptomatic mutation carriers, raise the question whether perhaps these subjects are approaching conversion. Further follow-up as part of the GENFI study will reveal whether or not this is the case.

The stable NfL levels in *C9orf72* and *MAPT* symptomatic carriers in the present study are consistent with observations in sporadic behavioural variant FTD,[18] ALS [20,22,23] and familial AD.[24] In *GRN* mutation carriers, on the other hand, an overall increase over time was seen with substantial fluctuations in NfL trajectories. Such fluctuations could hamper the use of NfL as a biomarker of treatment effect. Further research is needed to elucidate confounding factors of NfL in *GRN* mutation carriers. One possible explanation may lie in the severity of neuroinflammation, which is thought to play an important role in *GRN*-associated FTD.[25] Correlative analyses with longitudinal inflammatory biomarkers could be insightful for this purpose.

The correlation between rate of NfL change and atrophy rate of several brain regions is similar to previously reported associations for grey matter atrophy in primary progressive aphasia (PPA) and familial and sporadic AD.[24,26,27] It suggests that the speed of neuronal breakdown may determine the amount of NfL shed into the extracellular fluid and ultimately into the blood. The observed association with cerebellar volume could be driven by the *C9orf72* mutation carriers, for whom prominent cerebellar atrophy has been described.[28]

The prominent associations with subcortical structures support the hypothesis that areas rich in large-calibre myelinated axons contribute more strongly to NfL release, as NfL is an axonal protein.[7,18] It will be interesting to investigate whether NfL changes correlate with longitudinal white matter measures such as diffusion tensor imaging.

The lack of correlation between changes in NfL and changes in FTLD-CDR is not entirely surprising since most symptomatic mutation carriers had stable NfL despite functional deterioration. Possibly, NfL changes preceded major functional decline; more sensitive measures of early symptoms, such as neuropsychological test scores or behavioural measures, may be more suitable for these analyses.[10]

Thus far unexplained is why NfL increases around conversion, and appears to stabilise in most symptomatic mutation carriers. The release and accumulation of NfL is presumably counterbalanced by clearing mechanisms.[22] The presence of auto-antibodies against NfL, as previously described in ALS-patients, could contribute to this equilibrium.[29,30] The observed NfL increases and decreases in some symptomatic mutation carriers could be explained by disturbances in this equilibrium, e.g. during periods of more rapid or slow brain atrophy. Interestingly, NfL decreases were also previously described in some patients with behavioural variant FTD [18] and PPA.[26]

In two non-carriers and two presymptomatic mutation carriers, we found high NfL at baseline with rapid decreases over follow-up. We found no evidence of sample processing or assay-based causes for these unexpected fluctuations. Although brief medical history and neurological examination did not reveal any relevant neurological disorders, asymptomatic or minor (transient) neurological comorbidities as causative factors cannot be ruled out. A more detailed understanding of confounding factors of serum NfL is important for its clinical application and requires further study.

Major strengths of this study are the large number of presymptomatic and symptomatic mutation carriers, all of whom had multiple NfL measurements, and the availability of corresponding neuroimaging datasets. The inclusion of carriers of pathogenic mutations allowed us to create pathologically homogeneous cohorts, in contrast to studies of patients with clinically defined FTD. Accurate measurement of NfL was ensured using the ultrasensitive Simoa technology, which offers superior analytical sensitivity compared to ELISA and electrochemiluminescence.[7,31] Finally, we included samples from mutation carriers across the entire spectrum of disease, from presymptomatic to advanced stages of FTD.

A potential weakness is that symptom onset was based, as in a clinical setting, on retrospective estimations given by a caregiver, which could introduce a certain amount of

inaccuracy due to the insidious nature of FTD. Inevitably, in converters a certain time interval exists between symptom onset and the diagnosis of FTD. We ensured that this interval did not influence our estimates of NfL increase by plotting individual NfL changes against symptom onset rather than diagnosis. The risk of bias due to use of data from multiple centres was likely diminished through the use of standardised protocols and statistical correction for study site. The relationship between the slope of NfL change and changes over time in brain volume and clinical parameters must be interpreted in light of limitations of the applied statistical model, which used the estimated NfL slope as a fixed effect and therefore did not account for variability of this estimation. Finally, for correlative neuroimaging analyses, we used combined volumes for left and right hemispheres and therefore did not account for asymmetric atrophy.

In conclusion, this study underlines the value of serum NfL as an easily accessible biomarker in genetic FTD. Repeated measurements may be a suitable measure of disease activity in mutation carriers before symptom onset. Replication of our findings in a larger dataset with longer follow-up, allowing for longitudinal evaluation of NfL with more complex statistical models, is needed to confirm this. The characterisation of NfL over the course of genetic FTD provides valuable information for its use as a surrogate marker of treatment effect in therapeutic trials.

Acknowledgements

We thank all participants and their family members for taking part in this study.

This study was supported in the Netherlands by two Memorabel grants from Deltaplan Dementie (The Netherlands Organisation for Health Research and Development and Alzheimer Nederland; grant numbers 733050813 and 733050103), the Bluefield Project to Cure Frontotemporal Dementia, the Dioraphte foundation (grant number 1402 1300), and the European Joint Programme – Neurodegenerative Disease Research and the Netherlands Organisation for Health Research and Development (PreFrontALS: 733051042, RiMod-FTD: 733051024); in Spain by the EU Joint Programme – Neurodegenerative Disease Research (JPND) network PreFrontALS (01ED1512/AC14/00013) and Fundacio Marato de TV3 (grant number 20143810); in Sweden by grants from JPND Prefrontals Swedish Research Council (VR) 529-2014-7504, Swedish Research Council (VR) 2015-02926, Swedish Research Council (VR) 2018-02754, Swedish FTD Initiative- Schörling Foundation, Swedish Brain Foundation, Swedish Alzheimer Foundation, Stockholm County Council ALF, Karolinska Institutet Doctoral Funding and StratNeuro, Swedish Demensfonden, during the conduct of the study; in Italy

by the Italian Ministry of Health (Ricerca Corrente); in Germany by the JPND network PreFrontAls (01ED1512), the German Federal Ministry of Education and Research (FTLDc O1GI1007A), the EU (FAIR-PARK II), the German Research Foundation/DFG (VO2028, SFB1279), the foundation of the state Baden-Württemberg (D.3830) and the Thierry Latran Foundation; in the United Kingdom by the Medical Research Council UK (MR/M023664/1), Alzheimer Society (AS-PG-15-025) and Alzheimer's Research UK. J.D.R. is an MRC Clinical Scientist (MR/M008525/1) and has received funding from the NIHR Rare Diseases Translational Research Collaboration (BRC149/NS/MH). J.L. reports consulting fees from Aesku, speaker's fees from Bayer Vital, speaker's fees from Willi Gross Foundation, consulting fees from Axon Neuroscience, consulting fees from Ionis Pharmaceuticals, and non-financial support from Abbvie, all outside the submitted work. JBR is supported by the Wellcome Trust (103838) and the National Institute for Health Research Cambridge Biomedical Research Centre, and Holt Fellowship.

Author contributions

ELvdE and JCvS contributed to data acquisition, conception and design of the study, statistical analysis, and drafting of the manuscript and figures. JDR and LHM contributed to data acquisition and conception and design of the study. DR contributed to the statistical analyses. IV and CET performed NfL measurements. The remaining authors recruited patients and collected data. All authors critically reviewed the manuscript and approved the final draft.

Declaration of interest

The authors report no potential conflicts of interest with respect to this manuscript.

References

1. Rascovsky K, Hodges JR, Knopman D, et al. Sensitivity of revised diagnostic criteria for the behavioural variant of frontotemporal dementia. Brain. 2011;134(Pt 9):2456-77.
2. Gorno-Tempini ML, Hillis AE, Weintraub S, et al. Classification of primary progressive aphasia and its variants. Neurology. 2011;76(11):1006-14.
3. Lashley T, Rohrer JD, Mead S, et al. Review: an update on clinical, genetic and pathological aspects of frontotemporal lobar degenerations. Neuropathol Appl Neurobiol. 2015;41(7):858-81.
4. Meeter LH, Dopper EG, Jiskoot LC, et al. Neurofilament light chain: a biomarker for genetic frontotemporal dementia. Ann Clin Transl Neurol. 2016;3(8):623-36.
5. Rohrer JD, Woollacott IO, Dick KM, et al. Serum neurofilament light chain protein is a measure of disease intensity in frontotemporal dementia. Neurology. 2016;87(13):1329-36.
6. Scherling CS, Hall T, Berisha F, et al. Cerebrospinal fluid neurofilament concentration reflects disease severity in frontotemporal degeneration. Ann Neurol. 2014;75(1):116-26.
7. Khalil M, Teunissen CE, Otto M, et al. Neurofilaments as biomarkers in neurological disorders. Nat Rev Neurol. 2018;14(10):577-89.
8. Varhaug KN, Torkildsen O, Myhr KM, et al. Neurofilament Light Chain as a Biomarker in Multiple Sclerosis. Front Neurol. 2019;10:338.
9. Bacioglu M, Maia LF, Preische O, et al. Neurofilament Light Chain in Blood and CSF as Marker of Disease Progression in Mouse Models and in Neurodegenerative Diseases. Neuron. 2016;91(1):56-66.
10. Rohrer JD, Nicholas JM, Cash DM, et al. Presymptomatic cognitive and neuroanatomical changes in genetic frontotemporal dementia in the Genetic Frontotemporal dementia Initiative (GENFI) study: a cross-sectional analysis. Lancet Neurol. 2015;14(3):253-62.
11. Brooks BR, Miller RG, Swash M, et al. El Escorial revisited: revised criteria for the diagnosis of amyotrophic lateral sclerosis. Amyotroph Lateral Scler Other Motor Neuron Disord. 2000;1(5):293-9.
12. Cardoso MJ, Modat M, Wolz R, et al. Geodesic Information Flows: Spatially-Variant Graphs and Their Application to Segmentation and Fusion. IEEE Trans Med Imaging. 2015;34(9):1976-88.
13. Freeborough PA, Fox NC, Kitney RI. Interactive algorithms for the segmentation and quantitation of 3-D MRI brain scans. Comput Methods Programs Biomed. 1997;53(1):15-25.
14. Malone IB, Leung KK, Clegg S, et al. Accurate automatic estimation of total intracranial volume: a nuisance variable with less nuisance. Neuroimage. 2015;104:366-72.
15. Seelaar H, Kamphorst W, Rosso SM, et al. Distinct genetic forms of frontotemporal dementia. Neurology. 2008;71(16):1220-6.
16. van Swieten JC, Heutink P. Mutations in progranulin (GRN) within the spectrum of clinical and pathological phenotypes of frontotemporal dementia. Lancet Neurol. 2008;7(10):965-74.

17. Goossens J, Bjerke M, Van Mossevelde S, et al. Diagnostic value of cerebrospinal fluid tau, neurofilament, and progranulin in definite frontotemporal lobar degeneration. Alzheimers Res Ther. 2018;10(1):31.
18. Steinacker P, Anderl-Straub S, Diehl-Schmid J, et al. Serum neurofilament light chain in behavioral variant frontotemporal dementia. Neurology. 2018;91(15):e1390-e401.
19. Sudre CH, Bocchetta M, Cash D, et al. White matter hyperintensities are seen only in GRN mutation carriers in the GENFI cohort. Neuroimage Clin. 2017;15:171-80.
20. Benatar M, Wuu J, Andersen PM, et al. Neurofilament light: A candidate biomarker of presymptomatic amyotrophic lateral sclerosis and phenoconversion. Ann Neurol. 2018;84(1):130-9.
21. Weston PSJ, Poole T, O'Connor A, et al. Longitudinal measurement of serum neurofilament light in presymptomatic familial Alzheimer's disease. Alzheimers Res Ther. 2019;11(1):19.
22. Lu CH, Macdonald-Wallis C, Gray E, et al. Neurofilament light chain: A prognostic biomarker in amyotrophic lateral sclerosis. Neurology. 2015;84(22):2247-57.
23. Verde F, Steinacker P, Weishaupt JH, et al. Neurofilament light chain in serum for the diagnosis of amyotrophic lateral sclerosis. J Neurol Neurosurg Psychiatry. 2018.
24. Preische O, Schultz SA, Apel A, et al. Serum neurofilament dynamics predicts neurodegeneration and clinical progression in presymptomatic Alzheimer's disease. Nat Med. 2019.
25. Chitramuthu BP, Bennett HPJ, Bateman A. Progranulin: a new avenue towards the understanding and treatment of neurodegenerative disease. Brain. 2017;140(12):3081-104.
26. Steinacker P, Semler E, Anderl-Straub S, et al. Neurofilament as a blood marker for diagnosis and monitoring of primary progressive aphasias. Neurology. 2017;88(10):961-9.
27. Mattsson N, Cullen NC, Andreasson U, et al. Association Between Longitudinal Plasma Neurofilament Light and Neurodegeneration in Patients With Alzheimer Disease. JAMA Neurol. 2019.
28. Meeter LH, Kaat LD, Rohrer JD, et al. Imaging and fluid biomarkers in frontotemporal dementia. Nat Rev Neurol. 2017;13(7):406-19.
29. Fialova L, Svarcova J, Bartos A, et al. Cerebrospinal fluid and serum antibodies against neurofilaments in patients with amyotrophic lateral sclerosis. Eur J Neurol. 2010;17(4):562-6.
30. Puentes F, Topping J, Kuhle J, et al. Immune reactivity to neurofilament proteins in the clinical staging of amyotrophic lateral sclerosis. J Neurol Neurosurg Psychiatry. 2014;85(3):274-8.
31. Kuhle J, Barro C, Andreasson U, et al. Comparison of three analytical platforms for quantification of the neurofilament light chain in blood samples: ELISA, electrochemiluminescence immunoassay and Simoa. Clin Chem Lab Med. 2016;54(10):1655-61.

Supplementary file 1: Statistical analyses

All analyses were performed in *R* using linear regression or linear mixed-effects models through the nlme package (https://cran.r-project.org/web/packages/nlme/nlme.pdf).

Baseline linear regression NfL – brain volume (model A1):
lm(Log(NfL)~[brain_volume] + baseline_age + sex + scanner/study site)

Baseline linear regression NfL – MMSE (model A2):
lm(Log(NfL)~baseline_MMSE + baseline_age + sex + study_site)

Baseline linear regression NfL – FTLD-CDR (model A3):
lm(Log(NfL)~baseline_FTLD-CDR + baseline_age + sex + study_site)

Baseline NfL - age in asymptomatic mutation carriers (model B):
lm(Log(NfL)~baseline_age + carrier_status + baseline_age*carrier_status)

NfL change over time (model C):
lme(log(NfL)~time + clinical_status + time * clinical_status + baseline_age + sex + study site, random = ~time|subject_ID)

Post-hoc testing for different NfL trajectories by mutation group:
lme(log(NfL)~time + mutation_clinical + time * mutation_clinical + baseline_age + sex + study site, random = ~time|subject_ID)

Rate of biomarker change (model D):
lme([biomarker])~time, random=~time|subject_ID)
--coef() function used to generate individual regression coefficients per subject—

Relating extracted rate of NfL change with rate of brain volume change on longitudinal MRI (model E1):
lme([brain volume]~time + rate_NfL_change + time* rate_NfL_change + baseline_age + sex + scanner/study site, random=~time|subject_ID)

Relating extracted rate of NfL change with rate of MMSE decline (model E2):
lme(MMSE~time + rate_NfL_change + time* rate_NfL_change + baseline_age + sex + study site, random=~time|subject_ID)

Relating extracted rate of NfL change with rate of FTLD-CDR increase (model E3):
lme(FTLD-CDR~time + rate_NfL_change + time* rate_NfL_change + baseline_age + sex + study site, random=~time|subject_ID)

Abbreviations

time	Time in years since baseline sample
baseline_age	Age in years at baseline sample
brain_volume	Regional grey matter volume expressed as a percentage of total intracranial volume
biomarker	Log(NfL), regional brain volume (figure 4), or MMSE (figure S7)
carrier_status	Mutation carrier or non-carrier
clinical_status	Non-carrier, presymptomatic mutation carrier, symptomatic mutation carrier or converter
mutation_clinical	Combination of genetic mutation group and clinical status, i.e. non-carrier, presymptomatic *GRN* mutation carrier, presymptomatic *C9orf72* mutation carrier, presymptomatic *MAPT* mutation carrier, symptomatic *GRN* mutation carrier, symptomatic *C9orf72* mutation carrier, symptomatic *MAPT* mutation carrier, or converter.
scanner/study site	All combinations of study site and MRI scanner type

Supplementary file 2: Figures and tables

Supplementary figure S1. Number of samples collected at various time points during follow-up. Time = 0 indicates baseline sample collection (n=335).

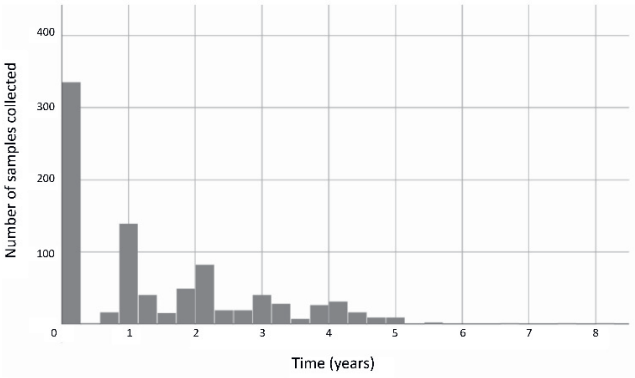

Supplementary figure S2. (A) Histogram plot showing distribution of baseline NfL levels across all clinical groups. (B) Residuals of log(NfL) at baseline for ANCOVA in different clinical groups (Kolmogorov-Smirnov statistic=0.041; p=0.200).

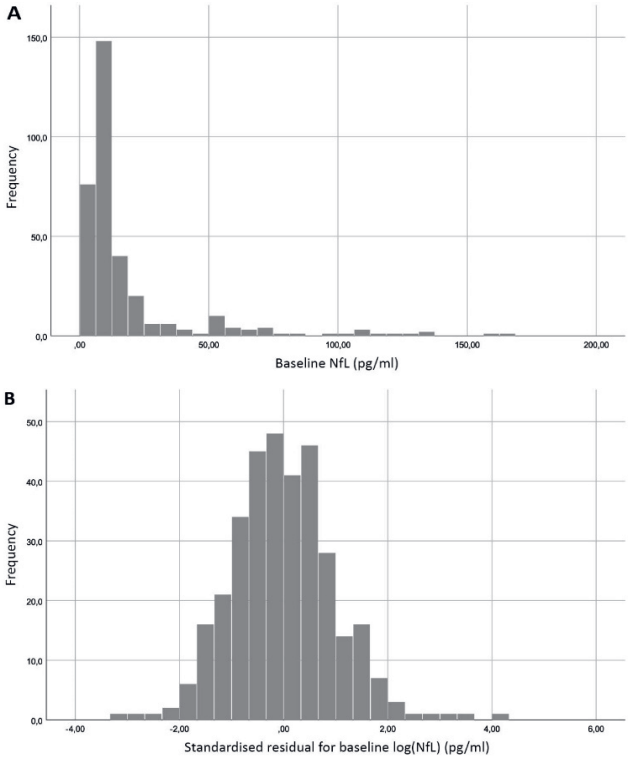

Supplementary figure S3. Receiver operating characteristic (ROC) curves for NfL at baseline. (A) symptomatic mutation carriers versus non-carriers (AUC 0.95 [95% CI 0.92-0.98]); (B) symptomatic mutation carriers versus presymptomatic mutation carriers (AUC 0.93 [95% CI 0.90-0.97]); (C) Presymptomatic mutation carriers who converted during follow-up versus non-converting presymptomatic mutation carriers (AUC 0.93 [95% CI 0.89-0.98]).

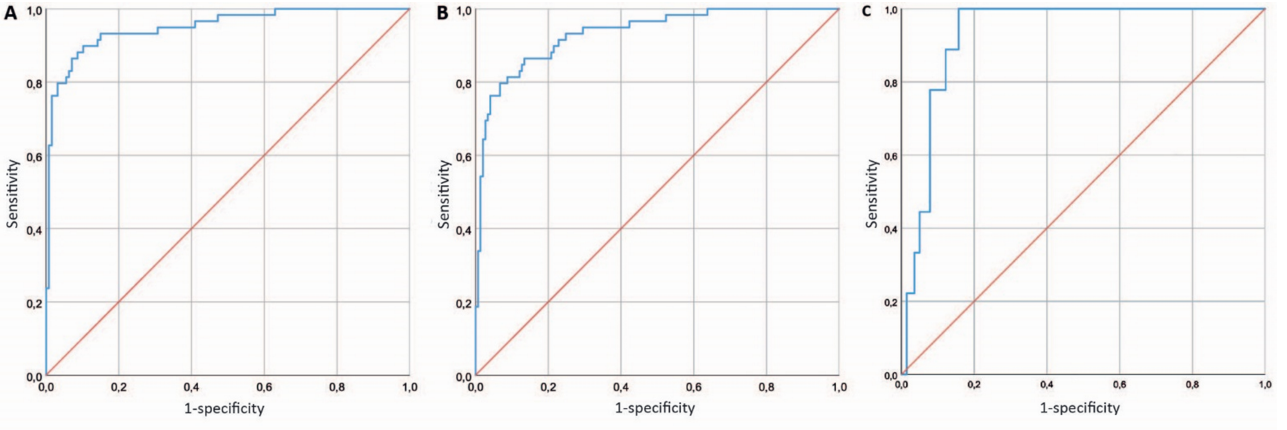

Supplementary figure S4. Individual NfL trajectories in non-carriers. To facilitate interpretation of visually unstable NfL trajectories, subjects with annualised changes of >5 pg/ml (calculated by subtracting the first from the last NfL measurement and dividing by total follow-up time) are highlighted in black. The remaining subjects are shown in grey.

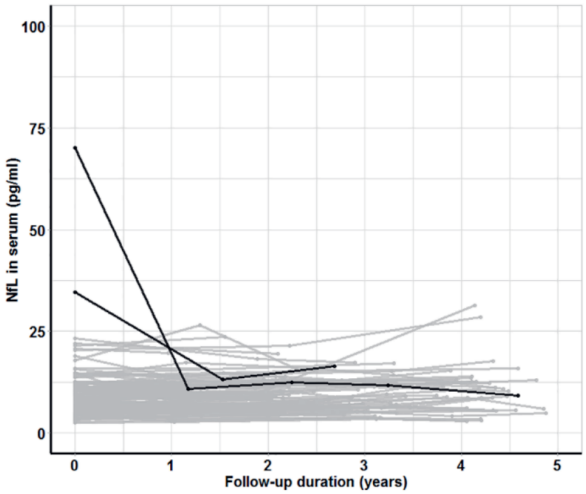

Supplementary figure S5. Individual NfL trajectories in presymptomatic and symptomatic mutation carriers. (A-C) Presymptomatic *GRN, C9orf72* and *MAPT* mutation carriers; (D-F) Symptomatic *GRN, C9orf72* and *MAPT* mutation carriers. To facilitate interpretation of visually unstable NfL trajectories, subjects with annualised changes of >5 pg/ml (calculated by subtracting the first from the last NfL measurement and dividing by total follow-up time) are highlighted in black. For visualisation purposes, follow-up duration was limited to six years; two symptomatic mutation carriers (1 *GRN*, 1 *C9orf72*) with longer follow-up durations (8.1 and 7.7 years) had visually stable NfL levels over time.

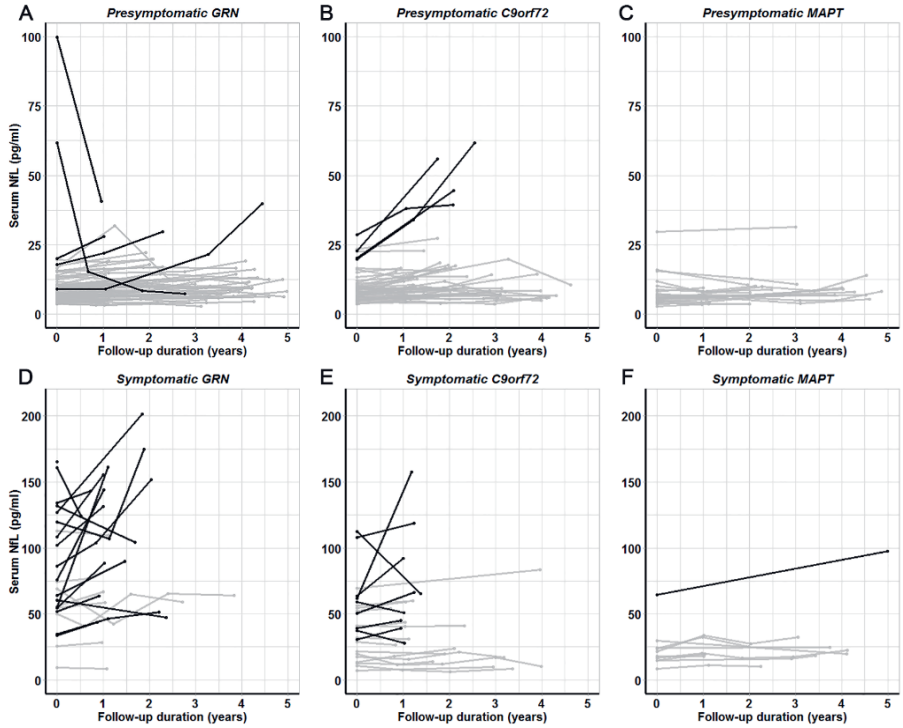

Supplementary figure S6. NfL and frontal lobe volume (as a percentage of total intracranial volume, TIV) in eight converters. The course of NfL over time is shown in red (left y-axis); frontal lobe volume is shown in blue (right y-axis). For converter no. 9 (not shown), no MRI scans were available.

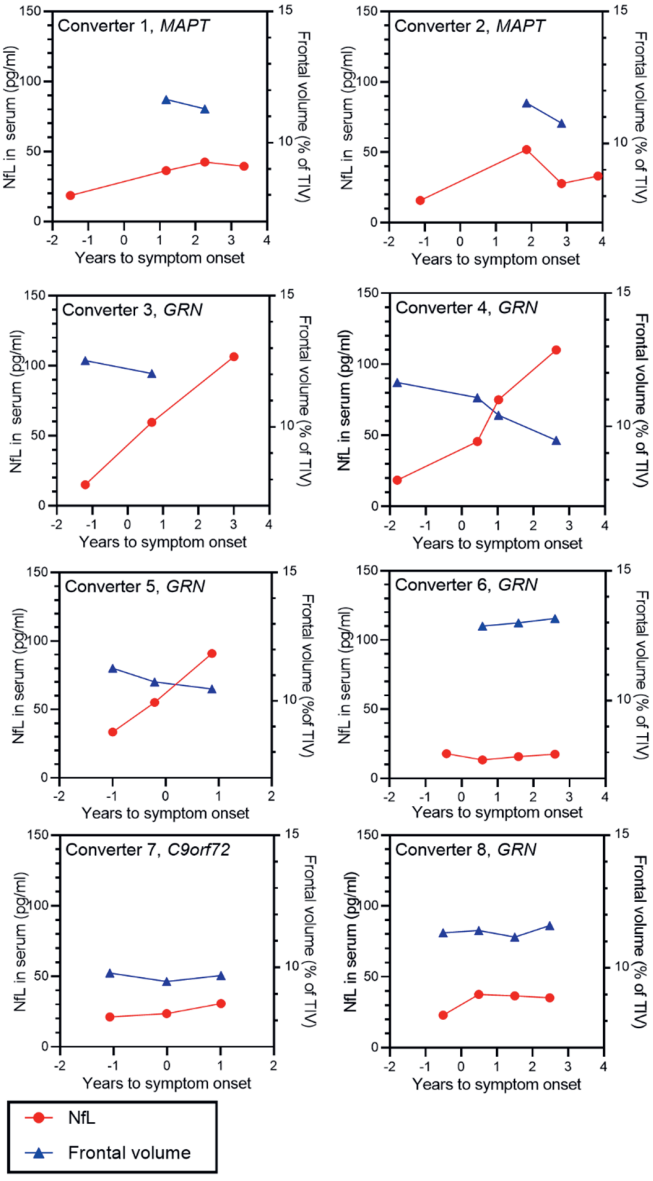

Supplementary figure S7. Relationship between the annual rate of log(NfL) change and the rate of MMSE change, as extracted from linear mixed effects models (model D) in symptomatic mutation carriers. Shaded areas represent 95% confidence intervals.

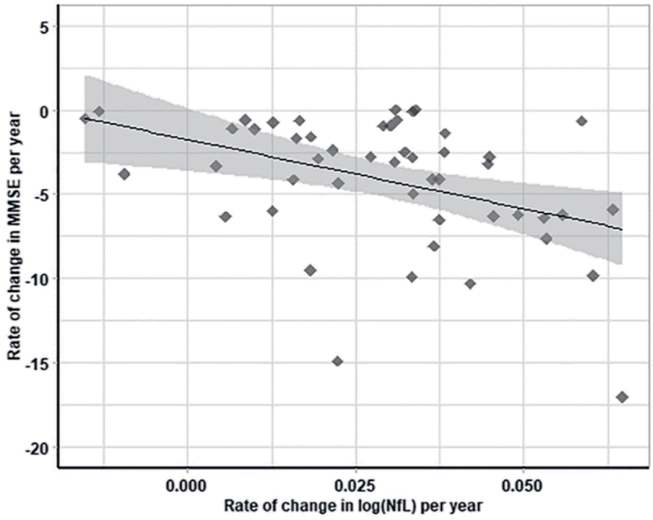

Supplementary table S1. Number of samples per subject and time since baseline sample (displayed as median (interquartile range)).

No. of samples	N	Time since baseline sample (years)
1 (baseline)	335	0
2	335	1.2 (1.0-2.0)
3	156	3.0 (2.1-3.9)
4	51	4.1 (2.7-6.6)
5	7	4.1 (3.9-7.7)
6	2	4.9 (4.9-5.9)

Supplementary table S2. Clinical characteristics and NfL levels for converters. Age at symptom onset is as reported retrospectively by a caregiver. bvFTD, behavioural variant FTD; PPA, primary progressive aphasia; MMSE, Mini Mental State Examination; FTLD-CDR, Frontotemporal Lobar Degeneration-Clinical Dementia Rating scale.

	Visit 1	Visit 2	Visit 3	Visit 4
Converter 1: MAPT mutation carrier; male; age at symptom onset 45 years.				
NfL	19	36	42	39
Age (years)	44.0	46.7	47.8	48.9
FTLD-CDR	0	10	13.5	11.5
MMSE	30	29	27	20
Diagnosis	Presymptomatic	bvFTD		
Converter 2: MAPT mutation carrier; male; age at symptom onset 40 years.				
NfL	16	52	28	33
Age (years)	39.6	42.6	43.6	44.6
FTLD-CDR	0	0	4.5	5.5
MMSE	30	29	29	28
Diagnosis	Presymptomatic		bvFTD	
Converter 3: GRN mutation carrier; female; age at symptom onset 57 years.				
NfL	15	60	106	
Age (years)	56.4	58.3	60.6	
FTLD-CDR	0	1	24	
MMSE	27	26	0	
Diagnosis	Presymptomatic	Non-fluent variant PPA		
Converter 4: GRN mutation carrier; female; age at symptom onset 51 years.				
NfL	19	46	75	110
Age (years)	50.0	52.2	52.8	54.4
FTLD-CDR	0	1	2	20
MMSE	28	29	27	0
Diagnosis	Presymptomatic	Non-fluent variant PPA		
Converter 5: GRN mutation carrier; female; age at symptom onset 55 years.				
NfL	34	55	91	
Age (years)	53.9	54.7	55.8	
FTLD-CDR	Not available	Not available	10.5	
MMSE	29	26	26	
Diagnosis	Presymptomatic			bvFTD
Converter 6: GRN mutation carrier; female; age at symptom onset 59 years.				
NfL	18	13	16	18
Age (years)	58.5	59.5	60.5	61.5
FTLD-CDR	Not available	2	3.5	Not available
MMSE	30	30	29	Not available
Diagnosis	Presymptomatic	bvFTD		
Converter 7: C9orf72 mutation carrier; male; age at symptom onset 68 years.				
NfL	21	24	31	
Age (years)	67.5	68.5	69.6	
FTLD-CDR	0	Not available	10	
MMSE	28	26	26	
Diagnosis	Presymptomatic			bvFTD

	Visit 1	Visit 2	Visit 3	Visit 4
Converter 8: GRN mutation carrier; female; age at symptom onset 71 years.				
NfL	23	38	37	35
Age (years)	70.5	71.5	72.5	73.5
FTLD-CDR	N/a	N/a	4	N/a
MMSE	25	25	21	20
Diagnosis	Presymptomatic	Memory-predominant FTD		
Converter 9: GRN mutation carrier; male; age at symptom onset 67 years.				
NfL	48	51		
Age (years)	67.7	68.8		
FTLD-CDR	0	8		
MMSE	28	27		
Diagnosis	Presymptomatic	PPA not otherwise specified		

Supplementary table S3a. Results of multiple linear regression models to study the association between baseline NfL and baseline brain volume (model A1). Linear regression models were constructed using the following formula: $Log(NfL) = \beta_1 * [brain\ volume] + \beta_2 * age + \beta_3 * sex + \beta_4 * scanner/study\ site$. Scanner/study site indicates the combination of study site and MRI scanner used. Each row represents a different model (n=276 for all models). Overall model statistics are shown as well as the regression coefficients for the brain volume variable. All brain volumes were expressed as a percentage of total intracranial volume. *b* denotes unstandardised regression coefficients; β denotes standardised regression coefficients. Abbreviations: SE: standard error; WBV: whole brain volume.

Brain volume	Overall model statistics			Brain volume coefficients per model				
	F (18, 257)	*p*	Adj. R^2	*b*	SE_b	B	T	*p**
Frontal	23.9	<0.0001	0.60	-0.115	0.016	-0.365	-7.01	<0.0001
Temporal	18.9	<0.0001	0.54	-0.084	0.029	-0.160	-2.95	0.045
Parietal	18.2	<0.0001	0.53	-0.054	0.029	-0.108	-1.93	0.717
Occipital	18.0	<0.0001	0.53	-0.035	0.028	-0.062	-1.27	0.999
WBV	20.1	<0.0001	0.56	-0.021	0.005	-0.448	-4.32	0.0003
Insula	19.9	<0.0001	0.55	-0.756	0.183	-0.212	-4.13	0.0006
Cingulate gyrus	19.4	<0.0001	0.55	-0.331	0.092	-0.172	-3.60	0.005
Cerebellum	17.7	<0.0001	0.52	-0.009	0.022	-0.021	-0.42	0.999
Thalamus	17.8	<0.0001	0.52	-0.112	0.230	-0.026	-0.49	0.999
Hippocampus	18.8	<0.0001	0.54	-0.778	0.272	-0.140	-2.86	0.059
Amygdala	18.1	<0.0001	0.53	-0.011	0.672	-0.078	-1.61	0.999
Putamen	18.5	<0.0001	0.53	-0.626	0.255	-0.120	-2.45	0.194
Caudate	17.9	<0.0001	0.53	-0.286	0.284	-0.047	-1.00	0.999

*After Bonferroni correction (p-value multiplied by 13 to correct for the use of 13 brain volume models)

Supplementary table S3b. Results of multiple linear regression models to study the association between baseline NfL and baseline Mini Mental State examination (MMSE) (n=55) and (2) Frontotemporal Lobar Degeneration Clinical Rating scale (FTLD-CDR) (n=48). Linear regression models were constructed using the following formula: Log(NfL) = β_1 * [cognitive test] + β_2 * age + β_3 * sex + β_4 * study site (model A2); For both models, overall model statistics are shown as well as the regression coefficients for MMSE and FTLD-CDR (i.e. β_1).

	b	SE_b	β	T	*p*
Intercept	0.324	0.058		5.54	<0.0001
Age at first sample	0.012	0.001	0.627	10.58	<0.0001
Carrier status	-0.100	0.082	-0.209	-1.22	0.222
Age at first sample * Carrier status	0.003	0.001	0.171	2.02	0.045

Supplementary table S4. Results of model B: baseline log(NfL) in presymptomatic mutation carriers and non-carriers by age. Reference category for carrier status: non-carriers. *b* denotes unstandardised regression coefficients, β denotes standardised regression coefficients. Overall model statistics: F(3,272)=95.4, p<0.001, R^2=0.51.

Cognitive test	Overall model statistics			Test coefficients per model				
	F	*p*	Adj. R^2	*b*	SE_b	β	T	*p*
MMSE	7.8 (11,4)	<0.0001	0.58	-0.021	0.007	-0.300	-3.10	0.003
FTLD-CDR	3.6 (10,4)	0.002	0.36	0.009	0.008	0.155	1.24	0.221

Supplementary table S5a. Fixed effects results from model C: NfL change over time. N=335 subjects; 886 observations. Abbreviations: SE: standard error; DF: degrees of freedom.

	Estimate	SE	DF	T	*p*
Intercept	0.318	0.053	547	5.96	<0.0001
Time	0.006	0.005	547	1.25	0.208
Clinical status (presymptomatic)	0.012	0.025	316	0.50	0.620
Clinical status (symptomatic)	0.464	0.037	316	12.54	<0.0001
Clinical status (converter)	0.351	0.068	316	5.19	<0.0001
Baseline age	0.012	0.001	316	13.60	<0.0001
Sex (female)	0.007	0.021	316	0.34	0.742
Time*Clinical status (Presymptomatic)	0.015	0.007	547	2.02	0.044
Time*Clinical status (Symptomatic)	0.017	0.010	547	1.59	0.101
Time*Clinical status (Converter)	0.097	0.018	547	5.56	<0.0001
Centre (2)	0.278	0.044	316	6.37	<0.0001
Centre (3)	-0.141	0.038	316	-3.75	0.0003
Centre (4)	0.010	0.051	316	0.20	0.841
Centre (5)	0.018	0.095	316	0.19	0.848
Centre (6)	-0.002	0.041	316	-0.05	0.962
Centre (7)	0.029	0.052	316	0.56	0.576
Centre (8)	0.023	0.046	316	0.51	0.610
Centre (9)	-0.039	0.049	316	-0.78	0.434
Centre (10)	0.055	0.047	316	1.15	0.250
Centre (11)	0.074	0.064	316	1.15	0.250
Centre (12)	-0.023	0.038	316	-0.61	0.545
Centre (13)	0.209	0.089	316	2.35	0.020
Centre (14)	0.050	0.086	316	0.59	0.557

Supplementary table S5b. F-tests for fixed effects from model C: NfL change over time.

	F	*p*
Intercept	11231.7 (1,547)	<0.0001
Time	24.4 (1,547)	<0.0001
Clinical status	255.4 (1,316)	<0.0001
Baseline age	187.0 (1,316)	<0.0001
Sex	0.4 (1,316)	0.529
Centre	5.8 (1,316)	<0.0001
Time*Clinical status	10.6 (1,547)	<0.0001

Supplementary table S5c. Standard deviation (SD) of random effects from model C: NfL change over time.

	SD
Intercept	0.017
Time	0.032
Residual	0.087

Supplementary table S6a. Fixed effects results from model C (NfL change over time) with post-hoc interaction term between time and mutation_clinical. Mutation_clinical was defined as the combination between the clinical status (i.e. non-carrier, presymptomatic mutation carrier, symptomatic mutation carrier or converter) and, in presymptomatic and symptomatic carriers, the genetic mutation group (i.e. *GRN, C9orf72, MAPT*). Due to the limited sample size, converters were not separated by genotype. SE: standard error; DF: degrees of freedom.

	Estimate	SE	DF	T	*p*
Intercept	0.298	0.049	543	6.14	<0.0001
Time	0.006	0.005	543	1.21	0.226
Presymptomatic *GRN*	-0.005	0.028	312	-0.20	0.844
Presymptomatic *C9orf72*	0.065	0.033	312	1.96	0.051
Presymptomatic *MAPT*	0.038	0.044	312	0.84	0.398
Symptomatic *GRN*	0.674	0.045	312	14.93	<0.0001
Symptomatic *C9orf72*	0.262	0.049	312	5.33	<0.0001
Symptomatic *MAPT*	0.303	0.062	312	4.92	<0.0001
Converter	0.344	0.063	312	5.48	<0.0001
Baseline age	0.013	0.001	312	15.56	<0.0001
Sex (female)	-0.001	0.019	312	-0.06	0.948
Time*Presymptomatic *GRN*	0.006	0.009	543	0.63	0.528
Time*Presymptomatic *C9orf72*	0.030	0.011	543	2.80	0.005
Time*Presymptomatic *MAPT*	0.013	0.013	543	1.04	0.298
Time*Symptomatic *GRN*	0.040	0.017	543	2.36	0.019
Time*Symptomatic *C9orf72*	0.007	0.016	543	0.45	0.650
Time*Symptomatic *MAPT*	0.013	0.018	543	0.73	0.464
Time*Converter	0.097	0.018	543	5.42	<0.0001
Centre (2)	0.214	0.042	312	5.13	<0.0001
Centre (3)	-0.117	0.034	312	-3.43	0.001
Centre (4)	-0.028	0.047	312	-0.58	0.559
Centre (5)	0.066	0.086	312	0.76	0.446
Centre (6)	0.012	0.037	312	0.32	0.746
Centre (7)	0.019	0.047	312	0.39	0.693
Centre (8)	0.015	0.041	312	0.36	0.719
Centre (9)	-0.052	0.046	312	-1.13	0.259
Centre (10)	0.028	0.043	312	0.64	0.525
Centre (11)	0.042	0.059	312	0.71	0.481
Centre (12)	-0.049	0.035	312	-1.37	0.170
Centre (13)	0.410	0.087	312	4.73	<0.0001
Centre (14)	0.128	0.079	312	1.62	0.106

Supplementary table S6b. F-tests for fixed effects from model C: NfL change over time with post-hoc interaction term between time and mutation_clinical.

	F	DF	*p*
Intercept	14367.4	543	<0.0001
Time	18.6	543	<0.0001
Mutation_clinical	154.4	312	<0.0001
Baseline age	242.8	312	<0.0001
Sex	0.2	312	0.660
Centre	5.9	312	<0.0001
Time*Mutation_clinical	5.4	543	<0.0001

Supplementary table S6c. Standard deviation (SD) of random effects from model model C: NfL change over time with post-hoc interaction term between time and mutation_clinical.

	SD
Intercept	0.163
Time	0.035
Residual	0.086

Supplementary table S7a. Results of mixed effects models to study the relationship between longitudinal regional brain volume and extracted longitudinal NfL change (model E1). The following formula was used: [brain volume] = time + time * rate_NfL_change + baseline_age + sex + study site, random=time|subject_ID. For these analyses, the primary variable of interest was time*rate_NfL_change; statistics of this variable are shown. Abbreviations: SE: standard error; DF: degrees of freedom; WBV: whole brain volume.

Brain volume	Model coefficients for Time*Rate_NfL change				
	F (1,348)	Estimate	SE	T	p*
Frontal	55.4	-3.124	0.420	-7.44	<0.0001
Temporal	16.5	-1.014	0.250	-4.06	0.001
Parietal	3.1	-0.555	0.328	-1.69	0.789
Occipital	0.0	-0.251	0.421	-0.60	0.552
WBV	15.8	-9.528	2.379	-4.01	0.001
Insula	31.1	-0.198	0.035	-5.59	<0.0001
Cingulate gyrus	27.6	-0.337	0.064	-5.27	<0.0001
Cerebellum	10.4	-0.409	0.129	-3.18	0.026
Thalamus	0.8	-0.035	0.046	-0.76	0.449
Hippocampus	20.2	-0.075	0.017	-4.52	<0.0001
Amygdala	11.1	-0.041	0.012	-3.35	0.012
Putamen	79.8	-0.213	0.023	-8.97	<0.0001
Caudate	3.0	-0.052	0.030	-1.74	0.997

* After Bonferroni correction (p-value multiplied by 13 to correct for the use of 13 brain volume models)

Supplementary table S7b. Results of mixed effects models to study the relationship between longitudinal cognitive tests scores (MMSE (n=49) (model E2) and FTLD-CDR (n=47) (model E3) and extracted longitudinal NfL change in symptomatic mutation carriers. The following formula was used:
[Cognitive test score] = Time + Time * rate_NfL_change + baseline_age + sex + study site, random=time|subject_ID. For these analyses, the primary variable of interest was time*rate_NfL_change; statistics of this variable are reported.

Cognitive test	Model coefficients for Time*Rate_NfL_change				
	F (df)	Estimate	SE	T	*p*
MMSE	7.8 (1,72)	-94.7	33.9	-3.10	0.003
FTLD-CDR	0.01 (1,55)	-3.46	46.3	-0.08	0.941

Chapter 2.2

Neuronal pentraxin 2: a synapse-derived CSF biomarker in genetic frontotemporal dementia

Emma L. van der Ende, Mei-Fang Xiao, Desheng Xu, Jackie M. Poos, Jessica L. Panman, Lize C. Jiskoot, Lieke H. Meeter, Elise G.P. Dopper, Janne M. Papma, Carolin Heller, Rhian Convery, Katrina M. Moore, Martina Bocchetta, Mollie Neason, Georgia Peakman, David M. Cash, Charlotte E. Teunissen, Caroline Graff, Matthis Synofzik, Fermin Moreno, Elizabeth Finger, Raquel Sanchez-Valle, Rik Vandenberghe, Robert Laforce Jr, Mario Masellis, Maria Carmela Tartaglia, James B. Rowe, Chris Butler, Simon Ducharme, Alex Gerhard, Adrian Danek, Johannes Levin, Yolande A.L. Pijnenburg, Markus Otto, Barbara Borroni, Fabrizio Tagliavini, Alexandre de Mendonça, Isabel Santana, Daniela Galimberti, Harro Seelaar, Jonathan D. Rohrer, Paul F. Worley, John C. van Swieten, on behalf of the Genetic Frontotemporal Dementia Initiative (GENFI)

Journal of Neurology, Neurosurgery and Psychiatry 2020;9(6):612-621

Abstract

Introduction: Synapse dysfunction is emerging as an early pathological event in frontotemporal dementia (FTD), however biomarkers are lacking. We aimed to investigate the value of cerebrospinal fluid (CSF) neuronal pentraxins (NPTXs), a family of proteins involved in homeostatic synapse plasticity, as novel biomarkers in genetic FTD.

Methods: We included 106 presymptomatic and 54 symptomatic carriers of a pathogenic mutation in *GRN*, *C9orf72* or *MAPT*, and 70 healthy non-carriers participating in the Genetic Frontotemporal dementia Initiative (GENFI), all of whom had at least one CSF sample. We measured CSF concentrations of NPTX2 using an in-house ELISA, and NPTX1 and NPTX receptor (NPTXR) by Western blot. We correlated NPTX2 with corresponding clinical and neuroimaging datasets as well as with CSF neurofilament light chain (NfL) using linear regression analyses.

Results: Symptomatic mutation carriers had lower NPTX2 concentrations (median 643pg/ml, interquartile range (301-872)) than presymptomatic carriers (1003pg/ml (632-1338), $p<0.001$) and non-carriers (990pg/ml (604-1373), $p<0.001$) (corrected for age). Similar results were found for NPTX1 and NPTXR. Among mutation carriers, NPTX2 concentration correlated with several clinical disease severity measures, NfL, and grey matter volume of the frontal and parietal lobes, insula and whole brain. NPTX2 predicted subsequent decline in phonemic verbal fluency and Clinical Dementia Rating scale (CDR) plus FTD modules. In longitudinal CSF samples, available in 13 subjects, NPTX2 decreased around symptom onset and in the symptomatic stage.

Discussion: We conclude that NPTX2 is a promising synapse-derived disease progression biomarker in genetic FTD.

Introduction

Frontotemporal dementia (FTD), a common form of early-onset dementia, has an autosomal dominant inheritance in 20-30% of patients, most often due to mutations in granulin (*GRN*), chromosome 9 open reading frame 72 (*C9orf72*) or microtubule-associated protein tau (*MAPT*).[1] Developing sensitive biomarkers to detect disease onset at an early, even preclinical stage is of utmost importance for upcoming therapeutic interventions. Genetic forms of FTD provide a unique opportunity to study disease progression from presymptomatic to overt FTD and to identify novel biomarkers.

Our previous proteomics study identified neuronal pentraxin receptor (NPTXR) in cerebrospinal fluid (CSF) as the most promising candidate biomarker in genetic FTD with markedly reduced levels in the symptomatic stage.[2] NPTXR forms complexes with NPTX1 and NPTX2 (also termed Neuronal activity related protein, Narp) at excitatory synapses of pyramidal neurons onto parvalbumin interneurons and contributes to synaptic homeostatic plasticity.[3,4] Increasing evidence suggests that dysfunction and degeneration of synapses is an early pathological event in FTD,[5-7] especially in *GRN*-associated FTD,[8-10] a concept widely recognised in other neurodegenerative diseases.[5,11] Fluid biomarkers reflecting synaptic integrity in FTD might therefore contribute to an early diagnosis and monitoring of disease progression in clinical practice and clinical trials. Following studies in Alzheimer's disease (AD) that identified NPTXs as candidate biomarkers,[12-20] we hypothesised that NPTXs could be valuable synapse-derived biomarkers in genetic FTD.

In the present study, we measured CSF NPTXs in a large cohort of *GRN*, *C9orf72* and *MAPT* mutation carriers participating in the international Genetic FTD Initiative (GENFI). We focused our attention on NPTX2, as the available ELISA for NPTX2 allowed for more accurate quantitative measurements than the Western blots used for NPTX1 and NPTXR. We explored the relationship between NPTX2 and clinical disease severity, grey matter volume and CSF neurofilament light chain (NfL), a marker of neuroaxonal damage.[21]

Methods

Subjects

Subjects were included from 16 centres across Europe and Canada participating in GENFI, a longitudinal cohort study of patients with FTD due to a pathogenic mutation in *GRN*, *C9orf72* or *MAPT* and healthy 50% at-risk relatives (either presymptomatic mutation carriers or non-carriers). Participants underwent an annual assessment as previously described,[22] including neurological and neuropsychological examination, magnetic resonance imaging

(MRI) of the brain, and collection of blood and CSF. Knowledgeable informants completed questionnaires about potential changes in cognition or behaviour.

For the present study, we included all participants with at least one CSF sample, amounting to 54 symptomatic mutation carriers (15 *GRN*, 31 *C9orf72*, 8 *MAPT*), 106 presymptomatic mutation carriers (47 *GRN*, 42 *C9orf72*, 17 *MAPT*), and 70 non-carriers. Longitudinal CSF samples were available in thirteen subjects.

Mutation carriers were considered symptomatic if they fulfilled international consensus criteria for FTD.[23,24] Furthermore, as *C9orf72* mutations are also associated with amyotrophic lateral sclerosis (ALS), which is increasingly considered part of the FTD disease spectrum,[1] *C9orf72* mutation carriers fulfilling criteria for ALS,[25] but not FTD, were also considered symptomatic. We calculated disease duration based on a caregiver's estimation of the emergence of first symptoms.

Global cognition was scored using the Mini Mental State Examination (MMSE) and Clinical Dementia Rating scale (CDR) plus FTD modules.[26] The Revised Cambridge Behavioural Inventory (CBI-R) was used to measure behavioural changes.[27] The Trail Making Test part B (TMT-B) and phonemic verbal fluency were included as measures of executive functioning.[28] TMT-B was truncated to 300 seconds for subjects that exceeded the time limit. All scores were collected within six months of CSF collection.

T1-weighted MRI on 3 Tesla scanners was obtained within six months of CSF collection in 190 participants (35 symptomatic and 91 presymptomatic mutation carriers, 64 non-carriers). All MRI scans were acquired using a standardised GENFI protocol.[22] T1-weighted volumetric MRI scans were parcellated into brain regions as previously described,[22] using an atlas propagation and fusion strategy [29] to generate volumes of the whole brain, frontal, temporal, parietal and occipital lobes, insula and cingulate gyrus. Brain volumes were expressed as a percentage of total intracranial volume (TIV), computed with SPM12 running under Matlab R2014b (Math Works, Natick, MA, USA).[30]

Sample collection and laboratory methods

CSF was collected in polypropylene tubes, centrifuged and stored at -80°C within two hours of withdrawal according to a standardised GENFI protocol.

NPTX2 concentrations were measured using an in-house ELISA as described previously.[12] The intra- and inter-assay coefficients of variation (CV) were <2% and <5% respectively. The lower limit of quantification (LLOQ) was 5 pg/ml; all NPTX2 measurements were above the LLOQ. NPTX1 and NPTXR were measured by Western blot. Rabbit anti-NPTX1 was described

previously[3]; sheep anti-NPTXR antibody is from R&D systems (Cat. Number: AF4414; RRID: AB_2153869). Immunoreactive bands were visualised by the enhanced chemiluminescent substrate (ECL, Pierce) on X-ray film and quantified using the image software TINA (www.tina-vision.net). Western blot results were expressed as a percentage of abundancy compared to non-carriers, i.e. mean abundancy in non-carriers was set at 100%. Detailed methods are reported in supplementary file 2.

All NPTX measurements were performed in two batches in the Neuroscience laboratory at Johns Hopkins University, Baltimore, USA. The mean CV of NPTX2 of the two batches was 5.4%. Longitudinal measurements were performed in one batch.

CSF NfL concentrations were measured in duplicate in one batch using the Simoa NF-Light Advantage Kit from Quanterix on a Simoa HD-1 analyser instrument according to manufacturer's instructions. The mean CV of duplicate measurements was 3.2% (range 0.1-15.6%). NfL measurements were missing in four subjects (two symptomatic *GRN* and two symptomatic *C9orf72* mutation carriers) due to insufficient CSF.

Standard protocol approvals and patient consents

Local ethics committees at each site approved the study, and all participants provided written informed consent. Clinical researchers were blinded to the genetic status of at-risk individuals unless they had undergone predictive testing. Laboratory technicians were blinded to all clinical and genetic information.

Statistical analysis

Statistical analyses were performed in IBM SPSS Statistics 24 and *R*. Graphs were drafted in *R* and GraphPad Prism 8. Statistical significance was set at 0.05 (two-sided). The primary analysis in the study was to investigate whether NPTX2, NPTX1 and NPTXR concentration differ among symptomatic mutation carriers, presymptomatic mutation carriers and non-carriers. We restricted correlative analyses of clinical and neuroimaging parameters to NPTX2 because an ELISA was available, which is more sensitive for quantitative analyses than Western blots used for NPTX1 and NPTXR.

Demographic and clinical variables were compared between groups using Kruskal-Wallis tests for continuous variables and a Chi-square test for sex. Normality of biomarker data was assessed using Kolmogorov-Smirnov tests and visual inspection of Q-Q plots. While raw biomarker values were not normally distributed, normal distributions were achieved after square-root transformation of NPTX2 and log-transformation of NfL. We performed ANCOVAs on transformed biomarker values with age as a covariate to test for group

differences. In comparisons between symptomatic mutation carriers, we also included disease duration as a covariate.

The diagnostic performance of NPTX2 to discriminate between the three clinical groups (symptomatic mutation carriers, presymptomatic mutation carriers, non-carriers) was assessed by the area under the curve (AUC) of receiver operating characteristic (ROC) analyses, with optimal cut-off levels determined by the highest Youden's index.[31]

Linear regression models were constructed to study the relationship between NPTX2 concentration (dependent variable; square-root transformed to meet model assumptions) and (1) regional grey matter volume, (2) clinical disease severity measures, and (3) NfL, with age, sex and study site as covariates. For analyses of cognitive tests (MMSE, TMT-B, phonemic verbal fluency) we also included years of education as a covariate. All analyses were performed for mutation carriers combined and for symptomatic and presymptomatic mutation carriers separately. Correction for multiple comparisons was done with the Bonferroni method.

Additional linear regression models were constructed to test whether NPTX2 could predict subsequent cognitive decline, as measured by annualised changes in clinical disease severity scores (score at the time of CSF collection subtracted from a later score and divided by time interval), correcting for age, sex and study site, and in cognitive tests for years of education.

Due to the limited sample size, statistical analyses on longitudinal NPTX2 measurements were limited to exploratory correlations between changes in NPTX2 and time interval, to test for an overall trend in NPTX2 concentration over time.

Data availability

The raw data of this project is part of GENFI and de-identified patient data can be accessed upon reasonable request to j.c.vanswieten@erasmusmc.nl and genfi@ucl.ac.uk.

Results

Demographic and clinical data

Subject characteristics are shown in table 1. Symptomatic mutation carriers were significantly older than presymptomatic carriers and non-carriers, both overall and for each genetic group (*GRN, C9orf72* and *MAPT*) separately. Three presymptomatic mutation carriers converted to the symptomatic stage ('converters') during follow-up (2 *GRN*, *1 MAPT*).

NPTX2 concentration

Overall, NPTX2 levels were lower in symptomatic mutation carriers (median 644 pg/ml, interquartile range (IQR) 301-872) than in presymptomatic carriers (1003 pg/ml (624-1358); p<0.001) and non-carriers (990 pg/ml (597-1373); p<0.001) (figure 1a). NPTX2 levels did not differ significantly between presymptomatic mutation carriers and non-carriers (p=0.859).

When analysed per genetic group, symptomatic *GRN* and *C9orf72* mutation carriers had significantly lower NPTX2 levels than their presymptomatic counterparts (*GRN*: 741 pg/ml versus 1072 pg/ml;p=0.003; *C9orf72*: 609 pg/ml versus 901 pg/ml; p=0.023) and non-carriers (*GRN*: p=0.007; *C9orf72*: p=0.004) (table 1, figure 1b). Symptomatic *MAPT* mutation carriers had lower NPTX2 levels than non-carriers (561 pg/ml; p=0.027) but not compared to presymptomatic *MAPT* mutation carriers (1079 pg/ml; p=0.213). NPTX2 levels did not differ between symptomatic carriers of different genetic groups (p=0.709). Similar results were obtained after excluding mutation carriers with ALS without FTD (n=3).

Overall, a correlation was found between NPTX2 and age (r_s=-0.141; p=0.033) (supplementary figure 1); this correlation was also found in mutation carriers alone (r_s=-0.205; p=0.009) but not in non-carriers alone (r_s=0.070; p=0.566). NPTX2 levels did not differ by sex (p=0.976).

Table 1. Subject characteristics. The clinical phenotype of symptomatic mutation carriers was behavioural variant FTD (n=37), primary progressive aphasia (n=7), FTD with ALS (n=4), ALS without FTD (n=3), memory-predominant FTD (n=1), progressive supranuclear palsy (n=1) and dementia not otherwise specified (n=1). Continuous variables are reported as medians ± interquartile range. Abbreviations: MMSE, Mini Mental State Examination; CDR, Clinical Dementia Rating scale.

	Non-carriers	Presymptomatic carriers			Symptomatic carriers			*p*
N	70	106			54			-
Sex, male (%)	31 (44%)	47 (44%)			32 (59%)			0.157[a]
Age at CSF collection, years	47 (40-58)	45 (34-56)			63 (56-69)			<0.001[b]
MMSE	30 (29-30)	30 (29-30)			26 (24-28)			<0.001[b]
CDR plus FTD modules	0 (0-0)	0 (0-0)			9 (3-10)			<0.001[b]
Disease duration, years	-	-			3 (2-6)			-
NPTX2, pg/ml	990 (597-1373)	1003 (624-1358)			644 (301-872)			<0.001[c]
		GRN	*C9orf72*	*MAPT*	*GRN*	*C9orf72*	*MAPT*	
N		47	42	17	15	31	8	-
Age at CSF collection, years		54 (41-58)	43 (32-53)	42 (34-46)	64 (61-69)	60 (55-70)	61 (53-64)	<0.001[b]
NPTX2, pg/ml		1072 (661-1406)	901 (534-1387)	1079 (389-1263)	741 (385-870)	609 (305-884)	561 (233-861)	<0.001[c]
Age at symptom onset, years		-	-	-	63 (54-66)	55 (49-62)	55 (52-58)	0.109[b]
Disease duration, years		-	-	-	2 (1-4)	4 (2-8)	3 (1-8)	0.238[b]

[a]By Chi-square; [b]by Kruskal-Wallis; [c]by ANCOVA with age as a covariate.

Figure 1. NPTX2 levels (A) in presymptomatic (n=106) and symptomatic mutation carriers (n=54) and non-carriers (n=70) and (B) separated by genetic group. Whiskers indicate minimum and maximum values. Orange squares indicate subjects who converted to the symptomatic stage during follow-up (n=3); grey asterisks indicate subjects with amyotrophic lateral sclerosis (ALS) without FTD (n=3); grey crosses indicate subjects with both FTD and ALS (n=4). P-values are from ANCOVAs with age as a covariate and Bonferroni correction for multiple comparisons. *p<0.05; **p<0.01; ***p<0.001. PRE: presymptomatic mutation carrier; SYM: symptomatic mutation carrier.

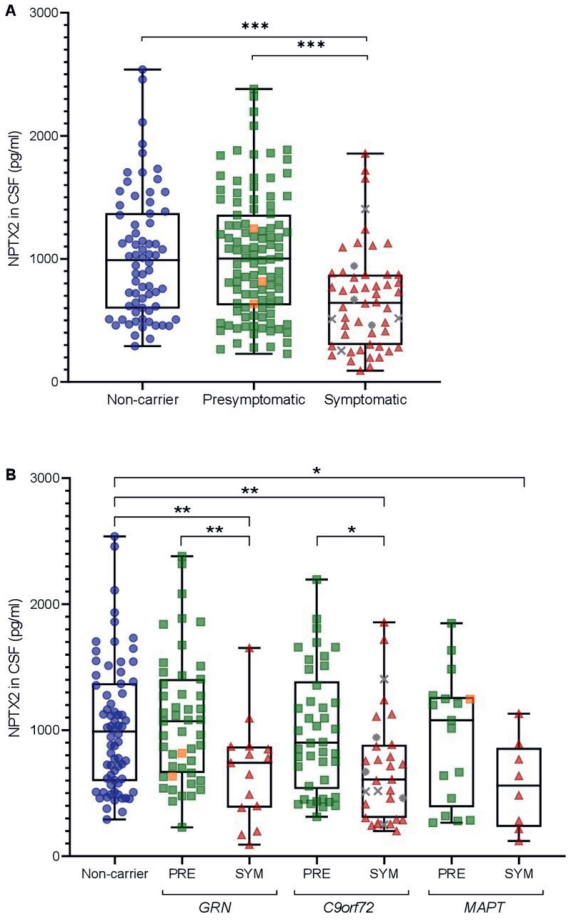

Diagnostic accuracy of NPTX2

The AUC for NPTX2 to distinguish symptomatic from presymptomatic mutation carriers was 0.71 (95% CI 0.63-0.80), with an optimal cut-off of 895 pg/ml (sensitivity 82%, specificity 56%) (supplementary figure 2). The AUC to distinguish symptomatic mutation carriers from non-carriers was 0.71 (95% CI 0.61-0.80), with an optimal cut-off of 945 pg/ml (sensitivity 83%, specificity 53%). NPTX2 did not distinguish presymptomatic mutation carriers from non-carriers (AUC 0.50 (95% CI 0.41-0.58)).

NPTX2 and clinical and neuroimaging data

NPTX2 levels in mutation carriers correlated significantly with grey matter volume of the whole brain, frontal, temporal and parietal lobes and insula, and in symptomatic mutation carriers alone, with whole brain volume, frontal lobe and insular volume (figure 2a-b, table 2, supplementary figure 3). In presymptomatic mutation carriers, NPTX2 levels were associated with frontal lobe volume but this was no longer significant after multiple testing correction (table 2). Among non-carriers (n=64), no significant associations were found with any of the regional grey matter volumes (supplementary table 1). Results were unchanged after repeating the analyses with raw grey matter volumes (i.e. not corrected for TIV).

Among mutation carriers, NPTX2 levels correlated with MMSE, TMT-B, phonemic verbal fluency, CDR plus FTD modules and CBI-R (table 3, figure 2c-d). In symptomatic mutation carriers alone, these correlations were similarly present for MMSE, TMT-B, CDR plus FTD modules and CBI-R. In presymptomatic mutation carriers alone, an association was found for TMT-B, which was no longer statistically significant after correction for multiple testing (table 3).

NPTX2 and NfL concentration

Symptomatic mutation carriers had significantly higher NfL levels than presymptomatic carriers (2575 pg/ml (1218-4592) versus 471 pg/ml (305-729); p<0.001) and non-carriers (421 pg/ml (298-555); p<0.001). These differences were also found for each genetic group separately (supplementary figure 4). No differences were seen between presymptomatic mutation carriers and non-carriers (p=0.517). Similar results were obtained after exclusion of nine outliers (values >3*IQR from the median) and after exclusion of subjects with ALS without FTD (n=3).

NPTX2 concentration across all mutation carriers was inversely associated with NfL concentration (*b*=-5.69E-4; p=0.010; n=156) (figure 3). This correlation was not observed for symptomatic (*b*=-3.61E-4; p=0.141; n=50) or presymptomatic mutation carriers (*b*=-3.64E-5; p=0.971; n=106) alone. Repeating the analyses for symptomatic mutation carriers after

exclusion of patients with concomitant or isolated ALS revealed a trend towards association between NfL and NPTX2 (b=-7.55E-4; p=0.061; n=43).

Figure 2. Relationship between NPTX2 and (A) frontal lobe volume (n=126), (B) insular volume (n=126), (C) Mini Mental State Examination (MMSE) (n=145), and (D) Clinical Dementia Rating scale (CDR) plus FTD modules (n=120) among mutation carriers. *b* and p were obtained through multiple linear regression with square-root transformed NPTX2 as the dependent variable, adjusting for age, sex and study site; for MMSE, we also included years of education as a covariate. Abbreviations: TIV, total intracranial volume.

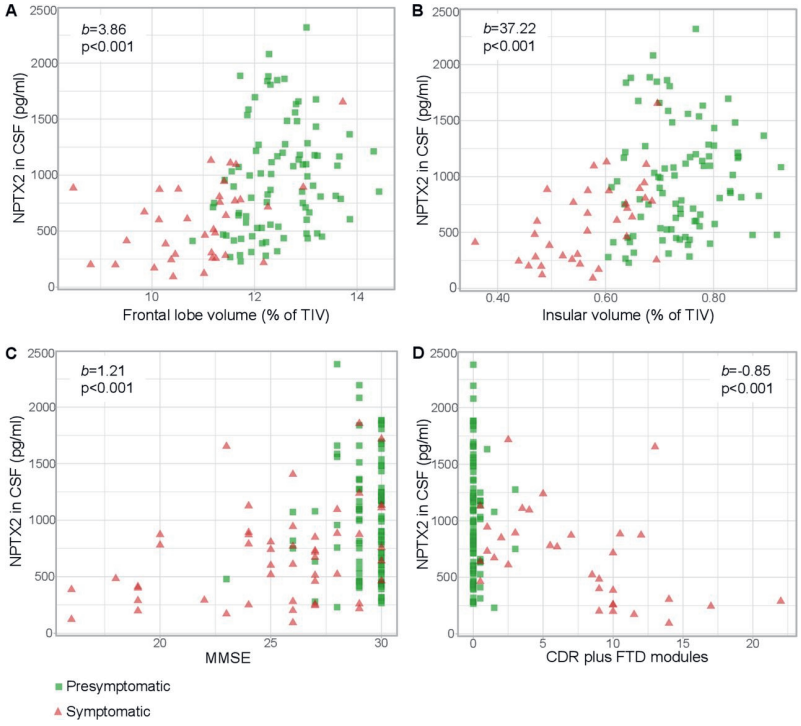

Table 2. Relationship between NPTX2 and grey matter volume. Results were obtained through multiple linear regression with square-root transformed NPTX2 as dependent variable, adjusting for age, sex and study site. All grey matter volumes were corrected for total intracranial volume. Displayed p-values are before multiple testing correction; p-values marked with an asterisk remained significant after Bonferroni correction. *b* indicates unstandardised regression coefficient; β indicates standardised regression coefficient; SE: standard error.

		All mutation carriers (n=126)	Symptomatic mutation carriers (n=35)	Presymptomatic mutation carriers (n=91)
Whole brain volume	*b (SE)*	1.07 (0.25)	1.21 (0.42)	0.58 (0.39)
	β	0.533	0.585	0.215
	p	<0.001*	0.007*	0.145
Frontal lobe	*b (SE)*	3.86 (0.83)	4.40 (1.33)	3.48 (1.44)
	β	0.516	0.623	0.331
	p	<0.001*	0.003*	0.018
Temporal lobe	*b (SE)*	4.01 (1.32)	5.00 (2.27)	0.67 (2.11)
	β	0.338	0.448	0.039
	p	0.003*	0.037	0.752
Parietal lobe	*b (SE)*	4.89 (1.77)	5.51 (4.25)	2.70 (2.18)
	β	0.323	0.319	0.169
	p	0.007*	0.208	0.218
Occipital lobe	*b (SE)*	1. 45 (1.77)	-6.65 (4.03)	3.10 (1.97)
	β	0.086	-0.341	0.185
	p	0.412	0.112	0.119
Cingulate gyrus	*b (SE)*	10.49 (5.27)	14.72 (11.32)	0.46 (7.27)
	β	0.205	0.285	0.008
	p	0.049	0.206	0.950
Insula	*b (SE)*	37.22 (8.69)	69.21 (13.09)	12.61 (13.16)
	β	0.482	0.786	0.119
	p	<0.001*	<0.001*	0.341

Table 3. Relationship between NPTX2 and disease severity scores, obtained through multiple linear regression with square-root transformed NPTX2 as dependent variable, adjusting for age, sex, study site and, in analyses of MMSE, TMT-B and letter fluency, years of education. Displayed p-values are before multiple testing correction; p-values marked with an asterisk remained significant after Bonferroni correction. *b* indicates unstandardised regression coefficient; β indicates standardised regression coefficient; SE: standard error; MMSE: Mini Mental State Examination; TMT-B: Trail Making Test part B; CDR: Clinical Dementia Rating scale; CBI-R: Revised Cambridge Behavioural Inventory.

		All mutation carriers	Symptomatic mutation carriers	Presymptomatic mutation carriers
MMSE	n	145	50	95
	b (SE)	1.21 (0.26)	0.98 (0.29)	1.58 (0.79)
	β	0.442	0.467	0.230
	p	<0.001*	0.002*	0.051
TMT-B	N	125	34	91
	b (SE)	-0.04 (0.01)	-0.02 (0.02)	-0.09 (0.04)
	β	-0.353	-0.234	-0.259
	p	<0.001*	<0.001*	0.030
Phonemic verbal fluency	N	132	39	93
	b (SE)	0.14 (0.05)	0.15 (0.10)	0.05 (0.08)
	β	0.255	0.250	0.076
	p	0.009*	0.151	0.536
CDR plus FTD modules	N	120	33	87
	b (SE)	-0.85 (0.19)	-0.72 (0.24)	-1.19 (1.67)
	β	-0.435	-0.479	-0.078
	p	<0.001*	0.007*	0.478
CBI-R	n	119	40	79
	b (SE)	-0.13 (0.03)	-0.10 (0.04)	-0.02 (0.14)
	β	-0.489	-0.394	-0.014
	p	<0.001*	0.017*	0.906

Figure 3. Correlation between NPTX2 and NfL levels in presymptomatic (n=106) and symptomatic (n=50) mutation carriers. NfL is plotted on a log-scale for visualisation purposes. *b* and p were obtained through multiple linear regression with square-root transformed NPTX2 as the dependent variable, adjusting for age, sex and study site.

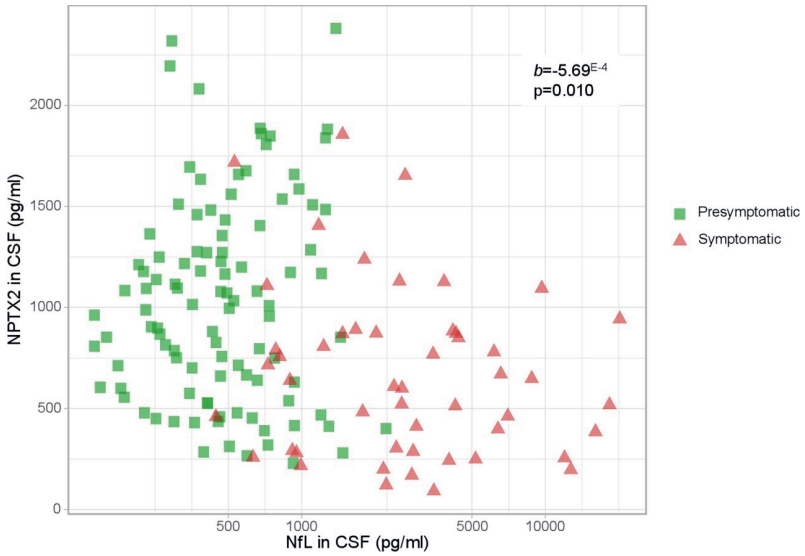

Longitudinal NPTX2 measurements

Longitudinal CSF samples were available in ten presymptomatic mutation carriers (of whom two had converted to the symptomatic stage at follow-up CSF collection), two symptomatic mutation carriers and one non-carrier. The median time between samples was 2.0 years (IQR 1.8-2.1).

In the *MAPT* converter, visually, a decrease in NPTX2 was observed in two presymptomatic samples, with a further decrease in the symptomatic sample (figure 4). In the *GRN* converter, NPTX2 was already below the proposed cut-off level 1.2 years before symptom onset, with a further decrease in the symptomatic sample. Both symptomatic mutation carriers demonstrated NPTX2 decreases over time. Lower NPTX2 levels at follow-up were observed in all presymptomatic mutation carriers over the age of 50 years, while in younger presymptomatic carriers, NPTX2 trajectories seemed to be more varied. NPTX2 in one non-carrier subject was visually stable (figure 4).

There was no correlation between change in NPTX2 levels and time interval between CSF collections (r_s=-0.116; p=0.705) (supplementary figure 5).

NPTX2 and subsequent cognitive decline

NPTX2 was significantly associated with annualised change in phonemic verbal fluency (*b*=0.004; p=0.001; n=118), and CDR plus FTD modules (*b*=-0.001; p=0.025; n=105). The former remained significant after adjusting for clinical status, frontal lobe volume and CSF NfL. A trend was found for annualised change in MMSE (*b*=0.001; p=0.077; n=136). NPTX2 level was not associated with annualised change in CBI-R (p=0.200; n=93) or TMT-B (p=0.693; n=107) (supplementary table 2, supplementary figure 6).

NPTX1 and NPTXR concentration

NPTX1 levels were significantly lower in symptomatic mutation carriers compared to presymptomatic carriers (median 54% (36-88) vs. 86% (55-118); p<0.001) and non-carriers (92% (61-123); p<0.001). Similar results were found for NPTXR (symptomatic vs presymptomatic: 51% (27-85) vs. 81% (51-147); p=0.002; symptomatic vs non-carriers: 51% vs. 76% (51-133); p<0.001) (figure 5). Separated by genetic group, symptomatic *C9orf72* and *MAPT* mutation carriers had significantly lower NPTX1 and NPTXR levels than non-carriers. In *GRN* mutation carriers, a similar pattern was observed, although not statistically significant. NPTX1- and NPTXR levels were strongly correlated with NPTX2 (r_s=0.828 and r_s=0.850 respectively, both p<0.001) (supplementary figure 7).

Figure 4. Longitudinal NPTX2 levels plotted against age in thirteen subjects with multiple CSF samples. A line is drawn between NPTX2 levels of follow-up samples. Presymptomatic samples are shown as green squares, symptomatic samples as red triangles and the non-carrier as blue circles. *GRN* mutation carriers are shown as open symbols, *C9orf72* mutation carriers as filled symbols and the *MAPT* mutation carrier as half-filled symbols. Dotted horizontal line indicates median NPTX2 level in presymptomatic mutation carriers (1003 pg/ml); dashed horizontal line indicates median in symptomatic mutation carriers (644 pg/ml). For blinding purposes, a jitter of ±2 years was applied to all subjects.

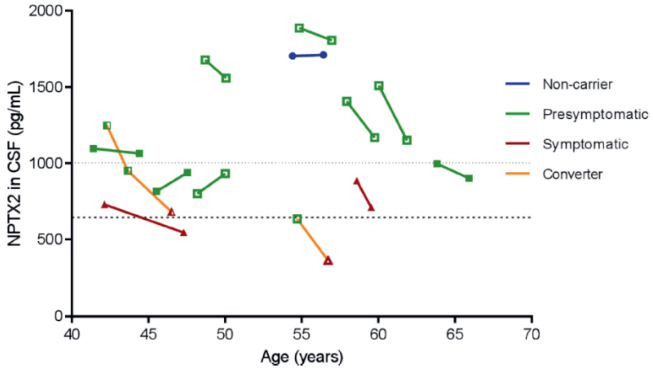

Figure 5. NPTX1 and NPTXR levels as measured by Western blot. (A) Representative (cropped) Western blots of NPTX1 and NPTXR (n=230); (B,C) NPTX1 and NPTXR levels across groups, expressed as a percentage of band intensity compared to non-carriers. Whiskers indicate minimum and maximum values. Displayed significance levels are from ANCOVA on square-root transformed relative band intensities of NPTX1 and NPTXR with age as a covariate. PRE: presymptomatic mutation carrier; SYM: symptomatic mutation carrier. *p<0.05; **p<0.01.

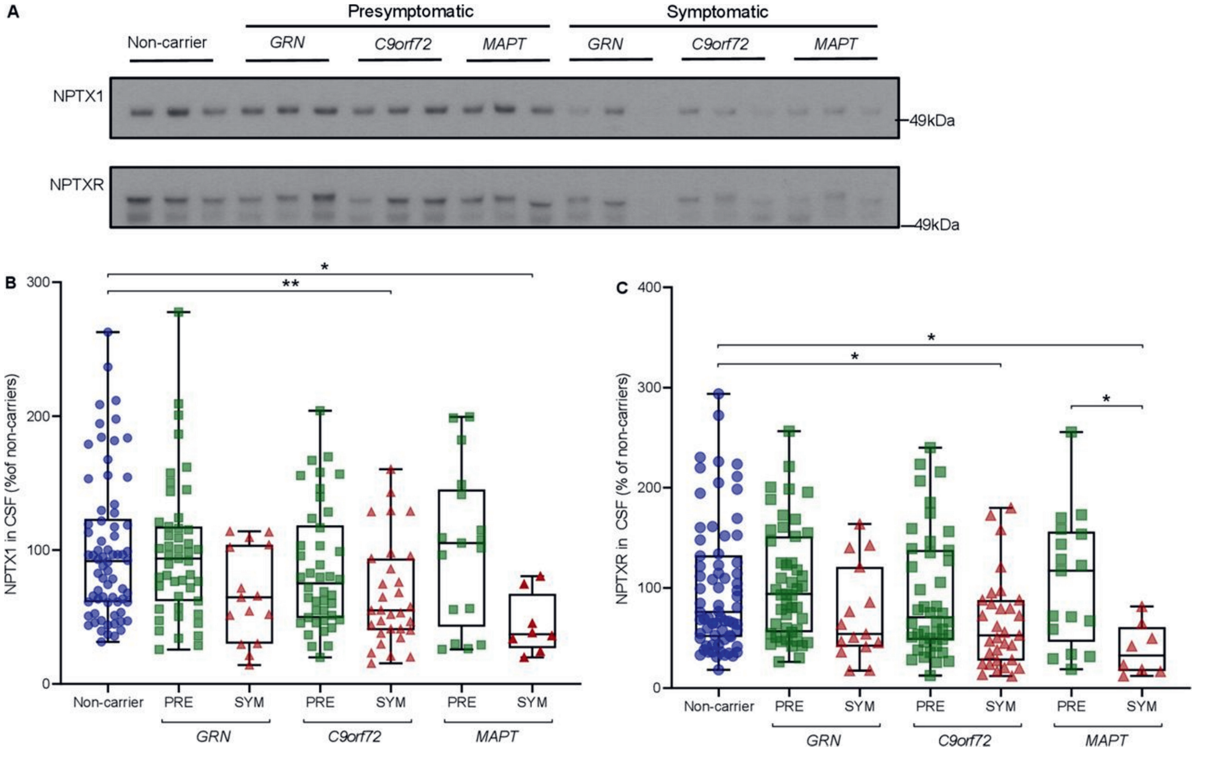

Discussion

The present study of a large international cohort of genetic FTD reports low levels of NPTX2, NPTX1 and NPTXR in the symptomatic stage, with correlations between NPTX2 and both disease severity and grey matter volume. We propose NPTX2 as a novel synapse-derived biomarker of disease progression in genetic FTD.

The decreased levels of CSF NPTXs in patients with *GRN*-, *C9orf72*- and *MAPT*-associated FTD probably reflect a loss or dysfunction of their synaptic sources.[32] Complexes of NPTXs accumulate at excitatory synapses between glutamatergic pyramidal neurons and parvalbumin-expressing (PV) interneurons in the cerebral cortex, hippocampus and cerebellum.[32] NPTXs modulate the strength of these synapses through recruitment of AMPA-type glutamate receptors (AMPARs) to the postsynaptic membrane, thereby regulating excitatory drive of pyramidal neurons onto PV-interneurons.[4,12,32] PV-interneurons in turn contact surrounding pyramidal neurons and prevent neural circuits from becoming too active (diagram provided in [33]).[34] The expression of NPTX2 – but not NPTX1 or NPTXR – is induced by synapse activity,[3,35] and the relative ratio of the NPTXs in the complex is dynamically dependent on the neuron's activity. Of the three proteins, NPTX2 is most effective at AMPAR recruitment, but their combined expression is synergistic.[3] *NPTX2* knockout mice have reduced AMPARs, resulting in less inhibitory PV-interneuron activity; the subsequent disruption of pyramidal neuron – PV-interneuron circuits is thought to underlie cognitive impairment, and NPTX2 loss has been hypothesised to drive neurodegeneration.[12] Restoring these circuits is emerging as a potential treatment strategy in neurodegenerative disease;[36] in this regard, measuring NPTX2 in CSF could be especially relevant to select and monitor patients with aberrant pyramidal neuron-PV interneuron circuits.[12,36] The lack of correlation in the current study between NPTX2 and brain volume in healthy non-carriers reflects that NPTX2 is not merely a measure of synapse density.

The present study reports low NPTX2 levels in all included forms of genetic FTD. The lack of significant differences between presymptomatic and symptomatic *MAPT* mutation carriers likely reflects insufficient statistical power given the small sample size, or could reflect differences in underlying pathology (eg. tau pathology in *MAPT*-associated FTD versus TDP-43 pathology in *GRN*- and *C9orf72*-associated FTD).[1] While these findings are novel in FTD, a few studies have identified reduced NPTXs in AD, both in brain and in CSF,[12-19] albeit mostly through mass spectrometry approaches (box 1). The observed reductions in both FTD and AD suggest that reduced NPTXs reflect general rather than gene- or disease-specific

pathological alterations. To date, CSF NPTX2 levels in other neurodegenerative diseases have not been reported; future research should focus on the measurement of CSF NPTXs across a broader range of neurodegenerative diseases, including sporadic FTD and Parkinson's disease.[37]

Box 1: CSF NPTXs in other neurodegenerative diseases

- CSF NPTX2 levels are reduced in patients with Alzheimer's disease (AD) compared to controls.[12,14,17] In AD, low CSF NPTX2 levels are associated with cognitive impairment and subsequent memory decline, as well as hippocampal atrophy and subsequent medial temporal lobe atrophy.[12,17]
- To date, CSF NPTX2 levels have not been reported in other neurodegenerative diseases, such as sporadic FTD and Parkinson's disease.
- Differentially regulated levels of CSF NPTX1 and NPTXR have been reported in patients with AD, mostly identified through mass spectrometry approaches.[13,15,16,18-20] In presymptomatic stages of autosomal dominant AD, mild cognitive impairment and early-stage AD, a transient increase in NPTXs has been observed.[15,16,19,20]
- In brain tissue, NPTX2 levels are decreased in patients with AD.[12] Conversely, one study has reported accumulation of NPTX2 in Lewy bodies in patients with Parkinson's disease.[37]

The correlations between NPTX2 concentration and several disease severity measures suggest that NPTX2 might further decrease with disease progression. This is supported by longitudinal NPTX2 decreases over time in two symptomatic mutation carriers and could reflect a link between progressive synapse pathology and cognitive decline; more longitudinal data is needed to confirm this. The association between NPTX2 levels and subsequent decline in phonemic verbal fluency and CDR plus FTD modules indicates that NPTX2 may have prognostic significance and is in line with previous findings in AD. The correlations between NPTX2 and grey matter volume in regions typically affected in FTD, including the frontal lobe and insula,[23] are comparable to the previously reported correlations with hippocampal volume in AD and provide further evidence for NPTX2 as a disease progression marker.[12,17]

Longitudinally, we observed strong NPTX2 decreases in two converters; in the *MAPT* converter, this decrease was already observed in two presymptomatic samples; similarly, in the *GRN* converter, NPTX2 levels were already low in the presymptomatic sample. Although these results must be interpreted with caution due to the small sample size, they provide tentative evidence that NPTX2 might be an early disease marker. The overall lack of differences in NPTXs between presymptomatic mutation carriers and non-carriers might reflect the inclusion of mutation carriers of all ages; therefore, time to symptom onset was highly variable. Remarkably, in presymptomatic autosomal dominant AD, mild cognitive impairment and early stage AD, a transient increase in NPTXs has been observed, with a

subsequent decline as the disease progresses.[15,16,19,20] This discrepancy in NPTXs dynamics may result from differences in underlying pathophysiology.

The diagnostic accuracy of NPTX2 of 71% to distinguish symptomatic from presymptomatic mutation carriers is comparable to that of neurogranin, the most evaluated synapse-derived CSF biomarker for AD.[38] Its longitudinal evaluation, especially in the late-presymptomatic stage, might be more valuable than cross-sectional measurements. It is promising that Ma et al.[39] observed a correlation between NPTX1 in plasma and brain tissue; further studies are warranted to investigate whether NPTX2 can also be reliably measured in the blood, which would offer opportunities for longitudinal studies with larger numbers of samples.

We found an inverse correlation between NPTX2 and NfL in mutation carriers. NfL is a sensitive marker of neuroaxonal degeneration which is elevated in CSF and blood in the symptomatic stage of genetic FTD [40] and in various other neurological disorders.[21] Although a trend was found for symptomatic carriers alone after exclusion of ALS patients (who are known to have very high NfL levels),[21] the lack of a stronger correlation probably reflects that NPTX2 and NfL are markers of different pathological processes which do not occur simultaneously.

Strengths of this study include the large sample size, despite the relative rarity of the disease, and the availability of corresponding clinical and brain imaging datasets. The inclusion of subjects with specific genetic defects allowed us to define pathologically homogeneous groups. Our NPTX2 findings are supported by similar results in NPTX1 and NPTXR, which correlated strongly with NPTX2, and indicate an overall reduction in NPTXs in genetic FTD.

The findings of this study must be viewed in light of some limitations. First, our longitudinal NPTX2 measurements were too limited in number to draw strong conclusions and require replication and more extensive statistical analyses in larger datasets. Second, using diagnostic criteria to label mutation carriers as presymptomatic or symptomatic may have failed to recognise subjects in a very early symptomatic stage. We calculated disease duration based on estimated time of symptom onset, rather than diagnosis, to ensure that any diagnostic delay did not affect correlative analyses. Third, three *C9orf72* mutation carriers had ALS without FTD, which, although increasingly recognised as part of the FTD spectrum,[1] represents a clinically distinct phenotype. We ensured that these subjects did not affect our main results by repeating group comparisons after exclusion of these subjects. Finally, although brief medical and neurological history and examination did not reveal any significant neurological comorbidities, asymptomatic diseases, including cerebrovascular

disease, could have confounded NPTX measurements. Future research focusing on potential confounding factors will be an important next step.

In conclusion, we provide evidence for NPTX2 as a novel CSF biomarker in genetic FTD. Its synaptic localisation and correlation with disease progression indicates that NPTX2 decreases probably reflect synaptic dysfunction or loss, providing novel opportunities for in vivo monitoring of synaptic integrity in genetic FTD. Treatment strategies aimed at improving synaptic connectivity may benefit from the use of NPTX2 as a tool to select and monitor patients with neural circuit dysfunction. More longitudinal data on NPTXs in presymptomatic and symptomatic mutation carriers might verify their value as (pre-)clinical biomarkers.

Acknowledgements

We thank all participants and their family members for taking part in this study. Several authors of this publication are members of the European Reference Network for Rare Neurological Diseases – Project ID no. 739510.

Funding

This study was supported in the Netherlands by two Memorabel grants from Deltaplan Dementie (The Netherlands Organisation for Health Research and Development and Alzheimer Nederland; grant numbers 733050813 and 733050103), the Bluefield Project to Cure Frontotemporal Dementia, the Dioraphte foundation (grant number 1402 1300), and the European Joint Programme – Neurodegenerative Disease Research and the Netherlands Organisation for Health Research and Development (PreFrontALS: 733051042, RiMod-FTD: 733051024); in Belgium by the Mady Browaeys Fonds voor Onderzoek naar Frontotemporale Degeneratie; in the UK by the MRC UK GENFI grant (MR/M023664/1); JDR is supported by an MRC Clinician Scientist Fellowship (MR/M008525/1) and has received funding from the NIHR Rare Disease Translational Research Collaboration (BRC149/NS/MH); KMM is supported by an Alzheimer's Society PhD Studentship (AS-PhD-2015-005); JBR is supported by the Wellcome Trust (103838); in Spain by the Fundació Marató de TV3 (20143810 to RSV); in Germany by the Deutsche Forschungsgemeinschaft (DFG, German Research Foundation) under Germany's Excellence Strategy within the framework of the Munich Cluster for Systems Neurology (EXC 2145 SyNergy – ID 390857198) and by grant 779357 "Solve-RD" from the Horizon 2020 Research and Innovation Programme (to MS); in Sweden by grants from the Swedish FTD Initiative funded by the Schörling Foundation, grants from JPND PreFrontALS Swedish Research Council (VR) 529-2014-7504, Swedish Research Council (VR) 2015-02926, Swedish Research Council (VR) 2018-02754, Swedish Brain Foundation,

Swedish Alzheimer Foundation, Stockholm County Council ALF, Swedish Demensfonden, Stohnes foundation, Gamla Tjänarinnor, Karolinska Institutet Doctoral Funding, and StratNeuro.

Author contributions

ELvdE and JCvS contributed to data acquisition, conception and design of the study, statistical analysis and drafting of the manuscript and figures. MFX, DX and PFW contributed to conception and design of the study, data acquisition (i.e. NPTX measurements) and drafting of the manuscript and figures. JDR contributed to data acquisition and design of the study. CET contributed to data acquisition (i.e. NfL measurements). The remaining authors recruited patients and collected data. All authors critically reviewed the manuscript and approved the final draft.

Competing interests

The authors report no competing interests relevant to this study.

References

1. Lashley T, Rohrer JD, Mead S, et al. Review: an update on clinical, genetic and pathological aspects of frontotemporal lobar degenerations. Neuropathol Appl Neurobiol. 2015;41(7):858-81.
2. van der Ende EL, Meeter HH, Stingl C, et al. Novel CSF biomarkers in genetic frontotemporal dementia identified by proteomics. Ann Clin Transl Neurol. 2019.
3. Xu D, Hopf C, Reddy R, et al. Narp and NP1 form heterocomplexes that function in developmental and activity-dependent synaptic plasticity. Neuron. 2003;39(3):513-28.
4. Pelkey KA, Barksdale E, Craig MT, et al. Pentraxins coordinate excitatory synapse maturation and circuit integration of parvalbumin interneurons. Neuron. 2015;85(6):1257-72.
5. Marttinen M, Kurkinen KM, Soininen H, et al. Synaptic dysfunction and septin protein family members in neurodegenerative diseases. Mol Neurodegener. 2015;10:16.
6. Ling SC. Synaptic Paths to Neurodegeneration: The Emerging Role of TDP-43 and FUS in Synaptic Functions. Neural Plast. 2018;2018:8413496.
7. Gong Y, Lippa CF. Review: disruption of the postsynaptic density in Alzheimer's disease and other neurodegenerative dementias. Am J Alzheimers Dis Other Demen. 2010;25(7):547-55.
8. Lui H, Zhang J, Makinson SR, et al. Progranulin Deficiency Promotes Circuit-Specific Synaptic Pruning by Microglia via Complement Activation. Cell. 2016;165(4):921-35.
9. Petkau TL, Neal SJ, Milnerwood A, et al. Synaptic dysfunction in progranulin-deficient mice. Neurobiol Dis. 2012;45(2):711-22.
10. Tapia L, Milnerwood A, Guo A, et al. Progranulin deficiency decreases gross neural connectivity but enhances transmission at individual synapses. J Neurosci. 2011;31(31):11126-32.
11. Terry RD, Masliah E, Salmon DP, et al. Physical basis of cognitive alterations in Alzheimer's disease: synapse loss is the major correlate of cognitive impairment. Ann Neurol. 1991;30(4):572-80.
12. Xiao MF, Xu D, Craig MT, et al. NPTX2 and cognitive dysfunction in Alzheimer's Disease. Elife. 2017;6.
13. Yin GN, Lee HW, Cho JY, et al. Neuronal pentraxin receptor in cerebrospinal fluid as a potential biomarker for neurodegenerative diseases. Brain Res. 2009;1265:158-70.
14. Spellman DS, Wildsmith KR, Honigberg LA, et al. Development and evaluation of a multiplexed mass spectrometry based assay for measuring candidate peptide biomarkers in Alzheimer's Disease Neuroimaging Initiative (ADNI) CSF. Proteomics Clin Appl. 2015;9(7-8):715-31.
15. Ringman JM, Schulman H, Becker C, et al. Proteomic changes in cerebrospinal fluid of presymptomatic and affected persons carrying familial Alzheimer disease mutations. Arch Neurol. 2012;69(1):96-104.
16. Llano DA, Bundela S, Mudar RA, et al. A multivariate predictive modeling approach reveals a novel CSF peptide signature for both Alzheimer's Disease state classification and for predicting future disease progression. PLoS One. 2017;12(8):e0182098.

17. Swanson A, Willette AA, Alzheimer's Disease Neuroimaging I. Neuronal Pentraxin 2 predicts medial temporal atrophy and memory decline across the Alzheimer's disease spectrum. Brain Behav Immun. 2016;58:201-8.
18. Begcevic I, Tsolaki M, Brinc D, et al. Neuronal pentraxin receptor-1 is a new cerebrospinal fluid biomarker of Alzheimer's disease progression. F1000Res. 2018;7:1012.
19. Duits FH, Brinkmalm G, Teunissen CE, et al. Synaptic proteins in CSF as potential novel biomarkers for prognosis in prodromal Alzheimer's disease. Alzheimers Res Ther. 2018;10(1):5.
20. Wildsmith KR, Schauer SP, Smith AM, et al. Identification of longitudinally dynamic biomarkers in Alzheimer's disease cerebrospinal fluid by targeted proteomics. Mol Neurodegener. 2014;9:22.
21. Khalil M, Teunissen CE, Otto M, et al. Neurofilaments as biomarkers in neurological disorders. Nat Rev Neurol. 2018;14(10):577-89.
22. Rohrer JD, Nicholas JM, Cash DM, et al. Presymptomatic cognitive and neuroanatomical changes in genetic frontotemporal dementia in the Genetic Frontotemporal dementia Initiative (GENFI) study: a cross-sectional analysis. Lancet Neurol. 2015;14(3):253-62.
23. Rascovsky K, Hodges JR, Knopman D, et al. Sensitivity of revised diagnostic criteria for the behavioural variant of frontotemporal dementia. Brain. 2011;134(Pt 9):2456-77.
24. Gorno-Tempini ML, Hillis AE, Weintraub S, et al. Classification of primary progressive aphasia and its variants. Neurology. 2011;76(11):1006-14.
25. Brooks BR, Miller RG, Swash M, et al. El Escorial revisited: revised criteria for the diagnosis of amyotrophic lateral sclerosis. Amyotroph Lateral Scler Other Motor Neuron Disord. 2000;1(5):293-9.
26. Miyagawa T, Brushaber D, Syrjanen J, et al. Use of the CDR(R) plus NACC FTLD in mild FTLD: Data from the ARTFL/LEFFTDS consortium. Alzheimers Dement. 2019.
27. Wear HJ, Wedderburn CJ, Mioshi E, et al. The Cambridge Behavioural Inventory revised. Dement Neuropsychol. 2008;2(2):102-7.
28. Spreen O SE. A compendium of neuropsychological tests: Administration, norms and commentary. In: Spreen O SE, editor. A compendium of neuropsychological tests: Administration, norms and commentary. 2nd edition ed: Oxford University Press; 1998.
29. Cardoso MJ, Modat M, Wolz R, et al. Geodesic Information Flows: Spatially-Variant Graphs and Their Application to Segmentation and Fusion. IEEE Trans Med Imaging. 2015;34(9):1976-88.
30. Malone IB, Leung KK, Clegg S, et al. Accurate automatic estimation of total intracranial volume: a nuisance variable with less nuisance. Neuroimage. 2015;104:366-72.
31. Youden WJ. Index for rating diagnostic tests. Cancer. 1950;3(1):32-5.
32. Chang MC, Park JM, Pelkey KA, et al. Narp regulates homeostatic scaling of excitatory synapses on parvalbumin-expressing interneurons. Nat Neurosci. 2010;13(9):1090-7.
33. Hanson JE. Identifying faulty brain circuits. Elife. 2017;6.
34. Ferguson BR, Gao WJ. PV Interneurons: Critical Regulators of E/I Balance for Prefrontal Cortex-Dependent Behavior and Psychiatric Disorders. Front Neural Circuits. 2018;12:37.

35. Tsui CC, Copeland NG, Gilbert DJ, et al. Narp, a novel member of the pentraxin family, promotes neurite outgrowth and is dynamically regulated by neuronal activity. J Neurosci. 1996;16(8):2463-78.
36. Palop JJ, Mucke L. Network abnormalities and interneuron dysfunction in Alzheimer disease. Nat Rev Neurosci. 2016;17(12):777-92.
37. Moran LB, Hickey L, Michael GJ, et al. Neuronal pentraxin II is highly upregulated in Parkinson's disease and a novel component of Lewy bodies. Acta Neuropathol. 2008;115(4):471-8.
38. Tarawneh R, D'Angelo G, Crimmins D, et al. Diagnostic and Prognostic Utility of the Synaptic Marker Neurogranin in Alzheimer Disease. JAMA Neurol. 2016;73(5):561-71.
39. Ma QL, Teng E, Zuo X, et al. Neuronal pentraxin 1: A synaptic-derived plasma biomarker in Alzheimer's disease. Neurobiol Dis. 2018;114:120-8.
40. van der Ende EL, Meeter LH, Poos JM, et al. Serum neurofilament light chain in genetic frontotemporal dementia: a longitudinal, multicentre cohort study Lancet Neurology. 2019;18(12):1103-11.

Supplementary file 1: Methods

NPTX2 concentrations were measured using an in-house ELISA. Briefly, 0.5 µg of rabbit anti-NPTX2 antibody in 50 mM Na_2CO_3 buffer (pH 9.5) was coated to a 96-well microtiter plate (Nunc) at 4°C overnight. The next day, after plates were blocked with 5% BSA at room temperature (RT) for 1 hour, 100 µl of the serially diluted NPTX2 standard proteins or CSF samples were added into wells and incubated at 4°C overnight with constant shaking. After plates were washed with TBS-Tween, 100 µl of biotinylated mouse anti-NPTX2 antibody was added and incubated at RT for 1 hour. After washing with TBS-Tween, 100 µl of HRP-conjugated streptavidin (Biolegend) was added and incubated for 1 hour. After washing with TBS-Tween, 100 µl of DAB substrate (Biolegend) was applied and incubated for 30 minutes at RT in the dark. In the end, 100 µl of 4 M H_2SO_4 stopping solution was added and the absorbance was measured at 450 nm. The absolute levels of NPTX2 in CSF were calculated from a standard curve.

NPTX1 and NPTXR concentrations were measured by Western blot. Briefly, human CSF was mixed with SDS loading buffer (2x: 125 mM Tris-HCl (pH 6.8), 4% SDS, 20% glycerol, 10% β-mercaptoethanol, 0.005% bromophenol blue) and heated at 70°C for 10 minutes. 10 µl of CSF were separated by 4-12% SDS-PAGE and transferred to PVDF membranes. After blocking with 5% non-fat milk, membranes were probed with primary antibodies overnight at 4°C. After washes with TBST (TBS with 0.1% Tween-20), membranes were incubated with HRP-conjugated secondary antibodies for 1 hour at RT. Immunoreactive bands were visualised by the enhanced chemiluminescent substrate (ECL, Pierce) on X-ray film and quantified using the image software TINA (www.tina-vision.net). Proteins migrating similarly in SDS-PAGE gel were assayed on different blots without stripping.

Supplementary file 2: Figures and tables

Supplementary figure 1. NPTX2 plotted against age in the entire group of subjects (n=230). For blinding purposes, a jitter of ±2 years was applied to all subjects (analyses were done on raw data). The correlation coefficient was obtained from Spearman's rank correlation.

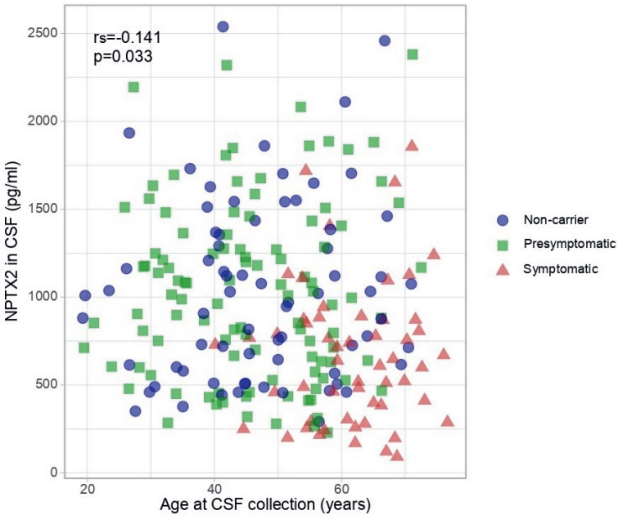

Supplementary figure 2. Receiver operating characteristic (ROC) curve to discriminate symptomatic from presymptomatic mutation carriers using NPTX2 (area under the curve=0.71; 95% CI 0.63-0.80).

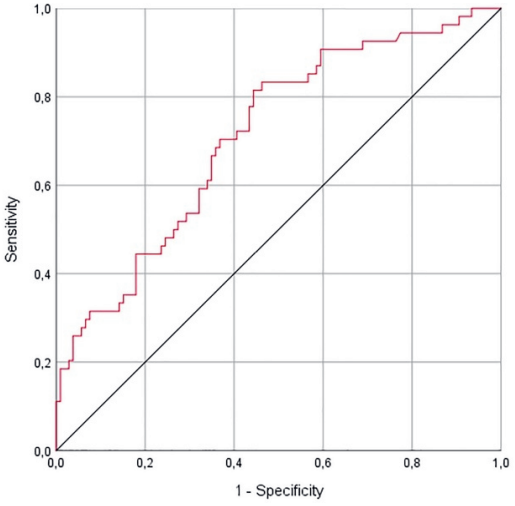

Supplementary figure 3. Grey matter volume of the (A) frontal lobe, and (B) insula in presymptomatic (n=91) and symptomatic mutation carriers (n=35) and non-carriers (n=64), expressed as a percentage of total intracranial volume (TIV). Whiskers indicate minimum and maximum values. P-values are from Kruskall-Wallis tests with Bonferroni correction for multiple comparisons. ***p<0.001.

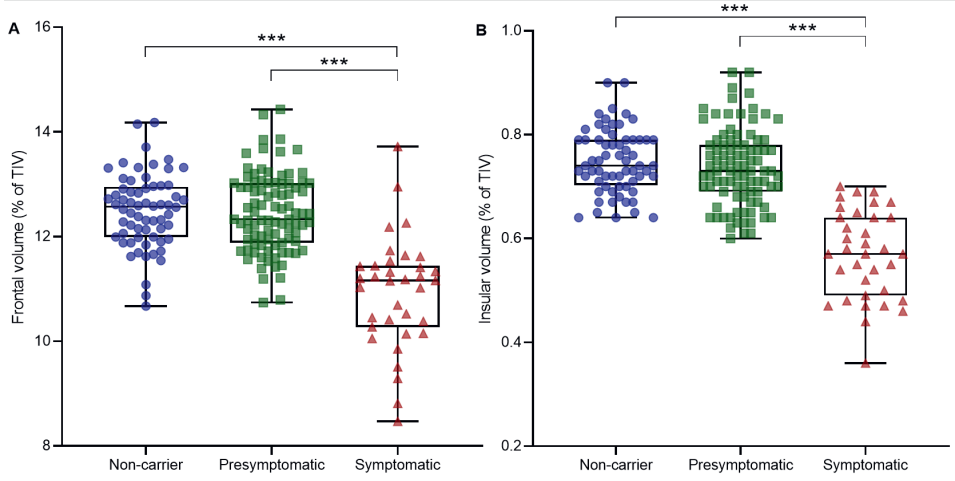

Supplementary figure 4. NfL concentrations in presymptomatic (n=106) and symptomatic mutation carriers (n=50) and non-carriers (n=70). Reported p-values are from ANCOVA with age as a covariate. Whiskers represent minimum and maximum values. Orange squares indicate subjects who converted to the symptomatic stage during follow-up (n=3). Grey asterisks indicate subjects with amyotrophic lateral sclerosis (ALS) without FTD (n=3); grey crosses indicate subjects with both FTD and ALS (n=4). PRE: presymptomatic; SYM: symptomatic. *p<0.05; **p<0.01; ***p<0.001.

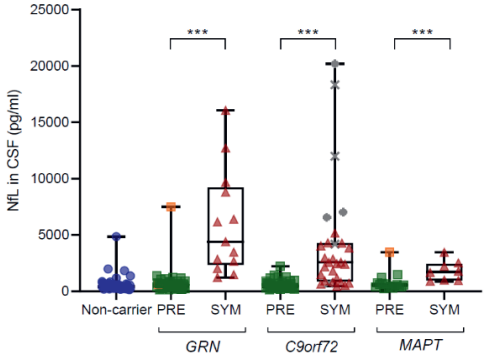

Supplementary figure 5. Relationship between changes in NPTX2 in longitudinal CSF samples (n=13) and time interval between CSF collections (r_s=0.116, p=0.705). Change in NPTX2 was defined as the difference in NPTX2 concentration between the first and the last CSF sample. Presymptomatic mutation carriers are shown as green squares; symptomatic mutation carriers as red triangles and converters are shown in orange. The non-carrier is shown as a blue circle. *GRN* mutation carriers are shown as open symbols, *C9orf72* mutation carriers as filled symbols and the *MAPT* mutation carrier as a half-filled symbol.

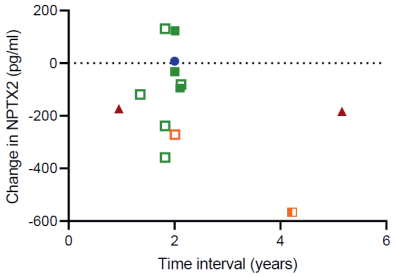

Supplementary figure 6. Relationship between NPTX2 concentration and subsequent annual change in phonemic verbal fluency among mutation carriers (n=118). Annualised change in phonemic verbal fluency was calculated by subtracting the score at CSF collection from the most recent score (collected through GENFI follow-up) and dividing by the time interval. *b* and p values are from linear regression analyses which included age, sex, centre and education level as covariates.

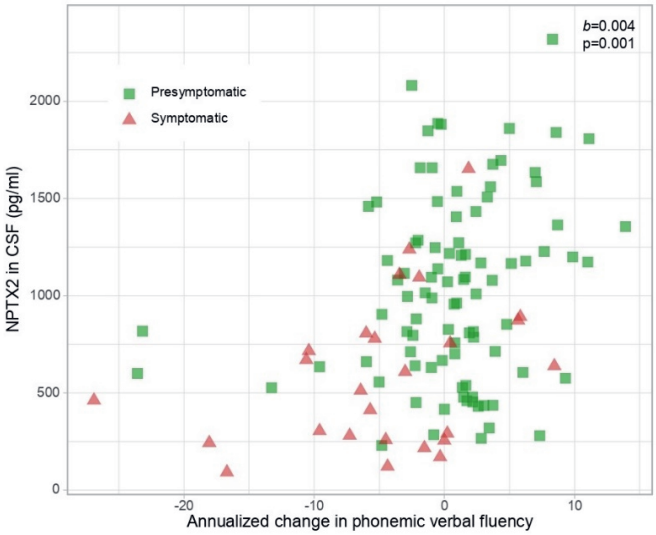

Supplementary figure 7. Correlation between NPTX2 and (A) NPTX1, and (B) NPTXR in the entire group (n=230). Correlation coefficients are from Spearman's rank correlations.

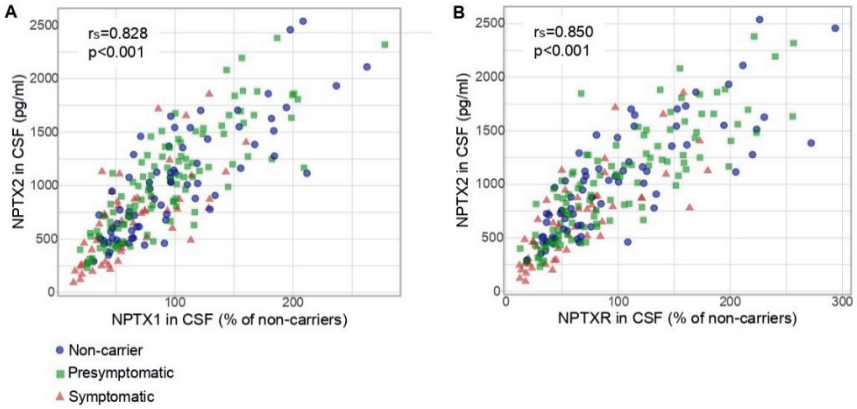

Supplementary table 1. Relationship between NPTX2 and grey matter volume among non-carriers (n=64). Results were obtained through multiple linear regression with square-root transformed NPTX2 as the dependent variable, adjusting for age, sex and study site. Section A shows results when brain volumes were corrected for total intracranial volume; section B shows results using raw (uncorrected) brain volumes. Displayed p-values are before multiple testing correction; none were significant after Bonferroni correction. *b* indicates regression coefficient; β indicates standardised regression coefficient; SE: standard error.

A. Brain volumes as percentage of total intracranial volume			
	b (SE)	β	*p*
Whole brain volume	-0.18 (0.42)	0.301	0.660
Frontal lobe	-1.18 (1.80)	0.187	0.515
Temporal lobe	1.88 (2.66)	0.422	0.484
Parietal lobe	1.27 (3.29)	0.314	0.700
Occipital lobe	0.62 (2.61)	0.205	0.814
Cingulate gyrus	1.65 (7.26)	0.215	0.821
Insula	-4.00 (19.89)	0.120	0.841
B. Raw brain volumes			
	b (SE)	β	*p*
Whole brain volume	2.08E-5 (7.42E-6)	0.293	0.106
Frontal lobe	8.17E-5 (4.51E-5)	0.195	0.228
Temporal lobe	2.47E-4 (7.28E-5)	0.400	0.029
Parietal lobe	2.54E-4 (1.02E-4)	0.322	0.065
Occipital lobe	1.88E-4 (1.08E-4)	0.211	0.157
Cingulate gyrus	4.45E-4 (1.15E-5	0.200	0.184
Insula	1.02E-3 (9.16E-4)	0.169	0.271

Supplementary table 2. Relationship between NPTX2 and annualised changes in MMSE, TMT-B, phonemic verbal fluency, FTD plus CDR modules and CBI-R in mutation carriers. Annualised change was calculated by subtracting the score at the time of CSF collection from the most recently collected score and dividing by the time interval. Results are from linear regression analysis which included age, sex, study site and for cognitive tests education level as covariates. *b* indicates unstandardised regression coefficient; β indicates standardised regression coefficient; SE: standard error; MMSE: Mini Mental State Examination; TMT-B: Trail Making Test part B; CDR: Clinical Dementia Rating scale; CBI-R: Revised Cambridge Behavioural Inventory.

	n	*b* (SE)	β	p
MMSE	136	0.001 (0.001)	0.159	0.077
TMT-B	107	-0.001 (0.004)	-0.040	0.693
Phonemic verbal fluency	118	0.004 (0.001)	0.302	0.001
FTD plus CDR modules	105	-0.001 (0.001)	-0.244	0.025
CBI-R	93	-0.004 (0.003)	-0.163	0.200

Chapter 3

Biomarkers of immune system dysregulation

Chapter 3.1

CSF sTREM2 is elevated in a subset in *GRN*-related frontotemporal dementia

Emma L. van der Ende, Estrella Morenas-Rodriguez, Corey McMillan, Murray Grossman, David Irwin, Raquel Sanchez-Valle, Caroline Graff, Rik Vandenberghe, Yolande A.L. Pijnenburg, Robert Laforce Jr, Isabelle Le Ber, Alberto Lleo, Christian Haass, Marc Suarez-Calvet, John C. van Swieten, Harro Seelaar

Neurobiology of Aging, 2021;103:158.e1-158.e5.

Abstract

Excessive microglial activation might be a central pathological process in *GRN*-related frontotemporal dementia (FTD-*GRN*). We measured soluble triggering receptor expressed on myeloid cells 2 (sTREM2), which is shed from disease-associated microglia following cleavage of TREM2, in cerebrospinal fluid of 34 presymptomatic and 35 symptomatic *GRN* mutation carriers, 6 presymptomatic and 32 symptomatic *C9orf72* mutation carriers and 67 healthy non-carriers by ELISA. Although no group differences in sTREM2 levels were observed (*GRN*: symptomatic (median 5.2 ng/ml, interquartile range [3.9-9.2]) vs. presymptomatic (4.3 ng/ml [2.6-6.1]) vs. non-carriers (4.2 ng/ml [2.6-5.5]): p=0.059; *C9orf72*: symptomatic (4.3 [2.9-7.0]) vs. presymptomatic (3.2 [2.2-4.2]) vs. non-carriers: p=0.294), high levels were seen in a subset of *GRN*, but not *C9orf72,* mutation carriers, which might reflect differential TREM2-related microglial activation. Interestingly, two presymptomatic carriers with low sTREM2 levels developed symptoms after 1 year, whereas two with high levels became symptomatic after >5 years. While sTREM2 is not a promising diagnostic biomarker for FTD-*GRN* or FTD-*C9orf72*, further research might elucidate its potential to monitor microglial activity and predict disease progression.

Introduction

Frontotemporal dementia (FTD) is frequently caused by autosomal dominant genetic mutations in granulin (*GRN*). Although the exact mechanisms by which *GRN* mutations lead to FTD are poorly understood, accumulating evidence suggests a role for dysregulation of microglial homeostasis.[1,2] *GRN*$^{-/-}$ mice display excessive microglial activation with subsequent release of pro-inflammatory factors and neuronal loss,[3-5] and suppression of genes characteristic for homeostatic microglia,[6] whereas *GRN* overexpression reduces microglial recruitment following nerve injury.[7] Biomarkers that accurately reflect microglial activity in vivo are currently lacking and might provide more insight into disease pathogenesis, as well as measure treatment effect in clinical trials aiming to restore immune dysregulation.

Triggering receptor expressed on myeloid cells 2 (TREM2) is a membrane-bound receptor expressed by microglia which regulates the transition from homeostatic to disease-associated microglia.[8-10] Cleavage of its extracellular domain produces a soluble fragment, sTREM2, which is measurable in cerebrospinal fluid (CSF).[11] CSF sTREM2 levels likely reflect cerebral TREM2 expression and TREM2-triggered microglial activity.[8,12-14] Elevated sTREM2 levels have been observed mainly in the prodromal stages of Alzheimer's disease (AD).[14-16] Reports of sTREM2 levels in FTD are inconsistent,[9,17,18] but high levels have been reported in a few FTD-*GRN* cases.[19]

In the present study, we measured CSF sTREM2 in an international cohort of presymptomatic and symptomatic *GRN* mutation carriers and non-carriers to determine its value as a biomarker in FTD-*GRN*. To study potential gene-specificity, we additionally measured sTREM2 in carriers of a *C9orf72* repeat expansion, the most common genetic cause of FTD.

Methods

Subjects were recruited from eight research centres in Europe and the USA through familial FTD studies. We included 34 presymptomatic and 35 symptomatic *GRN* mutation carriers, 6 presymptomatic and 32 symptomatic *C9orf72* mutation carriers, and 67 healthy non-carriers from *GRN* or *C9orf72* mutation families. Subjects were classified as symptomatic if they met international consensus criteria for behavioural variant FTD, primary progressive aphasia or amyotrophic lateral sclerosis (ALS).[20-22] Symptom onset and disease duration were based on caregivers' estimations of the emergence of first symptoms. Subjects had no known neurological or immunological co-morbidities. Global cognitive functioning was scored using the Mini Mental State Examination (MMSE).

CSF was collected in polypropylene tubes, centrifuged and stored at -80°C within two hours after withdrawal. sTREM2 levels were measured using an ELISA as previously described.[9] Samples were randomly distributed across plates and measured in duplicate; the median coefficient of variation (CV) of duplicate samples was 3.6%. One sample with a duplicate CV>15% was excluded. Samples were measured in two batches (median between-batch CV 4%) in the German Center for Neurodegenerative Diseases (DZNE), Munich, Germany. Laboratory technicians were blinded to all clinical and genetic information.

Statistical analyses were performed in IBM SPSS Statistics 24 applying a significance level of 0.05 (two-sided). Demographic variables were compared using Kruskal-Wallis tests for numerical variables and Chi square tests for categorical variables. Group comparisons of sTREM2 levels were performed by Mann Whitney U tests or Kruskal-Wallis tests as the data were not normally distributed. After log-transformation, sTREM2 levels were normally distributed, as confirmed by the Shapiro-Wilk test, and group comparisons were additionally performed by ANCOVA with correction for age, sex and assay batch. Spearman's rho was used for correlative analyses. Bonferroni correction for multiple testing was applied where appropriate.

Results

Demographics

Subject characteristics are shown in table 1. In both genetic groups (*GRN* and *C9orf72*), symptomatic mutation carriers were older at CSF collection than presymptomatic carriers and non-carriers ($p<0.001$). sTREM2 levels were positively correlated with age across the entire cohort ($r_s=0.271$, $p<0.001$) and in non-carriers alone ($r_s=0.247$, $p=0.044$) but not in symptomatic *GRN* or *C9orf72* mutation carriers (*GRN*: $r_s=0.020$, $p=0.911$; *C9orf72*: $r_s=0.206$, $p=0.258$) (supplementary figure 1). No differences were found in sTREM2 levels between males and females ($p=0.470$).

Table 1. Subject characteristics. All continuous variables are reported as medians (interquartile range). Abbreviations: CSF, cerebrospinal fluid; MMSE, Mini Mental State Examination; SYM, symptomatic; PRE, presymptomatic.

	GRN mutation carriers		*C9orf72* mutation carriers		Non-carriers	*p*
	SYM[a]	PRE	SYM[b]	PRE		
N	35	34	32	6	67	-
Sex, male (%)	16 (46%)	15 (44%)	18 (56%)	0 (0%)	27 (40%)	0.132[c]
Age at CSF collection, years	61 (57-65)	51 (41-59)	62 (54-67)	34 (26-43)	54 (42-59)	<0.001[d]
Disease duration, years	2.0 (1.5-3.1)	-	1.9 (0.7-5.1)	-	-	0.672
MMSE	23 (18-27)	29 (29-30)	26 (22-28)	29 (29-30)	30 (29-30)	<0.001[d]
sTREM2 (ng/ml)	5.2 (3.9-9.2)	4.3 (2.6-6.1)	4.3 (2.9-7.0)	3.2 (2.2-4.2)	4.2 (2.6-5.5)	0.090[e]

[a]Phenotypes: behavioural variant FTD (bvFTD) (n=20), primary progressive aphasia (PPA) (n=8), dementia not otherwise specified (n=4), memory-predominant FTD (n=2), and FTD with corticobasal syndrome (CBS) (n=1); [b]Phenotypes: bvFTD (n=13), PPA (n=3), FTD with amyotrophic lateral sclerosis (ALS) (n=9), ALS (n=5), memory-predominant FTD (n=1), and FTD with CBS (n=1); [c]By Chi-square test; [d]In both genetic groups, symptomatic mutation carriers were older and had lower MMSE scores than presymptomatic carriers and non-carriers (all comparisons p<0.001). There were no significant differences in age or MMSE between symptomatic *GRN* and *C9orf72* carriers (by Mann-Whitney U tests); [e]By Kruskall-Wallis test across all groups.

sTREM2 levels in GRN mutation carriers

No significant differences in sTREM2 levels were seen in symptomatic *GRN* mutation carriers (median 5.2 ng/ml, interquartile range [3.9-9.2]) compared to presymptomatic carriers (4.3 ng/ml [2.6-6.1]) and non-carriers (4.2 ng/ml [2.6-5.5]) (p=0.059 by Kruskal-Wallis test; p=0.513 by ANCOVA) (figure 1). sTREM2 levels did not correlate with disease duration (r_s=0.210, p=0.226) or MMSE score (r_s=-0.364, p=0.057, n=28) among symptomatic carriers. Furthermore, no significant differences in sTREM2 levels were seen between the various FTD phenotypes (p=0.830) (table 1).

Three presymptomatic *GRN* mutation carriers developed FTD respectively 1 year, 1.2 years and 7 years after CSF collection (figure 1). In addition, one presymptomatic *GRN* carrier developed mild behavioural abnormalities and cognitive deficits 5 years after CSF collection, although clinical diagnostic criteria for FTD were not fulfilled.

Visual inspection of figure 1 revealed high sTREM2 levels in eight symptomatic *GRN* mutation carriers (>10 ng/ml). We did not identify any association with specific clinical or genetic features in these subjects (i.e., disease severity or duration, phenotype, age at symptom onset, genetic mutation) (supplementary table 1).

Figure 1. sTREM2 levels in presymptomatic and symptomatic mutation carriers and non-carriers. Error bars represent median ± interquartile range. Red and blue triangles indicate subjects with isolated or concomitant amyotrophic lateral sclerosis, respectively. Green squares indicate subjects who developed symptoms after CSF collection; subject 1 developed FTD with corticobasal syndrome after seven years; subject 2 suffered cognitive decline after five years; subject 3 developed memory-predominant FTD after 1.2 years; subject 4 developed behavioural variant FTD after one year.

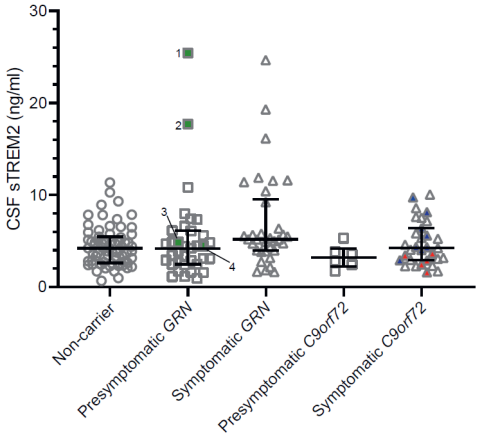

sTREM2 levels in C9orf72 mutation carriers

No significant differences in sTREM2 levels were seen between symptomatic (median 4.3 ng/ml [2.9-7.0])) and presymptomatic (3.2 ng/ml [2.2-4.2]) *C9orf72* mutation carriers or non-carriers (p=0.294 by Kruskal-Wallis test; p=0.433 by ANCOVA) (figure 1). Results were unchanged after exclusion of subjects with isolated ALS (n=4) or FTD with ALS (n=9). sTREM2 levels did not correlate with disease duration (r_s=0.199, p=0.275) or MMSE score (r_s=-0.037, p=0.856, n=27) among symptomatic carriers.

Comparison between GRN and C9orf72 mutation carriers

sTREM2 levels did not differ between symptomatic *GRN* and *C9orf72* mutation carriers (p=0.196) or between presymptomatic *GRN* and *C9orf72* mutation carriers (p=0.288) (both by Mann-Whitney U tests).

Discussion

The present study revealed no significant differences in CSF sTREM2 levels between presymptomatic and symptomatic *GRN* or *C9orf72* mutation carriers and non-carriers. Although the lack of group differences and overlap in sTREM2 levels between groups preclude its value as a diagnostic biomarker, a remarkable degree of variability in sTREM2 levels was observed among *GRN* mutation carriers, which warrants further study.

Several *GRN* mutation carriers had very high sTREM2 levels, whereas sTREM2 levels among *C9orf72* carriers and non-carriers appeared to be more consistent, which is in line with previous findings.[19] These high levels are unlikely to be measurement errors given the favorable assay characteristics [9] and low inter-plate and duplicate CVs. Elevated CSF sTREM2 levels are thought to reflect increased TREM2-dependent microglial activation, a hypothesis that is supported by more convincingly elevated levels in typical neuroinflammatory diseases such as multiple sclerosis [11] and by a correlation between brain sTREM2 levels and microglial activity on TSPO-PET imaging in mouse models.[23] Our findings might therefore reflect a variable degree of microglial involvement specifically among *GRN* mutation carriers. The identification of subsets of carriers with more or less microglial activation would be highly valuable for patient stratification in inflammation-directed clinical trials. Interestingly, much variability has also been observed for the microglia-derived proteins YKL-40 and chitotriosidase (CHIT-1) in FTD [24-26] and future studies that elucidate the relationship between these proteins in FTD-*GRN* would be of interest.

Three presymptomatic *GRN* mutation carriers developed FTD after CSF collection, and cognitive decline was reported in one. Interestingly, two of these subjects with very high sTREM2 levels only developed symptoms several years after CSF collection, while two subjects with low sTREM2 levels declined within two years. It is tempting to speculate that increased microglial activity and accordingly, high sTREM2 levels, in the late-presymptomatic stage might delay disease onset. In mild cognitive impairment and AD, higher CSF sTREM2 levels have been associated with reduced rates of clinical decline and attenuated amyloid-β accumulation on amyloid PET imaging, suggesting that TREM2-related processes might play a protective role.[12,13,27] In line with these findings, increased microglial activation on TSPO-PET imaging predicted slower disease progression in (prodromal) AD.[28] Such associations require further study in a much larger cohort of FTD-*GRN* patients, and could be highly relevant for clinical trial design as they could potentially confound outcome measures, i.e., slow progression rates could falsely be attributed to the study drug.

The positive correlation between sTREM2 levels and age is in line with previous studies [14,16,18,19,29] and is thought to reflect physiological age-related microglial activity.[30,31] Although we cannot rule out that co-existence of other (asymptomatic) neurodegenerative diseases such as AD might have affected sTREM2 levels in our cohort, several studies have found no correlation between sTREM2 levels and CSF amyloid-β;[14,18,29] therefore, the effect of concomitant amyloid pathology on sTREM2 levels in the present study is probably limited.

Neuroinflammation is thought to be the result of a highly complex and dynamic interaction between many factors.[1] Different disease stages might be characterised by variable degrees of microglial activation and subsequent sTREM2 shedding, making group comparisons difficult to interpret. This is exemplified by findings of elevated sTREM2 levels in preclinical and early-stage AD, followed by slightly attenuated levels in later disease stages.[14-16] Longitudinal measurements of sTREM2 in FTD-*GRN* might provide insights into its dynamics over the course of disease as well as determine its value as a disease monitoring marker.

A major strength of this study is the inclusion of presymptomatic and symptomatic carriers of *GRN* and *C9orf72* mutations, as opposed to clinically diagnosed FTD patients, enabling investigation of well-defined, pathologically homogeneous cohorts. Limitations include the relatively small sample size, which may have affected statistical power to detect group differences. Furthermore, the MMSE score might not be an optimal measure of disease severity in FTD, however it is a highly standardised instrument which we feel provides a suitable cognitive screening for this multicentre study. Finally, we cannot rule out that some subjects may have carried rare genetic variants in *TREM2*, which are known to affect sTREM2 levels.[9,14]

In conclusion, while sTREM2 is of limited diagnostic utility in FTD-*GRN*, its further study might help to elucidate the role of neuroinflammation in FTD pathogenesis. It would be interesting to further characterise the small number of *GRN* mutation carriers with very high sTREM2 levels and to investigate sTREM2 dynamics over the course of disease through longitudinal measurements.

Highlights

- CSF sTREM2 is not a promising diagnostic biomarker for FTD-*GRN*
- Elevated sTREM2 levels were observed in a subset of *GRN* mutation carriers
- Future studies might reveal utility of CSF sTREM2 for monitoring and stratification

Acknowledgements & Funding

This work was supported by two Memorabel grants from Deltaplan Dementie (The Netherlands Organisation for Health Research and Development and Alzheimer Nederland; grant numbers 7330550813 and 733050103); The Bluefield Project to Cure Frontotemporal Dementia; the Dioraphte foundation (grant number 1402 1300); the European Joint Programme – Neurodegenerative Disease Research (JPND, PreFrontALS); NIH (grant number AG017586); the Wyncote Foundation; Arking Family Fund; Invetissements d'avenir (grant number ANR-11-INBS-0011); the Schörling Foundation - Swedish FTD Initiative, Swedish

Research Council (2015-02926, 2018-02754 and 2019-02248: JPND GENFI-PROX), Swedish Alzheimer's foundation, Brain Foundation, Demensfonden, Stiftelsen för Gamla Tjänarinnor, Stohnes foundation, and Region Stockholm (ALF project).

Declarations of interest

C.H. collaborates with Denali Therapeutics, participated in one advisory board meeting of Biogen and received a speaker honorarium from Novartis and Roche. C.H. is chief advisor of ISAR Bioscience. The remaining authors declare no conflicts of interest.

Author contributions

ELvdE, JCvS and HS contributed to data acquisition, conception and design of the study, statistical analysis and drafting of the manuscript and figures. EMR, CMM, MG, DI, CH and MSC contributed to data acquisition and conception and design of the study. The remaining authors recruited patients and collected data. All authors criticially reviewed the manuscript and approved the final draft.

References

1. Bright F, Werry EL, Dobson-Stone C, et al. Neuroinflammation in frontotemporal dementia. Nat Rev Neurol. 2019;15(9):540-55.
2. Chitramuthu BP, Bennett HPJ, Bateman A. Progranulin: a new avenue towards the understanding and treatment of neurodegenerative disease. Brain. 2017;140(12):3081-104.
3. Lui H, Zhang J, Makinson SR, et al. Progranulin Deficiency Promotes Circuit-Specific Synaptic Pruning by Microglia via Complement Activation. Cell. 2016;165(4):921-35.
4. Martens LH, Zhang J, Barmada SJ, et al. Progranulin deficiency promotes neuroinflammation and neuron loss following toxin-induced injury. J Clin Invest. 2012;122(11):3955-9.
5. Tanaka Y, Matsuwaki T, Yamanouchi K, et al. Exacerbated inflammatory responses related to activated microglia after traumatic brain injury in progranulin-deficient mice. Neuroscience. 2013;231:49-60.
6. Götzl JK, Brendel M, Werner G, et al. Opposite microglial activation stages upon loss of PGRN or TREM2 result in reduced cerebral glucose metabolism. EMBO Mol Med. 2019;11(6).
7. Altmann C, Vasic V, Hardt S, et al. Progranulin promotes peripheral nerve regeneration and reinnervation: role of notch signaling. Mol Neurodegener. 2016;11(1):69.
8. Keren-Shaul H, Spinrad A, Weiner A, et al. A Unique Microglia Type Associated with Restricting Development of Alzheimer's Disease. Cell. 2017;169(7):1276-90 e17.
9. Kleinberger G, Yamanishi Y, Suarez-Calvet M, et al. TREM2 mutations implicated in neurodegeneration impair cell surface transport and phagocytosis. Sci Transl Med. 2014;6(243):243ra86.
10. Schlepckow K, Kleinberger G, Fukumori A, et al. An Alzheimer-associated TREM2 variant occurs at the ADAM cleavage site and affects shedding and phagocytic function. EMBO Mol Med. 2017;9(10):1356-65.
11. Piccio L, Buonsanti C, Cella M, et al. Identification of soluble TREM-2 in the cerebrospinal fluid and its association with multiple sclerosis and CNS inflammation. Brain. 2008;131(Pt 11):3081-91.
12. Ewers M, Biechele G, Suárez-Calvet M, et al. Higher CSF sTREM2 and microglia activation are associated with slower rates of beta-amyloid accumulation. EMBO Mol Med. 2020;12(9):e12308.
13. Ewers M, Franzmeier N, Suárez-Calvet M, et al. Increased soluble TREM2 in cerebrospinal fluid is associated with reduced cognitive and clinical decline in Alzheimer's disease. Sci Transl Med. 2019;11(507).
14. Suárez-Calvet M, Morenas-Rodríguez E, Kleinberger G, et al. Early increase of CSF sTREM2 in Alzheimer's disease is associated with tau related-neurodegeneration but not with amyloid-β pathology. Mol Neurodegener. 2019;14(1):1.
15. Liu D, Cao B, Zhao Y, et al. Soluble TREM2 changes during the clinical course of Alzheimer's disease: A meta-analysis. Neurosci Lett. 2018;686:10-6.
16. Ma LZ, Tan L, Bi YL, et al. Dynamic changes of CSF sTREM2 in preclinical Alzheimer's disease: the CABLE study. Mol Neurodegener. 2020;15(1):25.

17. Heslegrave A, Heywood W, Paterson R, et al. Increased cerebrospinal fluid soluble TREM2 concentration in Alzheimer's disease. Mol Neurodegener. 2016;11:3.
18. Piccio L, Deming Y, Del-Aguila JL, et al. Cerebrospinal fluid soluble TREM2 is higher in Alzheimer disease and associated with mutation status. Acta Neuropathol. 2016;131(6):925-33.
19. Woollacott IOC, Nicholas JM, Heslegrave A, et al. Cerebrospinal fluid soluble TREM2 levels in frontotemporal dementia differ by genetic and pathological subgroup. Alzheimers Res Ther. 2018;10(1):79.
20. Brooks BR, Miller RG, Swash M, et al. El Escorial revisited: revised criteria for the diagnosis of amyotrophic lateral sclerosis. Amyotroph Lateral Scler Other Motor Neuron Disord. 2000;1(5):293-9.
21. Gorno-Tempini ML, Hillis AE, Weintraub S, et al. Classification of primary progressive aphasia and its variants. Neurology. 2011;76(11):1006-14.
22. Rascovsky K, Hodges JR, Knopman D, et al. Sensitivity of revised diagnostic criteria for the behavioural variant of frontotemporal dementia. Brain. 2011;134(Pt 9):2456-77.
23. Brendel M, Kleinberger G, Probst F, et al. Increase of TREM2 during Aging of an Alzheimer's Disease Mouse Model Is Paralleled by Microglial Activation and Amyloidosis. Front Aging Neurosci. 2017;9:8.
24. Abu-Rumeileh S, Steinacker P, Polischi B, et al. CSF biomarkers of neuroinflammation in distinct forms and subtypes of neurodegenerative dementia. Alzheimers Res Ther. 2019;12(1):2.
25. Oeckl P, Weydt P, Steinacker P, et al. Different neuroinflammatory profile in amyotrophic lateral sclerosis and frontotemporal dementia is linked to the clinical phase. J Neurol Neurosurg Psychiatry. 2019;90(1):4-10.
26. Woollacott IOC, Nicholas JM, Heller C, et al. Cerebrospinal Fluid YKL-40 and Chitotriosidase Levels in Frontotemporal Dementia Vary by Clinical, Genetic and Pathological Subtype. Dement Geriatr Cogn Disord. 2020;49(1):56-76.
27. Franzmeier N, Suárez-Calvet M, Frontzkowski L, et al. Higher CSF sTREM2 attenuates ApoE4-related risk for cognitive decline and neurodegeneration. Mol Neurodegener. 2020;15(1):57.
28. Hamelin L, Lagarde J, Dorothée G, et al. Distinct dynamic profiles of microglial activation are associated with progression of Alzheimer's disease. Brain. 2018;141(6):1855-70.
29. Suárez-Calvet M, Kleinberger G, Araque Caballero M, et al. sTREM2 cerebrospinal fluid levels are a potential biomarker for microglia activity in early-stage Alzheimer's disease and associate with neuronal injury markers. EMBO Mol Med. 2016;8(5):466-76.
30. Kleinberger G, Brendel M, Mracsko E, et al. The FTD-like syndrome causing TREM2 T66M mutation impairs microglia function, brain perfusion, and glucose metabolism. Embo J. 2017;36(13):1837-53.
31. Heneka MT, Kummer MP, Latz E. Innate immune activation in neurodegenerative disease. Nat Rev Immunol. 2014;14(7):463-77.

Supplementary tables and figures

Supplementary table 1. Clinical and genetic data for symptomatic *GRN* mutation carriers with sTREM2 levels >10 ng/ml. Samples were measured in duplicate; duplicate coefficient of variation was <6% for all samples shown. To prevent potential identification of individuals, age at symptom onset is provided as a range rather than an exact age. Abbrevations: CSF, cerebrospinal fluid; bvFTD, behavioural variant FTD; nfvPPA, non-fluent variant primary progressive aphasia; FTD-CBS, FTD with corticobasal syndrome; MMSE, Mini Mental State Examination.

#	Age at symptom onset (years)	Disease duration at CSF (years)	Phenotype	MMSE score at CSF	sTREM2 (ng/ml)
1	50-55	2	bvFTD	8	24.7
2	56-60	3	bvFTD	N/A	19.3
3	56-60	2	nfvPPA	30	16.2
4	56-60	7	bvFTD	4	11.9
5	60-65	2	bvFTD	19	11.6
6	45-50	3	bvFTD	8	11.6
7	60-65	3	nfvPPA	24	11.4
8	60-65	3	FTD-CBS	8	10.4

Supplementary figure 1. Correlation between sTREM2 levels and age at CSF collection (r_s=0.271, p<0.001).

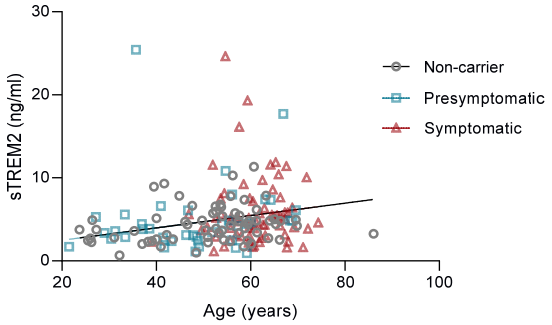

Chapter 4

Proteomic and genetic approaches to fluid biomarker identification

Chapter 4.1

Novel CSF biomarkers in genetic fronto temporal dementia identified by proteomics

Emma L. van der Ende*, Lieke H. Meeter*, Christoph Stingl, Jeroen G.J. van Rooij, Marcel P. Stoop, Diana A.T. Nijholt, Raquel Sanchez-Valle, Caroline Graff, Linn Öijerstedt, Murray Grossman, Corey McMillan, Yolande A.L. Pijnenburg, Robert Laforce Jr, Giuliano Binetti, Luisa Benussi, Roberta Ghidoni, Theo M. Luider, Harro Seelaar, John C. van Swieten

*Authors contributed equally to the manuscript

Annals of Clinical and Translational Neurology 2018;6(4):698-707

Abstract

Objective: To identify novel CSF biomarkers in *GRN*-associated frontotemporal dementia (FTD) by proteomics using mass spectrometry (MS).

Methods: Unbiased MS was applied to CSF samples from 19 presymptomatic and 9 symptomatic *GRN* mutation carriers and 24 non-carriers. Protein abundances were compared between these groups. Proteins were then selected for validation if identified by ≥4 peptides and if fold change was ≤0.5 or ≥2.0. Validation and absolute quantification by parallel reaction monitoring (PRM), a high-resolution targeted MS method, was performed on an international cohort (n=210) of presymptomatic and symptomatic *GRN, C9orf72* and *MAPT* mutation carriers.

Results: Unbiased MS revealed twenty differentially abundant proteins between symptomatic mutation carriers and non-carriers and nine between symptomatic and presymptomatic carriers. Seven of these proteins fulfilled our criteria for validation. PRM analyses revealed that symptomatic *GRN* mutation carriers had significantly lower levels of neuronal pentraxin receptor (NPTXR), receptor-type tyrosine-protein phosphatase N2 (PTPRN2), neurosecretory protein VGF, chromogranin-A (CHGA) and V-set and transmembrane domain-containing protein 2B (VSTM2B) than presymptomatic carriers and non-carriers. Symptomatic *C9orf72* mutation carriers had lower levels of NPTXR, PTPRN2, CHGA and VSTM2B than non-carriers, while symptomatic *MAPT* mutation carriers had lower levels of NPTXR and CHGA than non-carriers.

Interpretation: We identified and validated five novel CSF biomarkers in *GRN*-associated FTD. Our results show that synaptic, secretory vesicle and inflammatory proteins are dysregulated in the symptomatic stage and may provide new insights into the pathophysiology. Further validation is needed to investigate their clinical applicability as diagnostic or monitoring biomarkers.

Introduction

Frontotemporal dementia (FTD) is the second most common form of presenile dementia, with autosomal dominant inheritance in approximately 30% of cases.[1,2] Pathogenic mutations in granulin (*GRN*) are a major cause of hereditary FTD with underlying transactive response DNA-binding protein 43 (TDP-43) pathology.[2] The vast majority of *GRN* mutations result in reduction of progranulin (PGRN) protein levels in blood and cerebrospinal fluid (CSF) by haploinsufficiency.[3-6] However, the exact mechanism by which PGRN reduction leads to neurodegeneration is poorly understood. Upcoming therapeutic interventions should ideally be applied in the presymptomatic or prodromal stage of the disease, when neuronal damage is minimal, highlighting the need for biomarkers that reflect early pathologic processes.[7]
Most studies on fluid biomarkers in FTD have used targeted approaches, allowing measurement of known protein candidates only,[7,8] while unbiased approaches have scarcely been performed.[9,10] In autosomal dominant Alzheimer's disease, unbiased approaches have uncovered early changes in the proteome.[11]

In the present study, we investigated CSF proteomics by unbiased mass spectrometry (MS) in presymptomatic and symptomatic *GRN* mutation carriers. We aimed to identify novel proteins that reflect disease activity and/or give insight into the pathophysiology. We validated and quantified a selection of the identified proteins using parallel reaction monitoring (PRM), a high-resolution targeted MS-based approach, in an international cohort of *GRN* mutation carriers and other forms of genetic FTD, namely *C9orf72* and *MAPT* mutation carriers.[1]

Methods

Subjects

Discovery proteomics was applied on CSF of 9 symptomatic and 19 presymptomatic *GRN* mutation carriers and 24 healthy non-carriers ('discovery cohort'), who participate in the Dutch longitudinal FTD Risk Cohort (FTD-RisC).[12] Briefly, patients with genetic FTD and asymptomatic 50% at-risk individuals (either presymptomatic mutation carriers or non-carriers) from families with genetic FTD are followed yearly or two-yearly by means of neurological examination, neuropsychological testing, MRI scanning, structured informant interviews and collection of blood and, in a subset, CSF collection.

PRM was performed on a selection of the proteins identified by discovery proteomics in CSF of 61 *GRN* mutation carriers (31 presymptomatic, 30 symptomatic), 70 *C9orf72* mutation carriers (16 presymptomatic, 54 symptomatic), 27 *MAPT* mutation carriers (12 presymptomatic, 15 symptomatic) and 52 non-carriers ('validation cohort'). CSF samples were collected from six research centres in Europe and the USA. 46 samples in the validation cohort overlapped with those in the discovery cohort.

The study was approved by the local ethics committee and all participants (or a legal representative) provided written informed consent.

Sample collection

CSF was collected in polypropylene tubes according to standardised local procedures and stored at -80°C after centrifugation within two hours after withdrawal.

Discovery proteomics

Discovery proteomics was performed as described previously [13] and details are reported in the supplementary methods. In short, albumin and IgG were depleted from 50 µl of CSF sample to maximise peptide detection (Pierce, PN 85162). After overnight in-solution trypsin digestion, samples were analysed by LC-MS/MS in a randomised order on a nano LC system coupled to an Orbitrap Fusion Lumos mass spectrometer (Thermo Fisher Scientific). For peptide and protein identification, MS/MS spectra were extracted using ProteoWizard [14] software (version 3.0.9248) and analysed with the database search engine Mascot (Matrix Science, UK) against the Uniprot database [15] (downloaded November 12th 2015; taxonomy: Homo sapiens; 20,194 entries). Next we combined the search results of the individual samples, applied scoring of hits (local false discovery rate ≤ 1%) and conducted protein grouping using the software Scaffold.[16,17] For label-free quantitation MS raw data was processed with Progenesis QI (version 2.0) and linked with identification results to finally determine peptide and protein abundances. Abundances were normalised to the total ion current to compensate for experimental variations using an algorithm available in the analysis software. Subsequently, the data were exported in Excel format.

Statistical analyses of discovery proteomics

For all peptides identified by discovery proteomics, we compared peptide abundances in: 1) symptomatic mutation carriers versus non-carriers; 2) symptomatic versus presymptomatic mutation carriers; 3) presymptomatic mutation carriers versus non-carriers. As the data were not normally distributed, a Wilcoxon rank-sum test was used. Corresponding proteins were regarded as significantly differentially abundant when they satisfied all of the following criteria, as described before [18] with minor adjustments: 1) the protein was identified by two or more peptides; 2) 25% or more of the peptides of the protein were significant at

p<0.01; 3) 50% or more of the peptides of the protein were significant at *p*<0.05; 4) 75% or more of the peptides were changed in the same direction (i.e. up- or downregulated). Statistical background levels were determined by permutation tests on all samples and all identified peptides/proteins. The number of differentially abundant proteins was regarded as significant when the observed number in the true analysis exceeded the threshold from the permutation analysis: mean + three times the standard deviation. Fold changes based on median abundances were calculated for all group comparisons on peptide levels and peptides with a median of zero were excluded. Next, protein fold changes were calculated by the mean of corresponding peptide fold changes.

PRM validation

Differentially abundant proteins from discovery proteomics were selected for PRM validation based on the following criteria: 1) the protein was identified by four or more peptides and 2) protein fold change was ≤0.5 or ≥2.0.

PRM was essentially performed as described previously [19] and details are reported in the supplementary methods. In short, 20 µl of CSF was digested overnight by trypsin. LC-MS analysis was carried out on a nano LC system coupled to an Orbitrap Fusion mass spectrometer (Thermo Fisher Scientific). For PRM of the peptide panel of candidates a time scheduled targeted MS/MS method was used and the referring peptide-specific parameters are listed in supplementary table 1. To allow absolute quantification of peptides, synthetic stable isotope labelled (SIL) peptides were added as listed in supplementary table 1. As technical quality check (QC), a pool of 80 CSF samples was prepared and loaded as 8-fold replicate on each well-plate. During LC-MS measurements, every 12th run a QC sample was measured to determine the reproducibility of the assay. For assessment of sensitivity of the assay an eight-point dilutions series of the peptide panel in CSF digest matrix was prepared and measured in triplicate. MS data processing was conducted using the software package Skyline.[20] Peak ratios were exported and used for calculation of CSF concentrations of the samples and determining analytical parameters limit of detection (LOD), lower limit of quantitation (LLOQ) and coefficients of variance (CV) (supplementary tables 2a and 2b) using the software package R.[21]

Statistical analyses of demographic data and PRM validation

Statistical analyses were performed in IBM SPSS Statistics 24.0 applying a significance level of p<0.05. Demographic and PRM data for each genotype (*GRN, C9orf72* and *MAPT*) were compared between symptomatic mutation carriers, presymptomatic mutation carriers and non-carriers. For PRM results, per candidate protein one corresponding targeted peptide was chosen based on suitability for quantification and lowest LOD, LLOQ and CV as indicated

in supplementary tables 2a and 2b. Peptides with CV >15% were excluded from further analyses. As the data was not normally distributed, a Kruskall-Wallis test with post-hoc Dunn's test was performed to compare peptide concentrations between groups. ANCOVA of log-transformed peptide concentrations was used to correct for age at CSF sampling. All post-hoc analyses were adjusted for multiple testing by means of Bonferroni correction.

Mass spectrometry data has been made available via the PRIDE partner repository with the dataset identifiers PXD012178 (discovery study) and PXD012179 (validation study).[22]

Gene set enrichment analyses

Gene set enrichment analyses to the Gene Ontology database [23] were performed on a selection of proteins identified by discovery proteomics in symptomatic mutation carriers versus non-carriers, and separately on proteins identified in symptomatic versus presymptomatic mutation carriers. We relaxed the protein selection criteria to allow for separation of multiple enriched pathways in our dataset, aiming to include 50-150 proteins per enrichment analysis. Proteins with a fold change ≤0.83 or ≥1.2 and with ≥25% of peptides significantly up- or downregulated ($p<0.05$) were included. Enrichment was performed to the whole genome as statistical background, accepting false discovery rate (FDR)-corrected results of $p<0.05$ as significantly enriched Gene Ontology (GO) terms. The most significant non-redundant terms for Biological Processes (GOBP), Cellular Components (GOCC) and Molecular Functions (GOMF) were extracted and a protein network was created based on these terms using Cytoscape (v3.4.0).

Results

Subjects

Subject characteristics are shown in table 1. In the discovery cohort, no differences were found in age at CSF collection or sex among symptomatic and presymptomatic mutation carriers and non-carriers. In the validation cohort, symptomatic *GRN* (median 61 years) and *C9orf72* mutation carriers (59 years) were significantly older than presymptomatic *GRN* (54 years) and *C9orf72* mutation carriers (45 years, both $p<0.001$) and non-carriers (54 years, $p<0.001$) at the time of CSF sampling.

Table 1. Subject characteristics. Continuous variables are presented as medians (interquartile range). Abbreviations: FTD, frontotemporal dementia; CSF, cerebrospinal fluid.

	N	Age at CSF collection, years	Sex, male (%)	Age at symptom onset, years	Disease duration, years
Discovery cohort					
Non-carriers	24	51 (40-58)	14 (58%)	n/a	n/a
Presymptomatic *GRN*	19	56 (47-60)	9 (47%)	n/a	n/a
Symptomatic *GRN*	9	58 (53-60)	3 (33%)	57 (51-58)	2.3 (1.5-3.6)
Validation cohort					
Non-carriers	52	54 (43-59)	24 (46%)	n/a	n/a
Presymptomatic *GRN*	31	54 (42-59)	12 (39%)	n/a	n/a
Symptomatic *GRN*	30	61 (57-66)*	11 (37%)	58 (55-63)	1.9 (1.2-3.0)
Presymptomatic *C9orf72*	16	45(36-52)	3 (19%)	n/a	n/a
Symptomatic *C9orf72*	54	59 (54-65)†	31 (57%)‡	56 (50-62)	2.4 (1.2-5.2)
Presymptomatic *MAPT*	12	48 (44-53)	5 (42%)	n/a	n/a
Symptomatic *MAPT*	15	53 (51-60)	7 (47%)	51 (46-55)	3.0 (1.4-5.0)

*Symptomatic *GRN* mutation carriers significantly older than presymptomatic *GRN* mutation carriers and non-carriers ($p<0.001$); †Symptomatic *C9orf72* mutation carriers significantly older than presymptomatic *C9orf72* mutation carriers and non-carriers ($p<0.001$); ‡Symptomatic *C9orf72* mutation carriers and non-carriers significantly more males than presymptomatic *C9orf72* mutation carriers ($p=0.024$).

Discovery proteomics

We identified a total of 4539 peptides corresponding to 572 proteins, of which 503 proteins were identified by ≥2 peptides. 20 proteins were considered significantly differentially abundant in symptomatic *GRN* mutation carriers compared to non-carriers. In the comparison between symptomatic and presymptomatic *GRN* mutation carriers, nine differentially abundant proteins were found (figure 1, supplementary table 3). No significant differences were found between presymptomatic *GRN* mutation carriers and non-carriers. All differentially abundant proteins were identified by peptides which were matched exclusively to that protein.

Validation by PRM

Seven proteins fulfilled our criteria for validation by PRM (table 2). The protein Ig alpha-1 chain C region (IGHA1) was excluded from validation analyses as just one peptide was targeted and this peptide had a CV>15%.

Figure 1. Flow chart of differentially abundant proteins. The number of identified peptides and proteins are displayed and are then split to the differentially abundant proteins per group comparison: 1) symptomatic versus presymptomatic carriers, and 2) symptomatic versus non-carriers. No differentially abundant proteins were found in the comparison presymptomatic versus non-carriers (not shown). In the lower row, proteins are displayed that were selected for validation by PRM. CaM, Calcium/calmodulin-dependent; NPTXR, neuronal pentraxin receptor; PTPRN, receptor-type tyrosine-protein phosphatase-like N; PTPRN2, receptor-type tyrosine-protein phosphatase N2; TNF, tumor necrosis factor; VSTM2B, V-set and transmembrane domain-containing protein 2B.

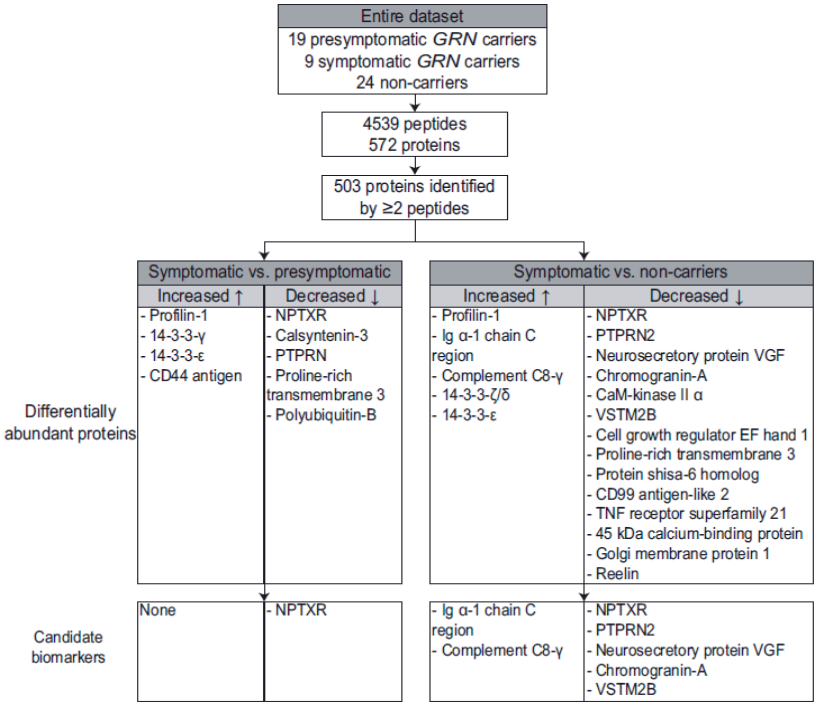

Table 2. Proteins selected for validation by PRM. Fold change (SYM/NC): fold change in discovery proteomics in the comparison between symptomatic *GRN* mutation carriers and non-carriers. Fold change (SYM/PRE): fold change in discovery proteomics in the comparison between symptomatic and presymptomatic *GRN* mutation carriers. Abbreviations: NPTXR, neuronal pentraxin receptor; PTPRN2, receptor-type tyrosine-protein phosphatase N2; VGF, neurosecretory protein VGF; CHGA, chromogranin-A; VSTM2B, V-set and transmembrane domain-containing protein 2B; C8G, complement component C8 gamma chain; IGHA1, Ig alpha-1 chain C region.

Protein	Peptides, *n*	Fold change (SYM/NC)	Fold change (SYM/PRE)
NPTXR	6	0.34	0.39
PTPRN2	5	0.35	-
VGF	21	0.45	-
CHGA	18	0.46	-
VSTM2B	4	0.49	-
C8G	4	2.00	-
IGHA1	6	2.39	-

Symptomatic *GRN* mutation carriers had significantly lower concentrations of Neuronal pentraxin receptor (NPTXR), Receptor-type tyrosine-protein phosphatase N2 (PTPRN2), Neurosecretory protein VGF (VGF), Chromogranin-A (CHGA) and V-set transmembrane domain-containing protein (VSTM2B) compared to both presymptomatic carriers and non-carriers by PRM (table 3, figure 2, supplementary figure 1). Complement component C8 gamma chain (C8G) levels were higher in symptomatic mutation carriers, however this difference was no longer statistically significant after correction for age at CSF sampling.

Symptomatic *MAPT* mutation carriers had significantly lower concentrations of NPTXR and CHGA compared to non-carriers, while the other proteins did not show any significant differences between groups (figure 2, supplementary figure 1).

Symptomatic *C9orf72* mutation carriers had significantly lower concentrations of NPTXR, PTPRN2, CHGA and VSTM2B compared to non-carriers (figure 2, supplementary figure 1). Lower concentrations of NPTXR, PTPRN2, CHGA and VSTM2B were found in presymptomatic mutation carriers than in non-carriers, although not statistically significant.

For all proteins included in validation analyses, no significant differences were found between presymptomatic carriers and non-carriers.

Table 3. Protein levels measured by PRM in *GRN* mutation carriers. Peptides used for quantification are indicated in supplementary table 2. P-values for analyses of covariance (correcting for age at CSF sampling) and after correction for multiple testing are displayed. Abbreviations: NPTXR: neuronal pentraxin receptor; PTPRN2: receptor-type tyrosine-protein phosphatase N2; VGF: neurosecretory protein VGF; CHGA: chromogranin-A; VSTM2B: V-set and transmembrane domain-containing protein 2B; C8G: complement component C8 gamma chain.

	Symptomatic carriers (ng/ml) [IQR] (n=30)	Presymptomatic carriers (ng/ml) [IQR] (n=31)	Non-carriers (ng/ml) [IQR] (n=52)	*p*
NPTXR	89.1 [68.3-117.2]	138.2 [114.2-171.0]	148.4 [118.2-167.0]	<0.001*
PTPRN2	8.7 [6.6-10.8]	15.1 [12.1-17.7]	13.6 [10.9-17.2]	<0.001**
VGF	117.6 [78.3-167.9]	203.3 [158.4-273.0]	171.7 [129.5-228.9]	<0.001†
CHGA	286.5 [233.6-343.6]	409.2 [293.6-471.9]	416.0 [337.7-509.6]	<0.001*
VSTM2B	13.6 [11.0-16.2]	17.7 [13.6-21.3]	17.7 [15.4-21.9]	<0.001‡
C8G	14.2 [10.2-20.6]	13.0 [9.2-17.5]	10.0 [7.9-15.6]	0.126

*Symptomatic *GRN* mutation carriers vs. non-carriers p<0.001; symptomatic vs. presymptomatic *GRN* mutation carriers <0.001; **Symptomatic *GRN* mutation carriers vs. non-carriers p=0.002; symptomatic vs. presymptomatic *GRN* mutation carriers <0.001; †Symptomatic *GRN* mutation carriers vs. non-carriers p=0.045; symptomatic vs. presymptomatic *GRN* mutation carriers p=0.005; ‡Symptomatic *GRN* mutation carriers vs. non-carriers p=0.002; symptomatic vs. presymptomatic *GRN* mutation carriers p=0.007

Figure 2. Neuronal pentraxin receptor (NPTXR) in presymptomatic and symptomatic *GRN, C9orf72* and *MAPT* mutation carriers by PRM. Error bars represent medians with interquartile ranges. Significances from the analysis of covariance (corrected for age at CSF sampling) and after correction for multiple testing are displayed. *p<0.05; **p<0.01; ***p<0.001.

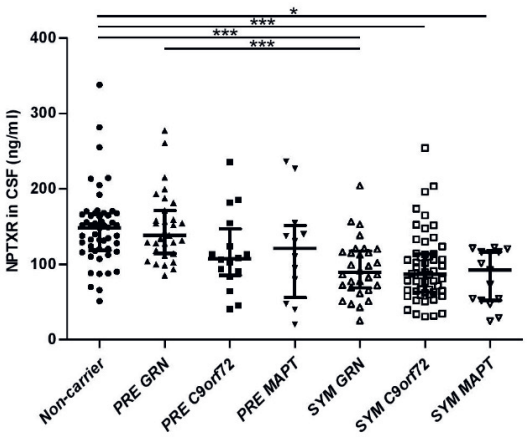

Gene set enrichment analyses

For gene set enrichment analyses, 116 proteins were included in the comparison of symptomatic mutation carriers versus non-carriers, and 72 proteins were included in the comparison of symptomatic versus presymptomatic mutation carriers. In total, 44 GOBP and 7 GOCC terms were significantly enriched (supplementary file 1). The most significantly enriched terms for both comparisons included acute inflammatory response, response to axonal injury and modulation of synaptic transmission. The generated protein interaction network is shown in supplementary figure 2.

Discussion

In this proteomics study, we identified several differentially regulated proteins in CSF of *GRN*-associated FTD. Validation of our results by targeted mass spectrometry revealed significantly lower levels of NPTXR, CHGA, VSTM2B, PTPRN2 and VGF in symptomatic *GRN* mutation carriers compared to presymptomatic and non-carriers. Here, we provide some background information on these proteins.

NPTXR is a transmembrane protein expressed on neurons and glia and is a member of the neuronal pentraxin (NP) family. NPs are multifunctional proteins that have been implicated in synaptic plasticity.[24,25] NPTXR has been identified as a progression biomarker in Alzheimer's disease (AD), with elevated levels in mild cognitive impairment and low levels in AD patients.[26-29] In autosomal dominant AD, NPTXR levels were elevated in

presymptomatic carriers,[11] an effect we did not observe in our presymptomatic *GRN* carriers. This discrepancy may result from differences in underlying pathophysiology, or because we studied presymptomatic carriers of all ages and thus of varying time from onset.

VGF and CHGA belong to the granin protein family and are precursors of peptides with numerous biological functions, including microglial activation (CHGA) and synaptic plasticity.[30-32] Decreased VGF and CHGA levels were also found in proteomics studies in AD.[11,26,29,33]

PTPRN2 is a transmembrane protein present in dense-core vesicles, implicated in secretory processes in the pancreatic islets, but also in the brain.[34] PTPRN, a highly homologous protein, was also found in our discovery proteomics, although it did not strictly fulfill our criteria for validation (fold change 0.56). PTPRN2 is also involved in secretory processes and is decreased in CSF of AD patients.[28] Both PTPRN2 and PTPRN also play more general roles in secretion of hormones and neurotransmitters, and knock-down of both these proteins result in behavioural and learning impairments in mice.[34]

C8G, a constituent of innate immunity was elevated in symptomatic *GRN* mutation carriers compared to non-carriers, although not statistically significant after correction for covariates.[35] An important role for inflammatory pathways in FTD is supported by prior studies that identified YKL-40, complement factors and interleukines as candidate biomarkers for FTD. The numerous enriched gene ontology terms related to inflammatory processes support this hypothesis. PGRN is implicated as an anti-inflammatory protein, with haploinsufficiency resulting in lysosomal dysfunction, complement production and microglial activation.[36]

The last candidate protein we identified is VSTM2B, this is a membrane protein but its exact function has scarcely been studied.

The observed decrease in synapse proteins could represent synaptic turnover or loss occurring during the course of the disease. Increasing evidence suggests that altered synaptic function may contribute to the early pathogenesis of FTD, especially in *GRN* mutations,[36-38] a concept previously recognised primarily in AD. In rat hippocampal neurons, knocking down PGRN decreases synapse density,[39] and in *GRN*-knockout mice, PGRN-deficiency causes synaptic dysfunction prior to the occurrence of other neuropathological changes.[40] It has been hypothesised that PGRN deficiency could cause synaptic pruning through activation of microglia and complement factors.[36] Strategies aimed at increasing or maintaining synaptic connectivity could prove beneficial in future therapeutic interventions.

Four of the five protein decreases (NPTXR, VSTM2B, CHGA and PTPRN2) observed in symptomatic *GRN* carriers were also seen in symptomatic *C9orf72* carriers, suggesting that these changes are not specific for *GRN*-associated FTD. The trend towards lower levels of these proteins in presymptomatic *C9orf72* carriers compared to non-carriers, must be interpreted with caution due to lack of statistical significance. However, if confirmed in a larger genetic FTD cohort, this could support the hypothesis that *C9orf72*-associated FTD has a more protracted onset than *GRN*-associated FTD.[41-43] In *MAPT* mutation carriers, significant differences in protein concentrations were only found for NPTXR and CHGA. This may reflect differences in underlying pathophysiology or it may be due to the smaller sample size in *MAPT* mutation carriers.[2,7]

Strengths of this study include the unique sample set with a large cohort of presymptomatic and symptomatic *GRN* mutation carriers. Restricting our discovery cohort to *GRN* mutation carriers allowed us to create a pathologically homogeneous group of FTD-patients. The unbiased proteomics approach enabled us to identify novel biomarkers without predefined hypotheses. Validation of our discovery proteomics results by PRM has provided convincing evidence for our findings.

The depletion step in the discovery proteomics, removing albumin and IgG, has considerably improved the detection of low abundancy proteins. Very low abundancy proteins could, however, be below the detection limit despite the depletion step. This may explain why we did not find PGRN, known to be decreased in *GRN* mutation carriers, or neurofilament light chain (NfL), known to be increased in symptomatic carriers, both of which have average CSF concentrations below 10 ng/ml.[4,41] Furthermore, relevant proteins may bind to the depleted proteins, thereby impeding their detection.[44] Finally, our stringent selection criteria for validation likely reduced the number of false-positive findings, however may also have excluded certain relevant potential biomarkers.

In conclusion, we present five promising novel CSF biomarkers in genetic FTD. Further verification and correlation with clinical features is needed in larger cohorts of genetic FTD, such as GENFI (Genetic FTD Initiative) and LEFFTDS (Longitudinal Evaluation of Familial Frontotemporal Dementia Subjects). Validation by immunoassays is necessary to reveal whether clinical implementation of these biomarkers is feasible.

Acknowledgements & Funding

We are greatly indebted to all participants of this study. We thank all local research coordinators for their help in collecting CSF samples and clinical data. This study was supported in the Netherlands by two Memorabel grants from Deltaplan Dementie (The

Netherlands Organisation for Health Research and Development and Alzheimer Nederland; grant numbers 733050813 and 733050103), the Bluefield Project to Cure Frontotemporal Dementia, the Dioraphte foundation (grant number 1402 1300), and the European Joint Programme – Neurodegenerative Disease Research and the Netherlands ORganisation for Health Research and Development (PreFrontALS: 733051042, RiMod-FTD: 733051024); in Spain by the Spanish National Institute of Health Carlos III (ISCIII) under the aegis of the EU Joint Programme – Neurodegenerative Disease Research (JPND) (AC14/00013) and Fundacio Marato de TV3 (grant number 20143810); in Sweden by the Swedish Alzheimer foundation, the Regional Agreement on Medical Training and Clinical Research (ALF) between Stockholm County Council and Karolinska Institutet, the Strategic Research Program in Neuroscience at Karolinska Institutet, Karolinska Institutet Doctoral Funding, Swedish Medical Research Council, Swedish Brain Foundation, the Old Servants foundation, Gun and Bertil Stohne's foundation and the Schörling Foundation - Swedish FTD Initiative; and in Italy by the Italian Ministry of Health (Ricerca Corrente).

Author contributions

E.L.v.d.E. and L.H.M. contributed to study design, data acquisition, statistical analysis and interpretation and drafting of the manuscript. C.S., M.P.S. and D.N. contributed to data acquisition and analysis (i.e. mass spectrometry experiments) and drafting of the manuscript. J.G. J. contributed to study design, data analysis and interpretation (i.e. gene set enrichment analysis) and drafting of the manuscript. J.C.v.S., H.S. and T.M.L. contributed to study design, data acquisition and interpretation and provided critical revision of the manuscript. All other authors contributed to data acquisition and revised the manuscript.

Potential conflicts of interest

The authors report no conflicts of interest relevant to this work.

References

1. Lashley T, Rohrer JD, Mead S, Revesz T. Review: an update on clinical, genetic and pathological aspects of frontotemporal lobar degenerations. Neuropathol Appl Neurobiol. 2015 Dec;41(7):858-81.
2. Seelaar H, Rohrer JD, Pijnenburg YAL, et al. Clinical, genetic and pathological heterogeneity of frontotemporal dementia: a review. Journal of Neurology, Neurosurgery & Psychiatry. 2011;82(5):476-86.
3. Ghidoni R, Benussi L, Glionna M, et al. Low plasma progranulin levels predict progranulin mutations in frontotemporal lobar degeneration. Neurology. 2008 Oct 14;71(16):1235-9.
4. Meeter LH, Patzke H, Loewen G, et al. Progranulin Levels in Plasma and Cerebrospinal Fluid in Granulin Mutation Carriers. Dement Geriatr Cogn Dis Extra. 2016 May-Aug;6(2):330-40.
5. Eriksen JL, Mackenzie IR. Progranulin: normal function and role in neurodegeneration. J Neurochem. 2008 Jan;104(2):287-97.
6. Sleegers K, Brouwers N, Van Damme P, et al. Serum biomarker for progranulin-associated frontotemporal lobar degeneration. Ann Neurol. 2009 May;65(5):603-9.
7. Meeter LH, Kaat LD, Rohrer JD, van Swieten JC. Imaging and fluid biomarkers in frontotemporal dementia. Nat Rev Neurol. 2017 Jul;13(7):406-19.
8. Oeckl P, Steinacker P, Feneberg E, Otto M. Cerebrospinal fluid proteomics and protein biomarkers in frontotemporal lobar degeneration: Current status and future perspectives. Biochim Biophys Acta. 2015 Jul;1854(7):757-68.
9. Teunissen CE, Elias N, Koel-Simmelink MJ, et al. Novel diagnostic cerebrospinal fluid biomarkers for pathologic subtypes of frontotemporal dementia identified by proteomics. Alzheimers Dement (Amst). 2016;2:86-94.
10. Agresta AM, De Palma A, Bardoni A, et al. Proteomics as an innovative tool to investigate frontotemporal disorders. Proteomics Clin Appl. 2016 Apr;10(4):457-69.
11. Ringman JM, Schulman H, Becker C, et al. Proteomic changes in cerebrospinal fluid of presymptomatic and affected persons carrying familial Alzheimer disease mutations. Arch Neurol. 2012 Jan;69(1):96-104.
12. Dopper EG, Rombouts SA, Jiskoot LC, et al. Structural and functional brain connectivity in presymptomatic familial frontotemporal dementia. Neurology. 2014 Jul 8;83(2):e19-26.
13. Stoop MP, Singh V, Stingl C, et al. Effects of natalizumab treatment on the cerebrospinal fluid proteome of multiple sclerosis patients. J Proteome Res. 2013 Mar 1;12(3):1101-7.
14. Chambers MC, Maclean B, Burke R, et al. A cross-platform toolkit for mass spectrometry and proteomics. Nat Biotechnol. 2012 Oct;30(10):918-20.
15. UniProt Consortium T. UniProt: the universal protein knowledgebase. Nucleic Acids Res. 2018 Mar 16;46(5):2699.
16. Nesvizhskii AI, Keller A, Kolker E, Aebersold R. A statistical model for identifying proteins by tandem mass spectrometry. Anal Chem. 2003 Sep 1;75(17):4646-58.
17. Hather G, Higdon R, Bauman A, et al. Estimating false discovery rates for peptide and protein identification using randomized databases. Proteomics. 2010 Jun;10(12):2369-76.

18. van den Berg CB, Duvekot JJ, Guzel C, et al. Elevated levels of protein AMBP in cerebrospinal fluid of women with preeclampsia compared to normotensive pregnant women. Proteomics Clin Appl. 2017 Jan;11(1-2).
19. Guzel C, Govorukhina NI, Wisman GBA, et al. Proteomic alterations in early stage cervical cancer. Oncotarget. 2018 Apr 6;9(26):18128-47.
20. MacLean B, Tomazela DM, Shulman N, et al. Skyline: an open source document editor for creating and analyzing targeted proteomics experiments. Bioinformatics. 2010 Apr 1;26(7):966-8.
21. R Development Core Team. R: A language and environment for statistical computing. Vienna, Austria: R Foundation for Statistical Computing; 2013.
22. Vizcaino JA, Csordas A, del-Toro N, et al. 2016 update of the PRIDE database and its related tools. Nucleic Acids Res. 2016 Jan 4;44(D1):D447-56.
23. Gene Ontology C. Creating the gene ontology resource: design and implementation. Genome Res. 2001 Aug;11(8):1425-33.
24. Osera C, Pascale A, Amadio M, et al. Pentraxins and Alzheimer's disease: at the interface between biomarkers and pharmacological targets. Ageing Res Rev. 2012 Apr;11(2):189-98.
25. Xiao MF, Xu D, Craig MT, et al. NPTX2 and cognitive dysfunction in Alzheimer's Disease. Elife. 2017 Mar 23;6.
26. Hendrickson RC, Lee AY, Song Q, et al. High Resolution Discovery Proteomics Reveals Candidate Disease Progression Markers of Alzheimer's Disease in Human Cerebrospinal Fluid. PLoS One. 2015;10(8):e0135365.
27. Wildsmith KR, Schauer SP, Smith AM, et al. Identification of longitudinally dynamic biomarkers in Alzheimer's disease cerebrospinal fluid by targeted proteomics. Mol Neurodegener. 2014 Jun 6;9:22.
28. Llano DA, Bundela S, Mudar RA, et al. A multivariate predictive modeling approach reveals a novel CSF peptide signature for both Alzheimer's Disease state classification and for predicting future disease progression. PLoS One. 2017;12(8):e0182098.
29. Spellman DS, Wildsmith KR, Honigberg LA, et al. Development and evaluation of a multiplexed mass spectrometry based assay for measuring candidate peptide biomarkers in Alzheimer's Disease Neuroimaging Initiative (ADNI) CSF. Proteomics Clin Appl. 2015 Aug;9(7-8):715-31.
30. Bartolomucci A, Possenti R, Mahata SK, et al. The extended granin family: structure, function, and biomedical implications. Endocr Rev. 2011 Dec;32(6):755-97.
31. Toshinai K, Nakazato M. Neuroendocrine regulatory peptide-1 and -2: novel bioactive peptides processed from VGF. Cell Mol Life Sci. 2009 Jun;66(11-12):1939-45.
32. Heneka MT, Kummer MP, Latz E. Innate immune activation in neurodegenerative disease. Nat Rev Immunol. 2014 Jul;14(7):463-77.
33. Brinkmalm G, Sjodin S, Simonsen AH, et al. A Parallel Reaction Monitoring Mass Spectrometric Method for Analysis of Potential CSF Biomarkers for Alzheimer's Disease. Proteomics Clin Appl. 2018 Jan;12(1).

34. Cai T, Notkins AL. Pathophysiologic changes in IA-2/IA-2beta null mice are secondary to alterations in the secretion of hormones and neurotransmitters. Acta Diabetol. 2016 Feb;53(1):7-12.
35. Bayly-Jones C, Bubeck D, Dunstone MA. The mystery behind membrane insertion: a review of the complement membrane attack complex. Philos Trans R Soc Lond B Biol Sci. 2017 Aug 5;372(1726).
36. Lui H, Zhang J, Makinson SR, et al. Progranulin Deficiency Promotes Circuit-Specific Synaptic Pruning by Microglia via Complement Activation. Cell. 2016 May 5;165(4):921-35.
37. Petkau TL, Leavitt BR. Progranulin in neurodegenerative disease. Trends Neurosci. 2014 Jul;37(7):388-98.
38. Marttinen M, Kurkinen KM, Soininen H, et al. Synaptic dysfunction and septin protein family members in neurodegenerative diseases. Mol Neurodegener. 2015 Apr 3;10:16.
39. Tapia L, Milnerwood A, Guo A, et al. Progranulin deficiency decreases gross neural connectivity but enhances transmission at individual synapses. J Neurosci. 2011 Aug 3;31(31):11126-32.
40. Petkau TL, Neal SJ, Milnerwood A, et al. Synaptic dysfunction in progranulin-deficient mice. Neurobiol Dis. 2012 Feb;45(2):711-22.
41. Meeter LH, Dopper EG, Jiskoot LC, et al. Neurofilament light chain: a biomarker for genetic frontotemporal dementia. Ann Clin Transl Neurol. 2016 Aug;3(8):623-36.
42. Rohrer JD, Nicholas JM, Cash DM, et al. Presymptomatic cognitive and neuroanatomical changes in genetic frontotemporal dementia in the Genetic Frontotemporal dementia Initiative (GENFI) study: a cross-sectional analysis. Lancet Neurol. 2015 Mar;14(3):253-62.
43. Jiskoot LC, Bocchetta M, Nicholas JM, et al. Presymptomatic white matter integrity loss in familial frontotemporal dementia in the GENFI cohort: A cross-sectional diffusion tensor imaging study. Ann Clin Transl Neurol. 2018 Sep;5(9):1025-36.
44. Gunther R, Krause E, Schumann M, et al. Depletion of highly abundant proteins from human cerebrospinal fluid: a cautionary note. Mol Neurodegener. 2015 Oct 15;10:53.

Supplementary file 1: Methods

Discovery proteomics

Fifty µL of CSF sample was depleted of albumin and immunoglobulin G using depletion spin columns (Pierce, PN 85162) according to manufacturers' recommendations. Samples were subsequently reduced (5 mM DTT), alkylated (15 mM IAA), dried (SpeedVac concentrator), then reconstituted in 50 µl 0.1% RapiGest (Waters) and 50mM ammoniumbicarbonate and digested overnight by addition of 500 ng trypsin (trypsin gold, Promega, Madison, WI) and incubation at 37°C with gentle shaking. Digests were stopped and detergent (RapiGest) was removed by acidification with trifluoroacetic acid (TFA) to pH<2 followed by incubation (45' at 37°C) and centrifugation (10' at 10,000 g). Samples were analysed by LC-MS/MS in a randomised order using an Ultimate 3000 nano RSLC system (Thermo Fischer Scientific, Germering, Germany) coupled online to an Orbitrap Fusion Lumos mass spectrometer (Thermo Fisher Scientific). Twelve microliter of digest was loaded onto a C18 trap column (C18 PepMap, 300 µm ID x 5 mm, 5 µm, 100 Å) and desalted for 10' using 0.1% TFA in water at a flow rate of 20 µl/min. Then the trap column was switched in-line with an analytical column (PepMap C18, 75 µm ID x 250 mm, 2 µm, 100 Å) and peptides were eluted using a binary gradient increasing solvent B from 4% to 38% over 90 minutes, whereby solvent A was 0.1% formic acid, solvent B 80% acetonitrile and 0.08% formic acid. The column flow rate was set to 300 nL/min and column oven temperature to 40°C. For electrospray ionisation, nano ESI emitter (New Objective) was used and a spray voltage of 1.7 kV applied. For MS/MS analysis a data dependent acquisition MS method was used with a high resolution survey scan from range 375 - 1500 m/z at 120,000 resolution, automatic gain control target 400,000), followed by consecutively isolation, fragmentation (HCD, 35% NCE) and detection (ion trap, AGC 10,000) of the peptide precursors detected in the survey scan until a duty cycle time of 3" was exceeded ('Top Speed' method). Precursor masses that were selected once for MS/MS were excluded for subsequent MS/MS fragmentation for 60".

For peptide and protein identification, MS/MS spectra were extracted using ProteoWizard [1] software (version 3.0.9248) and analysed with the database search engine Mascot (Matrix Science, UK) against the Uniprot database [2] (downloaded November 12th 2015, release v151112; taxonomy: Homo sapiens; 20,194 entries) using the following parameters: Carbamidomethylation of cysteine (+57.021 Da) as fixed modification and oxidation of methionine (+ 15.995 Da) as variable modification, allowing 2 missed cleavages, precursor mass tolerance of +/-10 ppm and fragment ions of +/- 0.5 Da. Next we combined the search results of the individual samples, applied scoring of hits (local false discovery rate ≤ 1%) and conducted protein grouping using the software Scaffold.[3,4] For label-free quantitation MS

raw data was processed with Progenesis QI (version 2.0, Waters) and linked with identification results to finally determine peptide and protein abundances. Abundances were normalised to the total ion current to compensate for experimental variations using an algorithm available in the analysis software. Subsequently the data were exported in Excel format and analysed using Excel, R and SPSS statistical software.

Parallel reaction monitoring (PRM)

Twenty µL of CSF were diluted in 50 µL digestion buffer (100 mM TEAB, 1% SDC, 10% ACN) and digested over-night by the addition of 400 ng trypsin (Promega, gold-grade) and incubation at 37°C with gentle shaking. Digests were stopped and detergent precipitated by addition of 60 µL 1% TFA. Next the mixture of synthetic stable isotope labelled (SIL) peptides was spiked and the detergent removed by centrifugation at 4,400 g and subsequent filtered through a 0.45 µm membrane (PALL Acroprep). The set of samples was distributed over 3 well-plates and prepared in two batches on two days. Digests were stored until measurements at 4 °C in sealed well-plates. LC-MS analysis was carried out on a nano LC system coupled to an Orbitrap Fusion mass spectrometer (Thermo Fisher Scientific). Eight uL of digest were loaded onto a trap column (C18 PepMap, 300 µm ID x 5 mm, 5 µm, 100 Å) and desalted for 10’ using 0.1% TFA at a flow rate of 20 µl/min. Then the trap column was switched in-line with an analytical column (EASY-Spray PepMap C18, 75 µm ID x 250 mm, 2 µm, 100 Å) and peptides were eluted using a binary 30´ gradient with increasing solvent B from 4% to 38%, whereby solvent A was 0.1% formic acid, solvent B 80% acetonitrile and 0.08% formic acid, flow rate 300 nL/min, column temperature 40°C and spray voltage 1.7 kV. For PRM of the peptide panel a time scheduled targeted MS/MS method was used and the referring peptide-specific parameters are listed in supplementary table 2. As technical quality check (QC), a pool of 80 CSF samples was prepared, loaded as 8-fold replicate on each well-plate, and processed otherwise identically as the other samples. During LC-MS measurements, every 12th run a QC sample was measured to determine the reproducibility of the assay. For assessment of sensitivity of the assay an eight-point dilutions series of the peptide panel in CSF digest matrix was prepared and measured in triplicate (supplementary table 2). MS data processing (peak picking, peak integration, and calculation of peak ratios) was conducted using the software package Skyline.[5] Peak ratios were exported and used for calculation of CSF concentrations of the samples and determining analytical parameters LOD (limit of detection), LLOQ (lower limit of quantitation) and CV (coefficients of variance) using the software package R.

Supplementary file 2: Figures and tables

Supplementary figure 1. Protein levels measured by PRM in presymptomatic and symptomatic *GRN, C9orf72* and *MAPT* mutation carriers. (A) Receptor-type tyrosine-protein phosphatase N2 (PTPRN2) (B) Neurosecretory protein VGF (VGF), (C) V-set and transmembrane domain-containing protein 2B (VSTM2B), (D) Chromogranin-A (CHGA), (E); Complement component C8 gamma chain (C8G). Peptides used for quantification are listed in supplementary table 2. Significances from the analysis of covariance (corrected for age at CSF sampling) and after correction for multiple testing are displayed. *p<0.05; **p<0.01; ***p<0.001. Abbreviations: SYM, symptomatic; PRE, presymptomatic.

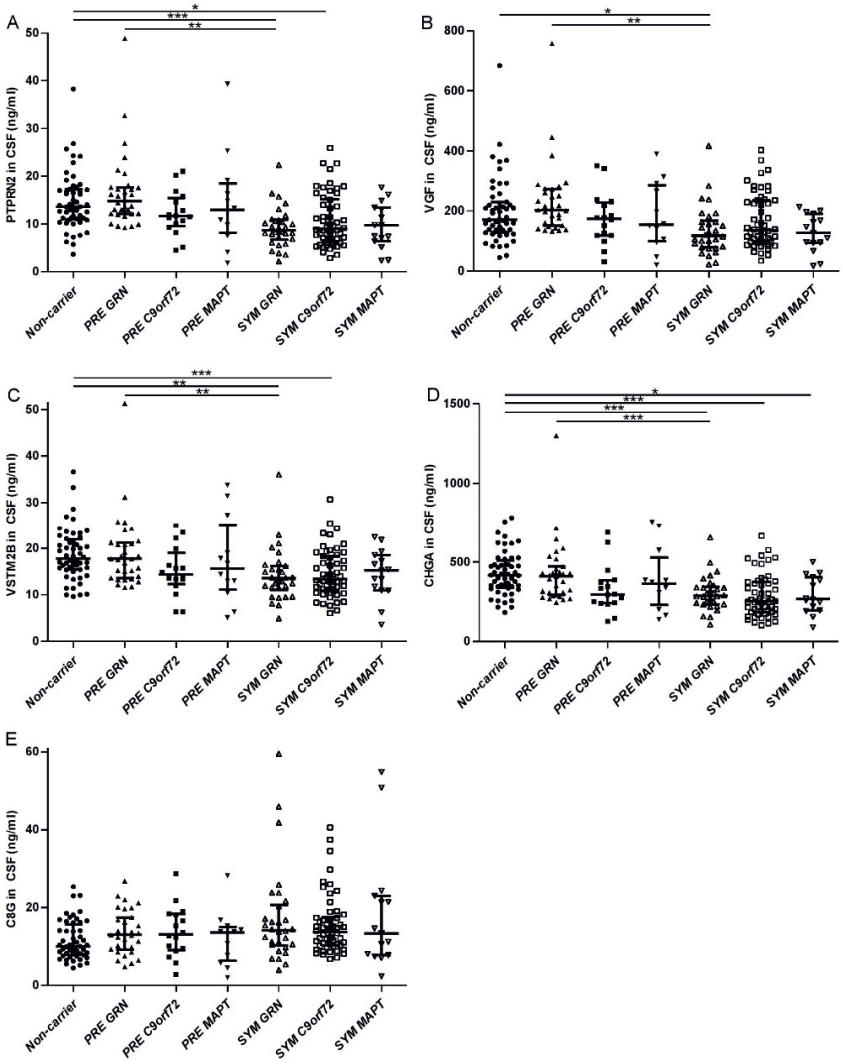

Supplementary figure 2. Network of enriched Gene Ontology (GO) terms coupled to related proteins. A selection of proteins identified by discovery proteomics was included in a gene set enrichment analysis to the GO database.[6] The most significantly enriched non-redundant GO terms for Biological Processes and Cellular Components coupled to the related proteins are shown. Proteins in green are upregulated in symptomatic mutation carriers, while proteins in red are downregulated in symptomatic mutation carriers; proteins up- or downregulated in symptomatic mutation carriers compared to non-carriers are shown in circles, those up- or downregulated compared to presymptomatic carriers in squares and those compared to both non-carriers and presymptomatic carriers are in octagons.

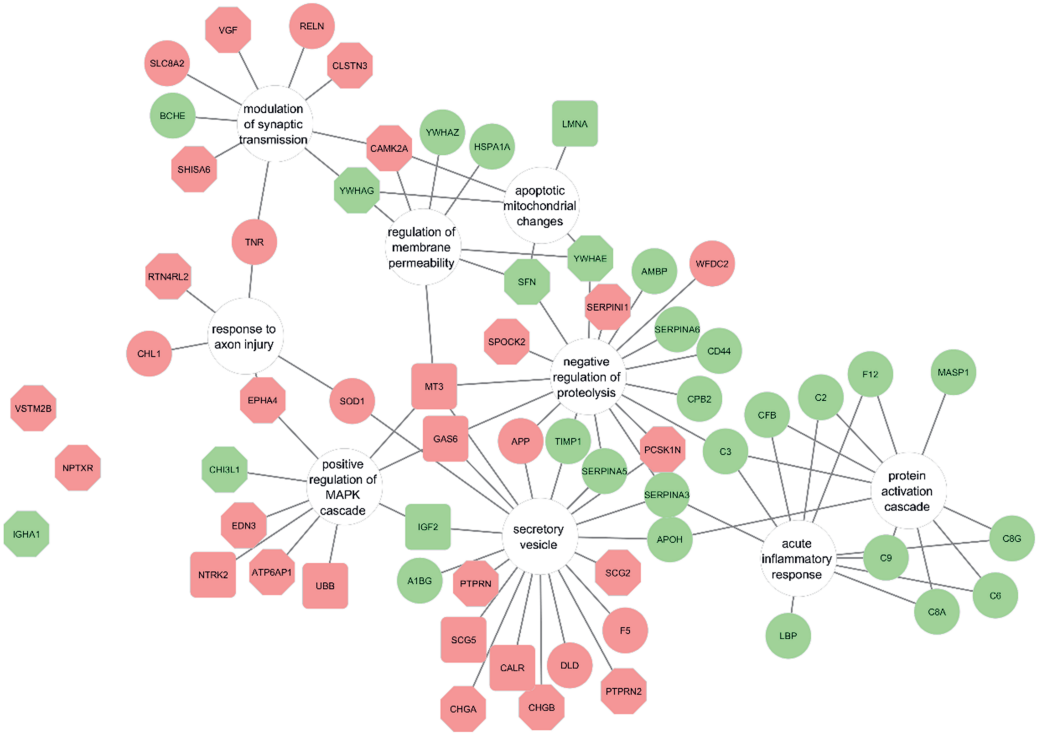

Supplementary table 1. Peptide specific settings of the PRM method. Peptide sequence: hash (#) indicates stable isotope labelled Lysine (L-Lysine-$^{13}C_6$, $^{15}N_2$) or Arginine (L-Arginine-$^{13}C_6$, $^{15}N_4$), respectively; z: charge state measured; CE: optimal normalised collision energy of HCD fragmentation; MIT: maximum ion injection time of scan (in ms, at a AGC target of 5 x 10^4); m/z: mass-over-charge ratio used; t(start) and t(stop): margins of scheduled PRM time windows; for all peptides the Orbitrap resolution was set to 120.000, and the isolation windows to 1 Da.

Gene	Peptide sequence	z	CE	MIT	m/z	t(start)	t(stop)
NPTXR	LVEAFGGATK	2	18	240	496.7742	8.5	10.2
NPTXR	LVEAFGGATK#	2	18	240	500.7813	8.5	10.2
NPTXR	VAELEHGSSAYSPPDAFK	2	28	400	952.9549	11	12.1
NPTXR	VAELEHGSSAYSPPDAFK#	2	28	400	956.962	11	12.1
PTPRN2	THTAQDRPPAEGDDR	2	30	400	833.3824	0	3.2
PTPRN2	THTAQDRPPAEGDDR#	2	30	400	838.3865	0	3.2
PTPRN2	AALGESGEQADGPK	2	23	400	665.3177	5.15	6.2
PTPRN2	AALGESGEQADGPK#	2	23	400	669.3248	5.15	6.2
VGF	EPVAGDAVPGPK	2	23	400	568.8009	7.5	8.5
VGF	EPVAGDAVPGPK#	2	23	400	572.808	7.5	8.5
VGF	THLGEALAPLSK	2	24	400	618.851	10.2	11
VGF	THLGEALAPLSK#	2	24	400	622.8581	10.2	11
CHGA	EAVEEPSSK	2	18	240	488.2351	3.2	4.5
CHGA	EAVEEPSSK#	2	18	240	492.2422	3.2	4.5
CHGA	RPEDQELESLSAIEAELEK	3	22	400	729.3656	21	40
CHGA	RPEDQELESLSAIEAELEK#	3	22	400	732.037	21	40
VSTM2B	VSDYSDDDTQEHK	2	25	240	769.8157	3.2	4.5
VSTM2B	VSDYSDDDTQEHK#	2	25	240	773.8228	3.2	4.5
VSTM2B	ELLHELALSVPGAR	2	28	240	752.9277	16	18
VSTM2B	ELLHELALSVPGAR#	2	28	240	757.9319	16	18
C8G	VQEAHLTEDQIFYFPK	2	25	240	982.9913	16	18
C8G	VQEAHLTEDQIFYFPK#	2	25	240	986.9984	16	18
C8G	SLPVSDSVLSGFEQR	2	27	240	810.915	18	21
C8G	SLPVSDSVLSGFEQR#	2	27	240	815.9192	18	21
IGHA1	TPLTATLSK	2	22	240	466.2766	8.5	10.2
IGHA1	TPLTATLSK#	2	22	240	470.2837	8.5	10.2

Supplementary table 2a. PRM settings: Peptide assay characteristics. Protein: name of protein (Gene ID); peptide: peptide sequence; n(LVL): number of levels used for calibration (with detected peaks); c range: calibration concentration range (in fmol/µL CSF); w range : calibration concentration range (in ng/mL CSF); R^2 (Cal): correlation coefficient of calibration curve; LOD: Limit of detection (3 x standard deviation of intercept / slope; in ng/mL CSF); LLOQ: Lower limit of detection (10 x standard deviation of intercept / slope; in ng/mL CSF); CV: inter batch coefficient of variance (CV) of QCs from 24 LC-MS measurements (all 3 well-plates); CV WP1, WP2, and WP3: intra batch CV from 8 LC-MS measurements of well-plate 1, 2, and 3. Asterisk (*) indicates peptide chosen for quantitative statistical analysis.

Protein	Peptide	n(LVL)	c range	w range	R^2 (Cal)	LOD	LLOQ	CV	CV WP1	CV WP2	CV WP3
NPTXR	LVEAFGGATK	8	[0.005..10]	[0.242..528.5]	0.9913	0.68	2.25	8.1	4.1	10.9	6.6
NPTXR	VAELEHGSSAYSPPDAF K*	7	[0.014..10]	[0.725..528.5]	0.9968	1.09	3.64	7.9	2	7.5	3.9
PTPRN2	AALGESGEQADGPK*	7	[0.001..1]	[0.153..111.3]	0.9985	0.11	0.37	9	2.6	8.8	5.3
PTPRN2	THTAQDRPPAEGDDR	7	[0.001..1]	[0.153..111.3]	0.8525	1.85	6.18	18.5	8.6	20.7	12.8
VGF	EPVAGDAVPGPK	8	[0.005..10]	[0.308..672.6]	0.9946	0.68	2.26	14.8	7.7	15	12.9
VGF	THLGEALAPLSK*	7	[0.014..10]	[0.923..672.6]	0.9982	0.73	2.42	14.2	6.9	7.1	7.4
CHGA	EAVEEPSSK*	8	[0.046..100]	[2.318..5068.8]	0.9859	8.30	27.65	5.4	2.9	7.3	4.1
CHGA	RPEDQELESLSAIEAELE K*	8	[0.046..100]	[2.318..5068.8]	0.998	3.09	10.29	8.6	5.8	9.1	10.1
VSTM2B	ELLHELALSVPGAR	6	[0.041..10]	[1.247..303]	0.9964	0.87	2.91	73.7	23.1	81.9	32.1
VSTM2B	VSDYSDDDTQEHK*	8	[0.005..10]	[0.139..303]	0.9875	0.54	1.81	5.2	3.3	7.8	2.8
C8G	SLPVSDSVLSGFEQR*	8	[0.005..10]	[0.102..222.8]	0.9896	0.31	1.04	10.2	3.2	10.6	4
C8G	VQEAHLTEDQIFYFPK	6	[0.005..10]	[0.102..222.8]	0.986	0.99	3.31	17.9	9	15.9	10.9
IGHA1	TPLTATLSK	8	[0.046..100]	[1.722..3765.5]	0.9984	2.06	6.88	17	5.3	10.7	4.8

Supplementary table 2b. Peptide quantification information. Protein: name of protein (Gene ID); peptide: peptide sequence; MW: molecular weight protein used for calculation (from uniprot.org); c(spike): spiked peptide concentration (fmol/µL CSF); w(spike): corresponding calculated protein concentration (in ng/mL); min(w): lowest concentration quantified (in ng/mL CSF); max(w): highest concentration quantified (in ng/mL CSF); n(<LOD): number of samples below LOD; n(<LLOQ): number of samples below LLOQ; suit: peptide suitable for quantification. Asterisk (*) indicates which peptide was chosen for quantitative statistical analysis.

Protein	Peptide	MW	c(spike)	w(spike)	n	min(w)	max(w)	n(<LOD)	n(<LLOQ)	suit
NPTXR	LVEAFGGATK	52,846	1	52.85	232	3.8	40.03	0	0	Yes
NPTXR	VAELEHGSSAYSPPDAI	52,846	1	52.85	232	20.41	337.95	0	0	Yes
PTPRN2	AALGESGEQADGPK*	111,271	0.1	11.13	232	1.85	48.82	0	0	Yes
PTPRN2	THTAQDRPPAEGDDR	111,271	0.1	11.13	232	0.33	30.65	9	91	No
VGF	EPVAGDAVPGPK	67,258	1	67.26	232	4.18	77.4	0	0	Yes
VGF	THLGEALAPLSK*	67,258	1	67.26	232	17.79	757.62	0	0	Yes
CHGA	EAVEEPSSK*	50,688	10	506.88	232	89.6	1298.79	0	0	Yes
CHGA	RPEDQELESLSAIEAELI	50,688	10	506.88	232	50.34	1583.82	0	0	Yes
VSTM2B	ELLHELALSVPGAR	30,297	1	30.3	232	6.24	344.73	0	0	No
VSTM2B	VSDYSDDDTQEHK*	30,297	1	30.3	232	3.62	51.32	0	0	Yes
C8G	SLPVSDSVLSGFEQR*	22,277	1	22.28	232	2.05	59.53	0	0	Yes
C8G	VQEAHLTEDQIFYFPK	22,277	1	22.28	232	0.48	113.86	3	14	No
IGHA1	TPLTATLSK	37,655	10	376.55	232	1.04	633.89	1	1	Yes

Supplementary table 3a. Differentially abundant proteins (n=20) in symptomatic *GRN* mutation carriers versus non-carriers. Proteins displayed were significantly abundant between symptomatic mutation carriers and non-carriers based on: ≥2 peptides identified, ≥25% of the peptides with a $p<0.01$, ≥50% of the peptides with a $p<0.05$, ≥75% of the peptides changed in the same direction. Bolded are the seven candidate proteins selected for further validation (based on: at least 4 identified peptides and a fold change of ≤0.5 or ≥2.0).

Protein (accession number)	Peptides	$p<0.01$, %	$p<0.05$, %	Peptides in same direction, %	Fold change (symptomatic/ non-carriers)
Higher abundance in symptomatic than non-carriers					
Profilin-1 (P07737)	2	100	100	100	2.47
Ig alpha-1 chain C region (P01876)	6	33	67	100	2.39
Complement component C8 gamma chain (P07360)	4	25	50	100	2.00
14-3-3 protein zeta/delta (P63104)	6	67	83	100	1.98
14-3-3 protein epsilon (P62258)	5	40	60	80	1.22
Lower abundance in symptomatic than non-carriers					
Neuronal pentraxin receptor (O95502)	6	67	100	100	0.34
Receptor-type tyrosine-protein phosphatase N2 (Q92932)	5	60	80	100	0.35
Neurosecretory protein VGF (O15240)	21	38	90	100	0.45
Chromogranin-A (P10645)	18	44	61	100	0.46
Calcium/calmodulin-dependent protein kinase type II alpha (Q9UQM7)	2	50	100	100	0.48
V-set and transmembrane domain-containing protein 2B (A6NLU5)	4	50	50	100	0.49
Cell growth regulator with EF hand domain protein 1 (Q99674)	4	50	50	100	0.54
Proline-rich transmembrane protein 3 (Q5FWE3)	2	50	100	100	0.57
Protein shisa-6 homolog (Q6ZSJ9)	2	50	100	100	0.60
CD99 antigen-like protein 2 (Q8TCZ2)	8	38	50	100	0.65
Reticulon-4 receptor-like 2 (Q86UN3)	4	25	50	75	0.69
Tumor necrosis factor receptor superfamily member 21 (O75509)	5	40	60	80	0.70
45 kDa calcium-binding protein (Q9BRK5)	2	50	50	100	0.73
Golgi membrane protein 1 (Q8NBJ4)	8	25	50	88	0.75
Reelin (P78509)	11	27	55	82	0.76

Supplementary table 3b. Differentially abundant proteins (n=9) in symptomatic versus presymptomatic *GRN* mutation carriers. Proteins displayed were significantly abundant between symptomatic and presymptomatic mutation carriers, based on: ≥2 peptides identified, ≥25% of the peptides with a $p<0.01$, ≥50% of the peptides with a $p<0.05$, ≥75% of the peptides changed in the same direction. Bolded are candidate proteins selected for further validation (based on: at least 4 identified peptides and a fold change of ≤0.5 or ≥2.0).

Protein (accession number)	Peptides	$p<0.01$, %	$p<0.05$, %	Peptides in same direction, %	Fold change (symptomatic / presymptomatic)
Higher abundance in symptomatic than presymptomatic carriers					
CD44 antigen (P16070)	4	25	50	75	1.11
14-3-3 protein epsilon (P62258)	5	60	80	80	1.40
14-3-3 protein gamma (P61981)	5	40	80	100	1.59
Profilin-1 (P07737)	2	50	50	100	1.68
Lower abundance in symptomatic than presymptomatic carriers					
Neuronal pentraxin receptor (O95502)	6	33	67	100	0.39
Calsyntenin-3 (Q9BQT9)	2	50	100	100	0.45
Receptor-type tyrosine-protein phosphatase-like N (Q16849)	8	25	50	88	0.56
Proline-rich transmembrane protein 3 (Q5FWE3)	2	50	50	100	0.68
Polyubiquitin-B (P0CG47)	4	25	50	100	0.78

Supplementary references

1. Chambers MC, Maclean B, Burke R, et al. A cross-platform toolkit for mass spectrometry and proteomics. Nat Biotechnol. 2012 Oct;30(10):918-20.
2. UniProt Consortium T. UniProt: the universal protein knowledgebase. Nucleic Acids Res. 2018 Mar 16;46(5):2699.
3. Nesvizhskii AI, Keller A, Kolker E, Aebersold R. A statistical model for identifying proteins by tandem mass spectrometry. Anal Chem. 2003 Sep 1;75(17):4646-58.
4. Hather G, Higdon R, Bauman A, et al. Estimating false discovery rates for peptide and protein identification using randomized databases. Proteomics. 2010 Jun;10(12):2369-76.
5. MacLean B, Tomazela DM, Shulman N, et al. Skyline: an open source document editor for creating and analyzing targeted proteomics experiments. Bioinformatics. 2010 Apr 1;26(7):966-8.
6. Gene Ontology C. Creating the gene ontology resource: design and implementation. Genome Res. 2001 Aug;11(8):1425-33.

Chapter 4.2

Unravelling the clinical spectrum and the role of repeat length in *C9orf72* repeat expansions

Emma L. van der Ende*, Jazmyne L. Jackson*, Adrianna White, Harro Seelaar, Marka van Blitterswijk#, John C. van Swieten#

*Authors contributed equally to the manuscript

#Authors contributed equally to the manuscript

Journal of Neurology, Neurosurgery and Psychiatry 2021;92(5):502-509

Abstract

Since the discovery of the *C9orf72* repeat expansion as the most common genetic cause of frontotemporal dementia (FTD) and amyotrophic lateral sclerosis (ALS), it has increasingly been associated with a wider spectrum of phenotypes, including other types of dementia, movement disorders, psychiatric symptoms and slowly-progressive FTD. Prompt recognition of patients with *C9orf72*-associated diseases is essential in light of upcoming clinical trials.

The striking clinical heterogeneity associated with *C9orf72* repeat expansions remains largely unexplained. In contrast to other repeat expansion disorders, evidence for an effect of repeat length on phenotype is inconclusive. Patients with *C9orf72*-associated diseases typically have very long repeat expansions, containing hundreds to thousands of GGGGCC-repeats, but smaller expansions might also have clinical significance. The exact threshold at which repeat expansions lead to neurodegeneration is unknown, and discordant cut-offs between laboratories pose a challenge for genetic counselling.

Accurate and large-scale measurement of repeat expansions has been severely hindered by technical difficulties in sizing long expansions and by variable repeat lengths across and within tissues. Novel long-read sequencing approaches have produced promising results and open up avenues to further investigate this enthralling repeat expansion, elucidating whether its length, purity, and methylation pattern might modulate clinical features of *C9orf72*-related diseases.

Introduction

A repeat expansion in *C9orf72* is the most common genetic cause of frontotemporal dementia (FTD) and amyotrophic lateral sclerosis (ALS) worldwide.[1,2] Besides typical features of FTD and ALS, the expansion is increasingly associated with a broader range of symptoms, including psychiatric manifestations and parkinsonism, and has also been identified in patients with no known family history for neurodegenerative disease.[3,4] Early recognition of *C9orf72*-related illnesses is becoming increasingly important with the advent of disease-modifying therapeutic trials.

The substantial clinical heterogeneity observed in *C9orf72* expansion carriers, in terms of phenotype, age at symptom onset and rate of disease progression, suggests that there are underlying disease modifiers which may serve as prognostic factors as well as targets for therapeutic interventions. Drawing on evidence from other neurodegenerative repeat expansion disorders, including Huntington's disease (HD), several spinocerebellar ataxias (SCA) and myotonic dystrophy (DM),[5] an explanation for this heterogeneity has primarily been sought in repeat length. Studies relating *C9orf72* repeat length to clinical features have produced inconsistent results, but they have been hampered by technical difficulties in detecting and sizing expansions.[6-8]

In this review, we present an overview of the clinical spectrum associated with *C9orf72* repeat expansions. We then discuss the role of repeat length in relation to the *C9orf72* phenotype. Finally, we provide an in-depth examination of the advantages and limitations of current and novel methods to identify and measure repeat expansions.

Genetics and pathophysiology of *C9orf72* repeat expansions

The *C9orf72* repeat expansion is located in a non-coding region and consists of an expanded GGGGCC-repeat. Healthy individuals commonly carry less than 30 repeats, whereas those with *C9orf72*-associated diseases usually have several hundreds to thousands of repeats.[1,2,9][S1] The exact function of the C9orf72 protein is unknown, but it is thought to play a role in autophagy and endosomal trafficking.[S2] Three possibly co-existing disease mechanisms have been proposed: (1) haploinsufficiency due to reduced expression of C9orf72 from the expanded allele, (2) formation of repeat-containing RNA foci through bidirectional transcription of the expansion, and (3) production of aggregation-prone dipeptide repeat (DPR) proteins via repeat-associated non-ATG translation. These mechanisms have in turn been associated with a wide range of downstream cellular defects, such as alterations in stress granules, proteostasis, nucleocytoplasmic and vesicular

transport, mitochondrial function and immunity.(reviewed in [10,11]) Each disease mechanism alone might not be sufficient to cause neurodegeneration, and a synergistic model in which C9orf72 loss-of-function exacerbates gain-of-function mechanisms has been proposed.[S3] A better understanding of their relative contributions across various disease stages is essential in order to determine viable treatment targets. Promising therapeutic strategies currently being researched include small molecules and gene-silencing tools that inhibit *C9orf72* transcription, antisense oligonucleotides (ASOs) that bind to and inactivate repeat-containing RNA, antibody-based approaches to inhibit accumulation of DPR proteins, and targeting downstream cellular defects.(reviewed in [10,11])

Pathologically, *C9orf72*-related diseases are characterised by cytoplasmic aggregates of TAR DNA-binding protein 43 (TDP-43) and p62-positive neuronal cytoplasmic inclusions containing DPR proteins.[1,2] While TDP-43 pathology coincides neuro-anatomically with affected regions of the central nervous system (CNS) in ALS and FTD, DPR proteins generally do not. Sense and antisense C9orf72 RNA foci are widely distributed throughout the CNS in affected expansion carriers.[10]

Epidemiology of *C9orf72* repeat expansions

A *C9orf72* expansion is identified in approximately 5-10% of all patients with FTD or ALS, and in up to 30% of patients with both diseases.[4,12] Collectively, these diseases are referred to as c9FTD/ALS. The prevalence varies strongly between ethnic groups: the highest rates are found in Caucasians and the lowest in Asians.[12] The expansion is highly penetrant, with cumulative percentages of 90.9 to 99.5% by the age of 83.[S4] The first symptoms usually manifest themselves in the fifth decade, but age at onset is highly variable, even within families, and can range from 20 to 90 years.[9,13,14][S4,S5] The initial presentation and disease course also vary widely (box 1, table 1); survival after symptom onset ranges from 2 months in rapidly progressive ALS to over 30 years in slowly progressive behavioural variant FTD (bvFTD).[14][S5]

Table 1. Common clinical presentations of *C9orf72* repeat expansion carriers. *Family history of neurodegenerative or neuropsychiatric diseases is enriched in all presentations. Abbreviations: FTD, frontotemporal dementia; bvFTD, behavioural variant FTD; nfvPPA, non-fluent variant primary progressive aphasia; ALS, amyotrophic lateral sclerosis.

Clinical presentation	Key clinical features	Features enriched in *C9orf72* expansion carriers*
FTD		
bvFTD	• Apathy, disinhibition, loss of empathy, perseverative or compulsive behaviour, hyperorality and dietary changes • Impairments in executive function, language, social cognition • Frontotemporal atrophy, often asymmetrical	• Concomitant motor neuron disease • Psychotic symptoms • Other psychiatric disturbances • Episodic memory impairment • Parkinsonism (usually late-stage) • Highly variable neuroimaging, including generalised symmetrical cortical, cerebellar or thalamic atrophy
nfvPPA	• Non-fluent, effortful speech, speech apraxia, agrammatism • Preserved single-word comprehension • Predominantly left-sided frontotemporal atrophy	
Benign-variant FTD	• As in bvFTD but lacking disease progression • Neuroimaging (near) normal	• Cognitive impairment
Motor neuron disease		
ALS	• Asymmetric limb weakness, dysphagia, dysarthria, pseudobulbar affect • Upper and lower motor neuron signs spreading to multiple regions • Cognitive / behavioural abnormalities, bvFTD	• Cognitive / behavioural abnormalities, bvFTD • Bulbar onset • Atrophy of non-motor frontal cortical areas, basal ganglia
Psychiatric		
	• Hallucinations and delusions, mood disorders, obsessive-compulsive disorder, catatonia, anxiety disorders, suicidality	• Late onset (age >40 years) • Cognitive deterioration • Psychosis, somatic delusions • Prominent cerebral or cerebellar atrophy

Box 1: Representative case histories of notable *C9orf72* expansion carriers. We describe four noteworthy patients with *C9orf72* expansions, highlighting the variability in clinical presentation, age at symptom onset and disease course.

Case 1: A middle-aged woman was admitted to the psychiatric ward due to severe vital depression and attempted suicide. She had experienced a similar episode of depression with psychosis two years previously which was unresponsive to antidepressants and eventually treated with electroconvulsive therapy (ECT). Before that time, she had no history of psychiatric disease. Her mother had exhibited strange social behaviour from her late sixties; her maternal grandfather had been diagnosed with Alzheimer's disease. Extensive laboratory testing and brain MR imaging were normal; an FDG-PET scan revealed bilateral temporal and mesiofrontal hypometabolism compatible with FTD. Her depression was treated successfully with ECT again, but she subsequently suffered progressive cognitive decline and was admitted to a nursing home five years after her first episode of depression.

Cases 2 and 3: A man in his thirties presented with a two-year history of word finding difficulties and memory complaints. Family members also reported mild behavioural changes. His father had been diagnosed with FTD in his seventies and several paternal relatives had suffered from ALS. MR imaging of the brain demonstrated mild bilateral frontotemporal atrophy, and neuropsychological assessment confirmed deficits in language and executive functioning domains. Very slow progression occurred over several years of follow-up, with behavioural abnormalities such as social disinhibition and loss of decorum becoming more noticeable. Currently, ten years after the initial presentation, he is still living independently. His brother presented in his forties with progressive difficulties speaking and swallowing since three months. He had subsequently developed weakness of the left arm and leg. His partner also reported increased emotional lability and memory decline. Neurological examination revealed a bulbar dysarthria, tongue wasting with fasciculations and brisk jaw jerk, as well as mild left-sided hemiparesis. Electromyography was compatible with ALS, neuropsychological testing showed mild impairments in social cognition and executive functioning, and MR imaging revealed moderate, predominantly left-sided frontotemporal atrophy. His condition deteriorated rapidly and he died within nine months of symptom onset.

Case 4: A middle-aged man was admitted to the psychiatric ward with a three-month history of somatic delusions. He had become convinced that there were foreign bodies inside his abdominal organs and refused to eat or drink. There was no history of neurodegenerative diseases on the maternal side of his family; his paternal family history was unknown. Neurological examination at the time did not reveal focal abnormalities except positive primitive reflexes and elevated muscle tone. Extensive laboratory testing, MR and FDG-PET imaging, and electro-encephalography were inconclusive. Despite antipsychotic medication, the patient deteriorated rapidly into a state of catatonia with limb myoclonus, cerebellar ataxia and apneas, and required continuous tube feeding. He remained in a fluctuating mute catatonic state over the following two years.

Clinical manifestations of *c9orf72* repeat expansions

Cognitive disorders

Frontotemporal dementia

A *C9orf72* expansion is found in 20-25% of familial and 6-8% of apparently sporadic FTD cases (c9FTD).[4,12] The median age at onset of 57 years is similar to that of FTD without a *C9orf72* expansion (non-c9FTD),[14,15] but survival after symptom onset is shorter (7 versus 11 years), even in the absence of concomitant ALS.[S6] The clinical presentation of c9FTD is usually bvFTD, which is characterised by progressive behavioural and personality changes,

prominent executive functioning deficits and relative sparing of other cognitive domains,[16] although language variants (non-fluent primary progressive aphasia and semantic dementia) may also occur (table 1).[14,15] Up to 30% of c9FTD patients develop concomitant ALS during the course of the disease, but routine screening for ALS symptoms in patients with c9FTD is not commonly performed.[15]

c9FTD cannot be reliably distinguished on clinical grounds from non-c9FTD. However, c9FTD patients may present with atypical signs and symptoms and frequently do not fulfill current diagnostic criteria for FTD.[16,17] First, memory impairment is more common in c9FTD and is often the presenting symptom in older subjects, which can lead to misdiagnosis of Alzheimer's disease (AD).[18,19][S5,S7] Second, psychotic symptoms and bizarre, irrational behaviour are common in c9FTD (see also section 4.3).[15] Third, some patients have a protracted or seemingly non-progressive disease course (see also section 4.1.2). Fourth, atrophy patterns in c9FTD are highly variable and can include generalised symmetrical cortical atrophy and atrophy of thalamus and cerebellum (figure 1, table 1).[19][S8]

Benign variant FTD

A slowly progressive variant of bvFTD, with isolated neuropsychiatric symptoms and minimal cognitive deterioration over many years of follow-up, has been described in several *C9orf72* expansion carriers.[20][S9-11] Furthermore, a recent meta-analysis showed that 2% of patients with so-called benign variant FTD, in whom neuroimaging abnormalities and disease progression are lacking, had a *C9orf72* expansion.[21] The identification of expansions in benign variant FTD suggests that it is a neurodegenerative condition in at least a subset and that genetic testing should be considered, especially in those with a positive family history.

Alzheimer's disease and other dementias

C9orf72 expansions have been identified in a small percentage (<1%) of clinically diagnosed AD patients in several large cohorts.[18,22] Most of these cases can probably be attributed to misdiagnoses, especially in older patients with memory impairment and atypical neuroimaging, and might not reflect a causative association between *C9orf72* expansions and AD. Accordingly, autopsy studies of expansion carriers with a clinical diagnosis of AD revealed either isolated FTD pathology, or FTD with concomitant AD pathology,[23,24] although more pathological studies are needed to confirm this. Importantly, concomitant AD pathology might modulate the clinical phenotype (i.e., more amnestic features) and thus conceal the existence of a *C9orf72* expansion. Pure AD pathology without FTD pathology reported in three expansion carriers possibly reflects incomplete penetrance.[S12] From a

clinical perspective, the presence of *C9orf72* expansions in clinical cohorts of AD highlights the need to screen FTD genes in AD patients with a positive family history.[22][S13]

Genetic screening of large series of Lewy body dementia (DLB) patients did not identify *C9orf72* expansion carriers,[S14,S15] but occasionally, carriers may present as DLB mimics or harbour DLB co-pathology.[S16,S17]

Motor neuron diseases

A *C9orf72* expansion is identified in 20-30% of familial and 5% of apparently sporadic ALS cases.[4,12] The median age at onset (57 years) in c9ALS is similar to that of ALS without a *C9orf72* expansion (non-c9ALS).[13,14] The clinical phenotype of c9ALS covers the entire ALS spectrum, typically presenting with muscle weakness starting in one segment and spreading throughout the motor system (table 1). A bulbar onset of disease, characterised by early dysphagia and dysarthria, is seen in 30-40% of c9ALS [13,14] and appears to be more common than in non-c9ALS and may explain the shorter overall survival in c9ALS reported in some studies.[13,14]

Cognitive impairment and dementia, mostly of the bvFTD subtype, are more common in c9ALS than in non-c9ALS.[15] Accordingly, c9ALS patients show more extensive atrophy of non-motor areas of the frontal cortex than those with non-c9ALS.[S18] Although only 20% of ALS patients fulfill FTD diagnostic criteria, an additional 20% has some degree of cognitive impairment, usually in executive functioning, social cognition or language, and 10% shows behavioural changes.[S19] Screening instruments that are specifically designed to detect cognitive and behavioural symptoms in ALS, such as the Edinburgh Cognitive and Behavioural Screen (ECAS), are increasingly used and may improve tailored patient care.[S20]

Other motor neuron diseases, including progressive muscular atrophy and primary lateral sclerosis, are rare in *C9orf72* expansion carriers.[14][S21]

Figure 1. Neuroimaging abnormalities in *C9orf72* repeat expansion carriers. T1-weighted MR imaging of four affected *C9orf72* expansion carriers is shown, demonstrating the diversity of atrophy patterns that can be encountered. MRI scans were made at the time of the initial presentation; subjects were between 55 and 62 years of age. A) Mild generalised cortical atrophy; B) Severe generalised cortical cerebral as well as cerebellar atrophy; C) Predominantly left-sided frontotemporal atrophy; D) Moderate symmetrical parietal atrophy as well as mild symmetrical frontotemporal atrophy.

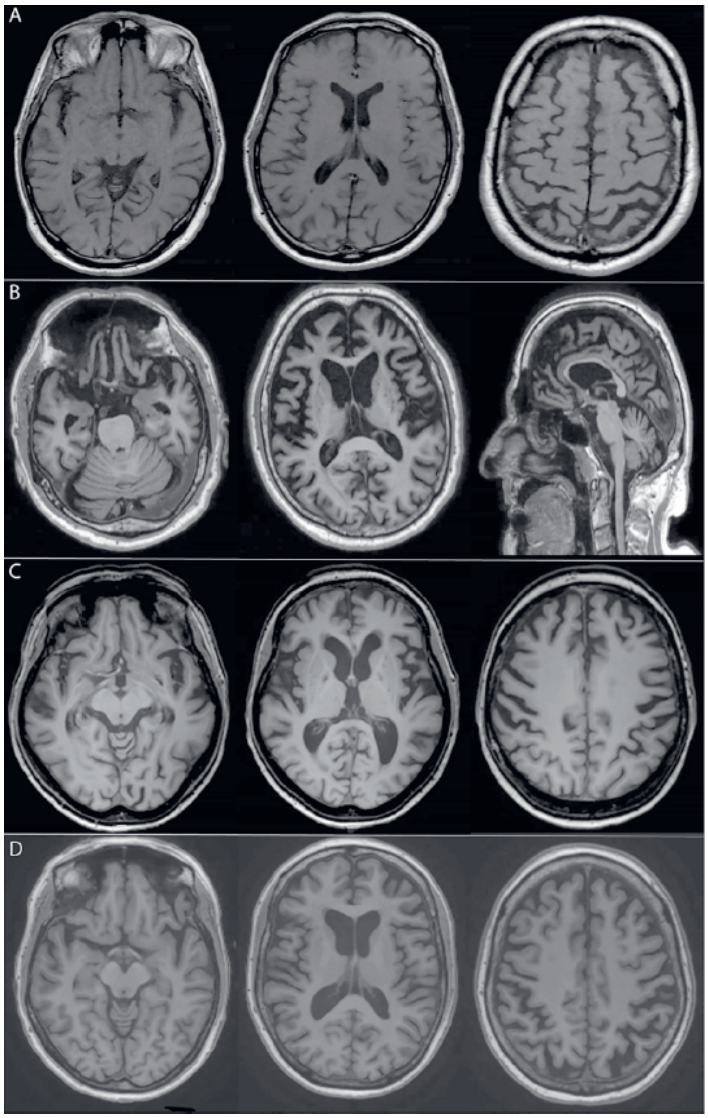

Psychiatric manifestations

Psychiatric symptoms occur at a much higher rate across the spectrum of *C9orf72*-related diseases than in non-c9FTD/ALS. Psychotic features are reported in 20-60% of c9FTD cases,[15,17,25][S22-S25] and include delusions and hallucinations in all sensory modalities, although somatic delusions are relatively common.[15][S24-S26] Other psychiatric manifestations include mood disorders, obsessive compulsive disorder and catatonia (table 1).[25-27][S27-S30] Psychiatric symptoms are occasionally the initial presentation and sometimes occur several years before the emergence of more typical FTD or ALS symptoms.[15,27][S23,S26] Misdiagnosis of a primary psychiatric disorder such as late-onset schizophrenia or late-onset bipolar disorder is not uncommon, especially in the case of (near-)normal neuroimaging.[27]

C9orf72 expansions in primary psychiatric disorders are rare, with prevalence rates below 0.2% in several large cohort studies.[28,29]

Movement disorders

Parkinsonism

Concomitant parkinsonism occurs more frequently in c9FTD/ALS than in non-c9FTD/ALS, and is especially common in bvFTD patients, with up to 75% developing a variable degree of parkinsonism during the disease course.[30][S31] Symptoms include symmetrical or asymmetrical bradykinesia, rigidity, falls and gaze palsy, often with little or no tremor.[30-32][S32,S33]

An initial presentation of parkinsonism, ataxia or apraxia has probably led to an erroneous diagnosis of Parkinson's disease (PD), progressive supranuclear palsy (PSP), corticobasal syndrome (CBS) or multisystem atrophy (MSA) in several expansion carriers.[31,33][S34,S35] Some of these patients lacked typical FTD or ALS signs for several years after presentation.[31-33] Parkinsonism in expansion carriers has been related to neuronal loss as well as TDP-43 and p62 pathology reported in the basal ganglia in a few pathology-proven studies.[34,35][S36] Accordingly, while some cohorts of clinically diagnosed PD report occasional (<1%) expansions,[33,36][S37] across two large studies of autopsy-proven PD (pooled sample size > 800 patients), just one expansion carrier was found who had both typical PD pathology as well as *C9orf72*-mediated pathology.[34,37]

Huntington's disease-like syndrome

A *C9orf72* expansion has been identified in up to 5% of patients with HD-like (HDL) syndrome, which is clinically indistinguishable from HD but without the typical CAG repeat expansion in the *HTT* gene, making it the most common genetic cause of HDL-syndromes.[38,39][S38,S39] There is no evidence for a causal relationship between *C9orf72* and HD, but these findings

are relevant for clinical practice as they demonstrate that expansion carriers may present with atypical signs including chorea, dystonia, tremor, rigidity, bradykinesia and myoclonus.[39] Neuropathological data is needed to determine whether *C9orf72*-linked pathology in HD-related brain regions might underlie these unusual presentations. Remarkably, repeat expansions in *HTT* were recently identified in a small number of non-c9FTD/ALS patients, supporting a phenotypical and possibly etiological overlap between HD and FTD/ALS.[S40]

Other movement disorders

Other movement disorders in expansion carriers include cerebellar ataxia and a case with a clinical diagnosis of Creutzfeldt-Jakob disease.[3,12] These cases probably represent misdiagnoses of unusual presentations of c9FTD/ALS and further highlight the diversity of the clinical spectrum.

Recommendations for genetic testing

Offering genetic testing for a *C9orf72* repeat expansion is generally recommended in patients with concomitant FTD/ALS or familial FTD or ALS,[S41] but the best approach for seemingly sporadic FTD or ALS is still under debate.[40][S42,S43] This is exemplified by two surveys published in 2017 which found that genetic testing is offered to 90% of familial ALS patients versus just 30-50% of seemingly sporadic cases.[S44,S45] The relatively frequent identification of expansions among seemingly sporadic cases, coupled with better availability of genetic testing and the promise of gene-targeted therapy, has led to an increasing tendency to consider genetic testing in all FTD (especially bvFTD) and ALS patients, regardless of family history.[40,41][S42,S43,S46] Importantly, although certain clinical features may prompt the clinician to suspect an underlying *C9orf72* expansion (table 1), many c9FTD/ALS patients do not show distinctive features; relying on such features to select patients for genetic testing therefore carries the risk of missing expansion carriers.[S7]

While the overall frequency of a *C9orf72* repeat expansion in psychiatric disease is very low, genetic testing should be considered in late-onset (>40 years) cases with cognitive decline, prominent cerebral or cerebellar atrophy, or a family history of FTD, ALS or psychiatric disease (table 1).[41][S47] Offering genetic testing has also been recommended for patients presenting with parkinsonism and concomitant upper- or lower motor neuron symptoms or early neuropsychiatric or cognitive impairment.[32]

All patients and their families should receive genetic counselling prior to genetic testing, emphasising limitations of current testing methods (see also sections 5 and 6) and potential implications of test results.[40,42][S43] In many situations, coupling *C9orf72* repeat

expansion assays with multigene sequencing panels, which screen for the most common genetic mutations causing neurodegenerative disorders, is advisable considering the substantial overlap in symptomatology between various mutations and the risk of mutations in multiple disease-causing genes (see also section 7).[40][S42]

Clinical significance of repeat length

Normal and pathological repeat length

There is no clear consensus on which *C9orf72* repeat length is pathogenic. Most laboratories consider a repeat length of less than 20-30 in blood to be normal, while more than 200 repeats are very likely pathogenic.[42] Small expansions (i.e., up to 200 repeats) represent a grey area in which some carriers develop symptoms, while others do not.[43-45][S1,S48,S49] The interpretation of small expansions presents a major challenge to clinical genetic counselling and can have far-reaching consequences for affected families.[42]

Repeat length variation across and within tissues

Measuring *C9orf72* repeat length, determining the threshold for pathogenic repeat length and identifying possible associations with clinical features is greatly complicated by instability of the expansion, which results in different repeat lengths across and within tissues of the same individual.[3,8,43,44,46-48] Furthermore, expansion sizes in blood might not accurately reflect sizes in the CNS and should be interpreted cautiously.[8,47]. Direct comparisons of blood and brain tissue from the same individual demonstrate similar sizes in some subjects, but completely different sizes in others.[8,47,48] This is illustrated by several cases with small expansions in blood, and long expansions in brain tissue.[8,43,45,48] The interpretability of repeat lengths is also hampered by somatic instability in blood, resulting in big smears spanning a range of expansion sizes and possibly extra bands (see also section 6.2).[3,47,49]

In cell lines, expansion sizes should also be interpreted carefully. Cell lines usually contain fairly small expansions as compared to patient tissues.[7,8][S50] Additionally, due to their oligoclonal nature, they may demonstrate multiple concise bands, as shown for fibroblasts, lymphoblastoid cells, induced pluripotent stem cells (iPSCs), iPSC-derived neurons, et cetera.[7,8,49][S50,S51]

The risk of false-negative genetic testing due to somatic instability in individuals with non-expanded alleles in blood is probably limited, since up to 30 repeats appear to be stable across tissues.[43,48] Accordingly, no expansions were found in neural tissue of a small number of ALS patients with non-expanded alleles in blood.[48,50]

Clinico-pathological associations with expansion sizes

Although significant associations between clinical features and expansion size have been reported, findings are inconsistent, which might, to some extent, be explained by the substantial differences between tissues and subjects investigated. Some studies detected differences in expansion size between c9FTD and c9ALS,[46,49] but others could not replicate these findings.[3,8,48]

Potential associations have been detected between repeat length in various tissues and age at symptom onset.[3,7,8,47-49,51][S52] For example, one study reported a positive association between repeat length in the frontal cortex and age at onset in c9FTD.[8] At the same time, the *C9orf72* expansion might further expand with increasing age.[8,47,49] Age at sample collection and age at symptom onset are generally highly correlated, making it unclear whether longer expansions actually delay symptom onset or simply reflect increased repeat length as an individual ages. Since smaller repeat lengths have been observed in young presymptomatic expansion carriers,[47,49] the latter explanation seems plausible. Interestingly, associations with survival after onset suggest that smaller expansions might be beneficial.[8,48,49]

To replicate these associations, in-depth studies are necessary, taking into consideration differences between tissues, disease subgroups (c9FTD and/or c9ALS), age at collection, and disease status (affected or unaffected). These studies could also reveal associations with pathological *C9orf72*-mediated features, such as levels of *C9orf72* transcripts, RNA foci, and DPR proteins.

Anticipation

A repeat expansion might lengthen in successive generations, which could lead to an earlier age at onset and/or more severe disease phenotype. This phenomenon – also known as anticipation – has been reported in numerous repeat expansion disorders.[5]

Interestingly, an increase of roughly 1,000 repeats from one generation to the next was described in a c9FTD family,[44] suggestive of anticipation. Moreover, in a subset of families, an earlier age at onset was observed in younger generations.[1,52] Because Southern blots were not performed in most parent-offspring pairs included in these studies, it remains unclear whether or not reported differences in age at onset can be attributed to an increase in expansion size. One could postulate that individuals with a family history of FTD or ALS may seek medical attention sooner. Furthermore, a growing awareness of FTD and ALS in the general population and among clinicians as well as the availability of unified diagnostic

criteria may lead to an earlier diagnosis. Besides, these findings could be (partially) driven by selection and/or recall bias.

Importantly, two recent studies actually provided evidence against anticipation in *C9orf72*-related diseases.[47,51] These studies detected a reduction of the expansion size in successive generations, accounting for more than 50% of transmissions.[47,51] Intriguingly, contractions were frequently encountered in paternal transmissions, but rarely in maternal transmissions.[47] It should be noted that both studies were based on repeat lengths in blood which may not correlate with those in the brain. This is exemplified by a case report of an unaffected father with approximately 70 repeats in blood, while his children harboured long expansions.[53] Although this could indicate a jump from a pre-mutation to a disease-causing expansion in the next generation,[53] post-mortem tissue of the father later revealed long expansions in his brain,[45] stressing the importance of determining expansion sizes in brain tissue. As such, to unravel whether anticipation contributes to *C9orf72*-linked diseases, large-scale studies focusing on brain tissue from multiple generations are needed.

Detecting and sizing *C9orf72* repeat expansions

Detection of C9orf72 repeat expansions with PCR-based approaches

The most commonly applied methods for detecting repeat expansions are PCR-based approaches; a 2-step protocol consisting of a fluorescent PCR fragment-length analysis followed by repeat-primed PCR is recommended (figure 2).[1] A fluorescent PCR can specify the size of alleles within the wild-type range. If an individual has two alleles with a different number of repeats (e.g., 2 repeats and 5 repeats), then two peaks are detected and no additional tests are required. If, however, a single peak is observed, then a repeat-primed PCR is warranted. A repeat-primed PCR is able to determine whether an apparently homozygous individual carries two wild-type alleles with exactly the same number of repeats, or whether a wild-type allele is present in addition to an expanded allele that is too long for detection using a fluorescent PCR, in which case a characteristic stutter pattern is seen.[S53] Reactions should be repeated (e.g., with more DNA), when results are difficult to interpret. If the fluorescent PCR repeatedly fails (i.e., does not reveal any peaks) in the presence of a stutter pattern on the repeat-primed PCR, then a homozygous expansion should be considered.[S54,S55]

Importantly, an international study demonstrated that 6 out of 14 participating laboratories misclassified at least one sample when using a repeat-primed PCR alone.[6] Given that the accuracy increased when both a fluorescent PCR and repeat-primed PCR were used,[6] a 2-step protocol is the preferred method to determine the presence or absence of a *C9orf72*

repeat expansion in a research setting. A subset of misclassifications should probably be attributed to the genomic complexity of the *C9orf72* region. Sequence variants (e.g., deletions and insertions) have been described downstream of the expansion.[9,54] Depending on how the repeat-primed PCR has been designed and whether it has been thoroughly optimised, the presence of sequence variants might hamper the amplification of the expansion, and therefore, lead to a false negative repeat-primed PCR.[S56] Interestingly, it has been suggested that a downstream deletion lengthens the expansion. A 10-bp deletion, for instance, removes several non-GC-bases, extending the GC-rich region with imperfect repeats.[9][S56]) Although this might be relevant for relatively small expansions, possibly decreasing stability of the repetitive area,[9] one could doubt whether the addition of a few extra GC-bases to a long expansion will have a major effect.[54] Regardless, these sequence variants should be taken into consideration since they may reduce the accuracy of the repeat-primed PCR

Figure 2. Stepwise approach for the detection of a *C9orf72* repeat expansion. Fluorescent PCR fragment-length analysis is used to determine the number of alleles in the wild-type range. If a single peak is observed, then repeat-primed PCR is warranted to determine whether the individual carries two wild-type alleles with the exact same number of repeats, or whether a repeat expansion is present that is too long for detection by fluorescent PCR. If a repeat expansion is present, a characteristic stutter pattern is observed on repeat-primed PCR. Especially in a clinical setting, it is recommended to confirm the presence of an expansion using Southern blotting.

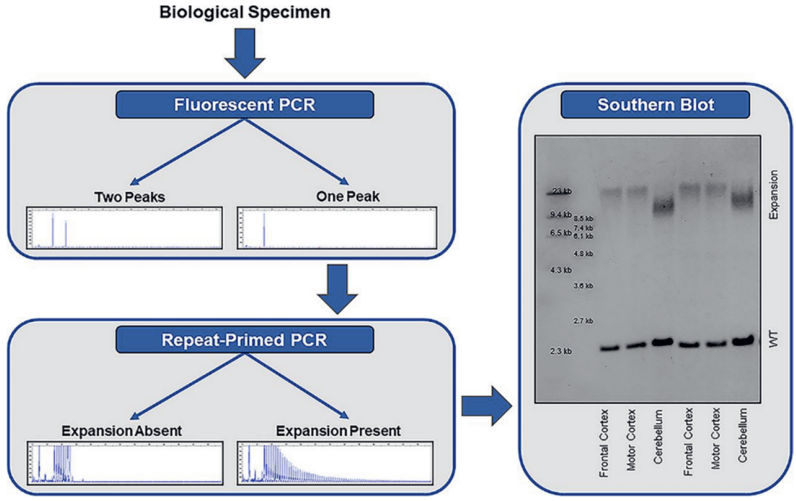

Detection and sizing of expanded C9orf72 repeats with Southern blotting

The gold standard to detect a *C9orf72* repeat expansion is a Southern blot (figure 2). Results are highly consistent across laboratories,[6] and Southern blotting should be used to confirm the presence of an expanded repeat, especially in a clinical setting. Moreover, Southern blotting can clarify whether an individual is heterozygous or homozygous for the expansion (i.e., presence or absence of a band corresponding to the wild-type allele).[S54,S55] As opposed to a repeat-primed PCR, Southern blotting is also capable of estimating the size of the expansion.

Various Southern blot protocols have been published to estimate the size of expanded *C9orf72* repeats using different restriction enzymes and probes.[3,8,46-49][S50,S52,S57] Whether an area close to the expansion is targeted [7,8,47] or the expansion itself,[3,49] also affects the Southern blot: while probes that target the repeat frequently produce a strong signal, they can hybridise to GGGGCC-repeats in other areas (outside of the *C9orf72* locus), and additionally, they may not visualise the wild-type allele, which is often used as an internal control that the Southern blot worked and which helps to elucidate whether someone is homozygous for the expansion.[7] Even though Southern blotting can accurately determine the presence or absence of an expanded *C9orf72* repeat and estimate its size, it is a time-consuming and technically challenging method requiring high-quality DNA.[8]

Detection of C9orf72 expansions with short-read sequencing

Several tools have been developed to detect a *C9orf72* repeat expansion in PCR-free short-read whole-genome sequencing (WGS) data.[S58-S61] The ExpansionHunter tool correctly identified all 212 *C9orf72* expansion carriers in a cohort of over 3,000 ALS patients.[55] Furthermore, a new version of this tool has been recently released that uses sequence graphs to handle complex loci.[S62] Despite encouraging results, it remains difficult to reconstruct expansions based on short-read sequencing techniques.[55]

Employing long-read sequencing to assess sizes, interruptions, and methylation patterns

Long--read sequencing techniques are a promising upcoming strategy to evaluate large repeat expansions. Popular platforms have been developed by Oxford Nanopore Technologies (ONT) and Pacific Biosciences (PacBio). ONT's nanopore technology measures changes in current as DNA passes through a nanopore,[56,57][S63] whereas PacBio's single molecule real-time (SMRT) technology measures fluorescence when nucleotides are added.[56,58] In theory, long-read sequencing can span the entire *C9orf72* expansion, which facilitates reliable estimation of expansion sizes. Another major advantage of long-read sequencing is its ability to evaluate sequence content. It is possible, for example, to determine the presence of interruptions in *C9orf72* repeat expansions,[59] which is highly relevant since interruptions serve as disease modifiers in other repeat expansion

disorders.[5][S64-S68] Furthermore, long-read sequencing provides the opportunity to examine the methylation status of expanded *C9orf72* repeats.[60] Interestingly, while hypermethylation of the *C9orf72* promoter is well documented,[S69-S72] little is known about the methylation status of the expanded repeat itself in c9FTD/ALS patients. It has been suggested that the expansion is methylated;[S73] however, quantitative assays have yet to be developed. Importantly, long-read sequencing requires high-molecular-weight genomic DNA, and DNA should be extracted using suitable protocols to ensure that the DNA, and therefore the expansion, remains intact.

Several long-read sequencing technologies have been tested for *C9orf72*-linked diseases.[59,60] Long-read WGS on ONT's MinION platform and PacBio's Sequel platform only yielded a relatively low number of reads covering the expanded allele. Newer CRISPR-Cas9-based enrichment strategies to specifically examine the *C9orf72* locus have considerably increased the yield.[59,60] These proof-of-concept studies demonstrate the feasibility of long-read sequencing approaches, and further protocol optimisation is expected to improve their accuracy and efficiency, facilitating implementation of long-read sequencing in research and eventually in clinical settings.

Other potential genetic disease modifiers

Besides repeat length, several other potential genetic disease modifiers have been identified, highlighting that a complex interplay of various genetic factors probably contributes to the phenotypic variability of the *C9orf72* repeat expansion. For example, intermediate repeat expansions in *ATXN2*, a known risk factor for ALS, appear to be more common in c9ALS than in c9FTD, suggesting that they might drive the clinical phenotype towards ALS rather than FTD.[S74,S75] Similarly, single nucleotide polymorphisms (SNPs) in *TMEM106B* appear to protect specifically against c9FTD, but not c9ALS,[S76,S77] and two CpG-SNPs (i.e., SNPs that affect DNA methylation patterns) at the *C6orf10/LOC101929163* locus are associated with age at symptom onset.[S78] The rare co-existence of pathogenic mutations in other FTD or ALS-associated genes, including *GRN, MAPT, TBK1, TARDBP, SOD1* and *FUS* might in some cases act synergistically to influence disease severity and / or phenotypic features.[S79,S80]

Conclusions and future directions

The *C9orf72* expansion is highly clinically heterogeneous, and clinicians need to be aware of the wide spectrum of associated symptoms in order to provide a timely diagnosis and management and to select patients for clinical trials. Despite extensive research, the genetic

basis of this heterogeneity remains poorly understood. Novel sequencing techniques that enable thorough assessment of the expansion size as well as its purity and methylation levels may reveal new associations with clinical features. The measurement and interpretation of repeat length is greatly complicated by the presence of somatic mosaicism, and a better understanding of repeat instability is needed to elucidate potential genotype-phenotype correlations as well as to determine the viability of therapeutic approaches aimed at stabilising repeat expansions.

The lack of consensus on clear cut-off values for pathogenicity poses a major challenge for clinical genetic counselling. Further research is also needed to determine whether intermediate repeat lengths have any clinical significance (reviewed in [S81]) which, remarkably, have been associated with normal to upregulated *C9orf72* expression,[45,47][S72,S82] in contrast to the downregulation seen in patients with long expansions.[S52]

Besides repeat length, several other potential genetic determinants have been identified. Possibly, multiple phenotypic modifiers are present at the same time, concealing clear associations with each individual modifier. Future research into the various modifiers will be essential to predict the expected disease course, which in turn will be valuable both for patient management and for patient stratification in clinical trials.

Funding

ELvdE, HS and JCvS are supported by two Memorabel grants from Deltaplan Dementie (The Netherlands Organisation for Health Research and Development and Alzheimer Nederland; grant numbers 7330550813 and 733050103), The Bluefield Project to Cure Frontotemporal Dementia, the Dioraphte foundation (grant number 1402 1300), and the European Joint Programme – Neurodegenerative Disease Research (JPND, PreFrontALS). MvB is supported by the Muscular Dystrophy Association (MDA), ALS Association, and National Institutes of Health (NIH) grants R21 NS110994 and R21 NS099631. The authors declare no conflicts of interest.

Author contributions

ELvdE, MvB, HS and JCvS contributed to conception and design of the review and drafting of the manuscript and figures. JLJ and AW contributed to the drafting of the manuscript and figures. All authors critically reviewed the manuscript and approved the final draft.

References

1. DeJesus-Hernandez M, Mackenzie IR, Boeve BF, et al. Expanded GGGGCC hexanucleotide repeat in noncoding region of C9ORF72 causes chromosome 9p-linked FTD and ALS. Neuron. 2011;72(2):245-56.
2. Renton AE, Majounie E, Waite A, et al. A hexanucleotide repeat expansion in C9ORF72 is the cause of chromosome 9p21-linked ALS-FTD. Neuron. 2011;72(2):257-68.
3. Beck J, Poulter M, Hensman D, et al. Large C9orf72 hexanucleotide repeat expansions are seen in multiple neurodegenerative syndromes and are more frequent than expected in the UK population. Am J Hum Genet. 2013;92(3):345-53.
4. Majounie E, Renton AE, Mok K, et al. Frequency of the C9orf72 hexanucleotide repeat expansion in patients with amyotrophic lateral sclerosis and frontotemporal dementia: a cross-sectional study. Lancet Neurol. 2012;11(4):323-30.
5. Paulson H. Repeat expansion diseases. Handb Clin Neurol. 2018;147:105-23.
6. Akimoto C, Volk AE, van Blitterswijk M, et al. A blinded international study on the reliability of genetic testing for GGGGCC-repeat expansions in C9orf72 reveals marked differences in results among 14 laboratories. J Med Genet. 2014;51(6):419-24.
7. Hübers A, Marroquin N, Schmoll B, et al. Polymerase chain reaction and Southern blot-based analysis of the C9orf72 hexanucleotide repeat in different motor neuron diseases. Neurobiol Aging. 2014;35(5):1214 e1-6.
8. van Blitterswijk M, DeJesus-Hernandez M, Niemantsverdriet E, et al. Association between repeat sizes and clinical and pathological characteristics in carriers of C9ORF72 repeat expansions (Xpansize-72): a cross-sectional cohort study. Lancet Neurol. 2013;12(10):978-88.
9. van der Zee J, Gijselinck I, Dillen L, et al. A pan-European study of the C9orf72 repeat associated with FTLD: geographic prevalence, genomic instability, and intermediate repeats. Hum Mutat. 2013;34(2):363-73.
10. Balendra R, Isaacs AM. C9orf72-mediated ALS and FTD: multiple pathways to disease. Nat Rev Neurol. 2018;14(9):544-58.
11. Tang X, Toro A, T GS, et al. Divergence, Convergence, and Therapeutic Implications: A Cell Biology Perspective of C9ORF72-ALS/FTD. Mol Neurodegener. 2020;15(1):34.
12. Marogianni C, Rikos D, Provatas A, et al. The role of C9orf72 in neurodegenerative disorders: a systematic review, an updated meta-analysis, and the creation of an online database. Neurobiol Aging. 2019;84:238 e25- e34.
13. Cammack AJ, Atassi N, Hyman T, et al. Prospective natural history study of C9orf72 ALS clinical characteristics and biomarkers. Neurology. 2019;93(17):e1605-e17.
14. Glasmacher SA, Wong C, Pearson IE, et al. Survival and Prognostic Factors in C9orf72 Repeat Expansion Carriers: A Systematic Review and Meta-analysis. JAMA Neurol. 2019;77(3):367-76.
15. Snowden JS, Rollinson S, Thompson JC, et al. Distinct clinical and pathological characteristics of frontotemporal dementia associated with C9ORF72 mutations. Brain. 2012;135(Pt 3):693-708.

16. Rascovsky K, Hodges JR, Knopman D, et al. Sensitivity of revised diagnostic criteria for the behavioural variant of frontotemporal dementia. Brain. 2011;134(Pt 9):2456-77.
17. Devenney E, Hornberger M, Irish M, et al. Frontotemporal dementia associated with the C9ORF72 mutation: a unique clinical profile. JAMA Neurol. 2014;71(3):331-9.
18. Cacace R, Van Cauwenberghe C, Bettens K, et al. C9orf72 G4C2 repeat expansions in Alzheimer's disease and mild cognitive impairment. Neurobiol Aging. 2013;34(6):1712 e1-7.
19. Mahoney CJ, Beck J, Rohrer JD, et al. Frontotemporal dementia with the C9ORF72 hexanucleotide repeat expansion: clinical, neuroanatomical and neuropathological features. Brain. 2012;135(Pt 3):736-50.
20. Khan BK, Yokoyama JS, Takada LT, et al. Atypical, slowly progressive behavioural variant frontotemporal dementia associated with C9ORF72 hexanucleotide expansion. J Neurol Neurosurg Psychiatry. 2012;83(4):358-64.
21. Llamas-Velasco S, García-Redondo A, Herrero-San Martín A, et al. Slowly progressive behavioral frontotemporal dementia with C9orf72 mutation. Case report and review of the literature. Neurocase. 2018;24(1):68-71.
22. Harms M, Benitez BA, Cairns N, et al. C9orf72 hexanucleotide repeat expansions in clinical Alzheimer disease. JAMA Neurol. 2013;70(6):736-41.
23. Bieniek KF, Murray ME, Rutherford NJ, et al. Tau pathology in frontotemporal lobar degeneration with C9ORF72 hexanucleotide repeat expansion. Acta Neuropathol. 2013;125(2):289-302.
24. Majounie E, Abramzon Y, Renton AE, et al. Repeat expansion in C9ORF72 in Alzheimer's disease. N Engl J Med. 2012;366(3):283-4.
25. Solje E, Aaltokallio H, Koivumaa-Honkanen H, et al. The Phenotype of the C9ORF72 Expansion Carriers According to Revised Criteria for bvFTD. PLoS One. 2015;10(7):e0131817.
26. Bieniek KF, van Blitterswijk M, Baker MC, et al. Expanded C9ORF72 hexanucleotide repeat in depressive pseudodementia. JAMA Neurol. 2014;71(6):775-81.
27. Block NR, Sha SJ, Karydas AM, et al. Frontotemporal Dementia and Psychiatric Illness: Emerging Clinical and Biological Links in Gene Carriers. Am J Geriatr Psychiatry. 2016;24(2):107-16.
28. Fahey C, Byrne S, McLaughlin R, et al. Analysis of the hexanucleotide repeat expansion and founder haplotype at C9ORF72 in an Irish psychosis case-control sample. Neurobiol Aging. 2014;35(6):1510 e1-5.
29. Solje E, Miettunen J, Marttila R, et al. The C9ORF72 expansion sizes in patients with psychosis: a population-based study on the Northern Finland Birth Cohort 1966. Psychiatr Genet. 2016;26(2):92-4.
30. Boeve BF, Boylan KB, Graff-Radford NR, et al. Characterization of frontotemporal dementia and/or amyotrophic lateral sclerosis associated with the GGGGCC repeat expansion in C9ORF72. Brain. 2012;135(Pt 3):765-83.
31. Carneiro F, Saracino D, Huin V, et al. Isolated parkinsonism is an atypical presentation of GRN and C9orf72 gene mutations. Parkinsonism Relat Disord. 2020;80:73-81.
32. Wilke C, Pomper JK, Biskup S, et al. Atypical parkinsonism in C9orf72 expansions: a case report and systematic review of 45 cases from the literature. J Neurol. 2016;263(3):558-74.

33. Lesage S, Le Ber I, Condroyer C, et al. C9orf72 repeat expansions are a rare genetic cause of parkinsonism. Brain. 2013;136(Pt 2):385-91.
34. Cooper-Knock J, Frolov A, Highley JR, et al. C9ORF72 expansions, parkinsonism, and Parkinson disease: a clinicopathologic study. Neurology. 2013;81(9):808-11.
35. Shivji S, Wong W, Fischer CE, et al. Parkinsonism in C9orf72 expansion without co-existing Lewy body pathology; a case report and review of the literature. Neuropathol Appl Neurobiol. 2020.
36. Theuns J, Verstraeten A, Sleegers K, et al. Global investigation and meta-analysis of the C9orf72 (G4C2)n repeat in Parkinson disease. Neurology. 2014;83(21):1906-13.
37. Nuytemans K, Inchausti V, Beecham GW, et al. Absence of C9ORF72 expanded or intermediate repeats in autopsy-confirmed Parkinson's disease. Mov Disord. 2014;29(6):827-30.
38. Hensman Moss DJ, Poulter M, Beck J, et al. C9orf72 expansions are the most common genetic cause of Huntington disease phenocopies. Neurology. 2014;82(4):292-9.
39. Martins J, Damásio J, Mendes A, et al. Clinical spectrum of C9orf72 expansion in a cohort of Huntington's disease phenocopies. Neurol Sci. 2018;39(4):741-4.
40. Roggenbuck J, Fong JC. Genetic Testing for Amyotrophic Lateral Sclerosis and Frontotemporal Dementia: Impact on Clinical Management. Clin Lab Med. 2020;40(3):271-87.
41. Ducharme S, Dols A, Laforce R, et al. Recommendations to distinguish behavioural variant frontotemporal dementia from psychiatric disorders. Brain. 2020;143(6):1632-50.
42. Crook A, McEwen A, Fifita JA, et al. The C9orf72 hexanucleotide repeat expansion presents a challenge for testing laboratories and genetic counseling. Amyotroph Lateral Scler Frontotemporal Degener. 2019;20(5-6):310-6.
43. Fratta P, Polke JM, Newcombe J, et al. Screening a UK amyotrophic lateral sclerosis cohort provides evidence of multiple origins of the C9orf72 expansion. Neurobiol Aging. 2015;36(1):546 e1-7.
44. Gijselinck I, Van Mossevelde S, van der Zee J, et al. The C9orf72 repeat size correlates with onset age of disease, DNA methylation and transcriptional downregulation of the promoter. Mol Psychiatry. 2016;21(8):1112-24.
45. McGoldrick P, Zhang M, van Blitterswijk M, et al. Unaffected mosaic C9orf72 case: RNA foci, dipeptide proteins, but upregulated C9orf72 expression. Neurology. 2018;90(4):e323-e31.
46. Dols-Icardo O, García-Redondo A, Rojas-García R, et al. Characterization of the repeat expansion size in C9orf72 in amyotrophic lateral sclerosis and frontotemporal dementia. Hum Mol Genet. 2014;23(3):749-54.
47. Jackson JL, Finch NA, Baker MC, et al. Elevated methylation levels, reduced expression levels, and frequent contractions in a clinical cohort of C9orf72 expansion carriers. Mol Neurodegener. 2020;15(1):7.
48. Nordin A, Akimoto C, Wuolikainen A, et al. Extensive size variability of the GGGGCC expansion in C9orf72 in both neuronal and non-neuronal tissues in 18 patients with ALS or FTD. Hum Mol Genet. 2015;24(11):3133-42.

49. Suh E, Lee EB, Neal D, et al. Semi-automated quantification of C9orf72 expansion size reveals inverse correlation between hexanucleotide repeat number and disease duration in frontotemporal degeneration. Acta Neuropathol. 2015;130(3):363-72.
50. Ross JP, Leblond CS, Catoire H, et al. Somatic expansion of the C9orf72 hexanucleotide repeat does not occur in ALS spinal cord tissues. Neurol Genet. 2019;5(2):e317.
51. Fournier C, Barbier M, Camuzat A, et al. Relations between C9orf72 expansion size in blood, age at onset, age at collection and transmission across generations in patients and presymptomatic carriers. Neurobiol Aging. 2019;74:234 e1- e8.
52. Van Mossevelde S, van der Zee J, Gijselinck I, et al. Clinical Evidence of Disease Anticipation in Families Segregating a C9orf72 Repeat Expansion. JAMA Neurol. 2017;74(4):445-52.
53. Xi Z, van Blitterswijk M, Zhang M, et al. Jump from pre-mutation to pathologic expansion in C9orf72. Am J Hum Genet. 2015;96(6):962-70.
54. Nordin A, Akimoto C, Wuolikainen A, et al. Sequence variations in C9orf72 downstream of the hexanucleotide repeat region and its effect on repeat-primed PCR interpretation: a large multinational screening study. Amyotroph Lateral Scler Frontotemporal Degener. 2017;18(3-4):256-64.
55. Dolzhenko E, van Vugt J, Shaw RJ, et al. Detection of long repeat expansions from PCR-free whole-genome sequence data. Genome Res. 2017;27(11):1895-903.
56. Amarasinghe SL, Su S, Dong X, et al. Opportunities and challenges in long-read sequencing data analysis. Genome Biol. 2020;21(1):30.
57. Jain M, Olsen HE, Paten B, et al. The Oxford Nanopore MinION: delivery of nanopore sequencing to the genomics community. Genome Biol. 2016;17(1):239.
58. Roberts RJ, Carneiro MO, Schatz MC. The advantages of SMRT sequencing. Genome Biol. 2013;14(7):405.
59. Ebbert MTW, Farrugia SL, Sens JP, et al. Long-read sequencing across the C9orf72 'GGGGCC' repeat expansion: implications for clinical use and genetic discovery efforts in human disease. Mol Neurodegener. 2018;13(1):46.
60. Giesselmann P, Brändl B, Raimondeau E, et al. Analysis of short tandem repeat expansions and their methylation state with nanopore sequencing. Nat Biotechnol. 2019;37(12):1478-81.

Supplementary references

S1. Kaivola K, Kiviharju A, Jansson L, et al. C9orf72 hexanucleotide repeat length in older population: normal variation and effects on cognition. Neurobiol Aging. 2019;84:242 e7- e12.

S2. Farg MA, Sundaramoorthy V, Sultana JM, et al. C9ORF72, implicated in amytrophic lateral sclerosis and frontotemporal dementia, regulates endosomal trafficking. Hum Mol Genet. 2014;23(13):3579-95.

S3. Murphy NA, Arthur KC, Tienari PJ, et al. Age-related penetrance of the C9orf72 repeat expansion. Sci Rep. 2017;7(1):2116.

S4. Moore KM, Nicholas J, Grossman M, et al. Age at symptom onset and death and disease duration in genetic frontotemporal dementia: an international retrospective cohort study. Lancet Neurol. 2020;19(2):145-56.

S5. Caswell C, McMillan CT, Xie SX, et al. Genetic predictors of survival in behavioral variant frontotemporal degeneration. Neurology. 2019;93(18):e1707-e14.

S6. Woollacott IO, Mead S. The C9ORF72 expansion mutation: gene structure, phenotypic and diagnostic issues. Acta Neuropathol. 2014;127(3):319-32.

S7. Rohrer JD, Isaacs AM, Mizielinska S, et al. C9orf72 expansions in frontotemporal dementia and amyotrophic lateral sclerosis. Lancet Neurol. 2015;14(3):291-301.

S8. Devenney E, Swinn T, Mioshi E, et al. The behavioural variant frontotemporal dementia phenocopy syndrome is a distinct entity - evidence from a longitudinal study. BMC Neurol. 2018;18(1):56.

S9. Gómez-Tortosa E, Serrano S, de Toledo M, et al. Familial benign frontotemporal deterioration with C9ORF72 hexanucleotide expansion. Alzheimers Dement. 2014;10(5 Suppl):S284-9.

S10. Suhonen NM, Kaivorinne AL, Moilanen V, et al. Slowly progressive frontotemporal lobar degeneration caused by the C9ORF72 repeat expansion: a 20-year follow-up study. Neurocase. 2015;21(1):85-9.

S11. Kohli MA, John-Williams K, Rajbhandary R, et al. Repeat expansions in the C9ORF72 gene contribute to Alzheimer's disease in Caucasians. Neurobiol Aging. 2013;34(5):1519 e5-12.

S12. Wojtas A, Heggeli KA, Finch N, et al. C9ORF72 repeat expansions and other FTD gene mutations in a clinical AD patient series from Mayo Clinic. Am J Neurodegener Dis. 2012;1(1):107-18.

S13. Geiger JT, Arthur KC, Dawson TM, et al. C9orf72 Hexanucleotide Repeat Analysis in Cases with Pathologically Confirmed Dementia with Lewy Bodies. Neurodegener Dis. 2016;16(5-6):370-2.

S14. Kun-Rodrigues C, Ross OA, Orme T, et al. Analysis of C9orf72 repeat expansions in a large international cohort of dementia with Lewy bodies. Neurobiol Aging. 2017;49:214 e13- e15.

S15. Forrest SL, Crockford DR, Sizemova A, et al. Coexisting Lewy body disease and clinical parkinsonism in frontotemporal lobar degeneration. Neurology. 2019;92(21):e2472-e82.

S16. Ramos-Campoy O, Ávila-Polo R, Grau-Rivera O, et al. Systematic Screening of Ubiquitin/p62 Aggregates in Cerebellar Cortex Expands the Neuropathological Phenotype of the C9orf72 Expansion Mutation. J Neuropathol Exp Neurol. 2018;77(8):703-9.
S17. Agosta F, Ferraro PM, Riva N, et al. Structural and functional brain signatures of C9orf72 in motor neuron disease. Neurobiol Aging. 2017;57:206-19.
S18. Chiò A, Moglia C, Canosa A, et al. Cognitive impairment across ALS clinical stages in a population-based cohort. Neurology. 2019;93(10):e984-e94.
S19. van Rheenen W, van Blitterswijk M, Huisman MH, et al. Hexanucleotide repeat expansions in C9ORF72 in the spectrum of motor neuron diseases. Neurology. 2012;79(9):878-82.
S20. Galimberti D, Fenoglio C, Serpente M, et al. Autosomal dominant frontotemporal lobar degeneration due to the C9ORF72 hexanucleotide repeat expansion: late-onset psychotic clinical presentation. Biol Psychiatry. 2013;74(5):384-91.
S21. Kaivorinne AL, Bode MK, Paavola L, et al. Clinical Characteristics of C9ORF72-Linked Frontotemporal Lobar Degeneration. Dement Geriatr Cogn Dis Extra. 2013;3(1):251-62.
S22. Landqvist Waldö M, Gustafson L, Nilsson K, et al. Frontotemporal dementia with a C9ORF72 expansion in a Swedish family: clinical and neuropathological characteristics. Am J Neurodegener Dis. 2013;2(4):276-86.
S23. Snowden JS, Adams J, Harris J, et al. Distinct clinical and pathological phenotypes in frontotemporal dementia associated with MAPT, PGRN and C9orf72 mutations. Amyotroph Lateral Scler Frontotemporal Degener. 2015;16(7-8):497-505.
S24. Shinagawa S, Nakajima S, Plitman E, et al. Psychosis in frontotemporal dementia. J Alzheimers Dis. 2014;42(2):485-99.
S25. Calvo A, Moglia C, Canosa A, et al. Amyotrophic lateral sclerosis/frontotemporal dementia with predominant manifestations of obsessive-compulsive disorder associated to GGGGCC expansion of the c9orf72 gene. J Neurol. 2012;259(12):2723-5.
S26. Galimberti D, Reif A, Dell'Osso B, et al. C9ORF72 hexanucleotide repeat expansion as a rare cause of bipolar disorder. Bipolar Disord. 2014;16(4):448-9.
S27. Holm AC. Neurodegenerative and psychiatric overlap in frontotemporal lobar degeneration: a case of familial frontotemporal dementia presenting with catatonia. Int Psychogeriatr. 2014;26(2):345-7.
S28. Meisler MH, Grant AE, Jones JM, et al. C9ORF72 expansion in a family with bipolar disorder. Bipolar Disord. 2013;15(3):326-32.
S29. Floris G, Borghero G, Di Stefano F, et al. Phenotypic variability related to C9orf72 mutation in a large Sardinian kindred. Amyotroph Lateral Scler Frontotemporal Degener. 2016;17(3-4):245-8.
S30. Majounie E, Abramzon Y, Renton AE, et al. Large C9orf72 repeat expansions are not a common cause of Parkinson's disease. Neurobiol Aging. 2012;33(10):2527 e1-2.
S31. O'Dowd S, Curtin D, Waite AJ, et al. C9ORF72 expansion in amyotrophic lateral sclerosis/frontotemporal dementia also causes parkinsonism. Mov Disord. 2012;27(8):1072-4.
S32. Goldman JS, Kuo SH. Multiple system atrophy and repeat expansions in C9orf72--reply. JAMA Neurol. 2014;71(9):1191-2.

S33. Lindquist SG, Duno M, Batbayli M, et al. Corticobasal and ataxia syndromes widen the spectrum of C9ORF72 hexanucleotide expansion disease. Clin Genet. 2013;83(3):279-83.

S34. Schipper LJ, Raaphorst J, Aronica E, et al. Prevalence of brain and spinal cord inclusions, including dipeptide repeat proteins, in patients with the C9ORF72 hexanucleotide repeat expansion: a systematic neuropathological review. Neuropathol Appl Neurobiol. 2016;42(6):547-60.

S35. Xi Z, Zinman L, Grinberg Y, et al. Investigation of c9orf72 in 4 neurodegenerative disorders. Arch Neurol. 2012;69(12):1583-90.

S36. Ida CM, Butz ML, Lundquist PA, et al. C9orf72 Repeat Expansion Frequency among Patients with Huntington Disease Genetic Testing. Neurodegener Dis. 2018;18(5-6):239-53.

S37. Kostić VS, Dobričić V, Stanković I, et al. C9orf72 expansion as a possible genetic cause of Huntington disease phenocopy syndrome. J Neurol. 2014;261(10):1917-21.

S38. Dobson-Stone C, Hallupp M, Loy CT, et al. C9ORF72 repeat expansion in Australian and Spanish frontotemporal dementia patients. PLoS One. 2013;8(2):e56899.

S39. García-Redondo A, Dols-Icardo O, Rojas-García R, et al. Analysis of the C9orf72 gene in patients with amyotrophic lateral sclerosis in Spain and different populations worldwide. Hum Mutat. 2013;34(1):79-82.

S40. Bardelli D, Sassone F, Colombrita C, et al. Reprogramming fibroblasts and peripheral blood cells from a C9ORF72 patient: A proof-of-principle study. J Cell Mol Med. 2020;24(7):4051-60.

S41. Zeier Z, Esanov R, Belle KC, et al. Bromodomain inhibitors regulate the C9ORF72 locus in ALS. Exp Neurol. 2015;271:241-50.

S42. Waite AJ, Bäumer D, East S, et al. Reduced C9orf72 protein levels in frontal cortex of amyotrophic lateral sclerosis and frontotemporal degeneration brain with the C9ORF72 hexanucleotide repeat expansion. Neurobiol Aging. 2014;35(7):1779 e5- e13.

S43. Hantash FM, Goos DG, Tsao D, et al. Qualitative assessment of FMR1 (CGG)n triplet repeat status in normal, intermediate, premutation, full mutation, and mosaic carriers in both sexes: implications for fragile X syndrome carrier and newborn screening. Genet Med. 2010;12(3):162-73.

S44. Fratta P, Poulter M, Lashley T, et al. Homozygosity for the C9orf72 GGGGCC repeat expansion in frontotemporal dementia. Acta Neuropathol. 2013;126(3):401-9.

S45. Ramos EM, Dokuru DR, Van Berlo V, et al. Genetic screening of a large series of North American sporadic and familial frontotemporal dementia cases. Alzheimers Dement. 2020;16(1):118-30.

S46. Buchman VL, Cooper-Knock J, Connor-Robson N, et al. Simultaneous and independent detection of C9ORF72 alleles with low and high number of GGGGCC repeats using an optimised protocol of Southern blot hybridisation. Mol Neurodegener. 2013;8:12.

S47. Dashnow H, Lek M, Phipson B, et al. STRetch: detecting and discovering pathogenic short tandem repeat expansions. Genome Biol. 2018;19(1):121.

S48. Mousavi N, Shleizer-Burko S, Yanicky R, et al. Profiling the genome-wide landscape of tandem repeat expansions. Nucleic Acids Res. 2019;47(15):e90.

S49. Tang H, Kirkness EF, Lippert C, et al. Profiling of Short-Tandem-Repeat Disease Alleles in 12,632 Human Whole Genomes. Am J Hum Genet. 2017;101(5):700-15.

S50. Tankard RM, Bennett MF, Degorski P, et al. Detecting Expansions of Tandem Repeats in Cohorts Sequenced with Short-Read Sequencing Data. Am J Hum Genet. 2018;103(6):858-73.

S51. Dolzhenko E, Deshpande V, Schlesinger F, et al. ExpansionHunter: a sequence-graph-based tool to analyze variation in short tandem repeat regions. Bioinformatics. 2019;35(22):4754-6.

S52. Dolzhenko E, Bennett MF, Richmond PA, et al. ExpansionHunter Denovo: a computational method for locating known and novel repeat expansions in short-read sequencing data. Genome Biol. 2020;21(1):102.

S53. Rang FJ, Kloosterman WP, de Ridder J. From squiggle to basepair: computational approaches for improving nanopore sequencing read accuracy. Genome Biol. 2018;19(1):90.

S54. Matsuura T, Fang P, Pearson CE, et al. Interruptions in the expanded ATTCT repeat of spinocerebellar ataxia type 10: repeat purity as a disease modifier? Am J Hum Genet. 2006;78(1):125-9.

S55. Matsuyama Z, Izumi Y, Kameyama M, et al. The effect of CAT trinucleotide interruptions on the age at onset of spinocerebellar ataxia type 1 (SCA1). J Med Genet. 1999;36(7):546-8.

S56. McFarland KN, Liu J, Landrian I, et al. Repeat interruptions in spinocerebellar ataxia type 10 expansions are strongly associated with epileptic seizures. Neurogenetics. 2014;15(1):59-64.

S57. Menon RP, Nethisinghe S, Faggiano S, et al. The role of interruptions in polyQ in the pathology of SCA1. PLoS Genet. 2013;9(7):e1003648.

S58. Pešović J, Perić S, Brkušanin M, et al. Repeat Interruptions Modify Age at Onset in Myotonic Dystrophy Type 1 by Stabilizing DMPK Expansions in Somatic Cells. Front Genet. 2018;9:601.

S59. Liu EY, Russ J, Wu K, et al. C9orf72 hypermethylation protects against repeat expansion-associated pathology in ALS/FTD. Acta Neuropathol. 2014;128(4):525-41.

S60. Xi Z, Rainero I, Rubino E, et al. Hypermethylation of the CpG-island near the C9orf72 G_4C_2-repeat expansion in FTLD patients. Hum Mol Genet. 2014;23(21):5630-7.

S61. Xi Z, Zinman L, Moreno D, et al. Hypermethylation of the CpG island near the G4C2 repeat in ALS with a C9orf72 expansion. Am J Hum Genet. 2013;92(6):981-9.

S62. Xi Z, Zhang M, Bruni AC, et al. The C9orf72 repeat expansion itself is methylated in ALS and FTLD patients. Acta Neuropathol. 2015;129(5):715-27.

S63. Ng ASL, Tan EK. Intermediate C9orf72 alleles in neurological disorders: does size really matter? J Med Genet. 2017;54(9):591-7.

S64. Cali CP, Patino M, Tai YK, et al. C9orf72 intermediate repeats are associated with corticobasal degeneration, increased C9orf72 expression and disruption of autophagy. Acta Neuropathol. 2019;138(5):795-811.

Chapter 5

Modelling biomarker trajectories in genetic frontotemporal dementia

Chapter 5.2

Modelling the cascade of biomarker changes in *GRN*-related frontotemporal dementia

Jessica L. Panman*, Vikram Venkatraghavan*, Emma L. van der Ende, Rebecca M.E. Steketee, Lize C. Jiskoot, Jackie M. Poos, Elise G.P. Dopper, Lieke H.H. Meeter, Laura Donker Kaat, Serge A.R.B. Rombouts, Meike W. Vernooij, Anneke J.A. Kievit, Enrico Premi, Maura Cosseddu, Elise Bonomi, Jaume Olives, Jonathan D. Rohrer, Raquel Sanchez-Valle, Barbara Borroni, Esther E. Bron, John C. van Swieten, Janne M. Papma, Stefan Klein, GENFI consortium investigators

*Authors contributed equally to the manuscript

Journal of Neurology, Neurosurgery and Psychiatry 2021;92(5):494-501

Abstract

Objective: Progranulin related frontotemporal dementia (FTD-*GRN*) is a fast progressive disease. Modelling the cascade of multimodal biomarker changes aids in understanding the etiology of this disease and enables monitoring of individual mutation carriers. In this cross-sectional study, we estimated the temporal cascade of biomarker changes for FTD-*GRN*, in a data-driven way.

Methods: We included 56 presymptomatic and 35 symptomatic *GRN* mutation carriers, and 35 healthy non-carriers. Selected biomarkers were neurofilament light chain (NfL), grey matter volume, white matter microstructure, and cognitive domains. We used discriminative event-based modelling to infer the cascade of biomarker changes in FTD-*GRN* and estimated individual disease severity through cross-validation. We derived the biomarker cascades in non-fluent variant primary progressive aphasia (nfvPPA) and behavioural variant FTD (bvFTD) to understand the differences between these phenotypes.

Results: Language functioning and NfL were the earliest abnormal biomarkers in FTD-*GRN*. White matter tracts were affected before grey matter volume, and the left hemisphere degenerated before the right. Based on individual disease severities, presymptomatic carriers could be delineated from symptomatic carriers with a sensitivity of 100% and specificity of 96.1%. The estimated disease severity strongly correlated with functional severity in nfvPPA, but not in bvFTD. In addition, the biomarker cascade in bvFTD showed more uncertainty than nfvPPA.

Conclusion: Degeneration of axons and language deficits are indicated to be the earliest biomarkers in FTD-*GRN*, with bvFTD being more heterogeneous in disease progression than nfvPPA. Our data-driven model could help identify presymptomatic *GRN* mutation carriers at risk of conversion to the clinical stage.

Introduction

Mutations in the progranulin (*GRN*) gene on chromosome 17q21 are a major cause of autosomal dominant inherited frontotemporal dementia (FTD).[1,2] The majority of mutation carriers develops a behavioural variant FTD (bvFTD) phenotype,[3] and another significant proportion of patients present with non-fluent variant primary progressive aphasia (nfvPPA)[3,4] The age of symptom onset varies between 35 and 90 in *GRN* mutation carriers.[1,2] without clear associations with familial age of onset.[4]. Brain changes in FTD-*GRN* patients can evolve symmetrically, or predominantly asymmetrically, in either the left or right hemisphere.[5,6]

Recent longitudinal studies have suggested that the time-window between emerging pathophysiological changes and the first clinical symptoms is short in *GRN* mutation carriers, and covers only two to four years.[7,8] During this period, the serum neurofilament light chain (NfL) level – a marker of axonal degeneration – increases two to three-fold.[9,10] loss of grey and white matter emerges.[7,11] and cognitive functioning declines.[8] However, most of the biomarker studies in FTD-*GRN* have investigated one type of biomarker, i.e. fluid, neuroimaging, or cognition, leaving the temporal relations and ordering of these biomarkers unknown. These temporal relations could potentially provide novel insights into disease progression mechanisms in *GRN* mutation carriers. Moreover, because of the fast progression of pathophysiological changes, determining the earliest abnormal biomarker is crucial, as the optimal window of opportunity for treatment might be small.

Recently, novel data-driven methods for disease progression modelling have emerged, focusing on the cascade of biomarker changes.[12,13] Event-based models are a class of disease progression models that estimate the cascade of biomarker changes derived from cross-sectional data.[6,13,14] This is done without strong *a priori* assumptions regarding the relationship between different biomarkers. A promising novel method that estimates the cascade of biomarker change is Discriminative Event-Based Modelling (DEBM).[13,15] This model is robust to disease phenotypic heterogeneity in a cohort and can handle missing data.

In this study, we use DEBM to estimate the temporal cascade of biomarker changes in presymptomatic and symptomatic FTD-*GRN* mutation carriers, distinguishing between early and late biomarkers. Furthermore, we determine phenotypic differences in patterns of biomarker changes in nfvPPA and bvFTD, to gain more insights into their distinct disease progression mechanisms.

Methods

Sample and study procedures

Subjects were recruited prospectively from three European centres of the Genetic Frontotemporal dementia Initiative (GENFI): Rotterdam (the Netherlands), Brescia (Italy), and Barcelona (Spain). We collected cognitive and clinical data, MRI, and serum samples from 126 participants. We included 35 symptomatic *GRN* mutation carriers (Rotterdam: n=11, Brescia: n=22, Barcelona: n=2), 56 presymptomatic *GRN* mutation carriers (Rotterdam: n=33, Brescia: n=17, Barcelona: n=6), and 35 cognitively healthy non-carriers (Rotterdam: n=34, Brescia: n=0, Barcelona: n=1). Local clinical genetics departments performed DNA genotyping to confirm the presence of a *GRN* mutation. Non-carriers were first-degree family members of *GRN* patients without a mutation. Symptomatic mutation carriers were diagnosed based on the established clinical criteria for bvFTD [16] (n=17), nfvPPA [17] (n=16), or cortico-basal syndrome [18] (n=2). Mutation carriers were defined as presymptomatic when clinical criteria were not fulfilled, i.e., behavioural or cognitive symptoms were absent,[19]. Clinical questionnaires were administered to the caregiver, spouse, or a family member, i.e. the Frontotemporal Lobar Degeneration Clinical Dementia Rating scale sum of boxes (FTD-CDR-SB),[20] the Neuropsychiatric Inventory (NPI),[21] and the Frontotemporal Dementia Rating scale (FRS).[22] The study was carried out according to the declaration of Helsinki, approved by the local medical ethics board at each site, and all participants provided written informed consent.

Biomarker collection and processing

Biomarker selection

For biomarker selection, we performed a literature search using Pubmed. We included studies that (i) performed research in presymptomatic *GRN* mutation carriers, and (ii) biomarker studies that examined biomarkers in blood or CSF, neuroimaging biomarkers and cognition. We selected serum NfL,[9] MMSE, cognitive domains of attention and processing speed, executive functioning, language, and social cognition;[8,23] left and right grey matter volumes of the insula, frontal lobe, parietal lobe and temporal lobe;[7,11] left and right white matter tracts of the anterior thalamic radiation, superior longitudinal fasciculus, uncinate fasciculus, and the forceps minor.[7,24] For detailed information about the literature review and subsequent biomarker selection, see supplementary file 1.

Neurofilament light chain

Serum samples were obtained through venepunctures and analysed with single molecular assay technology, as described previously.[10] Samples were measured in a single laboratory, in duplicate, with an intra-assay coefficient of variation below 5%. Inter-assay variation between batches was below 8%. NfL concentrations were expressed in pg/ml.

MRI

3D T1-weighted and diffusion tensor imaging were acquired with 3T MRI scanners across the three sites. MRI was missing in 25 participants due to unavailability (n=16) and insufficient quality due to motion artefacts (n=9). Availability of MRI and an overview of the scanning protocols are listed in supplementary table 1.1. Image processing was carried out in FMRIB Software Library,[25] using default pipelines for grey matter volumes and white matter tracts. For grey matter volumetric regions of interest (ROI), we used the Montreal Neurological Institute (MNI) atlas,[26] and for the fractional anisotropy of white matter tracts, we used the Johns Hopkins' University atlas.[27] Left and right regions and tracts were considered separately. Raw regional volumes and fractional anisotropy values were transformed to z-scores, based on the mean and standard deviation from the non-carriers. A detailed description of processing and ROI calculation is reported in supplementary file 1.

Cognitive assessment

Cognitive data were collected from all participants in four cognitive domains, described in detail in supplementary file 1. Raw cognitive test scores were transformed to z-scores based on the mean and standard deviation in non-carriers, and then combined into cognitive domain scores similar to previous studies.[8]

Confounding factors correction

All selected biomarkers were tested for normality (see supplementary file 1 for details) and log-transformed in case of a skewed distribution. As most non-carriers originated from one centre, we used presymptomatic subjects for regressing out possible confounding effects using multiple linear regression, before continuing with event-based modelling. NfL levels were corrected for age and sex. Grey matter volumes and fractional anisotropy values were corrected for age, sex, total intracranial volume and MRI scanning protocol. Cognitive domain scores were corrected for confounding effects of age, sex and total years of education.

Temporal cascade of biomarker changes

The DEBM model introduced in Venkatraghavan *et al.*,[13,15] estimates the cascade of biomarker changes in a three-step process. For each biomarker, it first estimates the distributions of normal and pathological (or abnormal) values using Gaussian mixture modelling (GMM), and uses these to compute, for each subject, the probability that the biomarker is abnormal (explained in detail in supplementary file 2). The method then estimates the biomarker cascade independently for each subject based on the biomarker values present for that subject. The mean cascade is estimated such that the sum of the probabilistic Kendall's Tau distance is minimised between mean cascade and all the subject-specific cascades. For subjects with missing biomarker values, only the corresponding subset

of biomarker cascade present in the subject-specific cascade is used to compute the probabilistic Kendall's Tau distance. Lastly, the severity of disease as a summary measure for each subject is computed by estimating the subject's progression along the resulting disease progression timeline. In this section, we describe the experiments we performed for estimating the cascade of biomarker changes for non-imaging biomarkers, as well as for neuroimaging and non-imaging biomarkers together.

DEBM model for non-imaging biomarkers

As imaging was missing in a lot of subjects (n=25), we first estimated the cascade of biomarker changes procedure with solely NfL and cognitive biomarkers. Since the non-carriers are healthy in this cohort, the normal Gaussians were fixed at the mean and standard deviation of the biomarker values of the non-carriers. We used GMM only to estimate the abnormal Gaussian and the mixing parameter for each biomarker. In order to estimate the positional variance in the estimated cascade, the entire dataset was randomly sampled using bootstrap sampling with 100 different random seeds, and the cascade of biomarker change was estimated for each of those randomly sampled datasets.[13,15]

DEBM model for neuroimaging and non-imaging biomarkers together

For the imaging biomarkers, we modified the GMM step in DEBM to make it better suited for the FTD-*GRN* population, known for its asymmetric pattern of atrophy.[5] Abnormal values of biomarkers that typically become abnormal late in the disease are usually under-represented in a specific patient population as compared to the early biomarkers. This could make the GMM of late biomarkers unstable, as previously reported.[15] Due to the asymmetrical atrophy patterns of FTD-*GRN,*[5,6] lateralised neuroimaging biomarkers that become abnormal early in the disease process may have a corresponding biomarker from the other hemisphere that remains stable until much later in the disease process. To exploit this, we assumed that the normal and abnormal Gaussians from the left and right hemispheric biomarkers (expressed as z-scores) are the same, and the biomarkers from both hemispheres only differ in their position along the disease progression timeline. With this assumption, we proposed a novel modification to the GMM optimisation called Siamese GMM, in which the biomarkers of the same region from left and right hemispheres are jointly optimised. The abnormal and normal Gaussians are shared between the left and right hemispheres, but the mixing parameters are independently estimated (see supplementary file 2 for details). In this way, the numerical stability of GMM optimisation in the late neuroimaging biomarkers improved.

For non-imaging biomarkers, GMM was performed as described in the previous section. After GMM, further steps of DEBM modelling were carried out as usual, to estimate the

complete cascade of neuroimaging and non-imaging biomarker changes in presymptomatic and symptomatic *GRN* mutation carriers. The positional variance in the estimated cascade was again estimated using bootstrap sampling with 100 different random seeds. For brevity, in the remainder of the paper we refer to this model, which integrates neuroimaging and non-imaging biomarkers, as the multimodal DEBM.

Validation

To validate the DEBM models, we used 10-fold cross-validation. In each fold of the cross-validation, the DEBM model was built in the training set and the disease severity was estimated in the test set. We distinghuished symptomatic mutation carriers from presymptomatic mutation carriers, and reported the corresponding sensitivity and specificity. Furthermore, in bvFTD and nfvPPA subjects, the estimated disease severity was correlated with years since symptom onset and FTD-CDR-SB scores, using Pearson correlation. Symptomatic carriers without imaging biomarkers were excluded for the validation of the multimodal DEBM but were included in the non-imaging DEBM.

Differential phenotype analysis

In order to examine the differences between bvFTD and nfvPPA variants of FTD-*GRN*, we built separate DEBM models. Presymptomatic subjects were excluded from this analysis as no phenotype information is available. The numbers of symptomatic subjects in each group (17 with bvFTD, 16 with nfvPPA) are too small to build complete DEBM models reliably. As a solution, we assumed that the biomarkers for the two phenotypes shared the same normal and abnormal biomarker distributions, and that they only differ in their position along the disease progression timeline. We hence optimised the GMM such that the normal and abnormal Gaussians were estimated without considering the phenotypes, whereas the mixing parameters were estimated separately for each phenotype. As before, we estimated the cascade of biomarker changes in the two phenotypes for non-imaging and multimodal (neuroimaging and non-imaging together) biomarkers.

Results

Sample

A total of 126 subjects were included in this study. Availability and characteristics of the data are presented in table 1. Details on biomarker availability and characteristics can be found in supplementary tables 1.2 and 1.3. Symptomatic mutation carriers were older, had fewer years of education, and had higher scores on the NPI and FTD-CDR-SB, and lower scores on the FRS than both presymptomatic mutation carriers and non-carriers. There were no

differences in demographic or clinical characteristics between presymptomatic mutation carriers and non-carriers.

Cascade of biomarker changes

Non-imaging and multimodal DEBM models

In figures 1A and 1B, we show the estimated mean cascade of biomarker changes and the uncertainty within the model for non-imaging and multimodal biomarkers. Language was the earliest biomarker to become abnormal followed by neurofilament light chain. It can be seen in figure 1B that, left anterior thalamic radiation, left insula, and bilateral uncinate fasciculi were the earliest imaging biomarkers. It can also be observed that imaging biomarkers from the left-hemisphere became abnormal earlier than their right counterpart. GMM estimations with normal and abnormal Gaussian distributions are shown in figure 2, where the estimated Gaussians are seen to fit the observed histograms well. Figure 1C shows the positional variance of the cascade of multimodal biomarker changes obtained when GMM of the imaging biomarkers was done without using Siamese GMM. Generally, the positional variance was smaller with Siamese GMM than without.

Table 1. Data availability and characteristics. Data availability variables represent numbers of cases and percentages of availability. Sample characteristic variables are expressed as mean ± standard deviation. Abbreviations: bvFTD, behavioural variant frontotemporal dementia; nfvPPA, non-fluent variant primary progressive aphasia; NfL, neurofilament light chain; DTI, diffusion tensor imaging; TIV, total intracranial volume; GM, grey matter; NPI, Neuropsychiatric inventory; FRS, Frontotemporal dementia rating scale; FTD-CDR-SB, Frontotemporal dementia Clinical Dementia Rating Scale Sum of Boxes.

	Symptomatic			Presymptomatic	Non-carriers
	Total	bvFTD	nfvPPA		
N					
Subjects (% female)	35[*] (60.0%)	17 (47.1%)	16 (75%)	56 (69.6%)	35 (54.4%)
Rotterdam	11	8	3	33	34
Brescia	22[*]	9	11	17	0
Barcelona	2	0	2	6	1
Data availability					
Serum NfL	91.7%	88.9%	93.8%	69.64%	91.67%
Cognitive assessment	91.7%	88.9%	93.8%	98.21%	91.67%
T1-weighted MRI	44.4%	38.9%	50.0%	96.4%	88.6%
DTI	50.0%	44.4%	56.3%	92.9%	91.4%
Sample characteristics					
Age (years)	62.57 ± 6.72[†]	62.93 ± 6.11[‡]	61.78 ± 7.78[§]	51.52 ± 11.42	55.15 ± 12.55
Education (years)	10.61 ± 4.59[†]	10.27 ± 4.91[‡]	11.79 ± 4.02	13.79 ± 3.27	13.21 ± 2.84
TIV (litres)	1.44 ± 0.17	1.50 ± 0.17	1.42 ± 0.14	1.39 ± 0.15	1.40 ± 0.14
NPI	23.77 ± 28.38[†]	28.90 ± 30.64[‡,¶]	6.67 ± 6.03[¶]	1.87 ± 3.37	2.24 ± 4.32
FRS	56.50 ± 30.43[†]	48.86 ± 29.91[‡]	67.20 ± 30.96[§]	97.27 ± 10.11	95.47 ± 7.45
FTD-CDR-SB	7.64 ± 6.52[†]	9.68 ± 7.47[‡,¶]	5.25 ± 4.37[§,¶]	0.04 ± 0.21	0.00 ± 0.00
Disease duration (years)	2.45 ± 2.01	2.37 ± 1.92	2.48 ± 2.29	N/A	N/A

[*]The two remaining patients presented with cortico-basal syndrome; [†]Significant difference between symptomatic carriers and presymptomatic as well as non-carriers; [‡]Significant difference between bvFTD patients and presymptomatic as well as non-carriers; [§]Significant difference between nfvPPA patients and presymptomatic as well as non-carriers; [¶]Significant difference between bvFTD patients and nfvPPA patients

Figure 1. Cascade of biomarker changes in FTD-*GRN* along with the uncertainty associated with it. (A) Non-imaging biomarkers, (B) Multimodal biomarkers with Siamese GMM, (C) Multimodal biomarkers without Siamese GMM. The biomarkers are ordered based on the position in the estimated cascade. The colour-map is based on the number of times a biomarker is at a position in 100 repetitions of bootstrapping.

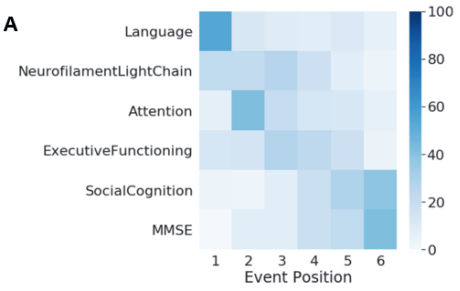

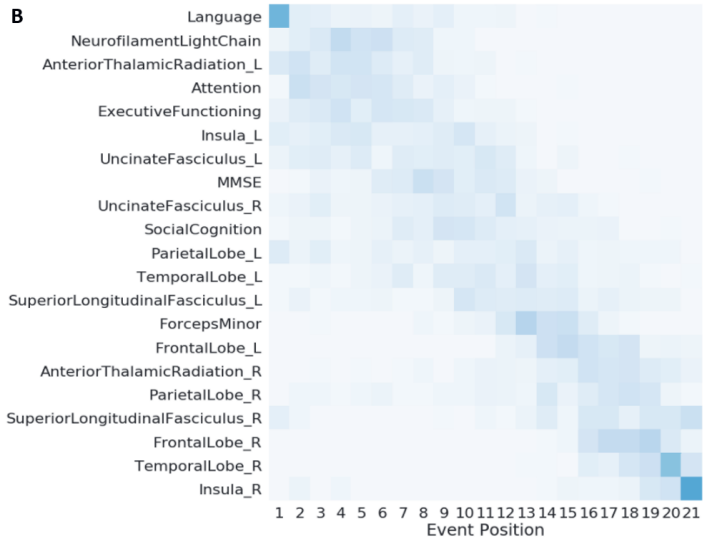

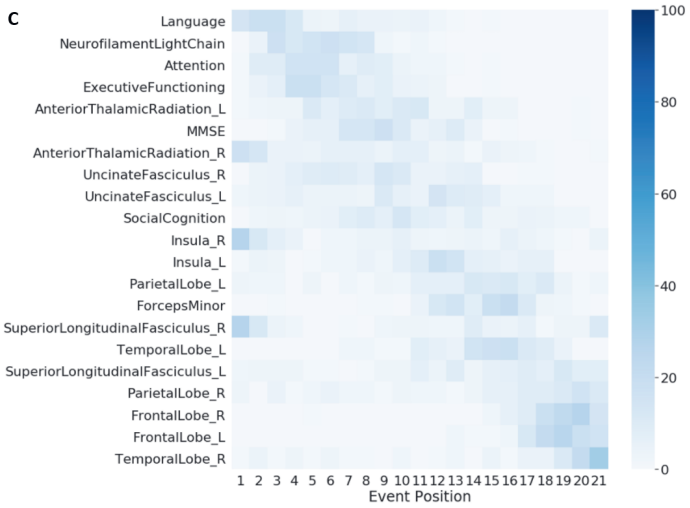
C
Language
NeurofilamentLightChain
Attention
ExecutiveFunctioning
AnteriorThalamicRadiation_L
MMSE
AnteriorThalamicRadiation_R
UncinateFasciculus_R
UncinateFasciculus_L
SocialCognition
Insula_R
Insula_L
ParietalLobe_L
ForcepsMinor
SuperiorLongitudinalFasciculus_R
TemporalLobe_L
SuperiorLongitudinalFasciculus_L
ParietalLobe_R
FrontalLobe_R
FrontalLobe_L
TemporalLobe_R
1 2 3 4 5 6 7 8 9 10 11 12 13 14 15 16 17 18 19 20 21
Event Position
100
80
60
40
20
0

Figure 2. Gaussian mixture modelling distributions. The histogram bins are divided in three colours, where the green part shows the proportion of non-carriers, the yellow part shows the proportion of presymptomatic carriers and the red part shows the proportion of symptomatic carriers. The Gaussians shown here are the ones that were estimated using Gaussian mixture modelling, where the green Gaussian is the normal one estimated using non-carriers and the red Gaussian is the abnormal one estimated using the carriers. The amplitudes of these Gaussians are based on the estimated mixing parameter. The grey curve shows the total estimated distribution, which is the summation of green and red Gaussians.

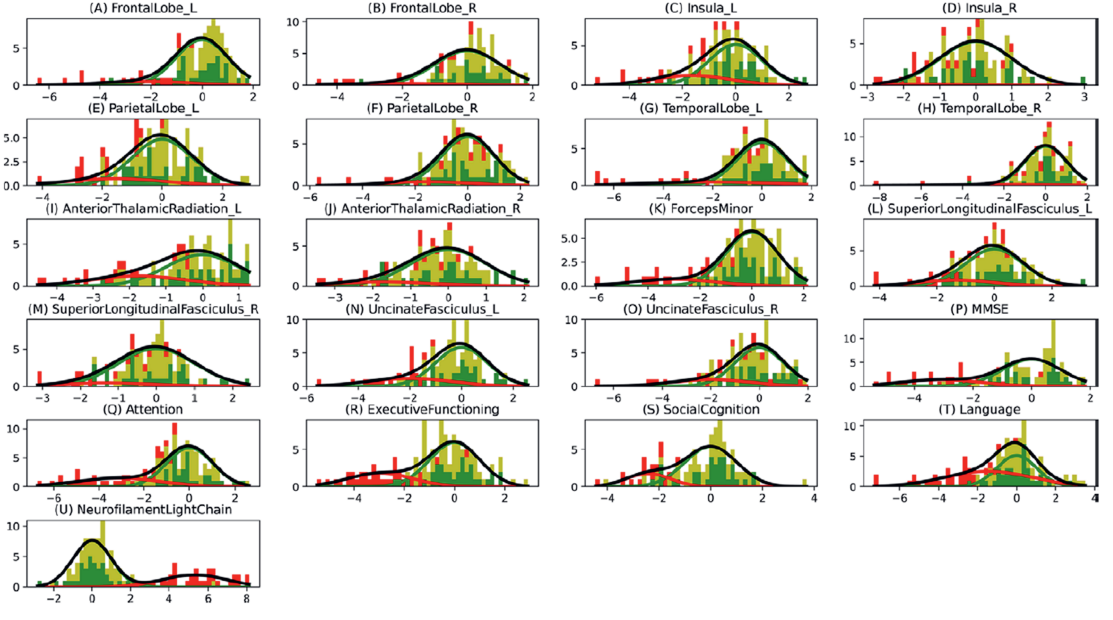

Validation

Figures 3A and 3B show the estimated disease severity when using non-imaging and multimodal biomarkers respectively. It can be seen that estimated disease severity delineated the symptomatic subjects from the pre-symptomatic subjects. The sensitivity and specificity of this delineation were 1.0 and 0.982 respectively while using non-imaging biomarkers, and 1.0 and 0.961 respectively while using multimodal biomarkers.

Figure 3. Relative frequency of occurrence of subjects with different disease severities, estimated using cross-validation. (A) Results using non-imaging biomarkers in DEBM, (B) results using multimodal biomarkers in DEBM.

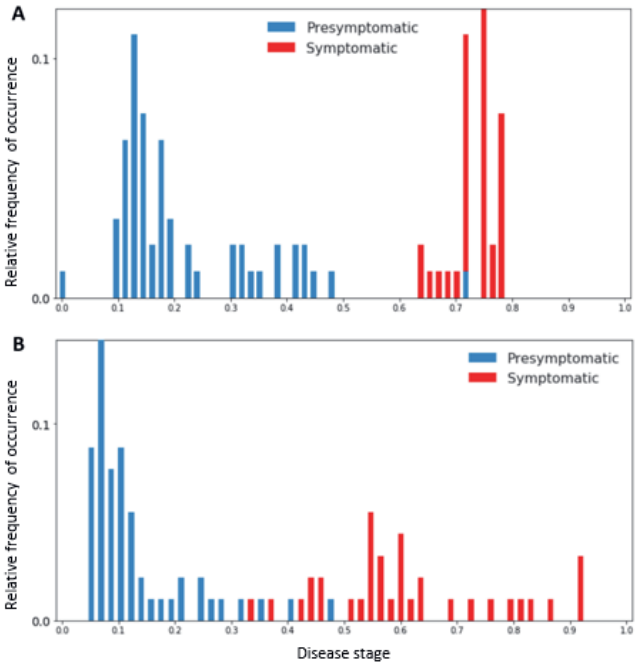

Figure 4 shows the correlation of the estimated disease severity with years since symptom onset and FTD-CDR-SB for nfvPPA and bvFTD subjects, when using multimodal DEBM. It can be seen from figure 4 that estimated disease severity strongly correlated with years since symptom onset (R=0.95, p=0.0003), and the FTD-CDR-SB (R=0.84, p=0.0189), in nfvPPA patients. However, estimated disease severity correlated poorly with years since symptom onset (R=0.22, p=0.6331) and the FTD-CDR-SB (R=0.28, p=0.5866) in bvFTD patients. Supplementary figure 2.2 shows a similar plot when using non-imaging biomarkers, where estimated disease severity did not correlate with years since symptom onset and FTD-CDR-SB, neither for nfvPPA nor for bvFTD subjects.

Figure 4. Correlation of disease severity (as estimated by multimodal DEBM using cross-validation) with years since onset and FTD-CDR-SOB. The 2D scatter plots in figures A and C show the correlations of disease severity with years since onset, for symptomatic nfvPPA and bvFTD subjects respectively. The 2D scatter plot in figures B and D show the correlations of disease severity with FTD-CDR-SOB. The plot on top of each subfigure shows the probability density function of the disease stages. The plots on the right of figures A and C show the probability density functions of years since symptom onset. The plots on the right of figures B and D show the probability density function of FTD-CDR-SOB.

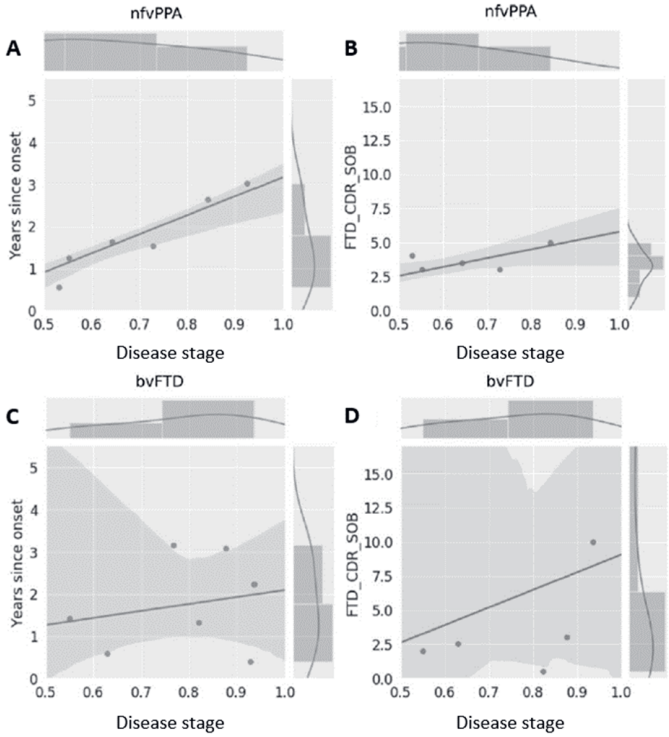

Differential phenotype analysis

Figure 5 shows the multimodal biomarker cascade for nfvPPA and bvFTD phenotypes. nfvPPA patients showed language and NfL as first abnormal biomarkers followed by other cognitive domains. Left-hemispheric imaging biomarkers became abnormal before right-hemispheric imaging biomarkers, starting with the uncinated fasciculus (white matter integrity), insula and temporal lobe (grey matter volume). Only the left superior longitudinal fasciculus was estimated as late biomarker, even later then its right-sided counterpart.

Interestingly, in bvFTD patients, the biomarker ordering also indicated that language and NfL were the earliest abnormal biomarkers. In contrast to the nfvPPA, the left superior longitudinal fasciculus (white matter integrity) was estimated as the first abnormal imaging

biomarker in bvFTD. However, the biomarker orderings in bvFTD were predominantly characterised by large uncertainty in the positioning of biomarkers in the disease timeline, with hardly any observable distinction between early and late biomarkers. Supplementary figure 2.3 presents the non-imaging biomarker cascade for the two phenotypes, showing that the uncertainty in the mean cascade in bvFTD is more than in nfvPPA.

Discussion

In this study, we estimated the cascade of biomarker changes in FTD-*GRN.* We validated our model by delineating the symptomatic mutation carriers from the presymptomatic mutation carriers using the estimated disease severity. We demonstrated that language and NfL levels are the earliest biomarkers to become abnormal in the FTD-*GRN* spectrum. Other early biomarkers were the white matter microstructure of the thalamic radiation and the cognitive domain of attention and mental processing speed.

Our findings support other studies that proposed NfL as an early biomarker for disease onset in FTD-*GRN*.[9,10] We demonstrated that the left anterior thalamic radiation also degenerated early. This is also supported by previous studies which suggested that white matter microstructure markers may correlate with changes in NfL.[9, 28] Cognitive changes in attention, mental processing speed, and executive functioning occurred relatively early in the estimated disease progression timeline. This corresponds well with the early white matter changes (i.e. NfL and fractional anisotropy changes), as attention and processing speed are cognitive functions that highly depend upon the integrity of axons and their myelin sheaths.[29,30] The early involvement of these biomarkers point towards axonal degeneration as one of the first pathological processes in *GRN* mutation carriers. However, it must be noted that the estimated cascade shows the sequence of biomarker events when they are detectably abnormal. One of the important factors that affects the detectability of biomarker abnormality in a cross-sectional data is the overlap between the normal and abnormal biomarker distributions. Therefore, the presented cross-sectional model cannot provide insight into the sequence of earliest changes in the carriers' biomarker levels. Figure 2 showed that the overlap in cognitive biomarkers is relatively smaller than the overlap in neuroimaging biomarkers, which could explain the relative early positioning of the cognitive biomarker events.

Figure 5. Cascade of multimodal biomarker changes in nfvPPA (A) and bvFTD (B) subjects along with the uncertainty associated with it. The biomarkers are ordered based on the position in the estimated cascade. The colour-map is based on the number of times a biomarker is at a position in 100 repetitions of bootstrapping.

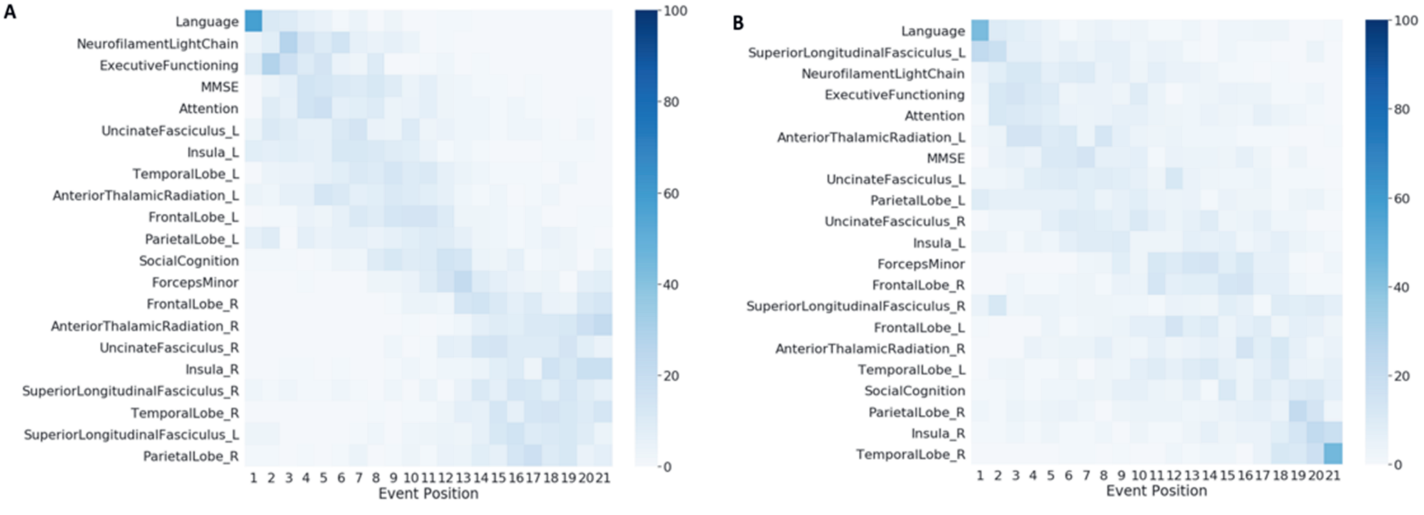

With the differential phenotypic analysis, we estimated the biomarker cascade for nfvPPA and bvFTD patients. Strikingly, language functions deteriorated early in both nfvPPA and bvFTD. While not currently embedded in the clinical criteria for bvFTD,[16] our results demonstrate the importance of decreased language functions in both phenotypes. This is in line with multiple previous studies.[31-33] In addition, multiple determinants of the complex language network were also affected early, for example the left insula, and uncinate fasciculus.[34] While language deficits were estimated as the first detectable abnormal biomarker, the overlap with the second, the elevation in NfL levels, complicates distinguishing the timeline of these disease events. Furthermore, as depicted in Figure 2, (subtle) language deficits were less specific for disease onset than NfL levels. However, the high sensitivity of the language biomarker in our study, and the relative uncomplicated administration of language tests (compared to neuroimaging techniques, for example) offers potential for longitudinal research in the preclinical stage of FTD-*GRN* – ideally in combination with NfL levels.

For nfvPPA, NfL levels and other cognitive domains became abnormal in early disease stages, consistent with findings from previous studies.[9,10,35] In addition, we showed that left hemispheric tracts and regions were affected in nfvPPA patients before right regions, accordant with the previously reported strong involvement of the left hemisphere in primary progressive aphasia.[36,37] We showed that NfL levels and cognitive domains may be possible biomarkers for disease onset, while neuroimaging markers were highly correlated with clinical indicators of progression (years since onset, FTD-CDR-SB).

For bvFTD, however, the biomarker cascade was characterised by large uncertainty, and the estimated disease severities did not correlate with actual years since onset or FTD-CDR-SB. This uncertainty could indicate large neuroanatomical heterogeneities between bvFTD patients. Differences in neuroanatomical atrophy patterns have been associated with FTD-*GRN* patients before.[5,6] Here, we demonstrated that this anatomical heterogeneity is predominantly associated with the bvFTD phenotype, while nfvPPA patients showed a clear pattern of left hemispheric degeneration before the right hemisphere was affected. Furthermore, bvFTD patients present with cognitive symptoms such as impaired social conduct and executive function but can also have severe memory problems. In summary, within the group of bvFTD, spatial and temporal brain degeneration and cognitive changes are more heterogeneous than in the nfvPPA group.

From a methodological point of view the strength of this paper lies in the introduction of the Siamese GMM approach in DEBM. We showed that Siamese GMM reduces the positional variance in neuroimaging biomarkers, most notably in the right insula, the right anterior

thalamic radiation and the right superior longitudinal fasciculus. This is because GMM is known to be unstable in the presence of biomarkers with a large overlap between the normal and abnormal Gaussians.[13] This is often the case in biomarkers becoming abnormal late in the disease and having very few samples representative of the typical abnormal values expected in the disease. The joint GMM in the Siamese counterpart exploits the knowledge that FTD-*GRN* is generally an asymmetric brain disease, and uses the neuroimaging biomarkers that become abnormal early in the disease process to aid the GMM of its hemispheric counterpart that becomes abnormal far later in the disease process. Another strong point about the DEBM model is that it infers disease progression from cross-sectional data, which is more readily available than longitudinal data, especially in a rare disease as FTD-*GRN*.

From the clinical point of view, a major strength of our study is the large, well-defined cohort of presymptomatic and symptomatic *GRN* mutation carriers, and availability of multimodal (i.e. fluid, imaging, and cognitive) biomarkers. Although we did not have FLAIR or T2 imaging data available for the current study, it would be interesting to incorporate white matter lesions in a future version of the model, as a number of studies have indicated the presence of white matter lesions in FTD-*GRN* carriers.[38] Additionally, including functional neuroimaging measures possibly provides new insights into the temporal biomarker sequence and underlying disease mechanism as well. Recent papers have addressed functional changes in FTD-GRN, showing thalamic-cortical hyperconnectivity in early preclinical stages [39] and presymptomatic abnormalities in neurophysiology.[40]

A minor limitation in our study is the difference in mean age between the non-carrier, presymptomatic, and symptomatic mutation carrier groups. We adjusted for this in the analysis rather than matching the groups. It should be noted that the small sample size may have caused a large part of the uncertainty of our model, especially in the case of missing (neuroimaging) biomarkers. Our bvFTD and nfvPPA samples due to *GRN* mutations were relatively large compared to previous studies.[41] However, the DEBM model would improve substantially if the phenotypic samples were larger, as we could only include symptomatic subjects for the phenotypic analysis. Uncertainties in the estimation of the phenotypic biomarker cascades may be improved with upcoming longitudinal data, when some of the converted mutation carriers can be included in the phenotypic models.

In conclusion, with this DEBM study in the FTD-*GRN* spectrum, we were able to demonstrate that language functions and NfL levels are the earliest abnormal biomarkers, regardless of phenotype. However, bvFTD show more heterogeneity and uncertainty in disease progression, pointing towards more variability in biomarkers than nfvPPA. Our analyses suggest axonal degeneration and damage to the language network as the earliest biomarkers

in *GRN* mutation carriers, which could potentially be used as endpoints in clinical trials for disease modifying treatments. Future efforts should be directed at confirmation and validation of these findings with longitudinal data. Validation of these results in an external cohort such as the LEFFTDS [42] could further aid in confirming these results and elucidate any ethnic variations in the disease progression timeline. We expect that DEBM modelling will benefit individual prediction of symptom onset in the future, and may optimise selection of eligible mutation carriers for clinical trials.

Acknowledgements

The authors wish to thank the patients and families for taking part in the FTD-RisC study and the GENFI cohort. Also, we thank Dr. Ir. Mark Bouts for the inspiration to commence this project.

Funding

V. Venkatraghavan, M.W. Vernooij, and S. Klein have received funding from the European Union's Horizon 2020 research and innovation programme under grant agreement No. 666992 (EuroPOND). E.E. Bron was supported by the Hartstichting (PPP Allowance, 2018B011). The Dutch genetic frontotemporal dementia cohort is supported by Dioraphte Foundation grant 09-02-00, the Association for frontotemporal Dementias Research Grant 2009, The Netherlands organization for Scientific Research (NWO) grant HCMI 056-13-018, ZonMw Memorabel project number 733050103 & 733050813, the Bluefield project, and JPND PreFrontAls consortium project number 733051042. L.H.H. Meeter was supported by Alzheimer Nederland project WE.09-2014-4. S.A.R.B. Rombouts was supported by NWO-Vici grant 016-130-677. This study was partially funded by Fundació Marató de TV3, Spain (grant no., 20143810 to R. Sanchez Valle). J.D. Rohrer is supported by an MRC Clinician Scientist Fellowship (MR/M008525/1) and has received funding from the NIHR Rare Disease Translational Research Collaboration (BRC149/NS/MH). This work was also supported by the MRC UK GENFI grant (MR/M023664/1). The authors of this publication are members of GENFI and of the European Reference Network for Rare Neurological Diseases - Project ID No 739510.

Competing interests

R. Sanchez-Valle received personal fees for participating in advisory meetings from Wave pharmaceuticals and Ionis. Other authors have no relevant disclosures to report.

References

1. Seelaar, H., Rohrer, J.D., Pijnenburg, Y.A. et al., Clinical, genetic and pathological heterogeneity of frontotemporal dementia: a review. J Neurol Neurosurg Psychiatry, 2011. 82(5): p. 476-86.
2. van Swieten, J.C. and P. Heutink, Mutations in progranulin (GRN) within the spectrum of clinical and pathological phenotypes of frontotemporal dementia. Lancet Neurol, 2008. 7(10): p. 965-74.
3. Mann, D.M.A. and J.S. Snowden, Frontotemporal lobar degeneration: Pathogenesis, pathology and pathways to phenotype. Brain Pathol, 2017. 27(6): p. 723-736.
4. Woollacott, I.O. and J.D. Rohrer, The clinical spectrum of sporadic and familial forms of frontotemporal dementia. J Neurochem, 2016. 138 Suppl 1: p. 6-31.
5. Chitramuthu, B.P., H.P.J. Bennett, and A. Bateman, Progranulin: a new avenue towards the understanding and treatment of neurodegenerative disease. Brain, 2017. 140(12): p. 3081-3104.
6. Young, A.L., Marinescu, R.V., Oxtoby, N.P., et al., Uncovering the heterogeneity and temporal complexity of neurodegenerative diseases with Subtype and Stage Inference. Nat Commun, 2018. 9(1): p. 4273.
7. Jiskoot, L.C., Panman, J.L., Meeter, L.H., et al., Longitudinal multimodal MRI as prognostic and diagnostic biomarker in presymptomatic familial frontotemporal dementia. Brain, 2019. 142(1): p. 193-208.
8. Jiskoot, L.C., Panman, J.L., van Asseldonk, L., et al., Longitudinal cognitive biomarkers predicting symptom onset in presymptomatic frontotemporal dementia. J Neurol, 2018.
9. Meeter, L.H., Dopper, E.G.P., Jiskoot, L.C., et al., Neurofilament light chain: a biomarker for genetic frontotemporal dementia. Ann Clin Transl Neurol, 2016. 3(8): p. 623-36.
10. van der Ende, E.L., Meeter, L.H., Poos, J.M., et al., Serum neurofilament light chain in genetic frontotemporal dementia: a longitudinal, multicentre cohort study. Lancet Neurol, 2019. 18(12): p. 1103-1111.
11. Rohrer, J.D., Nicholas, J.M., Cash, D.M., et al., Presymptomatic cognitive and neuroanatomical changes in genetic frontotemporal dementia in the Genetic Frontotemporal dementia Initiative (GENFI) study: a cross-sectional analysis. Lancet Neurol, 2015. 14(3): p. 253-62.
12. Donohue, M.C., Jacqmin-Gadda, H., Le Goff, M., et al., Estimating long-term multivariate progression from short-term data. Alzheimers Dement, 2014. 10(5 Suppl): p. S400-10.
13. Venkatraghavan, V., Bron, E.E., Niessen, W.J., et al., A discriminative event based model for Alzheimer's disease progression modelling. Information Processing in Medical Imaging, 2017: p. 121-133.
14. Fonteijn, H.M., Modat, M., Clarkson, M.J., et al., An event-based model for disease progression and its application in familial Alzheimer's disease and Huntington's disease. Neuroimage, 2012. 60(3): p. 1880-9.

15. Venkatraghavan, V., Bron, E.E., Niessen, W.J., et al., Disease progression timeline estimation for Alzheimer's disease using discriminative event based modeling. Neuroimage, 2019. 186: p. 518-532.
16. Rascovsky, K., Hodges, J.R., Knopman, D., et al., Sensitivity of revised diagnostic criteria for the behavioural variant of frontotemporal dementia. Brain, 2011. 134(Pt 9): p. 2456-77.
17. Gorno-Tempini, M.L., Hillis, A.E., Weintraub, S., et al., Classification of primary progressive aphasia and its variants. Neurology, 2011. 76(11): p. 1006-14.
18. Parmera, J.B., Rodriguez, R.D., Studart Neto, A., et al., Corticobasal syndrome: A diagnostic conundrum. Dement Neuropsychol, 2016. 10(4): p. 267-275.
19. Panman, J.L., Jiskoot, L.C., Bouts, M., et al., Gray and white matter changes in presymptomatic genetic frontotemporal dementia: a longitudinal MRI study. Neurobiol Aging, 2019. 76: p. 115-124.
20. Knopman, D.S., Kramer, J.H., Boeve, B.F., et al., Development of methodology for conducting clinical trials in frontotemporal lobar degeneration. Brain, 2008. 131(Pt 11): p. 2957-68.
21. Cummings, J.L., The Neuropsychiatric Inventory: comprehensive assessment of psychopathology in dementia. Neurology, 1994. 44(12): p. 2308-14.
22. Mioshi, E., Hsieh, S., Savage, S., et al., Clinical staging and disease progression in frontotemporal dementia. Neurology, 2010. 74(20): p. 1591-7.
23. Barandiaran, M., Moreno, F., de Arriba, M., et al., Longitudinal Neuropsychological Study of Presymptomatic c.709-1G>A Progranulin Mutation Carriers. J Int Neuropsychol Soc, 2019. 25(1): p. 39-47.
24. Jiskoot, L.C., Boccheta, M., Nicholas, J.M., et al., Presymptomatic white matter integrity loss in familial frontotemporal dementia in the GENFI cohort: A cross-sectional diffusion tensor imaging study. Ann Clin Transl Neurol, 2018. 5(9): p. 1025-1036.
25. Jenkinson, M., Beckmann, C.F., Behrens, T.E., et al., Fsl. Neuroimage, 2012. 62(2): p. 782-90.
26. Collins, D.L., Holmes, C.J., Peters, T.M., et al., Automated 3-D model-based neuroanatomical segmentation. Human Brain Mapping, 1995. 3(3): p. 190-208.
27. Mori, S., Wakana, S., van Zijl, P.C.M., et al., MRI atlas of Human White Matter. 2005, Amsterdam, the Netherlands: Elsevier.
28. Menke, R.A., Gray, E., Lu, C.H., et al., CSF neurofilament light chain reflects corticospinal tract degeneration in ALS. Ann Clin Transl Neurol, 2015. 2(7): p. 748-55.
29. Tomimoto, H., White matter integrity and cognitive dysfunction: Radiological and neuropsychological correlations. Geriatr Gerontol Int, 2015. 15 Suppl 1: p. 3-9.
30. Hase, Y., Horsburgh, K., Ihara, M., et al., White matter degeneration in vascular and other ageing-related dementias. J Neurochem, 2018. 144(5): p. 617-633.
31. Hardy, C.J., Buckley A.H., Downey, L.E., et al., The Language Profile of Behavioral Variant Frontotemporal Dementia. J Alzheimers Dis, 2016. 50(2): p. 359-71.
32. Ash, S., Nevler, N., Phillips, J., et al., A longitudinal study of speech production in primary progressive aphasia and behavioral variant frontotemporal dementia. Brain Lang, 2019. 194: p. 46-57.

33. Nevler, N., Ash, S., Jester, C., et al., Automatic measurement of prosody in behavioral variant FTD. Neurology, 2017. 89(7): p. 650-656.
34. Mesulam, M.M., Primary Progressive Aphasia and the Left Hemisphere Language Network. Dement Neurocogn Disord, 2016. 15(4): p. 93-102.
35. Staffaroni, A.M., Ljubenkov, P.A., Kornak, J., et al., Longitudinal multimodal imaging and clinical endpoints for frontotemporal dementia clinical trials. Brain, 2019. 142(2): p. 443-459.
36. Grossman, M., The non-fluent/agrammatic variant of primary progressive aphasia. Lancet Neurol, 2012. 11(6): p. 545-55.
37. Rohrer, J.D. and H.J. Rosen, Neuroimaging in frontotemporal dementia. Int Rev Psychiatry, 2013. 25(2): p. 221-9.
38. Sudre, C.H., Boccheta, M., Cash, D., et al., White matter hyperintensities are seen only in GRN mutation carriers in the GENFI cohort. Neuroimage Clin, 2017. 15: p. 171-180.
39. Lee, S.E., Sias, A.C., Kosik, E.L., et al., Thalamo-cortical network hyperconnectivity in preclinical progranulin mutation carriers. Neuroimage Clin, 2019. 22: 101751.
40. Benussi, A., Gazzina, S., Premi, E., et al., Clinical and biomarker changes in presymptomatic genetic frontotemporal dementia. Neurobiol Aging, 2019. 76: p. 133-140
41. Bonvicini, C., Milanesi, E., Pilotto, A., et al., Understanding phenotype variability in frontotemporal lobar degeneration due to granulin mutation. Neurobiol Aging, 2014. 35(5): p. 1206-11.
42. Rosen, H.J., Boeve, B.F, Boxer, A.L., et al., Tracking disease progression in familial and sporadic frontotemporal lobar degeneration: Recent findings from ARTFL and LEFFTDS. Alzheimers Dement. 16(1): p. 71-78.

Supplementary file 1: Biomarkers

Biomarker selection

For biomarker selection, we extensively searched for relevant literature about presymptomatic FTD-*GRN* in Pubmed. We reviewed all empirical studies that included at least a presymptomatic *GRN* mutation carrier group. Next, we determined which biomarkers were frequently reported as abnormal in previous empirical studies and included these biomarkers accordingly, restricted to fluid biomarkers, grey matter brain regions, white matter tracts, and cognition. The selected biomarkers were: serum NfL, [1-3] MMSE,[4-6] cognitive domains of language, attention and processing speed, executive functioning, and social cognition;[5,7-9] left and right volumes of the insula, frontal lobe, parietal lobe and the temporal lobe;[4,6,10-21] white matter tracts: left and right fractional anisotropy of anterior thalamic radiation, superior longitudinal fasciculus, uncinate fasciculus, and forceps minor.[10,17-19,22,23] Although the *GRN* mutation affects plasma progranulin protein levels, these levels were not selected as biomarker, as research has shown that these remain stable in both the presymptomatic and symptomatic stage.[6,24]

MRI processing and ROI calculation

An overview of MRI acquisition parameters is presented in supplementary table 1.1. The standard voxel-based morphometry pipeline from FSL [25-27] was used to process T1-weighted images. In brief, the brain was extracted from the images, and we carefully checked the brain extraction for missing brain tissue and areas of non-brain tissue, and adjusted the image accordingly. We corrected RF inhomogeneities by bias field correction with a Markov random field model and subsequently segmented the brain in grey matter, white matter, and cerebrospinal fluid images.[28] A study specific grey matter template was created in standard space using a balanced set of subjects, and all grey matter segmentations were registered to this template with non-linear registration, and then corrected for any local expansion or contraction by modulation of the Jacobian warp field.[26] Last, an isotropic Gaussian kernel with a sigma of 3mm was applied for smoothing of the grey matter images. Total intracranial volume (TIV) was calculated as the sum of the volumes from grey matter, white matter and cerebrospinal fluid in standard space. The structures from the MNI-atlas were used as grey matter ROIs. We extracted volumetric measurements from the ROIs by registering the structural MNI-atlas [29] to the grey matter images in standard space, and multiplying the grey matter density of the ROI with the total volume of the ROI, resulting in the grey matter volume within the ROI. Left and right regions were considered separately.

Diffusion tensor images were corrected for motion artefacts and eddy currents by alignment to the b=0 image, and subsequently, the tensor was fitted at each voxel to create fractional

anisotropy (FA) images. The FA images were processed with the tract-based spatial statistics (TBSS) pipeline as implemented in FSL.[30] Using non-linear registration, the images were aligned to the FMRIB58_FA template and then averaged into a mean FA image. The mean FA image was thresholded at 0.2 and thinned into a white matter skeleton. All individual FA images were projected onto this skeleton, resulting in skeletonised FA data for each participant. The probabilistic tracts from the Johns Hopkins University atlas [31] were applied as white matter ROIs to the skeleton mask, and the masked ROIs were used to extract FA values from the individual tracts. Left and right tracts were considered separately.

Cognitive assessment

The following cognitive tests were performed, depending on the protocol from the local site. For language, the Boston Naming Task [32] and semantic fluency (animals) [33] were used. Tests concerning attention and processing speed were the Trail making test part A,[34] Stroop part 1 and 2,[35] symbol substitution,[36] letter digit substitution task,[37] and forward digit span.[36] For executive functioning, we used Trail making test part B,[34] Stroop task part 3,[35] phonological fluency [33] and digit span backwards.[36] Tests for social cognition were the Ekman faces test,[38] emotion recognition from the mini social cognition and emotional assessment (MINI-SEA),[39] and Happé cartoon task.[40] Raw scores from tests in which a higher score indicates worse performance were reversed (i.e. Trail making test, Stroop). We transformed all raw test scores to z-scores, based on the mean and standard deviation of the non-carriers. Subsequently, cognitive domains were composed as the mean z-score of all available tests within that domain per individual, disregarding missing tests.

Supplementary table 1.1. MRI acquisition protocols. Abbrevations: s, symptomatic; p, presymptomatic; nc, non-carrier; TR, repetition time; TE, echo time; FOV, field of view.

	Rotterdam 1	Rotterdam 2	Brescia	Barcelona
N* (s/p/nc)	3/22/24	5/9/6	7/17/0	1/6/1
Scanner	Philips Achieva 3T	Philips Achieva 3T	Siemens Skyra	Siemens Trio Tim
Head Coil	8 channel SENSE	32 channel SENSE	32 channel	64 channel
T1 weighted imaging				
TR	9.8 ms	6.8 ms	2000 ms	2000 ms
TE	4.6 ms	3.1 ms	2.9 ms	2.9 ms
FOV	224x168 mm	256x256 mm	282x282 mm	282x282 mm
Voxel size	0.88x0.88x1.2 mm	1.1mm^3	1.1 mm^3	1.1mm^3
Flip angle	8°	8°	8°	8°
Slices	140	207	208	208
Diffusion tensor imaging				
TR	8250 ms	7000 ms	7300 ms	7300 ms
TE	80 ms	69 ms	90 ms	90 ms
FOV	256x256 mm	240x240 mm	240x240 mm	240x240 mm
Voxel size	2x2x2mm	2.5x2.5x2.5mm	2.5x2.5x2.5mm	2.5x2.5x2.5mm
Slices	70	59	59	59
Directions	60	68	68	68
B-values	0/1000 s/mm^2	0/1000 s/mm^2	0/1000 s/mm^2	0/1000 s/mm^2

*Number of subjects included after quality check.

Supplementary table 1.2. Availability and characteristics of cognitive data. Values are mean z-scores ± standard deviation based on non-carriers, uncorrected for confounding factors. Abbreviations: bvFTD, behavioural variant frontotemporal dementia; nfvPPA, non-fluent variant primary progressive aphasia; MMSE, Mini Mental State Examination; TMT, trail-making test; LDST, letter digit substitution task; mini-SEA, mini social cognition and emotional assessment; TOM, theory of mind.

	Symptomatic						Presymptomatic	
	Total (n=35)		bvFTD (n=17)		nfvPPA (n=16)		n=56	
	N	Mean±SD	N	Mean±SD	N	Mean±SD	N	Mean±SD
MMSE	29	-3.07 ± 1.50	15	-3.26 ± 1.69	14	-2.87 ± 1.28	55	0.22 ± 1.01
Language	32	-2.86 ± 1.37	16	-2.69 ± 1.58	14	-3.00 ± 1.24	55	0.28 ± 1.09
Boston naming test	25	-1.97 ± 1.32	13	-1.75 ± 1.44	12	-2.21 ± 1.19	55	0.57 ± 1.37
Semantic fluency	31	-3.28 ± 1.38	15	-3.14 ± 1.57	14	-3.45 ± 1.30	55	0.00 ± 1.31
Attention, concentration and mental processing speed	33	-2.35 ± 1.17	16	-2.43 ± 1.32	15	-2.26 ± 1.12	55	-0.05 ± 0.75
TMT-A	32	-2.65 ± 1.62	16	-2.91 ± 1.63	14	-2.23 ± 1.66	55	-0.01 ± 0.92
Stroop card 1&2	17	-3.05 ± 2.18	10	-2.96 ± 2.20	7	-3.18 ± 2.32	55	0.14 ± 1.02
LDST	4	-2.06 ± 1.59	2	-2.09 ± 1.99	2	-2.03 ± 1.90	17	0.22 ± 0.70
Symbol substitution	17	-2.35 ± 1.41	7	-3.01 ± 1.13	10	-1.89 ± 1.45	22	0.00 ± 1.29
Digit span forward	31	-1.66 ± 1.05	15	-1.41 ± 1.29	14	-1.95 ± 0.74	55	-0.26 ± 0.95
Executive functioning	32	-2.33 ± 0.97	15	-2.23 ± 1.19	15	-2.37 ± 0.79	55	-0.03 ± 0.75
TMT-B	28	-2.63 ± 0.97	13	-2.50 ± 1.11	13	-2.69 ± 0.89	55	0.03 ± 0.79
Stroop card 3	14	-3.84 ± 2.29	8	-3.73 ± 2.50	6	-3.98 ± 2.20	55	-0.36 ± 1.05
Phonological fluency	29	-2.12 ± 0.95	14	-1.92 ± 1.02	15	-2.30 ± 0.87	55	0.30 ± 1.36
Digit span backwards	30	-1.65 ± 1.14	15	-1.61 ± 1.44	13	-1.61 ± 0.75	55	-0.08 ± 1.11
Social cognition	15	-1.87 ± 0.76	7	-2.15 ± 0.92	8	-1.62 ± 0.52	51	-0.10 ± 1.02
Ekman faces	3	-0.70 ± 0.60	2	-0.37 ± 0.18	1	-1.36 ± N/A	26	0.14 ± 0.89
	N	Mean±SD	N	Mean±SD	N	Mean±SD	N	Mean±SD
Mini-SEA Emotion Recognition	10	-1.98 ± 0.83	3	-2.65 ± 1.13	7	-1.69 ± 0.52	22	-0.62 ± 0.98
HappeTOM	5	-2.07 ± 0.86	4	-2.32 ± 0.75	1	-1.05 ± N/A	28	0.42 ± 0.77
Happe non TOM	5	-1.65 ± 0.81	4	-1.81 ± 0.84	1	-1.03 ± N/A	28	0.34 ± 1.20

Biomarker statistics

Before modelling, we checked skewed distributions in the biomarkers with the following graphs and tests: histograms, q-q plots, skewness and kurtosis values (values between 2 and –2 indicate normality), Kolmogorov-Smirnov and Shapiro-Wilk's tests (values above 0.05 indicate normality). When three or more tests indicated skewness, the distributions were adjusted using log-transformations (log10), i.e. neurofilament light chain levels, MMSE, BNT, Trail Making Test, Stroop, facial emotion recognition. In the case of cognitive tests, log-transformation was performed before transforming raw scores to z-scores.

Biomarker characteristics and statistical differences between groups are presented in Table A.3. Symptomatic mutation carriers had higher NfL levels, lower grey matter volumes, impaired white matter microstructure, and worse cognitive functions than both presymptomatic mutation carriers and non-carriers in all selected biomarkers. Post-hoc analysis revealed that these differences in biomarkers were specifically driven by the bvFTD patients. For nfvPPA patients, we found higher NfL levels and worse cognitive performance than both presymptomatic mutation carriers and non-carriers. NfvPPA patients showed smaller grey matter volumes than both presymptomatic mutation carriers and non-carriers, especially in left-sided ROIs, and lower fractional anisotropy levels in the left anterior thalamic radiation, left uncinate fasciculus, and the forceps minor. The volume of the right frontal lobe was smaller in nfvPPA patients compared with presymptomatic mutation carriers. Furthermore, bvFTD patients had smaller volumes of the right frontal and temporal lobe than nfvPPA patients, and lower fractional anisotropy values in the forceps minor, left superior longitudinal fasciculus and right uncinate fasciculus. There were no differences in any of the selected biomarkers between presymptomatic mutation carriers and non-carriers.

Supplementary table 1.3. Biomarker characteristics after correction for confounding factors. Values are mean z-score (based on non-carriers) ± standard deviation, after correction for confounding factors of age, sex, MRI protocol, and years of education. Abbreviations: bvFTD, behavioural variant frontotemporal dementia; nfvPPA, non-fluent variant primary progressive aphasia; GM volume, grey matter volume; FA, fractional anisotropy; MMSE, Mini Mental State Examination.

		Symptomatic			Presymptomatic
		Total	bvFTD	nfvPPA	
Neurofilament light chain		1.90 ± 0.25[*]	1.89 ± 0.23[*]	1.91 ± 0.28[†]	1.10 ± 0.22
GM volume	Left frontal	-2.75 ± 1.8*	-3.42 ± 2.06[*]	-2.46 ± 1.40[†]	0.30 ± 0.65
	Right frontal	-1.72 ± 1.79[*]	-2.76 ± 1.43[*,‡]	-0.93 ± 1.79[§]	0.30 ± 0.65
	Left insula	-2.32 ± 1.56[*]	-2.45 ± 1.79[*]	-2.35 ± 1.51[†]	-0.32 ± 0.95
	Right insula	-1.02 ± 1.13[*]	-1.47 ± 1.26[*]	-0.74 ± 0.98	-0.08 ± 0.84
	Left parietal	-1.87 ± 1.11[*]	-2.18 ± 1.39[*]	-1.74 ± 0.84[†]	-0.03 ± 1.02
	Right parietal	-1.19 ± 2.00[*]	-1.42 ± 2.08[*]	-0.89 ± 2.15	-0.06 ± 0.96
	Left temporal	-2.97 ± 2.42[*]	-3.21 ± 2.59[*]	-2.98 ± 2.51[†]	-0.19 ± 0.96
	Right temporal	-1.14 ± 2.66[*]	-2.22 ± 3.40[*,‡]	-0.12 ± 1.69	-0.08 ± 0.94
FA	Left anterior thalamic radiation	-2.28 ± 1.34[*]	-2.73 ± 1.60[*]	-1.77 ± 0.98[†]	-0.33 ± 0.95
	Right anterior thalamic radiation	-1.24 ± 1.23[*]	-1.78 ± 1.51[*]	-0.66 ± 0.66	-0.27 ± 0.77
	Forceps minor	-3.00 ± 1.52[*]	-4.01 ± 1.52[*,‡]	-2.08 ± 0.96[†]	0.46 ± 0.93
	Left superior Longitudinal fasciculus	-1.50 ± 1.39[*]	-2.42 ± 1.28[*,‡]	-0.61 ± 0.96	0.02 ± 0.88
	Right superior Longitudinal fasciculus	-1.14 ± 1.12[*]	-1.47 ± 1.14[*]	-0.74 ± 1.06	-0.11 ± 0.60
	Left uncinate fasciculus	-2.63 ± 1.15[*]	-3.00 ± 1.43[*]	-2.29 ± 0.88[†]	-0.35 ± 0.86
	Right uncinate fasciculus	-1.92 ± 2.16[*]	-3.19 ± 2.07[*,‡]	-0.77 ± 1.74	-0.51 ± 1.12
MMSE		-2.71 ± 1.19[*]	-2.71 ± 1.28[*]	-2.71 ± 1.14[†]	0.06 ± 0.91
Attention / processing speed		-2.06 ± 1.09[*]	-2.11 ± 1.15[*]	-2.05 ± 1.12[†]	-0.22 ± 0.65
Executive functioning		-2.12 ± 0.88[*]	-2.00 ± 0.99[*]	-2.24 ± 0.82[†]	-0.14 ± 0.72
Language		-2.54 ± 1.23[*]	-2.35 ± 1.33[*]	-2.84 ± 1.17[†]	0.13 ± 0.97
Social cognition		-1.89 ± 0.64[*]	-2.13 ± 0.74[*]	-1.52 ± 0.42[†]	-0.19 ± 0.96

[*] Both the entire group of symptomatic carriers and only bvFTD patients significantly differed from presymptomatic carriers as well as non-carriers; [†] Significant difference between nfvPPA patients and presymptomatic mutation carriers as well as non-carriers ($p<0.05$, Bonferroni corrected); [‡] Significant difference between bvFTD patients and nfvPPA patients ($p<0.05$, Bonferroni corrected); [¶] Significant difference between nfvPPA patients and presymptomatic mutation carriers ($p<0.05$, Bonferroni corrected)

Supplementary references

1. Meeter, L.H., et al., Neurofilament light chain: a biomarker for genetic frontotemporal dementia. Ann Clin Transl Neurol, 2016. 3(8): p. 623-36.
2. Rohrer, J.D., et al., Serum neurofilament light chain protein is a measure of disease intensity in frontotemporal dementia. Neurology, 2016. 87(13): p. 1329-36.
3. van der Ende, E.L., et al., Serum neurofilament light chain in genetic frontotemporal dementia: a longitudinal, multicentre cohort study. Lancet Neurol, 2019. 18(12): p. 1103-1111.
4. Rohrer, J.D., et al., Presymptomatic cognitive and neuroanatomical changes in genetic frontotemporal dementia in the Genetic Frontotemporal dementia Initiative (GENFI) study: a cross-sectional analysis. Lancet Neurol, 2015. 14(3): p. 253-62.
5. Jiskoot, L.C., et al., Longitudinal cognitive biomarkers predicting symptom onset in presymptomatic frontotemporal dementia. J Neurol, 2018.
6. Benussi, A., et al., Clinical and biomarker changes in presymptomatic genetic frontotemporal dementia. Neurobiol Aging, 2019. 76: p. 133-140.
7. Barandiaran, M., et al., Neuropsychological features of asymptomatic c.709-1G>A progranulin mutation carriers. J Int Neuropsychol Soc, 2012. 18(6): p. 1086-90.
8. Barandiaran, M., et al., Longitudinal Neuropsychological Study of Presymptomatic c.709-1G>A Progranulin Mutation Carriers. J Int Neuropsychol Soc, 2019. 25(1): p. 39-47.
9. Jiskoot, L.C., et al., Presymptomatic cognitive decline in familial frontotemporal dementia: A longitudinal study. Neurology, 2016. 87(4): p. 384-91.
10. Borroni, B., et al., Brain magnetic resonance imaging structural changes in a pedigree of asymptomatic progranulin mutation carriers. Rejuvenation Res, 2008. 11(3): p. 585-95.
11. Cash, D.M., et al., Patterns of gray matter atrophy in genetic frontotemporal dementia: results from the GENFI study. Neurobiol Aging, 2017. 62: p. 191-196.
12. Premi, E., et al., Subcortical and Deep Cortical Atrophy in Frontotemporal Dementia due to Granulin Mutations. Dement Geriatr Cogn Dis Extra, 2014. 4(1): p. 95-102.
13. Young, A.L., et al., Uncovering the heterogeneity and temporal complexity of neurodegenerative diseases with Subtype and Stage Inference. Nat Commun, 2018. 9(1): p. 4273.
14. Jacova, C., et al., Anterior brain glucose hypometabolism predates dementia in progranulin mutation carriers. Neurology, 2013. 81(15): p. 1322-31.
15. Popuri, K., et al., Gray matter changes in asymptomatic C9orf72 and GRN mutation carriers. Neuroimage Clin, 2018. 18: p. 591-598.
16. Moreno, F., et al., Distinctive age-related temporal cortical thinning in asymptomatic granulin gene mutation carriers. Neurobiol Aging, 2013. 34(5): p. 1462-8.
17. Dopper, E.G., et al., Structural and functional brain connectivity in presymptomatic familial frontotemporal dementia. Neurology, 2014. 83(2): p. e19-26.

18. Jiskoot, L.C., et al., Longitudinal multimodal MRI as prognostic and diagnostic biomarker in presymptomatic familial frontotemporal dementia. Brain, 2019. 142(1): p. 193-208.
19. Panman, J.L., et al., Gray and white matter changes in presymptomatic genetic frontotemporal dementia: a longitudinal MRI study. Neurobiol Aging, 2019. 76: p. 115-124.
20. Pievani, M., et al., Pattern of structural and functional brain abnormalities in asymptomatic granulin mutation carriers. Alzheimers Dement, 2014. 10(5 Suppl): p. S354-S363 e1.
21. Caroppo, P., et al., Lateral Temporal Lobe: An Early Imaging Marker of the Presymptomatic GRN Disease? J Alzheimers Dis, 2015. 47(3): p. 751-9.
22. Jiskoot, L.C., et al., Presymptomatic white matter integrity loss in familial frontotemporal dementia in the GENFI cohort: A cross-sectional diffusion tensor imaging study. Ann Clin Transl Neurol, 2018. 5(9): p. 1025-1036.
23. Olm, C.A., et al., Longitudinal structural gray matter and white matter MRI changes in presymptomatic progranulin mutation carriers. Neuroimage Clin, 2018. 19: p. 497-506.
24. Meeter, L.H., et al., Progranulin Levels in Plasma and Cerebrospinal Fluid in Granulin Mutation Carriers. Dement Geriatr Cogn Dis Extra, 2016. 6(2): p. 330-340.
25. Douaud, G., et al., Anatomically related grey and white matter abnormalities in adolescent-onset schizophrenia. Brain, 2007. 130(Pt 9): p. 2375-86.
26. Jenkinson, M., et al., Fsl. Neuroimage, 2012. 62(2): p. 782-90.
27. Smith, S.M., et al., Advances in functional and structural MR image analysis and implementation as FSL. Neuroimage, 2004. 23 Suppl 1: p. S208-19.
28. Zhang, Y., M. Brady, and S. Smith, Segmentation of brain MR images through a hidden Markov random field model and the expectation-maximization algorithm. IEEE Trans Med Imaging, 2001. 20(1): p. 45-57.
29. Collins, D.L., Holmes, C.J., Peters, T.M., Evans, A.C., Automated 3-D model-based neuroanatomical segmentation. Human Brain Mapping, 1995. 3(3): p. 190-208.
30. Smith, S.M., et al., Tract-based spatial statistics: voxelwise analysis of multi-subject diffusion data. Neuroimage, 2006. 31(4): p. 1487-505.
31. Mori, S., Wakana, S, van Zijl, P.C.M, Nagae-Poetscher, L.M., MRI atlas of Human White Matter. 2005, Amsterdam, the Netherlands: Elsevier.
32. Kaplan, E., Goodglass, H., Weintraub, S., Boston Naming Test. 1983, Philadelphia: Lea & Febiger.
33. Thurstone, L.L., Thurstone, T.G., Primary Mental Abilities. 1962, Chicago: University of Chicago Press.
34. battery, A.i.t., Manual of directions and scoring. 1944, Washington, DC: War Department, Adjunct General's Office.
35. Stroop, J., Studies of interference in serial verbal reaction. Journal of Experimental Psychology, 1935. 18: p. 643-662.
36. Wechsler, D., WAIS-III Technische Handleiding. 2005, Amsterdam: Harcourt Test Publishers.
37. Jolles, J., Houx, P.K., van Boxtel, M.P.J., Ponds R.W.H.M., Maastricht aging study: Determinants of cognitive aging. 1995, Maastricht: Neuropsych Publishers.
38. Ekman, P., Friesen, W.V., Pictures of facial affect 1976, Palo Alto, CA: Consulting Psychological Press.

39. Funkiewiez, A., et al., The SEA (Social cognition and Emotional Assessment): a clinical neuropsychological tool for early diagnosis of frontal variant of frontotemporal lobar degeneration. Neuropsychology, 2012. 26(1): p. 81-90.
40. Happe, F., H. Brownell, and E. Winner, Acquired 'theory of mind' impairments following stroke. Cognition, 1999. 70(3): p. 211-40.

Supplementary file 2: Discriminative event-based modelling

Gaussian mixture modelling

Discriminative event-based modelling (DEBM) uses Gaussian mixture modelling to transform biomarker values to posterior probabilities of them being abnormal. This is done by assuming the probability density functions of normal and abnormal values are represented by Gaussians $N(\mu_{\sim E}, \sigma_{\sim E})$and $N(\mu_E, \sigma_E)$ respectively, where the occurrence of the biomarker abnormality event is denoted by E and the absence of such an event is denoted by $\sim E$.

Gaussian mixture modelling is an optimisation task to estimate these normal and abnormal Gaussians as well as the mixing parameter based on maximum log-likelihood, where the log-likelihood for biomarker B is computed as the summation over all *GRN* mutation carriers in the dataset as follows:

$$L_B = \sum_{\forall j \in Carriers} \log f(B_j)$$

Supplementary figure 2.1. Illustrations of the Gaussian probability density functions for normal and abnormal values of biomarker B.

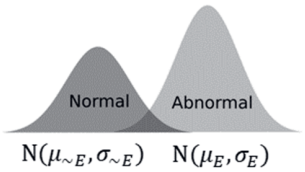

Here, the likelihood $f(B)$ is computed as follows:

$$f(B) = \theta_{\sim E} p(B|\mu_{\sim E}, \sigma_{\sim E}) + \theta_E p(B|\mu_E, \sigma_E),$$

Where $\theta_{\sim E} + \theta_E = 1$, and the mixing parameters $\theta_{\sim E}$ and θ_E show the relative proportions of the two Gaussians in the dataset. The abnormal Gaussian is initialised using the mean and standard deviation of the symptomatic subjects, while the normal Gaussian is initialised using the non-carriers. Since non-carriers are healthy controls, we fix $\mu_{\sim E}$ and $\sigma_{\sim E}$ to their initialised values and only optimise the remaining parameters in the Gaussian mixture model. The mixing parameter and the Gaussian parameters are optimised alternately until convergence as detailed previously.[1]

For imaging-biomarkers with left and right counter parts, we propose a novel modification to the Gaussian mixture model optimisation called Siamese Gaussian mixture model (Siamese GMM). We propose to jointly optimise the parameters of these biomarkers, by

taking advantage of symmetry in the brain. The log-likelihood for the joint optimisation for the imaging biomarkers I^L and I^R is given below:

$$L_I = \sum_{\forall j \in Carriers} \log f\left(I^L{}_j\right) + \log f\left(I^R{}_j\right)$$

where $f\left(I^L{}_j\right)$ and $f\left(I^R{}_j\right)$ are expressed mathematically as:

$$f\left(I^L{}_j\right) = \theta^L_{\sim E} p\left(I^L{}_j \middle| \mu_{\sim E}, \sigma_{\sim E}\right) + \theta^L_E p\left(I^L{}_j \middle| \mu_E, \sigma_E\right)$$

$$f\left(I^R{}_j\right) = \theta^R_{\sim E} p\left(I^R{}_j \middle| \mu_{\sim E}, \sigma_{\sim E}\right) + \theta^R_E p\left(I^R{}_j \middle| \mu_E, \sigma_E\right)$$

$\theta^L_{\sim E} + \theta^L_E = 1$ and $\theta^R_{\sim E} + \theta^R_E = 1$. The mixing parameters ($\theta^L_{\sim E}, \theta^L_E, \theta^R_{\sim E}, \theta^R_E$) and the abnormal Gaussian parameters (μ_E , σ_E) are again optimised alternately until convergence.[1] This joint optimisation of the left and right counter parts by sharing the normal and abnormal Gaussians reduces the number of parameters to be optimised, and thus improves the robustness. In case of asymmetrical atrophy patterns, where one of the biomarkers is stronger than the other, the joint optimisation also helps in making the GMM more stable for the weaker biomarker.

Supplementary figure 2.2. Correlation of disease severity (as estimated by non-imaging DEBM using cross-validation) with years since onset and FTD-CDR-SOB. The 2D scatter plots in figures A and C show the correlations of disease severity with years since onset, for symptomatic nfvPPA and bvFTD subjects respectively. The 2D scatter plot in figures B and D show the correlations of disease severity with FTD-CDR-SOB. The plot on top of each subfigure shows the probability density function of the disease stages. The plots on the right of figures A and C show the probability density functions of years since symptom onset. The plots on the right of figures B and D show the probability density function of FTD-CDR-SOB.

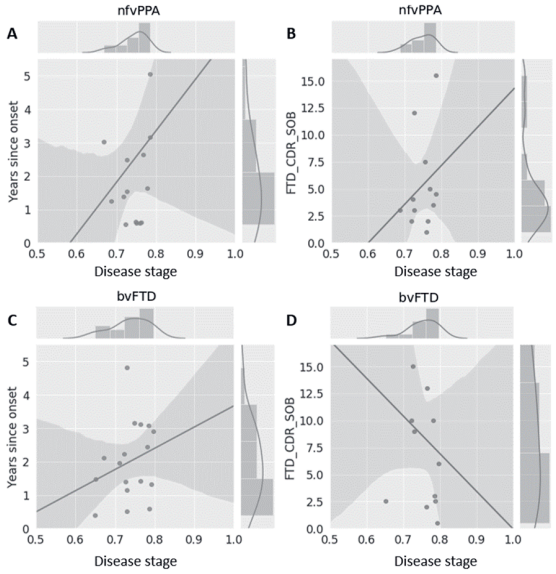

Supplementary figure 2.3. Cascade of non-imaging biomarker changes in nfvPPA (A) and bvFTD (B) subjects along with the uncertainty associated with it. The biomarkers are ordered based on the position in the estimated cascade. The colour-map is based on the number of times a biomarker is at a position in 100 repetitions of bootstrapping.

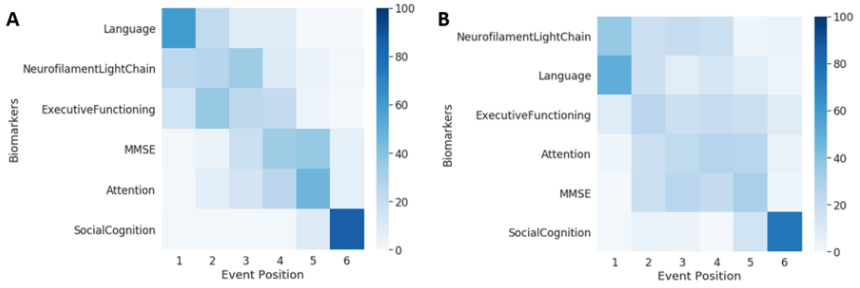

Supplementary references

1. Venkatraghavan, V., Bron, E.E., Wiessen, W.J., et al., Disease progression timeline estimation for Alzheimer's disease using discriminative event based modeling. Neuroimage, 2019. 186: p. 518-532.

Chapter 6

General discussion

Frontotemporal dementia (FTD) is a heterogeneous neurodegenerative disorder characterised by progressive neuronal loss of predominantly the frontal and / or temporal lobes. Patients usually present with changes in behaviour (behavioural variant, bvFTD) [1] and / or language (primary progressive aphasia, PPA),[2] although a wider clinical spectrum is increasingly recognised which includes other cognitive and psychiatric symptoms, motor neuron disease and Parkinsonian syndromes. In 10-20%, an underlying autosomal dominant genetic mutation is found, most commonly in *C9orf72*, *GRN* or *MAPT*.[3,4] Even within families, the clinical presentation, age at symptom onset, and disease course are highly variable.[4,5] Pharmacological treatment is currently limited to symptomatic management of behavioural disturbances, but large-scale clinical trials of disease-modifying drugs in genetic FTD are underway, which might ultimately delay functional decline or even postpone symptom onset.[6]

Biomarkers in cerebrospinal fluid (CSF) or blood that mirror pathological FTD-related changes are needed for both clinical trials and current clinical practice.[7] Various potential fluid biomarkers have been investigated, as described in chapter 1.2. CSF biomarkers might better reflect central nervous system changes, given the proximity to the brain and higher concentration of brain-derived proteins, whereas blood has the obvious advantage of minimally invasive collection, making it more convenient for repeated measurements. Genetic forms of FTD uniquely offer the opportunity to study presymptomatic and prodromal disease stages and therefore present a valuable platform for the discovery of early biomarkers.

In this thesis, I have utilised data from the Frontotemporal Dementia Risk Cohort (FTD-RisC) [8] and the Genetic Frontotemporal dementia Initiative (GENFI),[9] which follow genetic FTD patients and their at-risk relatives, to identify and validate biomarkers in CSF and blood. In this chapter, I present the results in light of current literature, discuss methodological considerations and suggest areas for further research.

Neurofilament light chain: a biomarker of neuroaxonal loss

Neurofilament light chain (NfL), a component of the axonal cytoskeleton, is released into the extracellular space upon neuroaxonal damage.[10] CSF and blood NfL levels are highly elevated in FTD and various other neurological disorders.[11] In chapter 2.1, we longitudinally measured serum NfL levels in the GENFI cohort and studied associations between NfL changes and disease progression.

NfL as a marker of early disease activity

Two major findings suggest that serum NfL increases before symptom onset. First, in nine presymptomatic mutation carriers who became symptomatic during follow-up ('converters'), NfL levels already exceeded the absolute threshold at baseline, i.e. 1-2 years before symptom onset. Second, we found higher NfL levels in presymptomatic carriers compared to non-carriers from the age of 48, which is considerably younger than the median age at symptom onset of 60 in the same cohort.

Strikingly, in presymptomatic familial Alzheimer's Disease (AD), NfL increases have been reported up to 22 years before the expected symptom onset.[12-14] Although these increases may initially be too small to be clinically meaningful,[13] they nevertheless provide fascinating pathophysiological insights and highlight the vast functional redundancy in the brain. In contrast, in amyotrophic lateral sclerosis (ALS) [15-18] and Parkinson's disease (PD),[19] NfL increases are only observed shortly before symptom onset. These discrepancies might reflect differences in disease pathogenesis, or might to some extent be due to differences in sample size, study design and statistical analyses. In contrast to familial AD, the age at symptom onset in FTD cannot be reliably predicted based on the parental age at symptom onset,[5] which greatly complicates the study of very early biomarker changes. More pre-conversion data from the GENFI and ARTFL LEFFTDS longitudinal FTLD (ALLFTD) [20] studies will allow us to estimate more accurately when NfL levels start to increase. Neuroimaging studies suggest that neurodegeneration starts at a much earlier stage in *C9orf72* mutation carriers than in *GRN* and *MAPT*,[21,22] which might also be reflected in presymptomatic NfL levels.

Elevated NfL levels could help identify presymptomatic mutation carriers with very early disease activity,[23] for whom therapeutic interventions may be the most effective, and serum NfL is currently being implemented as a tool to recruit presymptomatic carriers in the phase 3 clinical trial AL001-3 by Alector Inc. The longitudinal change of NfL over time might be more sensitive than single measurements,[12,15,19] and, given the relatively stable NfL levels in non-converting mutation carriers, periodic measurements could be used to monitor these individuals. Similar algorithms have been proposed for multiple sclerosis, with NfL increases prompting treatment initiation or modification even in the absence of clinical or neuroimaging changes.[24] The utility of NfL as a candidate selection tool might be the greatest in *GRN* mutation carriers, since NfL increases are especially pronounced in this group.

NfL as a surrogate marker of treatment effect

We showed that serum NfL remains elevated over the course of FTD, even in end-stage disease. In *C9orf72*- and *MAPT*-associated FTD, NfL levels appear to stabilise, whereas in *GRN* mutation carriers, they continue to rise. As short-term cognitive changes are difficult to quantify, NfL has garnered much interest as a surrogate marker of treatment effect in pharmaceutical trials.[7] Treatments that reduce the rate of neuroaxonal breakdown might be accompanied by a decrease in NfL levels, as has been shown extensively in multiple sclerosis.[25]

To use NfL as an outcome measure in trials, several issues need to be addressed. The NfL fluctuations observed mostly in *GRN* mutation carriers are poorly understood and could complicate the interpretation of NfL decreases following study drug administration. Furthermore, it is unknown when NfL changes in response to the study drug can be expected. Blood NfL peaks in the weeks after acute injury and remains elevated for several months, indicating a slow degeneration and long half-life,[26-28] which makes very frequent measurements unnecessary. Finally, intrathecal drug administration is expected to cause a transient NfL increase,[29] which may need to be accounted for in trials.

Prognostic value of NfL

Cross-sectional NfL levels predict the rate of subsequent functional decline, brain atrophy and survival in FTD,[30] and a rapid NfL increase over time is associated with a more aggressive disease course. NfL measurements could therefore provide prognostic information to the patient and caregiver, and prompt a more proactive approach for those expected to suffer rapid disease progression. Furthermore, in clinical trials, using NfL to stratify patients according to their expected disease course could significantly reduce heterogeneity in patient cohorts.

Confounding factors

NfL levels increase with healthy aging; interestingly, this association is non-linear, with steeper increases from the age of 60,[31] probably reflecting both increased physiological neuronal turnover and the accumulation of (subclinical) comorbidities. The large degree of variability in NfL levels in healthy older adults complicates the development of age-adjusted reference ranges.[31] Longitudinal measurements would allow for evaluation of individual NfL profiles without relying on reference values.

Confounding factors known to affect NfL levels include (unrecognised) head injuries, polyneuropathy, hypertension, diabetes mellitus, renal dysfunction, high body mass index and pregnancy.[32-34] The unexplained transient NfL elevations in a small number of individuals in our study suggest the presence of additional confounders. Therefore, we

recommend repeating NfL measurements before trial inclusion to ensure a valid measurement, especially in presymptomatic carriers with unexpectedly high NfL levels.

Conclusions

NfL is a highly promising biomarker with several potential applications, and we anticipate that it will soon find its place in clinical practice, where it could be used to distinguish neurological from non-neurological diseases and provide prognostic information. Ongoing international efforts to harmonise pre-analytical and analytical parameters and to develop universal reference values will enable us to establish guidelines for its measurement and interpretation.

Neuronal pentraxin: a biomarker of synapse integrity

Synapse dysfunction has long been considered a central event in neurodegenerative diseases, and therefore, synaptic biomarkers are a key area of interest.[35-37] In chapter 2.2, we describe the CSF measurement of neuronal pentraxins (NPTXs), a family of synaptic proteins which we previously identified as potential biomarkers through proteomics (chapter 4.1 and section 4 of this chapter).

We found reduced levels of NPTX1, NPTX2 and NPTX receptor (NPTXR) in the symptomatic stage of genetic FTD, probably reflecting dysfunction or loss of synapses. Other synaptic biomarkers identified in the context of AD, including neurogranin, SNAP-25 and synaptotagmin-1, are not consistently altered in FTD,[38,39] and NPTXs therefore provide a novel opportunity to measure synapse integrity in vivo. CSF NPTXs have recently received much attention and reduced levels have also been reported in mild cognitive impairment (MCI) and AD,[40-42] parkinsonism [43] and Lewy body dementia.[44]

NPTXs regulate the strength of excitatory synapses between pyramidal neurons and parvalbumin-containing inhibitory interneurons;[45,46] accordingly, NPTX knockout mice have inhibitory circuit disruption,[47] which in turn has been linked to cognitive impairment.[48] Since their expression is specific to these circuits,[45] NPTXs might not reflect the full extent of synapse loss in FTD. It would be interesting to investigate CSF NPTX levels in relation to other (non-fluid) measures of synapse integrity, such as [^{11}C]UCB-J position emission tomography (PET) imaging [49] and magneto-encephalography (MEG).[50]

The overlapping NPTX levels between presymptomatic and symptomatic mutation carriers indicate that single NPTX measurements will not be diagnostic for conversion, and their repeated measurement, preferably in blood, will probably be more informative. Promisingly,

recent studies have shown reduced NPTX2 levels in peripheral blood in vascular dementia [51] as well as in neuron-derived exosomes in blood of AD patients.[52]

Our NPTX2 measurements in a small number of longitudinal CSF samples tentatively suggest that NPTX2 might already decrease before symptom onset. This is in line with extensive evidence that synapse dysfunction occurs early and may precede neuronal loss.[53-57] Synaptic connectivity is a dynamic process, and synapse loss and dysfunction can be restored after removal of toxic stimuli.[58,59] Taken together, preservation and restoration of synapses could be a promising therapeutic strategy in early stages of neurodegeneration, and NPTXs might serve as biomarkers to monitor neural circuit defects and measure treatment effect.

To conclude, we demonstrated that CSF NPTXs are promising synaptic biomarkers in FTD. Future studies should measure NPTXs in blood of FTD patients in a longitudinal setting, and investigate which of the three NPTXs is the most robust biomarker.

Biomarkers of dysregulation of the immune system

Increasing clinical, genetic and cellular evidence suggests that chronic neuroinflammation plays an important role in FTD pathogenesis.[60] Specifically, microglial dysregulation and excessive activation of the complement system may be involved. In chapter 3, we measured the concentrations of soluble triggering receptor expressed on myeloid cells 2 (sTREM2) and complement proteins in CSF and blood to determine their value as biomarkers.

sTREM2 in *GRN*- and *C9orf72*-associated FTD

TREM2, a transmembrane receptor which is abundantly expressed by microglia, has garnered much interest as a potential biomarker since genetic variants in *TREM2* have been associated with AD, FTD, ALS and PD.[61-65] A soluble fragment, sTREM2, is measurable in CSF and is thought to reflect cerebral TREM2 expression.[66] We found no group differences in sTREM2 levels between presymptomatic and symptomatic *GRN* and *C9orf72* mutation carriers. In AD, sTREM2 levels fluctuate depending on the disease stage, with especially high levels in MCI and early-stage AD.[67-69] Similar dynamics might also be in place in FTD and could to some extent have masked group differences in our study.

While activated microglia were initially assumed to adopt either an M1 or an M2 phenotype,[70] recent research has identified multiple functionally diverse microglial populations which can dynamically change depending on the local microenvironment.[71] TREM2 expression is upregulated during neurodegeneration and is required for the transition from homeostatic to disease-associated microglia (DAMs).[71-74] sTREM2 levels may therefore specifically reflect the TREM2-mediated transition to DAMs. Interestingly,

TREM2-/- microglia are locked in homeostatic state, whereas in *GRN-/-* microglia, a persistently activated state is observed.[75,76] The fact that these seemingly opposing phenotypes are both associated with neurodegeneration highlights the complex nature of microglial dysregulation.

Higher CSF sTREM2 levels have been associated with slower disease progression in AD,[77-79] and increased microglial uptake on TSPO-PET imaging predicts a slower progression from MCI to AD.[80,81] Although not necessarily causal, these associations tentatively suggest that microglial activation in early neurodegeneration might be protective. Data from four converters in our study similarly suggested an association between high sTREM2 levels in the late-presymptomatic stage and delayed conversion. If confirmed in a larger number of subjects, sTREM2 levels would need to be taken into account for patient stratification in upcoming clinical trials. In line with one previous study,[82] we observed very high sTREM2 levels in a subset of *GRN* mutation carriers; it would be interesting to confirm the presumed microglial activation using other microglial markers, such as YKL-40, CHIT-1 (chapter 1.2) and TSPO-PET imaging,[83] and to determine whether these subjects have a slower rate of disease progression.

CSF and plasma complement factors

The complement system comprises a cascade of protein reactions which ultimately contribute to the innate immune response.[84] We found elevated levels of the complement factors C1q and C3b in CSF of symptomatic mutation carriers, which likely reflect increased complement synthesis by predominantly microglia,[85,86] providing further evidence of an inflammatory component in FTD. The substantial overlap between groups might be due to a variable degree of complement activation as well as within-individual fluctuations over the course of disease, and renders these proteins unsuitable as diagnostic markers.

C1q and C3b are thought to play crucial roles in the excessive pruning of synapses by microglia,[85,87] and deletion of *C1q* and *C3b* in *GRN-/-* mice mitigates synapse loss and neurodegeneration.[76,88] The inverse correlations between CSF C1q and C3b and grey matter volume in presymptomatic mutation carriers suggest that complement upregulation occurs in conjunction with early neuronal loss. Longitudinal measurements might elucidate the exact timing of complement activation and identify potential therapeutic windows for complement inhibition.

While the brain was long considered an immune-privileged organ, extensive research has revealed interactions between local and systemic immunity, and peripherally synthesised complement proteins might also contribute to neuroinflammation.[89,90] Our plasma

measurements revealed elevated levels of C2 and C3 in symptomatic mutation carriers, but the remaining nine complement factors did not differ between groups. Several potential explanations exist for these findings. First, pathological FTD-related changes might not elicit a strong systemic immune response; this is supported by the inconsistent reports of plasma cytokine levels in FTD.[60] Second, several confounding factors, including body mass index, cardiovascular risk factors and unrelated inflammatory diseases, were not adequately accounted for in our study. Third, we measured mostly intact complement proteins, the concentrations of which are subject to a delicate equilibrium between increased synthesis and cleavage into activated fragments.[91] Measuring activated complement fragments or using functional tests might provide a more robust measure of peripheral complement activation.[91,92]

Considerations for the identification of immunological biomarkers

Neuroinflammation in FTD is a highly complex and intricate process, which has proven difficult to capture in fluid biomarkers. The marker-based approaches used in most studies to date probably do not adequately reflect the heterogeneous populations of immune cells that may be involved in various stages of the disease.[71,74] Furthermore, the interpretation of differentially regulated molecules in biofluids is complicated by the fact that their downstream effects can be either pro- or anti-inflammatory, depending on prevailing conditions.[93] The significant variability in study populations, in terms of clinical phenotype, disease stage, underlying proteinopathy and genetic defects, as well as in pre-analytical and analytical parameters, have made it difficult to directly compare studies.[60]

The development of inflammation-targeted therapies is crucially hindered by a lack of understanding of the role of neuroinflammation in FTD pathogenesis. Current insights suggest a beneficial role for the initial immune response in the clearance of toxic protein species,[94] but its uncontrolled and persistent nature is thought to ultimately contribute to neurotoxicity.[60] Therapeutic interventions should therefore aim to encourage a protective inflammatory profile rather than inhibit inflammation in general. The need for robust biomarkers than can track different aspects of neuroinflammation over the course of disease in vivo is evident, and future biomarker research that better accounts for the dynamic and heterogeneous nature of neuroinflammation might prove fruitful.

The use of mass spectrometry to identify novel biomarkers

Mass spectrometry (MS)-based proteomics has emerged as a powerful exploratory tool to compare protein abundances between patient cohorts. We performed discovery proteomics followed by a targeted validation step to identify novel CSF biomarkers (chapter 4.1).

Novel CSF biomarkers in *GRN*-FTD

Unbiased liquid chromatography-tandem mass spectrometry (LC-MS/MS) enables the direct detection of thousands of proteins in biological samples without requiring predefined proteins of interest, creating an ideal framework for the discovery of novel biomarkers.[95-97] We identified 25 differentially regulated proteins between symptomatic and presymptomatic *GRN* mutation carriers and non-carriers.

Unbiased LC-MS/MS generates a large number of candidates including false discoveries, and therefore each candidate biomarker requires validation using independent methods.[96,98] We selected seven proteins of interest based on fold changes of the identified peptides for validation in a larger cohort of *GRN, C9orf72* and *MAPT* mutation carriers using parallel reaction monitoring (PRM), a targeted mass spectrometry(MS)-based approach which allows for more accurate peptide quantification.[95] The validation study confirmed downregulation of NPTXR, CHGA, VGF, VSTM2B and PTPRN2 in the symptomatic stages of FTD. These proteins are implicated in synaptic functioning, vesicle secretion and immunity and are discussed in detail in chapter 4.1. In a subsequent study (chapter 1.2 and section 2 of this chapter), we further validated NPTXR and related proteins using antibody-based methods, which are more feasible for clinical implementation.

Taken together, our studies demonstrate the multi-step workflow needed to find novel biomarkers by MS. While validation of unbiased LC-MS/MS findings can be done directly with immunoassays,[99-101] targeted MS may be preferred [102-105] as it enables validation of large panels of candidate biomarkers without the need for antibodies. Especially for new biomarkers, antibodies might not be readily available, and de novo assay development is costly and time-consuming.

Several proteins identified in our study have also been detected in MS studies of other neurodegenerative diseases,[103,105-112] which, while demonstrating the validity of our results, means that they reflect non-specific neurodegenerative changes. Comparing specific phenotypic, pathological or genetic dementia subtypes might identify markers that can contribute to differential diagnosis.[101,113]

Challenges for mass spectrometry in biomarker identification

Although MS-based biomarker identification has been reported on numerous occasions across a range of neurodegenerative diseases, there has been limited success in translating the findings to clinically useful biomarkers.[96] Results between studies have been largely inconsistent, possibly due to differences in patient cohorts (including the control population), disease phenotypes, environmental conditions affecting instrument parameters, and

technical MS parameters,[95,106,114-117] and biomarkers that are identified in multiple proteomics studies are probably the most promising.

A significant drawback of LC-MS/MS is that high-abundancy proteins, such as albumin and immunoglobulins, can mask or interfere with peptides of less abundant proteins. Consequently, the lower limit of detection is above the ng/ml range, which is much higher than the pg/ml level detectable by ELISA.[118,119] We depleted samples of the most abundant proteins using antibodies, which improves sensitivity, but might inadvertently remove proteins of interest due to interactions with the depletion matrix or with depletion targets.[120] These issues might explain why we did not detect key proteins such as progranulin and NfL, and NfL detection has been proposed as a potential quality check for upcoming MS studies.[106] Technical advances that resolve these problems might also facilitate the transition to blood proteomics. In any case, researchers should be encouraged to publish full results (e.g. in data repositories) rather than just proteins that reach statistical significance, to enable discrimination between proteins that were detected but not significantly different versus those that were simply not detected.[95]

Disease progression modelling

Since the seminal paper by Jack et al.,[121] which presented a hypothetical model of AD progression, various computational strategies have emerged to model biomarker changes based on real data. In chapter 5, we used discriminative event-based modelling (DEBM) to estimate the sequence in which biomarkers become abnormal over the course of FTD, which could facilitate disease staging and elucidate which biomarker is the most sensitive to early disease activity.[122]

Fluid biomarker modelling

DEBM of fluid biomarkers in the GENFI cohort revealed that NPTX2 and serum NfL are detectably abnormal first, followed by CSF NfL, phosphorylated neurofilament heavy chain (pNfH), glial acidic fibrillary protein (GFAP), C3b and C1q. Estimated disease stages based on this sequence could accurately delineate presymptomatic from symptomatic mutation carriers, demonstrating the validity of the model. Converters were assigned disease stages similar to symptomatic carriers, confirming the hypothesis that at least some these biomarkers become abnormal before symptom onset. Future studies with more converters should compare the ability to track presymptomatic carriers and predict conversion using NPTXs or NfL alone versus using a DEBM-based fluid biomarker profile.

Surprisingly, serum NfL abnormality was ordered before CSF NfL, suggesting that serum NfL is at least as good a measure to monitor disease activity in presymptomatic carriers. This

contrasts with the recently described elevations of CSF – but not blood – NfL in response to amyloid pathology in cognitively unimpaired subjects,[123] and might be explained by model-related parameters, such as the larger sample size and therefore greater statistical power to detect changes in serum compared to CSF.

Multimodal biomarker modelling

The combination of biomarkers from different modalities might better mirror the real-world assessment of mutation carriers and provide a more robust means to predict conversion and track disease progression. Our multimodal DEBM of *GRN*-FTD estimated that serum NfL, language decline and white matter integrity of the thalamic radiation were detectably abnormal first. The construction of phenotype-specific models yielded two interesting findings. First, the sequence of biomarker changes was much more uncertain in bvFTD than in PPA, which probably reflects the heterogeneity of bvFTD in terms of cognitive and neuroimaging measures.[4,124] Second, even among bvFTD patients, the language domain was the first to become abnormal. Possibly, an early decline in language functions is obscured in clinical practice by the often striking behavioural changes.[1,125] Given their relative ease of administration, cognitive tests of language might be a useful tool to detect not only PPA, but also early bvFTD.[125]

Estimated disease stages accurately distinguished between presymptomatic and symptomatic mutation carriers. However, in contrast to the fluid biomarker model, a certain degree of circularity must be acknowledged, given that several of the included biomarkers (e.g. cognitive test scores, grey matter volume) are also used to diagnose FTD. This is especially true for language tests in PPA, which by definition show early abnormalities.[2]

The role of event-based modelling in biomarker research

Our studies demonstrate great potential for DEBM in biomarker modelling. Here, we highlight some key strengths of these models, as well as challenges for future research.

First, in contrast to many other disease progression models which rely on (short-term) longitudinal data,[126-129] event-based models (EBMs) only requires cross-sectional data, which is particularly advantageous for CSF biomarkers, as longitudinal data is often not available. Second, as these models do not require predefined cut-off points, novel biomarkers for which reference ranges have not yet been established can be included in the models. Third, since pathological changes probably occur years before symptom onset, EBM's approach to genetic FTD as a disease continuum, rather than dichotomous (i.e. presymptomatic or symptomatic) probably better reflects the reality and should be encouraged in other biomarker studies.

Importantly, estimated disease stages are based on the average ordering of biomarker changes in a given population, and might therefore be inaccurate in subjects that undergo an atypical biomarker progression sequence. A promising modification to existing EBMs is Subtype and Stage Inference (SuStain),[130,131] which identifies clusters of subjects that share a differential sequence of events. SuStaIn was shown to recognise genetic subgroups in the GENFI cohort based on neuroimaging data, and intriguingly, two distinct subtypes of *C9orf72* disease progression (a frontotemporal and a subcortical subtype).[131] The existence of subtypes in *C9orf72* mutation carriers is in line with the vast clinical heterogeneity, as described in chapter 5.2, and is also reflected in the uncertainty in our fluid biomarker model for *C9orf72* mutation carriers. Detecting subgroups of mutation carriers that follow alternative sequences might help identify protective or risk factors.[132]

Biomarker studies of neurodegenerative diseases are inevitably hampered by a relative lack of data at end-stage disease, and the disease stages estimated by EBMs are therefore biased towards early FTD. The transition from CSF to blood biomarkers might facilitate on-site collection of samples in patients with advanced disease, which would reduce patient burden.

In conclusion, our models confirmed that NPTX2 and NfL are the earliest fluid biomarkers to become abnormal. Our findings should be validated in independent cohorts, preferably with longitudinal data. Future computational optimisations might enable us to estimate the relative time interval between biomarker changes,[122] creating an even more informative disease progression timeline.

The future of fluid biomarker research in FTD

Much progress has been made in the past two decades in identifying both general and gene-specific biomarkers of neurodegeneration.[133,134] Here, we discuss some important challenges for future fluid biomarker research.

Gaps in current fluid biomarkers

The diverse spectrum of presenting symptoms in FTD greatly complicates clinical practice, and diagnostic biomarkers are urgently needed to facilitate a more timely diagnosis. While NfL has proven useful to discriminate bvFTD from psychiatric disorders,[135] its capacity to discriminate between the various neurodegenerative disorders is limited.[136-138] Furthermore, in research settings, the use of a clinical diagnosis as a reference standard is potentially misleading given the high false positive rate of FTD diagnoses.[139] Although genetic forms offer a higher degree of certainty as to the diagnosis, co-existence of other neurodegenerative disorders could still affect biomarker identification.[139]

Biomarkers that reflect general neurodegenerative processes might translate well from genetic to sporadic FTD. However, since therapeutic interventions are likely to target specific proteinopathies, the ability to predict the underlying pathology during life in sporadic FTD will be crucial. Several previous attempts to identify biomarkers of TAR DNA-binding protein-43 (TDP-43) and tau pathology have been unsuccessful (chapter 1.2), although the recently described application of real-time quaking-induced conversion (RT-QuiC) technology to detect minute amounts of misfolded TDP-43 protein holds some promise for the future.[140] Until such time, genetic FTD, in which the underlying pathology is known based on the genetic defect, presents an ideal platform for therapeutic trials.[7]

Extensive evidence exists to support NfL as a predictor of clinical decline and survival once the disease has begun. However, to date, we are unable to predict at what age symptoms will commence, and which phenotype a mutation carrier will develop. These uncertainties contribute to the often devastating psychological and societal burden of carrying an FTD-related genetic mutation and are presumed to be the result of a complex interplay of environmental and (epi)genetic factors.[141] To date, a few genetic modifiers of phenotype have been identified, including variants in *TMEM106B* in *GRN* mutation carriers [142] and *ATXN2* in *C9orf72* mutation carriers.[143,144] Advances in genetic technologies might reveal additional contributory factors. In particular, novel techniques to characterise *C9orf72* repeat expansions are expected to elucidate the effect of their length and exact content on phenotype, as discussed in chapter 4.2.

Despite the remarkable capacity of statistical models such as DEBM to simulate disease progression based on cross-sectional data, there is an ever-present need for longitudinal biomarker data. Longitudinal biosamples from converters have proven invaluable to understand biomarker evolution over the course of disease, but statistical analyses have been hampered by the relative paucity of converters. Ongoing longitudinal studies such as GENFI and ALLFTD will inevitably identify more converters over time.

Although cell and animal models have provided valuable insights into FTD pathogenesis, the homozygous genetic mutations of most models to date might not accurately reflect the heterozygous mutations associated with FTD in humans. Post-mortem studies remain invaluable to improve our understanding of FTD, and discussing brain autopsy in all FTD patients and at-risk family members should be encouraged.

Novel strategies for biomarker identification

Although unbiased MS is a valuable tool to generate a large number of potential biomarkers, the acquisition of mass spectrometers and training of specialised staff is costly and time-consuming. Furthermore, since MS and immunoassays identify different things (i.e. experimentally fragmented vs. natively folded proteins and isoforms), candidates identified by MS might not necessarily translate well to immunoassays.[119] Multiplex immunoassays might therefore be an interesting alternative, which, although not entirely unbiased, are capable of measuring a very large number of analytes simultaneously in small sample volumes and are highly sensitive.[134] Promising examples include Mesoscale Discovery (MSD), Luminex, V-plex, and Olink, which have produced interesting results in AD and other neurological diseases.[145-149] These platforms might also help design panels of complementary biomarkers, which probably better reflect the complexities of FTD than single biomarkers.

The need for repeated measurements over time highlights the importance of using more easily accessible biofluids than CSF. Technological advances in the field of ultrasensitive assays (i.e. Single Molecule Arrays) have enabled detection of very low concentrations of brain-derived proteins in peripheral blood, such as NfL.[150] However, blood biomarker development poses several other challenges: the biomarker must be capable of crossing the blood-brain barrier, peripheral expression of biomarkers could contaminate blood concentrations, resident blood proteins could interfere with immunoassay platforms or degrade or mask potential biomarkers, and pre-analytical factors such as food intake and diurnal variation may be more relevant for blood than CSF.[151,152] Many of these issues might be overcome by using brain-derived exosomes (BDEs).

BDEs are secreted by various cell types in the brain, including neurons and glia, and play important roles in between-cell communication, synaptic plasticity and removal of unwanted proteins. Under pathological conditions, the number and composition of BDEs changes, probably in an attempt to dispose of potentially toxic protein species. BDEs cross the blood-brain barrier and can be isolated from peripheral blood based on cell-type specific surface markers.[153-156] Although their isolation is currently technically challenging, time-consuming and expensive, BDEs present a promising source for biomarker discovery. For example, elevated levels of BDEs have been found in symptomatic *GRN* mutation carriers, presumably as a compensatory reaction to lysosomal dysfunction,[153] and reduced synaptic protein levels in BDEs were found in FTD patients.[52]

Circulating nucleic acids might also prove to be useful blood-based biomarkers. microRNAs (miRNAs), which regulate the expression of mature RNAs, can be relatively easily obtained from blood or CSF,[157] and several recent studies have identified differential blood miRNA

signatures in sporadic and genetic FTD.[158-161] miRNAs in BDEs might be more stable over time and therefore be more robust biomarkers than those in serum or plasma.[157,162] Another promising source of biomarkers lies in cell-free DNA (cfDNA). cfDNA is normally present in very low concentrations in the blood, and increased levels are thought to reflect accelerated cell turnover.[163] Accordingly, elevated levels have been observed in AD following Aβ-induced cell death, even before the formation of Aβ-plaques.[164] Recent studies that have managed to identify brain-derived cfDNA based on tissue-specific methylation patterns suggest that cfDNA might provide a peripheral measure of neuronal loss.[165-167]

Implementing fluid biomarkers in clinical practice and treatment trials

An inevitable gap exists between identifying a potential fluid biomarker in a research setting, and applying it confidently to clinical practice and trials. We highlight some important considerations for biomarker implementation, which currently apply to NfL in particular.

First, an in-depth understanding of the biomarker's behaviour in the general population is required in order to establish accurate cut-off points. A strong correlation exists between most of the biomarkers described in this thesis and age, and since most are not disease-specific (NfL) or brain-specific (NPTXs, complement factors), neurological and systemic comorbidities can greatly affect their concentration. Furthermore, most studies to date are biased towards Caucasians and need to be replicated in other ethnicities. Finally, studies assessing the short- and long-term stability of a biomarker are crucial for its use in disease monitoring.[168]

Variability in sample collection, handling and storage can greatly affect biomarker measurements. More widespread dissemination of available biobanking guidelines should alleviate these issues.[169,170] Fortunately, blood NfL appears to be relatively robust to various pre-analytical parameters, enabling accurate quantification even under suboptimal conditions.[32,168,171] Furthermore, assays must be thoroughly validated across multiple centres.[172] Even when using the same assay, some variability in protein quantification might be inevitable, possibly due to user variability, matrix effects and lot variability of assay kits.[173] Longitudinal measurements for research purposes should therefore be performed in one batch of experiments.

Taken together, these factors highlight the importance of international initiatives such as BIOMARKAPD and the International CSF society to guide biomarker identification, validation and standardisation.[119,174]

Conclusions

This thesis adds to the rapidly expanding knowledge of CSF and blood biomarkers for genetic FTD. International collaborations have enabled large-scale cohort studies, such as GENFI and ALLFTD, together forming the FTD Prevention Initiative (FPI), which will continue to contribute to biomarker development and might ultimately pave the way towards an effective treatment.

References

1. Rascovsky K, Hodges JR, Knopman D, et al. Sensitivity of revised diagnostic criteria for the behavioural variant of frontotemporal dementia. Brain. 2011;134(Pt 9):2456-77.
2. Gorno-Tempini ML, Hillis AE, Weintraub S, et al. Classification of primary progressive aphasia and its variants. Neurology. 2011;76(11):1006-14.
3. Lashley T, Rohrer JD, Mead S, et al. Review: an update on clinical, genetic and pathological aspects of frontotemporal lobar degenerations. Neuropathol Appl Neurobiol. 2015;41(7):858-81.
4. Seelaar H, Rohrer JD, Pijnenburg YA, et al. Clinical, genetic and pathological heterogeneity of frontotemporal dementia: a review. J Neurol Neurosurg Psychiatry. 2011;82(5):476-86.
5. Moore KM, Nicholas J, Grossman M, et al. Age at symptom onset and death and disease duration in genetic frontotemporal dementia: an international retrospective cohort study. Lancet Neurol. 2020;19(2):145-56.
6. Ljubenkov PA, Boxer AL. FTLD Treatment: Current Practice and Future Possibilities. Adv Exp Med Biol. 2021;1281:297-310.
7. Boxer AL, Gold M, Feldman H, et al. New directions in clinical trials for frontotemporal lobar degeneration: Methods and outcome measures. Alzheimers Dement. 2020;16(1):131-43.
8. Dopper EG, Rombouts SA, Jiskoot LC, et al. Structural and functional brain connectivity in presymptomatic familial frontotemporal dementia. Neurology. 2013;80(9):814-23.
9. Rohrer JD, Nicholas JM, Cash DM, et al. Presymptomatic cognitive and neuroanatomical changes in genetic frontotemporal dementia in the Genetic Frontotemporal dementia Initiative (GENFI) study: a cross-sectional analysis. Lancet Neurol. 2015;14(3):253-62.
10. Petzold A. Neurofilament phosphoforms: surrogate markers for axonal injury, degeneration and loss. J Neurol Sci. 2005;233(1-2):183-98.
11. Khalil M, Teunissen CE, Otto M, et al. Neurofilaments as biomarkers in neurological disorders. Nat Rev Neurol. 2018;14(10):577-89.
12. Preische O, Schultz SA, Apel A, et al. Serum neurofilament dynamics predicts neurodegeneration and clinical progression in presymptomatic Alzheimer's disease. Nat Med. 2019.
13. Quiroz YT, Zetterberg H, Reiman EM, et al. Plasma neurofilament light chain in the presenilin 1 E280A autosomal dominant Alzheimer's disease kindred: a cross-sectional and longitudinal cohort study. Lancet Neurol. 2020;19(6):513-21.
14. Weston PSJ, Poole T, O'Connor A, et al. Longitudinal measurement of serum neurofilament light in presymptomatic familial Alzheimer's disease. Alzheimers Res Ther. 2019;11(1):19.
15. Benatar M, Wuu J, Andersen PM, et al. Neurofilament light: A candidate biomarker of presymptomatic amyotrophic lateral sclerosis and phenoconversion. Ann Neurol. 2018;84(1):130-9.
16. Benatar M, Wuu J, Lombardi V, et al. Neurofilaments in pre-symptomatic ALS and the impact of genotype. Amyotroph Lateral Scler Frontotemporal Degener. 2019;20(7-8):538-48.

17. Feneberg E, Oeckl P, Steinacker P, et al. Multicenter evaluation of neurofilaments in early symptom onset amyotrophic lateral sclerosis. Neurology. 2018;90(1):e22-e30.
18. Weydt P, Oeckl P, Huss A, et al. Neurofilament levels as biomarkers in asymptomatic and symptomatic familial amyotrophic lateral sclerosis. Ann Neurol. 2016;79(1):152-8.
19. Wilke C, Dos Santos MCT, Schulte C, et al. Intraindividual Neurofilament Dynamics in Serum Mark the Conversion to Sporadic Parkinson's Disease. Mov Disord. 2020;35(7):1233-8.
20. Boeve BF, Boxer AL, Rosen HJ, et al. Studying the natural history of frontotemporal lobar degeneration (FTLD): The ARTFL LEFFTDS longitudinal FTLD (ALLFTD) protocol. Alzheimer's & Dementia. 2020;16(S6):e045482.
21. Jiskoot LC, Bocchetta M, Nicholas JM, et al. Presymptomatic white matter integrity loss in familial frontotemporal dementia in the GENFI cohort: A cross-sectional diffusion tensor imaging study. Ann Clin Transl Neurol. 2018;5(9):1025-36.
22. Staffaroni AM, Goh SM, Cobigo Y, et al. Rates of Brain Atrophy Across Disease Stages in Familial Frontotemporal Dementia Associated With MAPT, GRN, and C9orf72 Pathogenic Variants. JAMA Netw Open. 2020;3(10):e2022847.
23. Rojas JC, Wang P, Staffaroni AM, et al. Plasma Neurofilament Light for Prediction of Disease Progression in Familial Frontotemporal Lobar Degeneration. Neurology. 2021.
24. Leppert D, Kuhle J. Blood neurofilament light chain at the doorstep of clinical application. Neurol Neuroimmunol Neuroinflamm. 2019;6(5):e599.
25. Thebault S, Bose G, Booth R, et al. Serum neurofilament light in MS: The first true blood-based biomarker? Mult Scler. 2021:1352458521993066.
26. Gattringer T, Pinter D, Enzinger C, et al. Serum neurofilament light is sensitive to active cerebral small vessel disease. Neurology. 2017;89(20):2108-14.
27. Shahim P, Zetterberg H, Tegner Y, et al. Serum neurofilament light as a biomarker for mild traumatic brain injury in contact sports. Neurology. 2017;88(19):1788-94.
28. Tiedt S, Duering M, Barro C, et al. Serum neurofilament light: A biomarker of neuroaxonal injury after ischemic stroke. Neurology. 2018;91(14):e1338-e47.
29. Bergman J, Dring A, Zetterberg H, et al. Neurofilament light in CSF and serum is a sensitive marker for axonal white matter injury in MS. Neurol Neuroimmunol Neuroinflamm. 2016;3(5):e271.
30. Meeter LH, Dopper EG, Jiskoot LC, et al. Neurofilament light chain: a biomarker for genetic frontotemporal dementia. Ann Clin Transl Neurol. 2016;3(8):623-36.
31. Khalil M, Pirpamer L, Hofer E, et al. Serum neurofilament light levels in normal aging and their association with morphologic brain changes. Nat Commun. 2020;11(1):812.
32. Barro C, Chitnis T, Weiner HL. Blood neurofilament light: a critical review of its application to neurologic disease. Ann Clin Transl Neurol. 2020;7(12):2508-23.
33. Korley FK, Goldstick J, Mastali M, et al. Serum NfL (Neurofilament Light Chain) Levels and Incident Stroke in Adults With Diabetes Mellitus. Stroke. 2019;50(7):1669-75.
34. Manouchehrinia A, Piehl F, Hillert J, et al. Confounding effect of blood volume and body mass index on blood neurofilament light chain levels. Ann Clin Transl Neurol. 2020;7(1):139-43.
35. Camporesi E, Nilsson J, Brinkmalm A, et al. Fluid Biomarkers for Synaptic Dysfunction and Loss. Biomark Insights. 2020;15:1177271920950319.

36. Marttinen M, Kurkinen KM, Soininen H, et al. Synaptic dysfunction and septin protein family members in neurodegenerative diseases. Mol Neurodegener. 2015;10:16.
37. Terry RD, Masliah E, Salmon DP, et al. Physical basis of cognitive alterations in Alzheimer's disease: synapse loss is the major correlate of cognitive impairment. Ann Neurol. 1991;30(4):572-80.
38. Antonell A, Tort-Merino A, Ríos J, et al. Synaptic, axonal damage and inflammatory cerebrospinal fluid biomarkers in neurodegenerative dementias. Alzheimers Dement. 2020;16(2):262-72.
39. Tible M, Sandelius Å, Höglund K, et al. Dissection of synaptic pathways through the CSF biomarkers for predicting Alzheimer disease. Neurology. 2020;95(8):e953-e61.
40. Belbin O, Xiao MF, Xu D, et al. Cerebrospinal fluid profile of NPTX2 supports role of Alzheimer's disease-related inhibitory circuit dysfunction in adults with Down syndrome. Mol Neurodegener. 2020;15(1):46.
41. Galasko D, Xiao M, Xu D, et al. Synaptic biomarkers in CSF aid in diagnosis, correlate with cognition and predict progression in MCI and Alzheimer's disease. Alzheimers Dement (N Y). 2019;5:871-82.
42. Xiao MF, Xu D, Craig MT, et al. NPTX2 and cognitive dysfunction in Alzheimer's Disease. Elife. 2017;6.
43. Magdalinou NK, Noyce AJ, Pinto R, et al. Identification of candidate cerebrospinal fluid biomarkers in parkinsonism using quantitative proteomics. Parkinsonism Relat Disord. 2017;37:65-71.
44. Boiten WA, van Steenoven I, Xiao M, et al. Pathologically Decreased CSF Levels of Synaptic Marker NPTX2 in DLB Are Correlated with Levels of Alpha-Synuclein and VGF. Cells. 2020;10(1).
45. Chang MC, Park JM, Pelkey KA, et al. Narp regulates homeostatic scaling of excitatory synapses on parvalbumin-expressing interneurons. Nat Neurosci. 2010;13(9):1090-7.
46. Xu D, Hopf C, Reddy R, et al. Narp and NP1 form heterocomplexes that function in developmental and activity-dependent synaptic plasticity. Neuron. 2003;39(3):513-28.
47. Pelkey KA, Barksdale E, Craig MT, et al. Pentraxins coordinate excitatory synapse maturation and circuit integration of parvalbumin interneurons. Neuron. 2015;85(6):1257-72.
48. Palop JJ, Mucke L. Network abnormalities and interneuron dysfunction in Alzheimer disease. Nat Rev Neurosci. 2016;17(12):777-92.
49. Chen MK, Mecca AP, Naganawa M, et al. Assessing Synaptic Density in Alzheimer Disease With Synaptic Vesicle Glycoprotein 2A Positron Emission Tomographic Imaging. JAMA Neurol. 2018;75(10):1215-24.
50. Adams NE, Hughes LE, Rouse MA, et al. GABAergic cortical network physiology in frontotemporal lobar degeneration. Brain. 2021.
51. Shao K, Shan S, Ru W, et al. Association between serum NPTX2 and cognitive function in patients with vascular dementia. Brain Behav. 2020;10(10):e01779.

52. Goetzl EJ, Abner EL, Jicha GA, et al. Declining levels of functionally specialized synaptic proteins in plasma neuronal exosomes with progression of Alzheimer's disease. Faseb J. 2018;32(2):888-93.
53. Handley EE, Pitman KA, Dawkins E, et al. Synapse Dysfunction of Layer V Pyramidal Neurons Precedes Neurodegeneration in a Mouse Model of TDP-43 Proteinopathies. Cereb Cortex. 2017;27(7):3630-47.
54. Lleó A, Núñez-Llaves R, Alcolea D, et al. Changes in Synaptic Proteins Precede Neurodegeneration Markers in Preclinical Alzheimer's Disease Cerebrospinal Fluid. Mol Cell Proteomics. 2019;18(3):546-60.
55. Starr A, Sattler R. Synaptic dysfunction and altered excitability in C9ORF72 ALS/FTD. Brain Res. 2018;1693(Pt A):98-108.
56. Tapia L, Milnerwood A, Guo A, et al. Progranulin deficiency decreases gross neural connectivity but enhances transmission at individual synapses. J Neurosci. 2011;31(31):11126-32.
57. Yoshiyama Y, Higuchi M, Zhang B, et al. Synapse loss and microglial activation precede tangles in a P301S tauopathy mouse model. Neuron. 2007;53(3):337-51.
58. Colom-Cadena M, Spires-Jones T, Zetterberg H, et al. The clinical promise of biomarkers of synapse damage or loss in Alzheimer's disease. Alzheimers Res Ther. 2020;12(1):21.
59. Jackson J, Jambrina E, Li J, et al. Targeting the Synapse in Alzheimer's Disease. Front Neurosci. 2019;13:735.
60. Bright F, Werry EL, Dobson-Stone C, et al. Neuroinflammation in frontotemporal dementia. Nat Rev Neurol. 2019;15(9):540-55.
61. Guerreiro R, Wojtas A, Bras J, et al. TREM2 variants in Alzheimer's disease. N Engl J Med. 2013;368(2):117-27.
62. Jonsson T, Stefansson H, Steinberg S, et al. Variant of TREM2 associated with the risk of Alzheimer's disease. N Engl J Med. 2013;368(2):107-16.
63. Su WH, Shi ZH, Liu SL, et al. The rs75932628 and rs2234253 polymorphisms of the TREM2 gene were associated with susceptibility to frontotemporal lobar degeneration in Caucasian populations. Ann Hum Genet. 2018;82(4):177-85.
64. Cady J, Koval ED, Benitez BA, et al. TREM2 variant p.R47H as a risk factor for sporadic amyotrophic lateral sclerosis. JAMA Neurol. 2014;71(4):449-53.
65. Rayaprolu S, Mullen B, Baker M, et al. TREM2 in neurodegeneration: evidence for association of the p.R47H variant with frontotemporal dementia and Parkinson's disease. Mol Neurodegener. 2013;8:19.
66. Piccio L, Buonsanti C, Cella M, et al. Identification of soluble TREM-2 in the cerebrospinal fluid and its association with multiple sclerosis and CNS inflammation. Brain. 2008;131(Pt 11):3081-91.
67. Liu D, Cao B, Zhao Y, et al. Soluble TREM2 changes during the clinical course of Alzheimer's disease: A meta-analysis. Neurosci Lett. 2018;686:10-6.
68. Ma LZ, Tan L, Bi YL, et al. Dynamic changes of CSF sTREM2 in preclinical Alzheimer's disease: the CABLE study. Mol Neurodegener. 2020;15(1):25.

69. Suárez-Calvet M, Morenas-Rodríguez E, Kleinberger G, et al. Early increase of CSF sTREM2 in Alzheimer's disease is associated with tau related-neurodegeneration but not with amyloid-β pathology. Mol Neurodegener. 2019;14(1):1.
70. Bachiller S, Jiménez-Ferrer I, Paulus A, et al. Microglia in Neurological Diseases: A Road Map to Brain-Disease Dependent-Inflammatory Response. Front Cell Neurosci. 2018;12:488.
71. Keren-Shaul H, Spinrad A, Weiner A, et al. A Unique Microglia Type Associated with Restricting Development of Alzheimer's Disease. Cell. 2017;169(7):1276-90 e17.
72. Chiu IM, Morimoto ET, Goodarzi H, et al. A neurodegeneration-specific gene-expression signature of acutely isolated microglia from an amyotrophic lateral sclerosis mouse model. Cell Rep. 2013;4(2):385-401.
73. Holtman IR, Raj DD, Miller JA, et al. Induction of a common microglia gene expression signature by aging and neurodegenerative conditions: a co-expression meta-analysis. Acta Neuropathol Commun. 2015;3:31.
74. Krasemann S, Madore C, Cialic R, et al. The TREM2-APOE Pathway Drives the Transcriptional Phenotype of Dysfunctional Microglia in Neurodegenerative Diseases. Immunity. 2017;47(3):566-81 e9.
75. Götzl JK, Brendel M, Werner G, et al. Opposite microglial activation stages upon loss of PGRN or TREM2 result in reduced cerebral glucose metabolism. EMBO Mol Med. 2019;11(6).
76. Zhang J, Velmeshev D, Hashimoto K, et al. Neurotoxic microglia promote TDP-43 proteinopathy in progranulin deficiency. Nature. 2020;588(7838):459-65.
77. Ewers M, Biechele G, Suárez-Calvet M, et al. Higher CSF sTREM2 and microglia activation are associated with slower rates of beta-amyloid accumulation. EMBO Mol Med. 2020;12(9):e12308.
78. Ewers M, Franzmeier N, Suárez-Calvet M, et al. Increased soluble TREM2 in cerebrospinal fluid is associated with reduced cognitive and clinical decline in Alzheimer's disease. Sci Transl Med. 2019;11(507).
79. Gispert JD, Suárez-Calvet M, Monté GC, et al. Cerebrospinal fluid sTREM2 levels are associated with gray matter volume increases and reduced diffusivity in early Alzheimer's disease. Alzheimers Dement. 2016;12(12):1259-72.
80. Hamelin L, Lagarde J, Dorothée G, et al. Early and protective microglial activation in Alzheimer's disease: a prospective study using 18F-DPA-714 PET imaging. Brain. 2016;139(Pt 4):1252-64.
81. Hamelin L, Lagarde J, Dorothée G, et al. Distinct dynamic profiles of microglial activation are associated with progression of Alzheimer's disease. Brain. 2018;141(6):1855-70.
82. Woollacott IOC, Nicholas JM, Heslegrave A, et al. Cerebrospinal fluid soluble TREM2 levels in frontotemporal dementia differ by genetic and pathological subgroup. Alzheimers Res Ther. 2018;10(1):79.
83. Zhang J. Mapping neuroinflammation in frontotemporal dementia with molecular PET imaging. J Neuroinflammation. 2015;12:108.

84. Rutkowski MJ, Sughrue ME, Kane AJ, et al. Complement and the central nervous system: emerging roles in development, protection and regeneration. Immunol Cell Biol. 2010;88(8):781-6.
85. Hong S, Beja-Glasser VF, Nfonoyim BM, et al. Complement and microglia mediate early synapse loss in Alzheimer mouse models. Science. 2016;352(6286):712-6.
86. Luchena C, Zuazo-Ibarra J, Alberdi E, et al. Contribution of Neurons and Glial Cells to Complement-Mediated Synapse Removal during Development, Aging and in Alzheimer's Disease. Mediators Inflamm. 2018;2018:2530414.
87. Dejanovic B, Huntley MA, De Mazière A, et al. Changes in the Synaptic Proteome in Tauopathy and Rescue of Tau-Induced Synapse Loss by C1q Antibodies. Neuron. 2018;100(6):1322-36 e7.
88. Lui H, Zhang J, Makinson SR, et al. Progranulin Deficiency Promotes Circuit-Specific Synaptic Pruning by Microglia via Complement Activation. Cell. 2016;165(4):921-35.
89. Dionisio-Santos DA, Olschowka JA, O'Banion MK. Exploiting microglial and peripheral immune cell crosstalk to treat Alzheimer's disease. J Neuroinflammation. 2019;16(1):74.
90. Louveau A, Harris TH, Kipnis J. Revisiting the Mechanisms of CNS Immune Privilege. Trends Immunol. 2015;36(10):569-77.
91. Ekdahl KN, Persson B, Mohlin C, et al. Interpretation of Serological Complement Biomarkers in Disease. Front Immunol. 2018;9:2237.
92. Nilsson B, Hamad OA, Ahlström H, et al. C3 and C4 are strongly related to adipose tissue variables and cardiovascular risk factors. Eur J Clin Invest. 2014;44(6):587-96.
93. Cavaillon JM. Pro- versus anti-inflammatory cytokines: myth or reality. Cell Mol Biol (Noisy-le-grand). 2001;47(4):695-702.
94. Spiller KJ, Restrepo CR, Khan T, et al. Microglia-mediated recovery from ALS-relevant motor neuron degeneration in a mouse model of TDP-43 proteinopathy. Nat Neurosci. 2018;21(3):329-40.
95. Carlyle BC, Trombetta BA, Arnold SE. Proteomic Approaches for the Discovery of Biofluid Biomarkers of Neurodegenerative Dementias. Proteomes. 2018;6(3).
96. Cilento EM, Jin L, Stewart T, et al. Mass spectrometry: A platform for biomarker discovery and validation for Alzheimer's and Parkinson's diseases. J Neurochem. 2019;151(4):397-416.
97. Guldbrandsen A, Vethe H, Farag Y, et al. In-depth characterization of the cerebrospinal fluid (CSF) proteome displayed through the CSF proteome resource (CSF-PR). Mol Cell Proteomics. 2014;13(11):3152-63.
98. Gupta N, Pevzner PA. False discovery rates of protein identifications: a strike against the two-peptide rule. J Proteome Res. 2009;8(9):4173-81.
99. Craig-Schapiro R, Perrin RJ, Roe CM, et al. YKL-40: a novel prognostic fluid biomarker for preclinical Alzheimer's disease. Biol Psychiatry. 2010;68(10):903-12.
100. Perrin RJ, Craig-Schapiro R, Malone JP, et al. Identification and validation of novel cerebrospinal fluid biomarkers for staging early Alzheimer's disease. PLoS One. 2011;6(1):e16032.

101. Teunissen CE, Elias N, Koel-Simmelink MJ, et al. Novel diagnostic cerebrospinal fluid biomarkers for pathologic subtypes of frontotemporal dementia identified by proteomics. Alzheimers Dement (Amst). 2016;2:86-94.
102. Begcevic I, Tsolaki M, Brinc D, et al. Neuronal pentraxin receptor-1 is a new cerebrospinal fluid biomarker of Alzheimer's disease progression. F1000Res. 2018;7:1012.
103. Brinkmalm G, Sjodin S, Simonsen AH, et al. A Parallel Reaction Monitoring Mass Spectrometric Method for Analysis of Potential CSF Biomarkers for Alzheimer's Disease. Proteomics Clin Appl. 2018;12(1).
104. Paterson RW, Slattery CF, Poole T, et al. Cerebrospinal fluid in the differential diagnosis of Alzheimer's disease: clinical utility of an extended panel of biomarkers in a specialist cognitive clinic. Alzheimers Res Ther. 2018;10(1):32.
105. Wildsmith KR, Schauer SP, Smith AM, et al. Identification of longitudinally dynamic biomarkers in Alzheimer's disease cerebrospinal fluid by targeted proteomics. Mol Neurodegener. 2014;9:22.
106. Barschke P, Oeckl P, Steinacker P, et al. Proteomic studies in the discovery of cerebrospinal fluid biomarkers for amyotrophic lateral sclerosis. Expert Rev Proteomics. 2017;14(9):769-77.
107. Duits FH, Brinkmalm G, Teunissen CE, et al. Synaptic proteins in CSF as potential novel biomarkers for prognosis in prodromal Alzheimer's disease. Alzheimers Res Ther. 2018;10(1):5.
108. Llano DA, Bundela S, Mudar RA, et al. A multivariate predictive modeling approach reveals a novel CSF peptide signature for both Alzheimer's Disease state classification and for predicting future disease progression. PLoS One. 2017;12(8):e0182098.
109. Ringman JM, Schulman H, Becker C, et al. Proteomic changes in cerebrospinal fluid of presymptomatic and affected persons carrying familial Alzheimer disease mutations. Arch Neurol. 2012;69(1):96-104.
110. Spellman DS, Wildsmith KR, Honigberg LA, et al. Development and evaluation of a multiplexed mass spectrometry based assay for measuring candidate peptide biomarkers in Alzheimer's Disease Neuroimaging Initiative (ADNI) CSF. Proteomics Clin Appl. 2015;9(7-8):715-31.
111. van Steenoven I, Koel-Simmelink MJA, Vergouw LJM, et al. Identification of novel cerebrospinal fluid biomarker candidates for dementia with Lewy bodies: a proteomic approach. Mol Neurodegener. 2020;15(1):36.
112. van Steenoven I, Noli B, Cocco C, et al. VGF Peptides in Cerebrospinal Fluid of Patients with Dementia with Lewy Bodies. Int J Mol Sci. 2019;20(19).
113. Barschke P, Oeckl P, Steinacker P, et al. Different CSF protein profiles in amyotrophic lateral sclerosis and frontotemporal dementia with C9orf72 hexanucleotide repeat expansion. J Neurol Neurosurg Psychiatry. 2020;91(5):503-11.
114. Bastos P, Ferreira R, Manadas B, et al. Insights into the human brain proteome: Disclosing the biological meaning of protein networks in cerebrospinal fluid. Crit Rev Clin Lab Sci. 2017;54(3):185-204.
115. Hedl TJ, San Gil R, Cheng F, et al. Proteomics Approaches for Biomarker and Drug Target Discovery in ALS and FTD. Front Neurosci. 2019;13:548.

116. Rehiman SH, Lim SM, Neoh CF, et al. Proteomics as a reliable approach for discovery of blood-based Alzheimer's disease biomarkers: A systematic review and meta-analysis. Ageing Res Rev. 2020;60:101066.
117. Wesenhagen KEJ, Teunissen CE, Visser PJ, et al. Cerebrospinal fluid proteomics and biological heterogeneity in Alzheimer's disease: A literature review. Crit Rev Clin Lab Sci. 2020;57(2):86-98.
118. Surinova S, Schiess R, Hüttenhain R, et al. On the development of plasma protein biomarkers. J Proteome Res. 2011;10(1):5-16.
119. Teunissen CE, Otto M, Engelborghs S, et al. White paper by the Society for CSF Analysis and Clinical Neurochemistry: Overcoming barriers in biomarker development and clinical translation. Alzheimers Res Ther. 2018;10(1):30.
120. Günther R, Krause E, Schümann M, et al. Depletion of highly abundant proteins from human cerebrospinal fluid: a cautionary note. Mol Neurodegener. 2015;10:53.
121. Jack CR, Jr., Knopman DS, Jagust WJ, et al. Hypothetical model of dynamic biomarkers of the Alzheimer's pathological cascade. Lancet Neurol. 2010;9(1):119-28.
122. Venkatraghavan V, Bron EE, Niessen WJ, et al. Disease progression timeline estimation for Alzheimer's disease using discriminative event based modeling. Neuroimage. 2019;186:518-32.
123. Andersson E, Janelidze S, Lampinen B, et al. Blood and cerebrospinal fluid neurofilament light differentially detect neurodegeneration in early Alzheimer's disease. Neurobiol Aging. 2020;95:143-53.
124. Boeve BF, Rosen H. Clinical and Neuroimaging Aspects of Familial Frontotemporal Lobar Degeneration Associated with MAPT and GRN Mutations. Adv Exp Med Biol. 2021;1281:77-92.
125. Hardy CJ, Buckley AH, Downey LE, et al. The Language Profile of Behavioral Variant Frontotemporal Dementia. J Alzheimers Dis. 2016;50(2):359-71.
126. Donohue MC, Jacqmin-Gadda H, Le Goff M, et al. Estimating long-term multivariate progression from short-term data. Alzheimers Dement. 2014;10(5 Suppl):S400-10.
127. Jedynak BM, Lang A, Liu B, et al. A computational neurodegenerative disease progression score: method and results with the Alzheimer's disease Neuroimaging Initiative cohort. Neuroimage. 2012;63(3):1478-86.
128. Sabuncu MR, Desikan RS, Sepulcre J, et al. The dynamics of cortical and hippocampal atrophy in Alzheimer disease. Arch Neurol. 2011;68(8):1040-8.
129. Villemagne VL, Burnham S, Bourgeat P, et al. Amyloid β deposition, neurodegeneration, and cognitive decline in sporadic Alzheimer's disease: a prospective cohort study. Lancet Neurol. 2013;12(4):357-67.
130. Young AL, Bragman FJS, Rangelov B, et al. Disease Progression Modeling in Chronic Obstructive Pulmonary Disease. Am J Respir Crit Care Med. 2020;201(3):294-302.
131. Young AL, Marinescu RV, Oxtoby NP, et al. Uncovering the heterogeneity and temporal complexity of neurodegenerative diseases with Subtype and Stage Inference. Nat Commun. 2018;9(1):4273.

132. Li D, Donohue MC. Disease progression models for dominantly-inherited Alzheimer's disease. Brain. 2018;141(5):1244-6.
133. Meeter LH, Kaat LD, Rohrer JD, et al. Imaging and fluid biomarkers in frontotemporal dementia. Nat Rev Neurol. 2017;13(7):406-19.
134. Swift IJ, Sogorb-Esteve A, Heller C, et al. Fluid biomarkers in frontotemporal dementia: past, present and future. J Neurol Neurosurg Psychiatry. 2021;92(2):204-15.
135. Katisko K, Cajanus A, Jaaskelainen O, et al. Serum neurofilament light chain is a discriminative biomarker between frontotemporal lobar degeneration and primary psychiatric disorders. J Neurol. 2020;267(1):162-7.
136. Bridel C, van Wieringen WN, Zetterberg H, et al. Diagnostic Value of Cerebrospinal Fluid Neurofilament Light Protein in Neurology: A Systematic Review and Meta-analysis. JAMA Neurol. 2019.
137. Forgrave LM, Ma M, Best JR, et al. The diagnostic performance of neurofilament light chain in CSF and blood for Alzheimer's disease, frontotemporal dementia, and amyotrophic lateral sclerosis: A systematic review and meta-analysis. Alzheimers Dement (Amst). 2019;11:730-43.
138. Zhao Y, Xin Y, Meng S, et al. Neurofilament light chain protein in neurodegenerative dementia: A systematic review and network meta-analysis. Neurosci Biobehav Rev. 2019;102:123-38.
139. Irwin DJ, Trojanowski JQ, Grossman M. Cerebrospinal fluid biomarkers for differentiation of frontotemporal lobar degeneration from Alzheimer's disease. Front Aging Neurosci. 2013;5:6.
140. Scialò C, Tran TH, Salzano G, et al. TDP-43 real-time quaking induced conversion reaction optimization and detection of seeding activity in CSF of amyotrophic lateral sclerosis and frontotemporal dementia patients. Brain Commun. 2020;2(2):fcaa142.
141. Fenoglio C, Scarpini E, Serpente M, et al. Role of Genetics and Epigenetics in the Pathogenesis of Alzheimer's Disease and Frontotemporal Dementia. J Alzheimers Dis. 2018;62(3):913-32.
142. Cruchaga C, Graff C, Chiang HH, et al. Association of TMEM106B gene polymorphism with age at onset in granulin mutation carriers and plasma granulin protein levels. Arch Neurol. 2011;68(5):581-6.
143. Lattante S, Millecamps S, Stevanin G, et al. Contribution of ATXN2 intermediary polyQ expansions in a spectrum of neurodegenerative disorders. Neurology. 2014;83(11):990-5.
144. van Blitterswijk M, Mullen B, Heckman MG, et al. Ataxin-2 as potential disease modifier in C9ORF72 expansion carriers. Neurobiol Aging. 2014;35(10):2421 e13-7.
145. Brodovitch A, Boucraut J, Delmont E, et al. Combination of serum and CSF neurofilament-light and neuroinflammatory biomarkers to evaluate ALS. Sci Rep. 2021;11(1):703.
146. Janelidze S, Mattsson N, Stomrud E, et al. CSF biomarkers of neuroinflammation and cerebrovascular dysfunction in early Alzheimer disease. Neurology. 2018;91(9):e867-e77.
147. King E, O'Brien JT, Donaghy P, et al. Peripheral inflammation in prodromal Alzheimer's and Lewy body dementias. J Neurol Neurosurg Psychiatry. 2018;89(4):339-45.

148. Westwood S, Baird AL, Anand SN, et al. Validation of Plasma Proteomic Biomarkers Relating to Brain Amyloid Burden in the EMIF-Alzheimer's Disease Multimodal Biomarker Discovery Cohort. J Alzheimers Dis. 2020;74(1):213-25.
149. Whelan CD, Mattsson N, Nagle MW, et al. Multiplex proteomics identifies novel CSF and plasma biomarkers of early Alzheimer's disease. Acta Neuropathol Commun. 2019;7(1):169.
150. Kuhle J, Barro C, Andreasson U, et al. Comparison of three analytical platforms for quantification of the neurofilament light chain in blood samples: ELISA, electrochemiluminescence immunoassay and Simoa. Clin Chem Lab Med. 2016;54(10):1655-61.
151. Hampel H, O'Bryant SE, Molinuevo JL, et al. Blood-based biomarkers for Alzheimer disease: mapping the road to the clinic. Nat Rev Neurol. 2018;14(11):639-52.
152. Sancesario G, Bernardini S. AD biomarker discovery in CSF and in alternative matrices. Clin Biochem. 2019;72:52-7.
153. Arrant AE, Davis SE, Vollmer RM, et al. Elevated levels of extracellular vesicles in progranulin-deficient mice and FTD-GRN Patients. Ann Clin Transl Neurol. 2020;7(12):2433-49.
154. Badhwar A, Haqqani AS. Biomarker potential of brain-secreted extracellular vesicles in blood in Alzheimer's disease. Alzheimers Dement (Amst). 2020;12(1):e12001.
155. Hornung S, Dutta S, Bitan G. CNS-Derived Blood Exosomes as a Promising Source of Biomarkers: Opportunities and Challenges. Front Mol Neurosci. 2020;13:38.
156. Thompson AG, Gray E, Heman-Ackah SM, et al. Extracellular vesicles in neurodegenerative disease - pathogenesis to biomarkers. Nat Rev Neurol. 2016;12(6):346-57.
157. Dong X, Zheng D, Nao J. Circulating Exosome microRNAs as Diagnostic Biomarkers of Dementia. Front Aging Neurosci. 2020;12:580199.
158. Denk J, Oberhauser F, Kornhuber J, et al. Specific serum and CSF microRNA profiles distinguish sporadic behavioural variant of frontotemporal dementia compared with Alzheimer patients and cognitively healthy controls. PLoS One. 2018;13(5):e0197329.
159. Grasso M, Piscopo P, Talarico G, et al. Plasma microRNA profiling distinguishes patients with frontotemporal dementia from healthy subjects. Neurobiol Aging. 2019;84:240 e1- e12.
160. Kmetzsch V, Anquetil V, Saracino D, et al. Plasma microRNA signature in presymptomatic and symptomatic subjects with C9orf72-associated frontotemporal dementia and amyotrophic lateral sclerosis. J Neurol Neurosurg Psychiatry. 2020.
161. Piscopo P, Grasso M, Puopolo M, et al. Circulating miR-127-3p as a Potential Biomarker for Differential Diagnosis in Frontotemporal Dementia. J Alzheimers Dis. 2018;65(2):455-64.
162. Schneider R, McKeever P, Kim T, et al. Downregulation of exosomal miR-204-5p and miR-632 as a biomarker for FTD: a GENFI study. J Neurol Neurosurg Psychiatry. 2018;89(8):851-8.
163. Nandi K, Verma R, Dawar R, et al. Cell free DNA: revolution in molecular diagnostics - the journey so far. Horm Mol Biol Clin Investig. 2020;41(1).
164. Pai MC, Kuo YM, Wang IF, et al. The Role of Methylated Circulating Nucleic Acids as a Potential Biomarker in Alzheimer's Disease. Mol Neurobiol. 2019;56(4):2440-9.
165. Lehmann-Werman R, Neiman D, Zemmour H, et al. Identification of tissue-specific cell death using methylation patterns of circulating DNA. Proc Natl Acad Sci U S A. 2016;113(13):E1826-34.

166. Moss J, Magenheim J, Neiman D, et al. Comprehensive human cell-type methylation atlas reveals origins of circulating cell-free DNA in health and disease. Nat Commun. 2018;9(1):5068.
167. Ye Z, Chatterton Z, Pflueger J, et al. Cerebrospinal fluid liquid biopsy for detecting somatic mosaicism in brain. Brain Commun. 2021;3(1):fcaa235.
168. Hviid CVB, Madsen AT, Winther-Larsen A. Biological variation of serum neurofilament light chain. Clin Chem Lab Med. 2021.
169. Hok AHYS, Willemse EAJ, Teunissen CE, et al. Guidelines for CSF Processing and Biobanking: Impact on the Identification and Development of Optimal CSF Protein Biomarkers. Methods Mol Biol. 2019;2044:27-50.
170. Teunissen CE, Tumani H, Engelborghs S, et al. Biobanking of CSF: international standardization to optimize biomarker development. Clin Biochem. 2014;47(4-5):288-92.
171. Simrén J, Ashton NJ, Blennow K, et al. Blood neurofilament light in remote settings: Alternative protocols to support sample collection in challenging pre-analytical conditions. Alzheimers Dement (Amst). 2021;13(1):e12145.
172. Andreasson U, Perret-Liaudet A, van Waalwijk van Doorn LJ, et al. A Practical Guide to Immunoassay Method Validation. Front Neurol. 2015;6:179.
173. Breen EC, Reynolds SM, Cox C, et al. Multisite comparison of high-sensitivity multiplex cytokine assays. Clin Vaccine Immunol. 2011;18(8):1229-42.
174. Reijs BL, Teunissen CE, Goncharenko N, et al. The Central Biobank and Virtual Biobank of BIOMARKAPD: A Resource for Studies on Neurodegenerative Diseases. Front Neurol. 2015;6:216.

Chapter 7

Summary & Samenvatting

Summary

Frontotemporal dementia (FTD) is a clinically, genetically and pathologically heterogeneous condition most commonly characterised by progressive changes in behaviour (behavioural variant FTD) and / or language (primary progressive aphasia). An underlying autosomal dominant mutation in *GRN, C9orf72* or *MAPT* is identified in 10-20% of patients. Fluid biomarkers that enable detection and monitoring of FTD pathology in vivo could be instrumental both in clinical practice and pharmaceutical trials. This thesis investigated fluid biomarkers in genetic forms of FTD, using data from two observational cohort studies: the Dutch Frontotemporal Dementia Risk Cohort (FTD-RisC study) and the international Genetic Frontotemporal dementia Initiative (GENFI).

Chapter 1 introduces the aims of this thesis (chapter 1.1) and provides an overview of fluid biomarker research in FTD to date (chapter 1.2). Recent years have seen significant advances in the field of fluid biomarkers in neurodegenerative diseases. In particular, neurofilament light chain (NfL) is emerging as a highly sensitive, albeit non-specific, marker of neuroaxonal degeneration. Gene-specific biomarkers include PGRN in *GRN* mutation carriers and dipeptide repeat proteins in *C9orf72* mutation carriers. There is an unmet need for a biomarker that can reliably differentiate between FTD and other cognitive disorders and predict the underlying neuropathological substrate in sporadic FTD. Technological advances are facilitating biomarker identification in blood as a minimally invasive alternative to CSF, which is expected to greatly accelerate future biomarker research.

Chapter 2 describes the measurement of biomarkers of neuroaxonal and synaptic degeneration. In chapter 2.1, we longitudinally measured serum NfL in 335 GENFI participants over a mean follow-up duration of two years. Serum NfL levels were stable over time in presymptomatic mutation carriers, strongly increased around symptom onset and remained elevated over the course of FTD. Data from nine converters, i.e. presymptomatic carriers who developed symptoms during follow-up, revealed elevated NfL levels at least 1-2 years before symptom onset. The rate of NfL increase was associated with the rate of atrophy and clinical disease progression. Our data support NfL as a tool to identify preclinical disease in mutation carriers and to monitor disease progression. Chapter 2.2 describes the measurement of CSF neuronal pentraxins (NPTXs), a family of proteins implicated in synaptic plasticity, in 230 GENFI participants. We found decreased levels of NPTXs in the symptomatic stage of genetic FTD, probably reflecting the loss or dysfunction of synapses. Longitudinal measurements of NPTX2 in twelve mutation carriers suggested that NPTX2 levels might already decrease before symptom onset. NPTX2 correlated with clinical and neuroimaging measures of disease severity, demonstrating its potential as a disease progression biomarker.

NPTX2 might serve as a useful biomarker of synaptic integrity in future trials aimed at restoring synapse function.

Chapter 3 focuses on biomarkers that reflect immune system dysregulation in FTD. In chapter 3.1, we measured CSF levels of soluble triggering receptor expressed on myeloid cells 2 (sTREM2), which are thought to reflect microglial activation, in an international cohort of 107 *GRN* and *C9orf72* mutation carriers and 67 controls. We found no group differences in sTREM2 levels, precluding its use as a diagnostic biomarker. Interestingly, strongly elevated levels of sTREM2 were seen in some *GRN* mutation carriers, suggesting the presence of a subset with differential microglial activation. Based on data from four converters, we tentatively hypothesize that high sTREM2 levels in the presymptomatic stage might predict a delayed symptom onset. Chapter 3.2 reports on CSF and plasma complement levels in the GENFI cohort. We found elevated levels of CSF C1q and C3b, as well as plasma C2 and C3, in symptomatic mutation carriers, providing in vivo evidence of complement system dysregulation in FTD, although the substantial overlap between diagnostic groups diminishes their diagnostic value. Complement protein levels correlated with brain atrophy and NfL in the presymptomatic stage, suggesting that they might increase in conjunction with early neuronal loss. Further research is needed to determine their potential to monitor complement system dysregulation.

In chapter 4, we focus on the identification of novel biomarkers through proteomic and genetic approaches. Chapter 4.1 describes discovery mass spectrometry experiments on CSF of 28 *GRN* mutation carriers (19 presymptomatic, 9 symptomatic) and 24 non-carriers from the FTD-RisC study, revealing 25 differentially regulated proteins. We selected six proteins for validation by targeted mass spectrometry in a larger cohort of *GRN, C9orf72* and *MAPT* mutation carriers, revealing reduced levels of NPTXR, CHGA, VGF, PTPRN2 and VSTM2B in symptomatic carriers of all genetic subgroups. These proteins are primarily involved in synapse function, innate immunity and vesicle secretion and, if further validated in independent cohorts, might present novel biomarkers. In chapter 4.2, we first review the extensive spectrum of clinical presentations and the heterogeneous disease course associated with the *C9orf72* repeat expansion. Next, we explore possible genetic factors that might predict the phenotype and disease course in *C9orf72*, with particular emphasis on the length of the repeat expansion. Finally, we discuss recent advances in genetic technologies to characterise the length and content of repeat expansions, which might help identify novel prognostic factors.

Chapter 5 describes the use of discriminative event-based models to estimate the sequence in which biomarkers become abnormal over the course of FTD. In chapter 5.1, we

constructed a model of fluid biomarker changes in the GENFI cohort. NfL and NPTX2 were the first biomarkers to become detectably abnormal. Although this biomarker ordering did not differ between genetic subgroups, much more uncertainty was noted among *C9orf72* mutation carriers. Chapter 5.2 describes a similar DEBM model of blood NfL, neuroimaging and cognitive biomarkers, revealing that blood NfL and language domains were the first to become abnormal. Interestingly, language deficits were also one of the first abnormalities noted in models of behavioural variant FTD (bvFTD), suggesting that this might be an overlooked early feature.

In chapter 6, we discuss the main findings of this thesis in the context of current literature, review methodological considerations and suggest areas for future research.

Samenvatting

Frontotemporale dementie is een klinisch, genetisch en pathologisch heterogeen ziektebeeld wat meestal wordt gekenmerkt door progressieve veranderingen in het gedrag en / of de taal. Bij 10-20% van de patienten wordt een autosomaal dominant overervende mutatie gevonden in *GRN, C9orf72* of *MAPT*. Biomarkers in bloed of hersenvocht die de vroege detectie en monitoring van FTD faciliteren zouden bij kunnen dragen aan de huidige klinische praktijk als ook aan medicijnstudies. Dit proefschrift beschrijft de identificatie en validatie van fluïde biomarkers in genetische vormen van FTD. Hiervoor is gebruik gemaakt van twee observationele cohortstudies: het Nederlandse Frontotemporale Dementie Risico Cohort (FTD-RisC), en het internationale Genetic Frontotemporal Dementia Initiative (GENFI).

Hoofdstuk 1 geeft een inleiding op dit proefschrift (hoofdstuk 1.1) en een overzicht van de huidige status van biomarker-onderzoek in FTD (hoofdstuk 1.2). De afgelopen jaren is grote vooruitgang geboekt op gebied van biomarkerontwikkeling. Veelbelovend is neurofilament light chain (NfL), een zeer sensitieve, doch aspecifieke marker van neuroaxonale schade. Tevens zijn enkele gen-specifieke biomarkers beschreven, waaronder PGRN bij *GRN* mutatiedragers, en dipeptide repeat eiwitten in *C9orf72* mutatiedragers. Tot op heden ontbreken biomarkers die FTD van andere cognitieve stoornissen kunnen onderscheiden, en die bij leven de onderliggende neuropathologie kunnen voorspellen. De transitie naar biomarkers in bloed, in plaats van hersenvocht, is grotendeels te danken aan belangrijke technische ontwikkelingen in het veld, en zal naar verwachting het biomarker-onderzoek versnellen.

Hoofdstuk 2 is gewijd aan biomarkers die degeneratie van axonen en synapsen weerspiegelen. In hoofdstuk 2.1 beschrijven we de longitudinale metingen van serum NfL in 335 deelnemers van de GENFI studie, over een gemiddeld tijdsbestek van 2 jaar. Wij vonden stabiele NfL waarden in presymptomatische mutatiedragers, met een sterke stijging rondom het ontstaan van klachten. Gedurende de symptomatische fase bleven NfL waarden verhoogd. Bij negen converters, oftewel presymptomatische mutatiedragers die gedurende follow-up FTD-verschijnselen ontwikkelden, vonden wij verhoogde NfL waarden minstens 1-2 jaar voor het ontstaan van klachten. Tenslotte toonden we aan dat de snelheid waarmee NfL toeneemt correleert met de snelheid van ziekteprogressie. Deze bevindingen onderschrijven de waarde van NfL om (vroege) ziekte-activiteit op te sporen en te monitoren. Hoofdstuk 2.2 beschrijft metingen van neuronal pentraxins (NPTXs) in hersenvocht van 230 GENFI deelnemers. NPTXs worden in verband gebracht met plasticiteit van synapsen. De concentratie van NPTXs bleek verlaagd in symptomatische mutatiedragers, hetgeen

waarschijnlijk een verlies of dysfunctie van synapsen reflecteert. Longitudinale metingen van NPTX2 bij twaalf mutatiedragers doen vermoeden dat NPTX2 al daalt voor het ontstaan van klachten. De correlaties tussen NPTX2 en verscheidene maten van ziekte-ernst tonen aan dat NPTX2 een interessante marker van ziekteprogressie kan zijn. Toekomstige medicijnonderzoeken die zijn gericht op herstel van synapsfunctie hebben mogelijk baat bij NPTX2 als marker van synapsintegriteit.

Hoofdstuk 3 behelst biomarkers die betrokken zijn bij ontregelede immunologische processen in FTD. In hoofdstuk 3.1 beschrijven wij de meting van soluble triggering receptor expressed on myeloid cells 2 (sTREM2), een maat voor microglia-activatie, in hersenvocht van 107 *GRN* en *C9orf72* mutatiedragers en 67 controles. Wij vonden geen verschillen in sTREM2 waarden tussen de verschillende groepen, en sTREM2 heeft dan ook een beperkte waarde in de diagnostiek van FTD. Enkele *GRN* mutatiedragers hadden opvallend hoge sTREM2 waarden, hetgeen een subgroep van patienten met versterkte microglia-activatie suggereert. Op basis van vier converters veronderstellen wij dat hoge sTREM2 waarden in de presymptomatische fase mogelijk prognostisch gunstig zijn. Hoofdstuk 3.2 beschrijft de meting van complement-eiwitten in hersenvocht en plasma in de GENFI studie. De verhoogde waarden van C1q en C3b in hersenvocht, alsook C2 en C3 in plasma, zijn een aanwijzing voor ontregeling van het complementsysteem in de symptomatische fase van genetische FTD. Eventuele diagnostische waarde wordt tenietgedaan door de grotendeels overlappende resultaten tussen klinische groepen. Een opvallende correlatie werd waargenomen tussen complement-eiwitten en grijze stof atrofie als ook NfL in de presymptomatische fase, hetgeen suggereert dat complementactivatie simultaan met vroege neuronale schade optreedt. Meer onderzoek zal uitwijzen of complement-eiwitten kunnen dienen voor ziektemonitoring.

Hoofdstuk 4 richt zich op de ontwikkeling van biomarkers door proteomics en genetische strategieen. In hoofdstuk 4.1 beschrijven wij de identificatie van 25 potentiele biomarkers in hersenvocht middels massaspectrometrie op 28 *GRN* mutatiedragers (19 symptomatisch, 9 presymptomatisch) en 24 controles uit de FTD-RisC studie. Validatie van zes van deze eiwitten in een groter cohort van *GRN, C9orf72* en *MAPT* mutatiedragers middels parallel reaction monitoring toonde verlaagde concentraties van NPTXR, CHGA, VGF, PTPRN2 en VSTM2B in de symptomatische fase van FTD. Deze eiwitten zijn betrokken bij synapsfunctie, immunologische processen en exocytose. In hoofdstuk 4.2 geven wij een overzicht van het klinische spectrum van *C9orf72* mutatiedragers en beschrijven wij de huidige kennis omtrent genetische factoren die het fenotype en de snelheid van progressie mogelijk beinvloeden. In het bijzonder bespreken we het effect van de lengte van de *C9orf72* repeat expansie, en

lichten enkele nieuwe genetische technieken toe waarmee de repeat expansie in de toekomst beter in kaart kan worden gebracht.

In hoofdstuk 5 onderzoeken wij de relatie in de tijd tussen verschillende biomarkers middels discriminative event-based modelling. Het model beschreven in hoofdstuk 5.1, over fluïde biomarkers in het GENFI cohort, toont aan dat NPTX2 en NfL al vroeg in het ziektebeloop abnormaal worden. Hoewel de volgorde van biomarkerverandering niet verschilde tussen genetische subgroepen, was deze onzekerder in de *C9orf72* groep. In hoofdstuk 5.2 wordt een multimodaal ziekteprogressiemodel beschreven met NfL, neuroimaging en cognitieve biomarkers. NfL en achteruitgang van de taal bleken de eerste abnormale biomarkers te zijn. Zelfs in de gedragsvariant van FTD werd een vroege achteruitgang van de taal waargenomen; mogelijk wordt dit in de klinische praktijk onderschat.

In hoofdstuk 6 bespreken wij de belangrijkste bevindingen van dit proefschrift in het kader van de huidige literatuur en doen wij suggesties voor toekomstig biomarkeronderzoek.

GENFI consortium author list

Sónia Afonso; Maria Rosario Almeida; Sarah Anderl-Straub; Christin Andersson; Anna Antonell; Silvana Archetti; Andrea Arighi; Mircea Balasa; Myriam Barandiaran; Nuria Bargalló; Robart Bartha; Benjamin Bender; Alberto Benussi; Luisa Benussi; Valentina Bessi; Giuliano Binetti; Sandra Black; Martina Bocchetta; Sergi Borrego-Ecija; Jose Bras; Rose Bruffaerts; Marta Cañada; Valentina Cantoni; Paola Caroppo; David Cash; Miguel Castelo-Branco; Rhian Convery; Thomas Cope; Giuseppe Di Fede; Alina Díez; Diana Duro; Chiara Fenoglio; Camilla Ferrari; Catarina B. Ferreira; Nick Fox; Morris Freedman; Giorgio Fumagalli; Alazne Gabilondo; Roberto Gasparotti; Serge Gauthier; Stefano Gazzina; Giorgio Giaccone; Ana Gorostidi; Caroline Greaves; Rita Guerreiro; Carolin Heller; Tobias Hoegen; Begoña Indakoetxea; Vesna Jelic; Hans-Otto Karnath; Ron Keren; Tobias Langheinrich; Maria João Leitão; Albert Lladó; Gemma Lombardi; Sandra Loosli; Carolina Maruta; Simon Mead; Gabriel Miltenberger; Rick van Minkelen; Sara Mitchell; Katrina Moore; Benedetta Nacmias; Jennifer Nicholas; Linn Öijerstedt; Jaume Olives; Sebastien Ourselin; Alessandro Padovani; Georgia Peakman; Michela Pievani; Yolande Pijnenburg; Cristina Polito; Enrico Premi; Sara Prioni; Catharina Prix; Rosa Rademakers; Veronica Redaelli; Tim Rittman; Ekaterina Rogaeva; Pedro Rosa-Neto; Giacomina Rossi; Martin Rosser; Beatriz Santiago; Elio Scarpini; Sonja Schönecker; Elisa Semler; Rachelle Shafei; Christen Shoesmith; Miguel Tábuas-Pereira; Mikel Tainta; Ricardo Taipa; David Tang-Wai; David L Thomas; Paul Thompson; Hakan Thonberg; Carolyn Timberlake; Pietro Tiraboschi; Emily Todd; Philip Van Damme; Mathieu Vandenbulcke; Michele Veldsman; Ana Verdelho; Jorge Villanua; Jason Warren; Carlo Wilke; Ione Woollacott; Elisabeth Wlasich; Henrik Zetterberg; Miren Zulaica.

Curriculum vitae

Emma van der Ende was born on June 23rd, 1993 in Vlaardingen, the Netherlands. She attended the Stedelijk Gymnasium in Schiedam (secondary school) and subsequently obtained a degree in Medicine in December 2016 from the Erasmus University in Rotterdam. Following her graduation, she worked as a medical doctor in the Neurology department of the Maasstad ziekenhuis in Rotterdam. In June 2017, she began her PhD research on fluid biomarkers in genetic frontotemporal dementia under supervision of prof. dr. John van Swieten at the Erasmus University Medical Center. The author currently works as a medical doctor in the Neurology department of the Erasmus University Medical Center and lives with her partner in Oud-Beijerland.

Portfolio

	Year	ECTS
PhD Training		
Courses		
Pathology of neurodegenerative diseases (European Confederation of Neuropathological societies, Amsterdam)	2017	1.5
Markers and prediction research (NIHES)	2017	0.7
Introduction to data analysis (NIHES)	2017	1
Repeated measurements (NIHES)	2017	1.7
Good Clinical Practice (BROK)	2018	1.5
Research integrity	2018	0.3
Introduction to Linux (LUMC)	2018	0.3
Molecular Neurodegeneration (Wellcome Genome Campus, UK)	2019	2,5
Protein aggregation disorders (LUMC)	2019	1
Conferences and symposia		
Alzheimer's Association International Congress, London, United Kingdom *Poster presentation*	2017	1
International Conference on Frontotemporal Dementias, Sydney, Australia *Oral presentation & Poster presentation*	2018	2
2nd meeting of the International CSF Society, Amsterdam, the Netherlands *Poster presentation*	2018	1
JPND / JPco-fuND Symposium , Brussels, Belgium *Poster presentation*	2019	0.3
FTD Europe workshop, Tricase, Italy *Oral presentation*	2020	1
GENFI Investigator meetings *Oral presentations*	2017-2021	2
Other		
Mix&Match meetings ZonMw/Alzheimer Nederland (including organizing committee in 2018)	2017-2020	1
Alzheimer center weekly research meeting	2017-2021	4
Member of the Dutch FTD Experts working group (quarterly meetings)	2017-2021	1
Sub-investigator clinical trial Alector AL001-2	2020-2021	10
Teaching		
Supervision of Master's theses (two students)	2018-2020	3
Dutch FTD Caregivers society and other dementia support groups *Oral presentations*	2017-2021	1
Total		37.8

List of publications

E.L. van der Ende, E.E. Bron, J.M. Poos, L.C. Jiskoot, J.L. Panman, J.M. Papma, H.H. Meeter, C. Wilke, M. Synofzik, C. Heller, I.J. Swift, A. Sogorb-Esteve, A. Bouzigues, B. Borroni, R. Ghidoni, R. Sanchez-Valle, F. Moreno, C. Graff, R. Laforce Jr, D. Galimberti, M. Masellis, M.C. Tartaglia, E. Finger, R. Vandenberghe, J.B. Rowe, A. de Mendonça, F. Tagliavini, I. Santana, S. Ducharme, C.R. Butler, A. Gerhard, J. Levin, A. Danek, M. Otto, Y.A.L. Pijnenburg, G. Frisoni, S. Sorbi, W.J. Niessen, J.D. Rohrer, S. Klein, J.C. van Swieten, V. Venkatraghavan*, H. Seelaar*, on behalf of the GENFI consortium. A data-driven disease progression model of fluid biomarkers in genetic frontotemporal dementia. *Brain, revisions under review.*

E.L. van der Ende*, C. Heller*, A. Sogorb-Esteve, I.J. Swift, D. McFall, G. Peakman, A. Bouzigues, J.M. Poos, L.C. Jiskoot, J.L. Panman, J.M. Papma, C. Graff, M. Synofzik, F. Moreno, E. Finger, R. Sanchez-Valle, R. Vandenberghe, R. Laforce Jr, M. Masellis, M.C. Tartaglia, J.B. Rowe, C. Butler, S. Ducharme, A. Gerhard, A. Danek, J. Levin, Y.A.L. Pijnenburg, M. Otto, B. Borroni, F. Tagliavini, A. de Mendonça, I. Santana, D. Galimberti, G. Frisoni, S. Sorbi, R. Ghidoni, E. Huang, J.C. van Swieten, J.D. Rohrer[#], H. Seelaar[#], on behalf of the GENFI consortium. Elevated CSF and plasma complement proteins in genetic frontotemporal dementia: results from the GENFI study. *Under review*

E.L. van der Ende, E. Morenas-Rodriguez, C. McMillan, M. Grossman, D. Irwin, R. Sanchez-Valle, C. Graff, R. Vandenberghe, Y.A.L. Pijnenburg, R. Laforce Jr, I. Le Ber, A. Lleo, C. Haass, M. Suarez-Calvet, J.C. van Swieten, H. Seelaar. CSF sTREM2 is elevated in a subset in *GRN*-related frontotemporal dementia. *Neurobiology of Aging.* 2021 Jul;103:158.e1-158.e5.

E.L. van der Ende*, J. L. Jackson*, A. White, H. Seelaar, M. van Blitterswijk[#], J.C. van Swieten[#]. Unravelling the clinical spectrum and the role of repeat length in *C9orf72* repeat expansions. *Journal of Neurology, Neurosurgery and Psychiatry.* 2021 May;92(5):502-509.

J.L. Panman*, V. Venkatraghavan*, **E.L. van der Ende**, R.M.E. Steketee, L.C. Jiskoot, J.M. Poos, E.G.P. Dopper, H.H. Meeter, L. Donker Kaat, S.A.R.B. Rombouts, M.W. Vernooij, A.J.A. Kievit, E. Premi, M. Cosseddu, E. Bonomi, J. Olives, J.D. Rohrer, R. Sanchez-Valle, B. Borroni, E.E. Bron, J.C. van Swieten, J.M. Papma, S. Klein, on behalf of the GENFI consortium. Modelling the cascade of biomarker changes in GRN related frontotemporal dementia. *Journal of Neurology, Neurosurgery and Psychiatry*. 2021 May;92(5):494-501.

E.L. van der Ende, J.C. van Swieten. Fluid biomarkers of frontotemporal lobar degeneration. In: B. Ghetti, E. Buratti, B. Boeve, R Rademakers (eds.) *Frontotemporal Dementias. Advances in Experimental Medicine and Biology.* Vol. 1281. Cham: Springer; 2021; p.123-139.

I.J. Swift, A. Sogorb-Esteve, C. Heller, M. Synofzik, M. Otto, C. Graff, D. Galimberti, E. Todd, A.J. Heslegrave, **E.L. van der Ende**, J.C. van Swieten, H. Zetterberg, J.D. Rohrer. Fluid biomarkers in frontotemporal dementia: past, present and future. *Journal of Neurology, Neurosurgery and Psychiatry*. 2021 Feb;92(2):204-215.

E.L. van der Ende, M.F. Xiao, D. Xu, J.M. Poos, J.L. Panman, L.C. Jiskoot, H.H. Meeter, E.G.P. Dopper, J.M. Papma, C. Heller, R.S. Convery, K.M. Moore, M. Bocchetta, M. Neason, G. Peakman, D.M. Cash, C.E. Teunissen, C. Graff, M. Synofzik, F. Moreno, E. Finger, R. Sanchez-Valle, R. Vandenberghe, R. Laforce Jr, M. Masellis, M.C. Tartaglia, J.B. Rowe, C. Butler, S. Ducharme, A. Gerhard, A. Danek, J. Levin, Y.A.L. Pijnenburg, M. Otto, B. Borroni, F. Tagliavini, A. de Mendonça, I. Santana, D. Galimberti, H. Seelaar, J.D. Rohrer, P.F. Worley, J.C. van Swieten, on behalf of the Genetic Frontotemporal Dementia Initiative (GENFI). Neuronal pentraxin 2: A novel synapse-derived CSF biomarker in genetic frontotemporal dementia. *Journal of Neurology, Neurosurgery and Psychiatry.* 2020 Jun;91(6):612-621.

P. Barschke, P. Oeckl, P. Steinacker, M.R. Al Shweiki, J.H. Weishaupt, G.B. Landwehrmeyer, S. Anderl-Straub, P. Weydt, J. Diehl-Schmid, A. Danek, J. Kornhuber, M.L. Schroeter, J. Prudlo, H. Jahn, K. Fassbender, M. Lauer, **E.L. van der Ende**, J.C. van Swieten, A.E. Volk, A.C. Ludolph, M. Otto; German FTLD consortium. Different CSF protein profiles in amyotrophic lateral sclerosis and frontotemporal dementia with *C9orf72* repeat expansions. *Journal of Neurology, Neurosurgery and Psychiatry*. 2020 May;91(5):503-511.

J.M. Poos, L.C. Jiskoot, S.M.J. Leijdesdorff, H. Seelaar, J.L. Panman, **E.L. van der Ende**, M.O. Mol, H.H. Meeter, Y.A.L. Pijnenburg, L. Donker Kaat, F.J. de Jong, J.C. van Swieten, J.M. Papma, E. van den Berg. Cognitive profiles discriminate between genetic variants of behavioral frontotemporal dementia. *Journal of Neurology.* 2020 Jun;267(6):1603-1612.

E.L. van der Ende, H.H. Meeter, J.M. Poos, J.L. Panman, L.C. Jiskoot, E.G.P. Dopper, J.M. Papma, F.J. de Jong, I. Verberk, C.E. Teunissen, D. Rizopoulos, C. Heller, R.S. Convery, K.M. Moore, M. Bocchetta, M. Neason, D.M. Cash, B. Borroni, D. Galimberti, R. Sanchez-Valle, R. Laforce Jr, F. Moreno, M. Synofzik, C. Graff, M. Masellis, M.C. Tartaglia, J.B. Rowe, R. Vandenberghe, E. Finger, F. Tagliavini, A. de Mendonça, I. Santana, C. Butler, S. Ducharme, A. Gerhard, A. Danek, J. Levin, M. Otto, G. B. Frisoni, S. Cappa, Y.A.L. Pijnenburg, J.D. Rohrer, J.C. van Swieten, on behalf of the Genetic Frontotemporal dementia Initiative (GENFI). Serum

neurofilament light chain in genetic frontotemporal dementia: a longitudinal, multicentre cohort study. *The Lancet Neurology*. 2019 Dec;18(12):1103-1111.

J.L. Panman, Y.Y. To, **E.L. van der Ende**, J.M. Poos, L.C. Jiskoot, H.H. Meeter, E.G.P. Dopper, M.J.R.J. Bouts, M.J.P. van Osch, S.A.R.B. Rombouts, J.C. van Swieten, J. van der Grond, J.M. Papma, A. Hafkemeijer. Bias introduced by multiple head coils in MRI research: an 8 channel and 32 channel coil comparison. *Frontiers in Neuroscience*. 2019 Jul 15;13:729.

E.L. van der Ende, E. van den Berg, H. Seelaar, M.P. Coesmans, M.W. Vernooij, J.C. van Swieten. Frontotemporale dementie: een uitdaging in de klinische praktijk. *Tijdschrift voor Neurologie en Neurochirurgie*. 2019;120(3):87-93.

E.L. van der Ende*, H.H. Meeter*, C. Stingl, J.G.J. van Rooij, M.P. Stoop, D.A.T. Nijholt, R. Sanchez-Valle, C. Graff, L. Öijerstedt, M. Grossman, C. McMillan, Y.A.L. Pijnenburg, R. Laforce Jr, G. Binetti, L. Benussi, R. Ghidoni, T.M. Luider, H. Seelaar, J.C. van Swieten. Novel CSF biomarkers in *GRN*-associated frontotemporal dementia identified by proteomics. *Annals of Clinical and Translational Neurology.* 2019 Mar 7;6(4):698-707.

J.L. Panman, L.C. Jiskoot, M.J.R.J. Bouts, H.H. Meeter, **E.L. van der Ende,** J.M. Poos, R.A. Feis, A.J.A. Kievit, R. van Minkelen, E.G.P. Dopper, S.A.R.B. Rombouts, J.C. van Swieten, J.M. Papma. Gray and white matter changes in presymptomatic genetic frontotemporal dementia: a longitudinal MRI study. *Neurobiol Aging*. 2019 Apr;76:115-124.

J.L. Panman, L.C. Jiskoot, M.J.R.J. Bouts, H.H. Meeter, **E.L. van der Ende**, J.M. Poos, R.A. Feis, A.J.A. Kievit, R. van Minkelen, E.G.P. Dopper, S.A.R.B. Rombouts, J.C. van Swieten, J.M. Papma. Gray and white matter changes in presymptomatic genetic frontotemporal dementia: a longitudinal MRI study. *Neurobiology of Aging.* 2019 Apr;76:115-124.

L.C. Jiskoot, J.L. Panman, H.H. Meeter, E.G.P. Dopper, L. Donker Kaat, S. Franzen, **E.L. van der Ende**, R. van Minkelen, S.A.R.B. Rombouts, J.M. Papma, J.C. van Swieten. Longitudinal multimodal MRI as prognostic and diagnostic biomarker in presymptomatic familial frontotemporal dementia. *Brain*. 2019 Jan 1;142(1):193-208.

L.C. Jiskoot, M. Bocchetta, J.M. Nicholas, D.M. Cash, D. Thomas, M. Modat, S. Ourselin, S.A.R.B. Rombouts, E.G.P. Dopper, H.H. Meeter, J.L. Panman, R. van Minkelen, **E.L. van der Ende**, L. Donker Kaat, Y.A.L. Pijnenburg, B. Borroni, D. Galimberti, M. Masellis, M.C. Tartaglia, J.B. Rowe, C. Graff, F. Tagliavini, G.B. Frisoni, R. Laforce Jr, E. Finger, A. de Mendonça, S. Sorbi; Genetic Frontotemporal dementia Initiative (GENFI), J.M. Papma, J.C. van Swieten, J.D.

Rohrer. Presymptomatic white matter integrity loss in familial frontotemporal dementia in the GENFI cohort: a cross-sectional diffusion tensor imaging study. *Annals of Clinical and Translational Neurology.* 2018 Jul 11;5(9):1025-1036.

L.C. Jiskoot, J.L. Panman, L. van Asseldonk, S. Franzen, H.H. Meeter, L. Donker Kaat, E**.L. van der Ende**, E.G.P. Dopper, R. Timman, R. van Minkelen, J.C. van Swieten, E. van den Berg, J.M. Papma. Longitudinal cognitive biomarkers predicting symptom onset in presymptomatic frontotemporal dementia. *Journal of Neurology*. 2018 Jun;265(6):1381-1392.

H.H. Meeter, T.F. Gendron, A.C. Sias, L.C. Jiskoot, S.P. Russo, L. Donker Kaat, J.M. Papma, J.L. Panman, **E.L. van der Ende**, E.G.P. Dopper, S. Franzen, C. Graff, A.L. Boxer, H.J. Rosen, R. Sanchez-Valle, D. Galimberti, Y.A.L. Pijnenburg, L. Benussi, R. Ghidoni, B. Borroni, R. Laforce Jr, M. Del Campo, C.E. Teunissen, R. van Minkelen, J.C. Rojas, G. Coppola, D.H. Geschwind, R. Rademakers, A.M. Karydas, K. Öijerstedt, E. Scarpini, G. Binetti, A. Padovani, D.M. Cash, K.M. Dick, M. Bocchetta, B.L. Miller, J.D. Rohrer, L. Petrucelli, J.C. van Swieten, S.E. Lee. Poly(GP), neurofilament and grey matter deficits in *C9orf72* expansion carriers. *Annals of Clinical and Translational Neurology.* 2018 Apr 6;5(5):583-597.

List of abbreviations

Aβ	Amyloid-β
AD	Alzheimer's disease
ALLFTD	ARTFL-LEFFTDS Longitudinal Frontotemporal Lobar Degeneration
ALS	Amyotrophic lateral sclerosis
AMPAR	AMPA-type glutamate receptor
ANCOVA	Analysis of covariance
APP	Amyloid precursor protein
ARTFL	Advancing Research and Treatment in Frontotemporal Lobar degeneration
ASO	Antisense oligonucleotide
AUC	Area under the curve
BDE	Brain-derived exosomes
BNT	Boston Naming Test
bvFTD	Behavioural variant frontotemporal dementia
C8G	Complement component C8 gamma chain
C9orf72	Chromosome 9 open reading frame 72
CBI-R	Revised Cambridge Behavioural Inventory
CBS	Corticobasal syndrome
CDR	Clinical Dementia Rating scale
cfDNA	Cell-free DNA
CHGA	Chromogranin A
CHIT-1	Chitotriosidase-1
CI	Confidence interval
CNS	Central nervous system
CSF	Cerebrospinal fluid
CV	Coefficient of variation
DEBM	Discriminative event-based modelling
DLB	Dementia with Lewy bodies
DM	Myotonic dystrophy
DPR	Dipeptide repeat
EBM	Event-based modelling
ECAS	Edinburgh Cognitive and behavioural Screen
ECL	Electrochemiluminescence

ELISA	Enzyme-linked immunosorbent assay
FA	Fractional aniosotropy
FDG-PET	Fluorodeoxyglucose positron emission tomography
FDR	False discovery rate
FPI	Frontotemporal dementia Prevention Initiative
FSL	FMRIB Software Library
FTD	Frontotemporal dementia
FTD-MND	Frontotemporal dementia with motor neuron disease
FTD-RisC	Frontotemporal Dementia Risk Cohort
FTLD	Frontotemporal lobar degeneration
FTLD-CDR	Frontotemporal lobar degeneration – Clinical Dementia Rating scale
FRS	Frontotemporal dementia Rating Scale
FUS	Fused in sarcoma
GENFI	Genetic Frontotemporal dementia Initiative
GFAP	Glial fibrillary acidic protein
GMM	Gaussian mixture modelling
GO	Gene Ontology
GOBP	Gene Ontology – Biological Processes
GOCC	Gene Ontology – Cellular Components
GOMF	Gene Ontology – Molecular Functions
GRN	Granulin
HD	Huntington's disease
HDL	Huntington-like syndrome
IGHA1	Immunoglobulin heavy constant alpha 1
iPSC	Induced pluripotent stem cell
IQR	Interquartile range
LC-MS/MS	Liquid chromatography-tandem mass spectrometry
LDST	Letter digit substitution task
LEFFTDS	Longitudinal Evaluation of Familial Frontotemporal Dementia Study
LLOQ	Lower limit of quantification
MAPT	Microtubule-associated protein tau
MBL	Mannose-binding lectin
MCP-1	Monocyte chemoattractant protein 1
MEG	Magneto-encephalography
miRNA	micro-RNA

Mini-SEA	Mini Social cognition and Emotional Assessment
MMSE	Mini Mental State Examination
MND	Motor neuron disease
MNI	Montréal Neurological Institute
MRI	Magnetic resonance imaging
MS	Mass spectrometry
NfL	Neurofilament light chain
NfM	Neurofilament medium chain
nfvPPA	Non-fluent primary progressive aphasia
NPI	Neuropsychiatric Inventory
NPTX	Neuronal pentraxin
NPTXR	Neuronal pentraxin receptor
ONT	Oxford nanopore technology
PBMC	Peripheral blood mononuclear cells
PCR	Polymerase chain reaction
PD	Parkinson's disease
PET	Positron emission tomography
PGRN	Progranulin
pNfH	Phosphorylated neurofilament heavy chain
PPA	Primary progressive aphasia
PRM	Parallel reaction monitoring
PSP	Progressive supranuclear palsy
p-tau$_{181}$	Phosphorylated tau-181
PTPRN2	Protein tyrosine phosphatase receptor type N2
PV	Parvalbumin
QC	Quality control
RAN-translation	Repeat-associated non-ATG initiated translation
ROI	Region of interest
RT	Room temperature
RT-QuiC	Real-time quaking-induced conversion
SB	Sum of boxes
SCA	Spinocerebellar ataxia
SE	Standard error
Simoa	Single molecule array
SMRT	Single-molecule real-time
SPM	Statistical Parametric Mapping

sTREM2	Soluble triggering receptor expressed on myeloid cells 2
SuStaIn	Subtype and Stage Inference
svPPA	Semantic variant primary progressive aphasia
TBSS	Tract-based spatial statistics
TDP-43	TAR DNA-binding protein 43
TIV	Total intracranial volume
TOM	Theory of Mind
TMT	Trail Making Test
TREM2	Triggering receptor expressed on myeloid cells 2
TSPO-PET	Translocator protein positron emission tomography
t-tau	Total tau
ULOQ	Upper limit of quantification
UPS	Ubiquitin proteasome system
VGF	Vascular growth factor
VSTM2B	V-set and transmembrane domain-containing protein 2B
WGS	Whole genome sequencing
YKL-40	Chitinase-3-like protein 1